GEAR TOOTH SCORING INVESTIGATION

P. M. Ku, et al

Southwest Research Institute

Prepared for:

Army Air Mobility Research and
Development Laboratory

July 1975

USAAMRDL-TR- 75-33

233097

GEAR TOOTH SCORING INVESTIGATION

SOUTHWEST RESEARCH INSTITUTE
8500 Culebra Road
San Antonio , Tex. 78284

July 1975

Final Report for Period June 1970 - April 1975

Prepared for

EUSTIS DIRECTORATE
U. S. ARMY AIR MOBILITY RESEARCH AND DEVELOPMENT LABORATORY
Fort Eustis, Va. 23604

Unclassified

SECURITY CLASSIFICATION OF THIS PAGE (When Data Entered)

REPORT DOCUMENTATION PAGE		READ INSTRUCTIONS BEFORE COMPLETING FORM
1. REPORT NUMBER USAAMRDL-TR-75-33	2. GOVT ACCESSION NO.	3. RECIPIENT'S CATALOG NUMBER AD-A013 527
4. TITLE (and Subtitle) GEAR TOOTH SCORING INVESTIGATION		5. TYPE OF REPORT & PERIOD COVERED Final Report 6-29-70 to 4-24-75 6. PERFORMING ORG. REPORT NUMBER
7. AUTHOR(s) P. M. Ku H. E. Staph H. J. Carper		8. CONTRACT OR GRANT NUMBER(s) DAAJ02-70-C-0071
9. PERFORMING ORGANIZATION NAME AND ADDRESS Southwest Research Institute 8500 Culebra Road San Antonio, Texas 78284		10. PROGRAM ELEMENT, PROJECT, TASK AREA & WORK UNIT NUMBERS 62207A 1G162207AA72 02 002 EK
11. CONTROLLING OFFICE NAME AND ADDRESS Eustis Directorate U.S. Army Air Mobility R & D Laboratory Fort Eustis, Virginia 23604		12. REPORT DATE July 1975 13. NUMBER OF PAGES 316
14. MONITORING AGENCY NAME & ADDRESS (if different from Controlling Office) Same		15. SECURITY CLASS. (of this report) Unclassified 15a. DECLASSIFICATION/DOWNGRADING SCHEDULE

16. DISTRIBUTION STATEMENT (of this Report)

Approved for public release; distribution unlimited.

17. DISTRIBUTION STATEMENT (of the abstract entered in Block 20, if different from Report)

18. SUPPLEMENTARY NOTES

None

19. KEY WORDS (Continue on reverse side if necessary and identify by block number)

Gear tooth scoring
Gear performance
Gear design

20. ABSTRACT (Continue on reverse side if necessary and identify by block number)

A method has been devised for predicting the scoring potential and scoring-limited power-transmitting capacity of spur, helical, and spiral bevel gears. Computer programs for making such predictions for the three gear types have been written and are presented.

DD FORM 1 JAN 73 1473 EDITION OF 1 NOV 65 IS OBSOLETE

Unclassified

SECURITY CLASSIFICATION OF THIS PAGE (When Data Entered)

20. Continued

The predictive scheme comprises basically two steps. The first step involves the prediction of the ideal scoring-limited power-transmitting capacity, assuming perfect tooth alignment and no dynamic tooth load. The probable, actual scoring-limited power-transmitting capacity is then deduced from the ideal scoring-limited power-transmitting capacity by applying corrections for the misalignment and dynamic effects.

In order to evaluate the quality of the predictions, scoring tests have been performed on typical aircraft-quality gears, including spur gears of the same design but of two different surface characteristics, and spiral bevel gears of one design. The experimentally determined scoring-limited power-transmitting capacities have all been found to be within ten percent of the predictions.

EUSTIS DIRECTORATE POSITION STATEMENT

The work reported herein is the result of controlled disk tests, analytical computations, and verification gear tests. The resulting computer programs predict the scoring potential and scoring-limited, power-transmitting capacity of spur, helical, and spiral bevel gears. The verification gear test data have all been found to be within 10 percent of the predictions.

E. Rousee Givens of the Technology Applications Division served as Project Engineer for this effort.

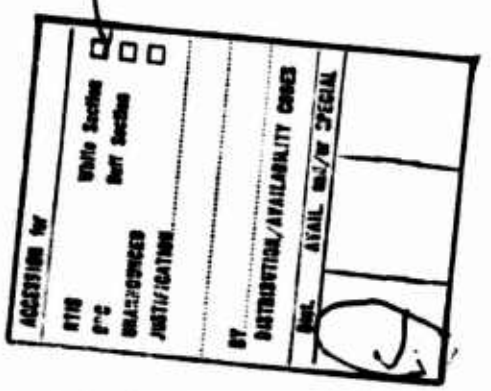

DISCLAIMERS

The findings in this report are not to be construed as an official Department of the Army position unless so designated by other authorized documents.

When Government drawings, specifications, or other data are used for any purpose other than in connection with a definitely related Government procurement operation, the United States Government thereby incurs no responsibility nor any obligation whatsoever; and the fact that the Government may have formulated, furnished, or in any way supplied the said drawings, specifications, or other data is not to be regarded by implication or otherwise as in any manner licensing the holder or any other person or corporation, or conveying any rights or permission, to manufacture, use, or sell any patented invention that may in any way be related thereto.

Trade names cited in this report do not constitute an official endorsement or approval of the use of such commercial hardware or software.

DISPOSITION INSTRUCTIONS

Destroy this report when no longer needed. Do not return it to the originator.

PREFACE

This report presents the results of a program conducted by Southwest Research Institute for the Eustis Directorate, U.S. Army Air Mobility Research and Development Laboratory, under Contract DAAJ02-70-C-0071. The USAAMRDL technical direction was provided by Mr. R. Givens.

The work described herein was performed with Southwest Research Institute as the prime contractor and Bell Helicopter Company as the subcontractor. SwRI had overall responsibility in the administration of the program, in addition to the development of the gear scoring predictive technique, the performance of sliding-rolling disk tests, and the analyses of all disk-test and gear-test results. BHC was responsible for the manufacture of all test disks and test gears, as well as gear testing.

In addition to the above gear tests, valuable spur gear test results were made available to this program by Mr. P. Lynwander, Chairman, Tribology Division, Aerospace Gearing Committee, American Gear Manufacturers Association. These test results were utilized in the formulation of the gear scoring predictive methodology.

Active participants of this program included P. M. Ku (principal investigator), H. E. Staph, H. J. Carper, D. M. Deffenbaugh, and H. Haufler of SwRI; C. E. Braddock, R. Battles, and R. T. Jenkins of BHC; as well as other supporting personnel of the two organizations.

TABLE OF CONTENTS

TABLE OF CONTENTS (Cont'd)

TABLE OF CONTENTS (Cont'd)

LIST OF ILLUSTRATIONS

LIST OF ILLUSTRATIONS (Cont'd)

LIST OF ILLUSTRATIONS (Cont'd)

LIST OF TABLES

LIST OF TABLES (Cont'd)

LIST OF TABLES (Cont'd)

CHAPTER I
INTRODUCTION

The investigation reported herein had as its basic objective the development of an improved methodology for predicting the power-transmitting capacity of gears as limited by gear-tooth scoring, with special reference to aircraft power gears. The gear types of interest included spur gears, straight helical gears, and spiral bevel gears. The gear material selected for study was carburized vacuum-melt AISI 9310 steel. The lubricants were MIL-L-7808 and MIL-L-23699 synthetic lubricants, with emphasis on a MIL-L-7808G lubricant.

In order to accomplish the above objective, pertinent information in the literature was reviewed and made use of where deemed applicable; controlled sliding-rolling disk tests were performed and their results analyzed and generalized to provide the basic inputs to the predictive scheme; computer programs were written for predicting the scoring-limited power-transmitting capacity of spur, helical, and spiral bevel gears; and full-scale gear tests were conducted to test the validity of the computer predictions.

Aircraft power gears should ideally be designed to give maximum power-transmitting capacity per unit size and weight, and at the same time possess a high degree of operating reliability. Obviously, it is not possible to assess operating reliability and hence the maximum permissible power-transmitting capacity of gears as limited by all possible modes of failure without considering the nature of these failure modes and their respective impact on gear performance. A comprehensive gear failure analysis of this character is not only beyond the scope of this investigation, but also impossible to accomplish in many respects. However, in order to provide some perspective to the overall problem, a brief qualitative discussion of the major gear-tooth failure modes and their effects will be given in the next chapter. It suffices to state at this juncture that gear teeth may fail basically by either strength-related or lubrication-related causes. However, many strength-related failures are influenced by lubrication or can be induced by lubrication-related failures. The importance of lubrication to gear performance is thus abundantly clear.

The current investigation is concerned with gear-tooth scoring, which is one particular mode of lubrication-related gear failure. In contrast to the other modes of lubrication-related gear failure which generally take time to develop or reach destructive magnitude, scoring

occurs quite precipitously and is therefore the most urgent one confronting the designer. Obviously, as long as scoring cannot be overcome, all time-dependent modes of gear failure are essentially academic. In other words, with gears that are adequately designed and manufactured strengthwise, scoring is the first performance barrier that must be crossed. It is only after scoring can assuredly be controlled that the other failure modes become truly relevant.

As will be seen later, the existing technology of gear design is such that the risk of strength-related failures can be quantitatively assessed with some confidence, especially for gears of relatively simple geometry operating under conditions such that misalignment and dynamic effects are not large. However, the same cannot be said of all lubrication-related failures due to the enormous complexity of the phenomena involved. This investigation emphasizes the scoring problem. Assuming that a scoring criterion can be established and quantitatively related to gear performance, then the next logical step will be the development of criteria for quantitative assessment of the effects of the other lubrication-related failures, as well as further refinements in handling the strength-related failures particularly for the complex gear types and the subtle influence of gear mechanics on lubrication. Unfortunately, all such information is not yet at hand; hence meaningful optimization of gear design is now not possible.

In view of the overwhelming importance of scoring, it is understandable that the gear designer's concern, other than the strength considerations, has so far been directed primarily toward the avoidance of scoring almost at any cost. In this connection, it is well to emphasize the difference between the avoidance of scoring and the quantitative prediction of scoring in the design stage. Thanks to decades of efforts on the part of many workers, the existing gear design technology is such that although the onset of scoring cannot yet be predicted accurately, nevertheless enough is known in a general way to avoid scoring by design without regard to the price to be paid. The advancement that is being sought in this program is to be able to predict scoring in the design stage and estimate the scoring-limited power-transmitting capacity. It is a far more difficult task than mere avoidance of scoring without inquiring as to what penalties are thereby entailed.

The program was essentially in the nature of engineering application, and as such no serious effort has been made to delve into the basic mechanism of scoring. Nevertheless, tangible progress is believed to have been made in the phenomenological sense to provide a

methodology for predicting the scoring-limiting power-transmitting capacity of gears. As outlined in Chapter VII, the basic procedure involves first the prediction of the ideal scoring-limited power-transmitting capacity of a gear set, assuming perfect tooth alignment and no dynamic tooth load. The probable, actual scoring-limited power-transmitting capacity is then deduced from the ideal scoring-limited power-transmitting capacity by applying corrections for the misalignment and dynamic effects.

As will be shown in Chapter VII, the prediction of the ideal scoring-limited power-transmitting capacity requires the use of certain numerical coefficients, and the prediction of the actual scoring-limited power-transmitting capacity further requires quantitative estimates of the misalignment and dynamic correction factors. Tentative values for these coefficients and correction factors were derived from the results of the sliding-rolling disk tests performed under this program, supplemented by several sets of full-scale spur gear test results made available by the Aerospace Gearing Committee of the American Gear Manufacturers Association. It is realized that these coefficients and correction factors are subject to refinements as additional disk and gear test results become available. Nevertheless, using the tentative values thus far developed, predictions were made for the full-scale gear tests performed under this program. As will be seen in Chapter VIII, the predicted scoring-limited power-transmitting capacities were within 10 percent of the statistically deduced test results from two series of tests on spur gears and one series of tests on spiral bevel gears. Helical gears were not tested in this program, due to difficulties encountered by the subcontractor in the scheduling of gear manufacturing and testing.

The investigation has brought out certain fundamental issues related to gear lubrication and gear mechanics, the resolution of which is believed to be essential before gear design, performance prediction, and performance optimization can be put on a truly rational basis. These problems are discussed in Chapter IX.

CHAPTER II
GEAR-TOOTH FAILURE AND LUBRICATION

A. Major Modes of Gear-Tooth Failure

Since this investigation is concerned with gear design and performance analysis, the nomenclature and symbols employed herein follow generally those adopted by the American Gear Manufacturers Association.[1-6] However, departures from the AGMA practice are made in several instances for the sake of clarity, as evident from the List of Symbols presented at the end of the report.

AGMA cites 21 modes of gear-tooth failure,[2] divided into four broad categories of wear, surface fatigue, plastic flow, and breakage. For the purpose of the present discussion, it is convenient to classify the major gear-tooth failure modes as shown in Table 1.

There are two broad classes of gear-tooth failures, namely, lubrication-related failures and strength-related failures. Major modes of lubrication-related failure are rubbing wear, scoring, and pitting. Major modes of strength-related failure are plastic flow and breakage.

Rubbing wear is a loss of metal by the rubbing action between two relatively moving surfaces, when there is a lack of an intact oil film of sufficient thickness to separate the surfaces.[7,8] One form of rubbing wear is adhesive wear, caused by metal transfer due to localized adhesion or a solid-phase welding process, and subsequent detachment of particles from one or both surfaces. The other form of rubbing wear is abrasive wear, caused by abrasive action between the relatively moving surfaces, or by the presence of abrasive particles between them. These particles may be dirt or other solid contaminants, or particles detached from the surfaces themselves due to severe pitting or wear.

Rubbing wear takes time to reach damaging proportion. It is of course harmful if severe and continued at an undiminishing rate. However, rubbing wear which diminishes with time, such as that associated with a break-in process, is not damaging but in fact beneficial.

Scoring (or scuffing) is a severe form of adhesive wear, which results in rapid damage to one or both surfaces in relative motion.[9,10] In contrast to the other modes of lubrication-related tooth failure which generally take time to develop or reach destructive magnitude, scoring occurs quite precipitously and is therefore the most urgent one

TABLE 1. MAJOR MODES OF GEAR-TOOTH FAILURE

Mode	Basic cause
Lubrication-related failure	
1. Rubbing wear	Lack of an intact oil film of sufficient thickness.
a. Adhesive wear	Metal transfer by localized adhesion, and subsequent detachment of particles.
b. Abrasive wear	Abrasive action.
2. Scoring	Lack of intact oil film coupled with intense localized frictional heating.
3. Pitting	Repeated surface stress cycling.
Strength-related failure	
1. Plastic flow	Surface deformation under heavy load, often aggravated by inadequate lubrication.
2. Breakage	Bending fatigue, severe pitting or abrasive wear.

confronting the designer. Obviously, as long as scoring cannot be avoided, all time-dependent modes of failure are essentially academic. In other words, with gears that are adequately designed and manufactured strengthwise, scoring is the first performance barrier that must be crossed. It is only after scoring can assuredly be controlled that the other failure modes become truly relevant. This accounts for the enormous emphasis to date on gear scoring by researchers and designers alike.

Since scoring is a form of adhesive wear, it cannot occur if an oil film of sufficient thickness separates the surfaces. However, mere lack of an intact oil film, while it inevitably leads to adhesive wear, may not cause scoring. In order for adhesive wear to advance to scoring, another necessary condition must be satisfied. Although the precise mechanism of scoring is at present not yet understood, the concensus is that it is the result of intense, localized frictional heating at the rubbing contact and is thus thermal in character.

Pitting (or surface fatigue) is the consequence of repeated stress cycling of the surfaces beyond the metal's endurance limit, which leads to surface or subsurface cracks and eventually the detachment of fragments from and the formation of pits on one or both surfaces.[9-11] Being a fatigue phenomenon, pitting takes time to develop. However, while rubbing wear and scoring cannot take place if an intact oil film of adequate thickness separates the two surfaces, pitting can occur even though it takes more time. This is because the presence of such an oil film merely modulates the intensity of the repeated surface stressing, but does not eliminate it altogether.

Plastic flow is the surface deformation resulting from plastic yielding of one or both surfaces in relative motion, usually associated with heavy loads or high temperatures. Although basically a strength-related phenomenon, it can nevertheless be influenced by lubrication. For example, high temperature which results in a reduction of the metal's yield strength may be due to inadequate lubrication. Moreover, rippling (a form of plastic flow) is apparently related to a complex interaction between the oil film and surfaces.[12]

Breakage of a gear tooth is caused by the bending stress imposed on it by the transmitted torque.[4-6] Outright breakage due to excessive bending stress beyond the fracture strength of the tooth is rather rare. A more common form of tooth breakage is that due to bending fatigue. Breakage is basically a strength-related failure. However, severe pitting or wear may so weaken the tooth (otherwise

adequate for the service) as to cause breakage. In this connection, a lubrication-related failure may lead to a breakage failure.

Consideration of the strength-related modes of gear-tooth failure is beyond the scope of this report. However, the subject is well covered by the standard treatises.[13-15] Moreover, the AGMA Standards for rating the strength of several gear types[4-6] provide tangible, straightforward, and quantitative guides to design, provided the many correction factors contained therein are selected with care.

In Chapters III, IV, and V which follow, the mechanics of spur, helical, and spiral bevel gears will be briefly discussed, with the objective of providing a background for assessing the risks of gear-tooth scoring as well as the other modes of lubrication-related failure.

It is only necessary to emphasize here that although gear-tooth failures may be due to either strength-related causes or lubrication-related causes, many strength-related failures are directly or indirectly influenced by lubrication.

B. Nature of Gear-Tooth Scoring

Although the basic mechanism of the scoring phenomenon is still largely not understood, there is good agreement that the lack of an intact oil film between the relatively moving surfaces is only a necessary but insufficient condition for scoring.[9, 10, 16-31] In other words, in order for scoring to occur, the operation not only must move into the boundary lubrication regime* but also must meet an additional requirement. However, largely because the mechanism of scoring is basically unsettled, what form this additional scoring criterion must take is still very much an open question. All available evidence appears to suggest that how deeply the operation may safely extend into the boundary lubrication regime without resulting in scoring depends upon the physical and chemical nature of the oil, the metal surface, and the surrounding atmosphere, as well as the operating conditions. Moreover, if there is a generalized scoring criterion, the concensus is that it is thermal in character, i.e., it is the consequence of the intense frictional heat generation at the potential scoring site.

* The term "boundary lubrication" is used herein to designate collectively the rather ill-defined modes of classical boundary lubrication, mixed lubrication, partial-elastohydrodynamic lubrication, and micro-elastohydrodynamic lubrication.

Of the various thermal scoring criteria that have been proposed, the most famous is no doubt the critical temperature criterion.[16,17] Other principal criteria include the critical power intensity criterion[21] and the critical power criterion.[28] These criteria have been compared,[27-30] but the comparisons are basically inconclusive. In short, there is no lack of data or arguments either to support or to refute any of these criteria in some way. However, from the point of view of generality, i.e., the potential of the criterion to account for the greatest number of design, material, lubricant, surface, and operating variables, it appears at this time that Blok's critical temperature criterion is the most promising, provided suitable refinements are added to Blok's original hypothesis. Such refinements will be discussed later in Chapter VI as applied to sliding-rolling disks and in Chapter VII as applied to gears.

Critical Temperature Hypothesis. In a sliding-rolling system, the friction due to the relative motion results in a localized, instantaneous rise in the temperatures of the surfaces in the conjunction which, under steady-operating conditions, establishes the quasi-steady temperatures of the two surfaces and the bulk temperatures of the two bodies. In most practical cases, the partition of the frictional heat and the general heat transfer conditions at the conjunction are such that the two surface temperatures are approximately equal.[32] The very unusual case when this is not so requires a more elaborate treatment.[23] However, such a refinement is hardly warranted at this time, inasmuch as the basic mechanism of scoring is, as previously stated, still not understood.

Taking the two surface temperatures as being equal, then one may write for the sliding-rolling system

$$T_c = T_s + \Delta T \qquad (1)$$

where T_c = maximum instantaneous surface temperature in the conjunction, °F

T_s = quasi-steady surface temperature, °F (often erroneously taken as the "bulk temperature")

ΔT = maximum rise of instantaneous surface temperature in the conjunction above the quasi-steady surface temperature, °F (also called the "flash temperature" by Blok)

Note that the transient temperature, T_c, is made up of two components: a quasi-steady component, T_s, and a transient component, ΔT. Both of these components are basically caused by the frictional heat generation at the conjunction. Their principal difference is that the ΔT component arises almost instantaneously, so practically no heat loss can take place in the process. On the other hand, the T_s component can be influenced by the heat loss from the conjunction, because it is taken over a period of time.[28] This problem will be considered further in Chapters VI and VII.

The basic premise of Blok's critical temperature hypothesis is that scoring will occur when T_c reaches a critical value.[16,17] In other words, the criterion for scoring is

$$T_{cr} = T_s + \Delta T \tag{2}$$

where T_{cr} = critical temperature, °F.

In Blok's postulate, T_{cr} is considered as a constant for a given metal-oil combination, regardless of the surface and operating conditions. However, this has not been found to be quite true by other investigators.[24-26, 28-30] The matter will be considered in some detail in Chapter VI.

If the critical temperature hypothesis is accepted, then scoring prediction for a given gear set becomes basically a problem of establishing the proper value of T_{cr} and estimating the value of T_s for various operating conditions, from which the ΔT required to reach scoring may be determined. Once this scoring-limited ΔT is known, the scoring-limited power-transmitting capacity may readily be computed.

The basic expression for computing the scoring-limited power-transmitting capacity is Blok's equation for a steady-operating sliding-rolling system with a rectangular conjunction (the so-called "line contact"), such as a system comprising a pair of perfectly aligned, straight cylinders.[19] This equation relates ΔT to the unit normal load as follows:

$$\Delta T = \frac{1.11\, f w \left| \sqrt{V_1} - \sqrt{V_2} \right|}{\beta \sqrt{B}} \tag{3}$$

where f = coefficient of friction

w = unit normal load, ppi

V_1, V_2 = surface velocities (absolute) of the two bodies, ips

β = Blok's thermal coefficient, lb/°F-in.-$sec^{\frac{1}{2}}$

B = width of Hertzian band in the direction of motion, in.

The various quantities involved in Equation (3) will be discussed in Chapter VI for steady-operating sliding-rolling disks. Application to gears, which undergo transient operation, must consider the effect of gear mechanics as given in Chapter VII.

Note that Equation (3) applies strictly to a sliding-rolling system with a rectangular conjunction. In case the conjunction is elliptic in shape, B must be replaced by the width of the Hertzian ellipse and w be replaced by an "equivalent unit normal load" such as that proposed by Kelley.[18]

C. Elastohydrodynamic Lubrication

It follows from Section A of this chapter that the presence of an intact oil film between the surfaces of mating gear teeth appears to be a desirable design goal, as it precludes rubbing wear and scoring, and minimizes pitting danger. However, whether or not such a design goal is practical or even achievable requires critical examination.

When counterformal bodies are loaded against each other, their surfaces experience significant localized elastic deformations. Elastohydrodynamic lubrication deals with the interaction between the hydrodynamic action of the lubricant and the localized elastic deformations of the surfaces. It basically explains why an intact oil film may exist under certain conditions between highly-loaded counterformal systems.

It has been found, both analytically and experimentally,[33, 34] that the oil film thickness in an EHD conjunction is not uniform. Accordingly, the oil film thickness of particular interest is the minimum oil film thickness, because if rubbing contact were to occur, it would be apt to occur where the oil film thickness is the least.

The basic equation for the minimum oil film thickness in a

rectangular EHD conjunction of perfectly smooth surfaces, in a steady-state, flooded, and isothermal flow, has been given in dimensionless form by Dowson.[34] This equation may be written in conventional engineering units as follows:

$$h_m = 26.5 \frac{\alpha_o^{0.54} (\mu_o V_t)^{0.70} R^{0.43}}{w^{0.13} E^{*0.03}} \quad (4)$$

where h_m = minimum oil film thickness, μin.

α_o = pressure-viscosity coefficient of oil at conjunction-inlet temperature and near-atmospheric pressure, psi^{-1}

μ_o = absolute viscosity of oil at conjunction-inlet temperature and near-atmospheric pressure, cp

V_t = sum velocity, ips

R = equivalent radius of curvature at the conjunction, in.

w = unit normal load, ppi

E^* = equivalent Young's modulus, psi

The above equation applies strictly to a sliding-rolling system with a rectangular conjunction, provided the numerous assumptions stated above are met. In practical applications, the conjunction shape may not be rectangular, but may be elliptic in shape. If the aspect ratio of the ellipse normal to the motion is large (> 5), little error results from the rectangular assumption. However, if the aspect ratio is small, then the problem becomes more complex. In that event, an approximate correction for "side flow effect," due to Cheng,[35] may be used, provided all the other assumptions are not substantially violated.

Additionally, the assumption of an isothermal flow process may not be approached in practice, due to heating caused by the viscous shear of the oil in the inlet region. This effect can be very significant at high sum velocities, particularly when the oil viscosity is high. In that event, another approximate correction for the "inlet-shear thermal effect," also due to Cheng,[36] may be applied, provided again all the other assumptions are not substantially violated.

When Cheng's side flow and inlet-shear thermal corrections are applied to Equation (4), the minimum oil film thickness for a flooded, elliptic EHD conjunction of perfectly smooth surfaces is obtained:

$$h'_m = 26.5 \frac{\alpha_o^{0.54}(\mu_o V_t)^{0.70} R^{0.43} \phi_s \phi_t}{w^{0.13} E^{*0.03}} \qquad (5)$$

where h'_m = minimum oil film thickness, μin.

ϕ_s = side flow correction factor

ϕ_t = inlet-shear thermal correction factor

The procedure for estimating the values of ϕ_s and ϕ_t is conveniently summarized in a recent paper by Cheng.[37] The other quantities involved in Equation (5) will be further dealt with in Appendix C, primarily as a matter of general interest. However, the calculation of the EHD film thickness will not be emphasized in this report. The reasons are many;[9,10] but the crucial ones are as follows:

1. The inlet-shear thermal correction factor does not account for the nonuniform temperature distribution across the oil film, yet this effect can be quite significant in practice.[38] Reliable assessment of the temperature gradient across the film, particularly considering sliding[39] and the complex participating flow and heat transfer involved, is currently not available.

2. Similarly, an improved method for estimating the side flow correction factor is required.

3. Actual surfaces are never perfectly smooth. Surface roughness and surface texture affect the EHD film formation in a complex manner;[25,40-42] but there is as yet no confident way to assess these effects. Indeed, if the composite surface roughness involved is about the same order of magnitude as the nominal film thickness, EHD lubrication in the classical sense no longer prevails. In that event, the meaning of classical EHD lubrication becomes quite obscure, and the computed EHD film thickness resulting therefrom is apt to be very misleading.

4. Due to the action of the gear teeth and the conventional manner of oil supply, the state of gear-tooth lubrication is probably always starved, or far from the flooded assumption. Although the effect of starvation on film thickness behavior is quite well understood by assuming an arbitrary inlet boundary location and shape with a uniform temperature distribution across the film,[43] these assumptions are, as stated above, not realistic for gears. In any case, there is presently no reliable way to relate the extent of starvation (i.e., the inlet boundary location) to lubricant, design, and operating parameters, even under these idealized conditions.

5. Gear-tooth action also introduces dynamic tooth loading, augments oil film development due to normal approach of the tooth surfaces, and causes flow acceleration and deceleration which affect film formation. These effects are difficult to account for quantitatively.

6. As stated previously, it is now well established that the lack of an intact oil film between the relatively moving surfaces is only a necessary but insufficient condition for scoring. In other words, scoring always occurs in the boundary lubrication regime, and the scoring risk is more realistically assessed by another criterion, such as the critical temperature. Accordingly, gear design based on obtaining full EHD lubrication is not only unnecessary, but far too conservative from the standpoint of size and weight.

7. Even if one chooses to employ full EHD lubrication as a design goal, he has no assurance that it will be achieved in practice, since the current film thickness predictive technique is inadequate for this purpose, for reasons stated above. It can be readily seen from Equation (5) that, everything else being equal, h'_m is inversely proportional to $w^{0.13}$, or w is inversely proportional to $(h'_m)^{7.7}$. Thus, any errors in predicting the minimum oil film thickness will be greatly magnified in the prediction of the scoring-limited power-transmitting capacity.

D. Boundary Lubrication

The above remarks are not intended to minimize the important contributions of the EHD theory to the current understanding of the lubrication of counterformal surfaces. It is only that as knowledge on the details of EHD lubrication expands, complications begin to emerge and further refinements appear necessary. In particular, once the operation leaves the full EHD lubrication regime, a continuous and undisturbed oil film no longer exists between the mating surfaces. The operation then enters the boundary lubrication regime, and the

complex chemical interactions involved cannot be ignored.

It has been argued previously that of the three major lubrication-related gear-tooth failure modes, EHD lubrication is not a necessary condition for pitting and not a sufficient condition for scoring. Therefore, in assessing the effect of lubrication-related failure modes on gear performance, the crucial question is not when and how full EHD film ceases to prevail; but rather when and how the boundary film formed by the oil-metal-atmosphere interaction ceases to inhibit or minimize surface failures.

Boundary lubrication is of course the most investigated but perplexed subject in lubrication. Literally thousands of references exist that pertain to various aspects of boundary lubrication; but a few broad treatises should suffice to illustrate its scope and tremendous complexity.[44-47] It is not possible to deal with the subject of boundary lubrication in simple terms. What appears particularly important as pertains to the lubrication-related failure modes of gear teeth will be commented on later, mainly in Chapter VI. In any case, as the operation moves into the boundary lubrication regime, i.e., when contact between the gear-tooth surfaces takes place, rubbing wear becomes inevitable, scoring becomes a possibility, and pitting becomes more likely. The manifestation of rubbing wear and pitting damages is time-dependent, and their rates of damage depend upon the physical and chemical oil-metal-atmosphere interactions. The occurrence of scoring is quite precipitous, and is also controlled by boundary lubrication considerations in some way.

E. Lubrication-Limited Gear Performance

It is very difficult to describe the lubrication-related modes of gear-tooth failure, or to evaluate their impact on gear performance with much confidence, mainly because the mechanisms of the failure modes are still not well understood and the effect of gear mechanics on these failure modes—while known to be large—cannot be accurately assessed. However, regardless of the approximations involved, an analysis made by Blok[19] is instructive.

In his analysis, Blok derived general expressions for the maximum power transmittable by a set of homologous gears, or gears having similar design and materials, using a straight mineral oil. He assumed that rubbing wear would not take place if the operation is in the full EHD regime. He considered that scoring was governed by his critical temperature hypothesis, with the critical temperature and

instantaneous coefficient of tooth friction assumed constant. He regarded pitting as strictly a mechanical consideration by ignoring the effect of lubrication. Using these assumptions, Blok concluded that in the absence of strength-related failures, the maximum power transmittable through a set of homologous gears is primarily limited at low speeds by rubbing wear, at intermediate speeds by pitting or scoring, and at high speeds by scoring.

As has been discussed in the preceding sections of this chapter, Blok's assumptions are rather drastic oversimplifications of very complex phenomena. Quite apart from the difficulty of defining the mechanisms of the failure phenomena, which will hopefully come about in due time, it is believed that the time-dependent nature of the damages due to rubbing wear and pitting can be introduced in the scheme of analysis. While such refinements will alter Blok's predicted trends substantially in some regimes of gear operation, it is not believed that his major conclusions will be greatly altered. The Blok analysis gives probably the most convincing reason for the practical importance of scoring, especially for aircraft power gears.

F. Impact of Gear Mechanics

Lubrication is concerned with the behavior of interacting surfaces in relative motion. Accordingly, the study of the lubrication of any machine element must, by necessity, include a consideration of the total effect of the following participating factors:

1. Motions without regard to the forces acting, or a study of kinematics.

2. Forces, displacements, and motions, which are the concern of what may be termed statics (where a state of rest is assumed) and dynamics (the general case).

3. Material and surface characteristics, both physical and chemical.

4. Lubricant characteristics, both physical and chemical.

5. Characteristics of the surrounding atmosphere, both physical and chemical.

In other words, lubrication deals with the total interaction including all physical and chemical causes and effects, which are in most respects time-dependent in character. In an effort to gain an insight into some specific aspects of the total problem, one customarily begins by isolating the problem into neat, individual packages that can

be more readily attacked. This is a logical and necessary learning process; but one must not lose sight of the fact that these prescribed packages may or may not neatly simulate gear operation. As explained previously, although much has been learned about the lubrication of idealized sliding-rolling systems in steady-state operation, certain basic issues still remain. Additionally, in order to translate such idealized knowledge into practice, the mechanical behavior of gears must be brought into focus; but this is an area that has not engaged the needed attention of lubrication engineers.

Gears employ counterformal surfaces and are thus subject to high normal stresses. As they go through a mesh cycle, the tooth load, sum velocity, and sliding velocity all vary in manners dependent on the gear type and design.

Gear kinematics can be precisely defined by assuming completely rigid gears.[13-15,48] Even so, the matter acquires much complexity with such gear types as the hypoids and spiral bevels. In reality, gears are never completely rigid, hence one must deal with the interactions between forces and displacements or motions. One then encounters the problems of statics and dynamics of gears, which will now be highlighted.

Surface Deformation — Since gears are not completely rigid, one must consider the consequences of this fact. One important consequence is the local elastic deformation of the counterformal surfaces under load, which gives rise to elastohydrodynamic lubrication, the application of which to gear lubrication has been discussed.

Tooth Deflection — The elastic deflection of the gear teeth affects tooth profile modification and the manner of load sharing among the teeth. Although the subject of load sharing will be covered later, some general remarks appear in order here. Consider, for example, a set of involute spur gears (assuming no manufacturing errors) with a contact ratio of less than 2, for which the load is carried by two pairs of teeth at the beginning and end of the mesh cycle, and by only one pair of teeth during the remaining portion of the mesh cycle. In this simple case, the relation between the load sharing pattern and tooth profile modification for a particular design load can be established by statics with relative ease, but still with some measure of empiricism. If the contact ratio is, say, between 2 and 3, the load is carried by three pairs of teeth at the beginning, middle, and end of the mesh cycle, and by two pairs of teeth during the remaining portions of the mesh cycle. The load sharing and profile modification problem of

high-contact-ratio gears is considerably more difficult to solve. Design optimization is far more complex, because the propensity of both strength-related and lubrication-related failures depends markedly on how the high contact ratio is achieved.[49] Nevertheless, high contact ratio normally exists in such gears as the helicals and spiral bevels; and it is gaining in popularity for aircraft spur gears.

Other Deflections — The gear bodies, shafts, support bearings, and housing also deflect under load. These deflections may modify load sharing among the teeth, or cause tooth misalignment. Analysis of these deflections is even more difficult than that of tooth deflection; a rational approach is currently lacking.

Tooth Misalignment — Tooth misalignment may be due to the numerous bulk deflections mentioned above, manufacturing errors, stackup of tolerances in the assembly process, or differential thermal expansion. Whatever the causes, misalignment can greatly affect both strength-related failures[4-6] and lubrication-related failures.[22] Misalignment is one of the most nasty problems to handle, because it is difficult to measure and control in practice, and reliable prediction of its effects is still not available.

Dynamics — The dynamics of gear-tooth behavior, due to the transient nature of tooth engagement, operation away from the profile-modified design point, manufacturing errors, and externally imposed dynamic conditions, is an exceedingly complex subject. Clearly, if the actual tooth load is much higher than that derived for the static case, then estimates for both strength-related and lubrication-related failures based on the static load can be overly optimistic. As will be seen later, the dynamics of gear teeth of simple geometry, under idealized conditions, has been a subject of much study, mainly with regard to strength-related failures. Even so, the dynamics of a complete gear system, and also the dynamics of lubricant flow to and over the gear teeth, are quite different matters. The effects of gear and lubricant flow dynamics on lubrication-related failures, as well as the time-dependent chemical interactions involved in the failure processes, are by and large not well understood at present.

CHAPTER III
SPUR GEAR MECHANICS

A. Spur Gear Kinematics

Spur gears are the most common form of gears in use. They operate on parallel shafts and all elements of a gear tooth are parallel to those shafts. The shape of a gear tooth may take one of many forms, provided the contact between mating pairs of teeth results in a conjugate motion; i.e., the transmission of motion at constant angular velocity. The most commonly used tooth form is derived from the involute of a circle.

This chapter will discuss several important aspects of involute gear mechanics as applicable to the problem of gear scoring. More detailed treatment of involute gear mechanics may be found in standard texts.[13-15]

Figure 1 shows a transverse view of two involute gears in mesh. The smaller one of the pair, usually called the pinion, is the driving member in this illustration. The larger one, usually called the gear, is the driven member. Contact initiates at point A between a pair of teeth and continues along the line AD until the pair of teeth disengage at point D. The line AD is the path of contact. To avoid interference between the tooth profiles, contact must lie between points V and W, the interference points.

The line VW is tangent to the base circles of the pinion and gear, which are unique to any given pair of involute gears. This line, of which AD is a part, makes an angle ϕ with the normal to the line of centers. This angle is the pressure angle, as shown in the lower portion of Figure 1.

Figure 1 shows two adjacent pairs of teeth in contact, one pair at A and the second pair at B. If the line VW, assumed to be a flexible but inextensible cord, were loosened at point W and wrapped around the pinion base circle, and then loosened at point V and wrapped around the gear base circle, scribers attached at points A and B would alternately trace involutes on the pinion and gear blanks which would form part of the active portions of the mating tooth surfaces. The length AB is equal to the arc length A'B', the normal base pitch.

The distance from any point of tooth contact to the interference

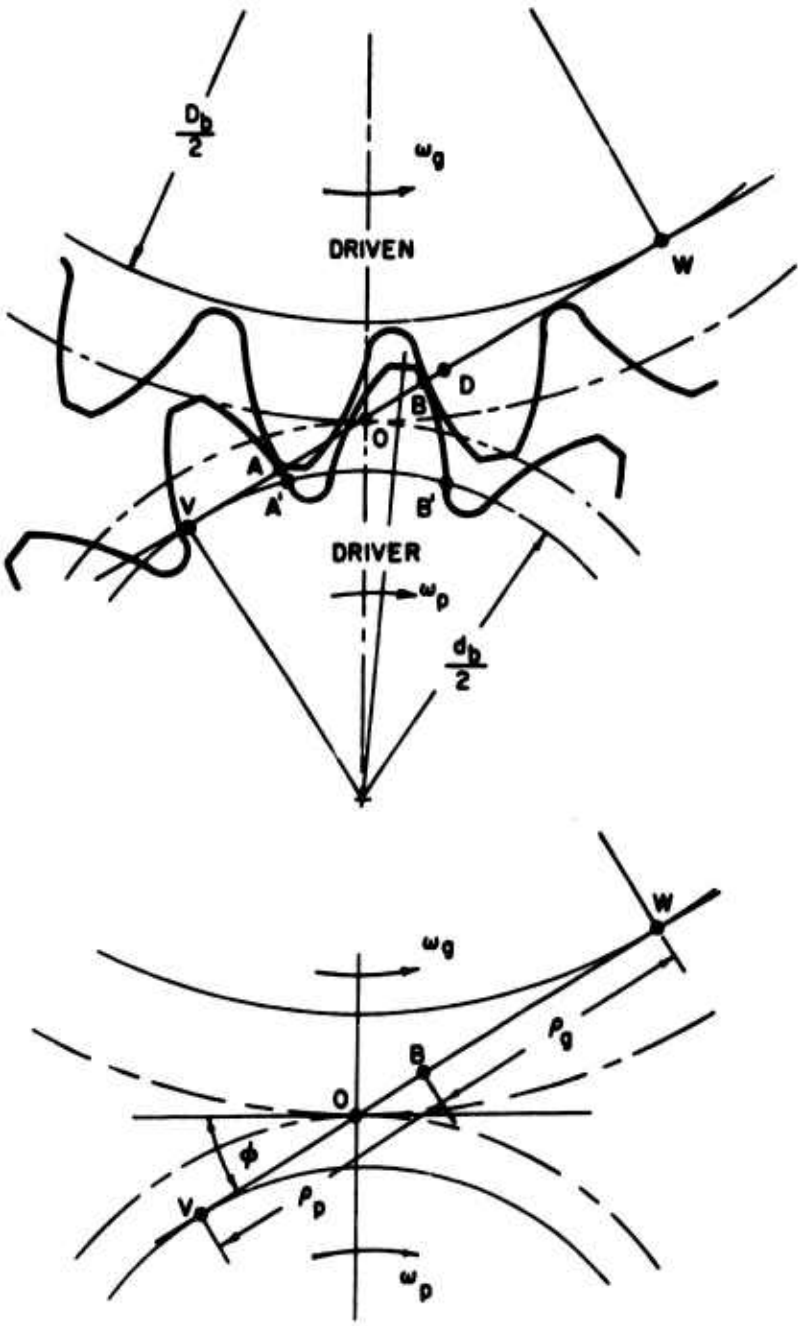

Figure 1. Spur gear geometry and kinematics

point is the instantaneous radius of curvature of the tooth profile at the point of contact. Thus in Figure 1, the radii of curvature at A are AV for the pinion tooth and AW for the gear tooth. Similarly at B, the radii are BV and BW.

The instantaneous sliding and sum velocities at the contact point may be determined from the instantaneous radii of curvature of the two teeth at that point and the angular velocities of the pinion and gear. Referring to Figure 1, they are

$$V_s = \rho_p \omega_p - \rho_g \omega_g \tag{6}$$

$$V_t = \rho_p \omega_p + \rho_g \omega_g \tag{7}$$

where V_s = instantaneous sliding velocity, ips

V_t = instantaneous sum velocity, ips

ρ_p = instantaneous radius of curvature of pinion tooth, in.

ρ_g = instantaneous radius of curvature of gear tooth, in.

ω_p = angular velocity of pinion, rad/sec

ω_g = angular velocity of gear, rad/sec

The gear ratio, or the ratio of the larger to the smaller number of teeth in the mating gears, is

$$G = \frac{N_g}{N_p} = \frac{D}{d} = \frac{\omega_p}{\omega_g} \tag{8}$$

where G = gear ratio

d = pitch diameter of pinion, in.

D = pitch diameter of gear, in.

N_p = number of pinion teeth

N_g = number of gear teeth

It can be readily shown that as a pair of teeth go through the mesh, the sum velocity remains positive throughout the mesh cycle. On the other hand, the sliding velocity starts at a maximum negative value at point A, rises to zero at the pitch point O, then it becomes positive and increases to a maximum positive value at point D. For the case of G = 1, the sum velocity is constant throughout the mesh cycle, while the absolute value of the sliding velocity variation is symmetrical with respect to the pitch point. If the pinion is the driver, as shown in Figure 1, the sum velocity will increase as the mesh progresses from A to D, and the absolute value of the sliding velocity will be greater at A than at D. With the gear as the driver, the sum velocity will decrease as the mesh progresses from A to D, and the absolute value of the sliding velocity will be less at A than at D.

B. Spur Gear Statics

It has been pointed out that a pair of spur gear teeth first engage at point A (Fig. 1) and finally disengage at point D. Figure 2 shows two involute spur gears at the instant that a pair of teeth engage at A. A second pair of teeth are already in mesh at B. As the gears rotate, the pair of teeth previously in mesh at B will move to point D, where they are ready to disengage. The pair of teeth previously at A are engaged at point C. Any further motion will result in the teeth at D separating and the teeth at C being the only pair of teeth in contact. It is obvious that as the pair of teeth at A move to C, and the pair of teeth at B move to D, the load is shared between these two tooth pairs. However, as the pair of teeth at C move to B, the load is carried entirely by this single pair of teeth. A measure of the portion of the total contact time during which two pairs of teeth share the load is given by the contact ratio, defined as

$$m_c = \frac{AD}{p_b} \tag{9}$$

where m_c = contact ratio

AD = length of path of contact, in.

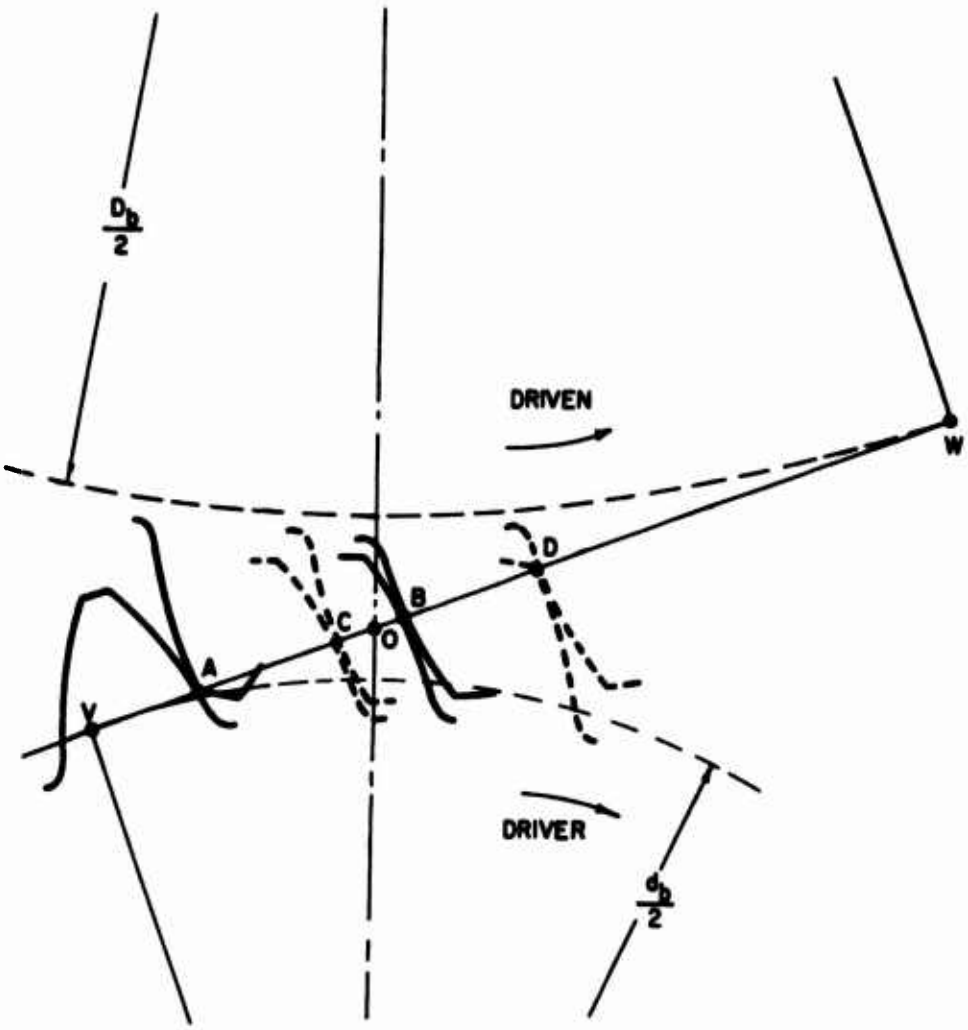

Figure 2. Spur gear contact condition

P_b = base pitch, in.

Contact ratios of properly designed spur gears are normally in the range of 1.3 to 1.7; and the greater the contact ratio, the longer two pairs of teeth share the load during the mesh cycle.

The load distribution between the two pairs of teeth simultaneously in contact between AC and BD is a function of the tooth deflection under load and the tooth profile modification.

Walker[50-52] has shown to an engineering approximation that the normal deflection at an arbitrary point M of a full-depth involute spur gear tooth under a normal load at M is given by the expression

$$\delta_m = \frac{14 w_m}{E} \frac{h}{t} \cos\theta \qquad (10)$$

where δ_m = normal deflection of tooth, in.

w_m = unit normal load on a single tooth at point M, lb/in.

E = Young's modulus, psi

h = height of inscribed parabola, in.

t = width of inscribed parabola, in.

θ = load angle, deg.

The parabola height and width are those associated with the tooth-equivalent beam of uniform bending stress inscribed in the tooth profile[4, 52] and illustrated in Figure 3. The load angle is the angle between the load line and a line normal to the center line of the tooth. It is also shown in Figure 3.

The total deflection between a pair of teeth in contact at M is the sum of the individual deflections of each tooth, or

$$\delta_m = \delta_{mp} + \delta_{mg} \qquad (11)$$

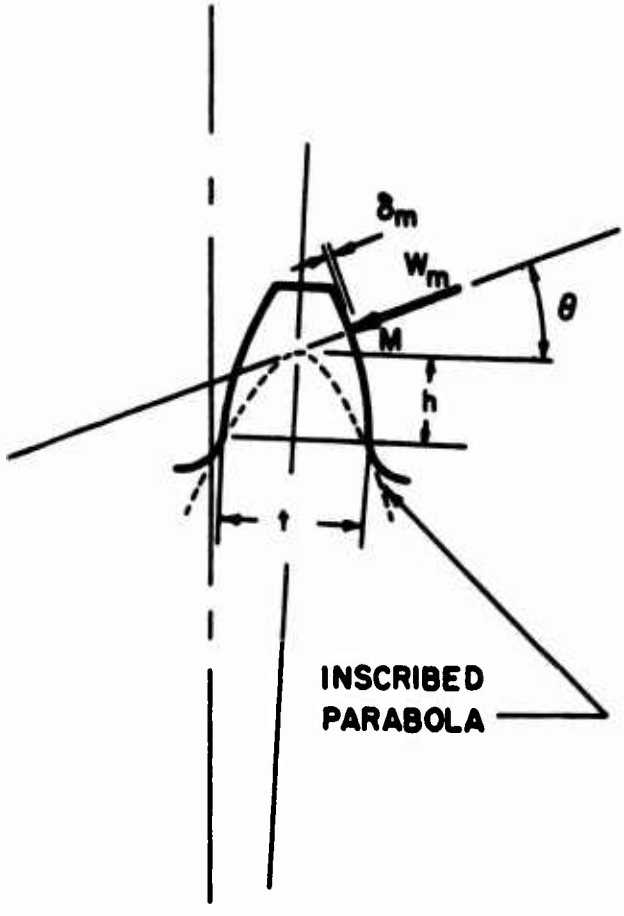

Figure 3. Load on a single tooth

When the gear teeth are loaded, they deflect; and the deflection manifests itself as a relative angular shift between the gears. The result is that the teeth interfere with each other at the point of load engagement. This is illustrated in Figure 4. The interference at point A may be eliminated if the tooth on the driven gear were to have the "overlapping" material at its tip removed. Then the tip of this gear tooth would once again make initial contact with the driver gear tooth at the point A. To ensure smooth engagement of the teeth as the mesh continues, material is removed along the entire tip of the working face of the driven gear tooth from A to C. To avoid a similar interference during the mesh cycle from B to D, the driver gear tooth profile is relieved from B to D. It is seen from Figure 4 that the maximum profile modification to be applied to the tip of the driven gear tooth is equal to the total tooth deflection at point B. Similarly, the maximum profile modification to be applied to the tip of the driver gear tooth is the total tooth deflection at point C. The amount of modification between points A and C, and between points D and B, usually reduces linearly along the profile.*

It should be apparent that if the modification is determined by the deflection of the teeth at some given load, then the modification will not be ideal at other loads. If the load is greater than that for which modification was selected, some interference will occur, but certainly not to the extent had there been no modification at all. If, on the other hand, the load is less than that for which modification was selected, the teeth will be slightly late in engaging and early in disengaging, but no interference will occur. The usual practice is to choose the modification to give a smooth load transfer at the load level most often encountered during operation.

If it is assumed that during contact between two pairs of teeth (double tooth contact), the total deflections at each contact pair are equal, and that the sum of the loads at each pair are equal to the total transmitted load, the individual normal tooth loads may be determined.

For contact between A and C (Fig. 2), the normal load at an arbitrary point i is

$$W_i = W \frac{\delta_j + \Delta_j - \Delta_i}{\delta_i + \delta_j} \qquad (12)$$

* In practice, the calculated modification is applied fully at the first point of contact, but only partially at the last point of contact, in an effort to allow the gear set to run smoother at less than the design load.

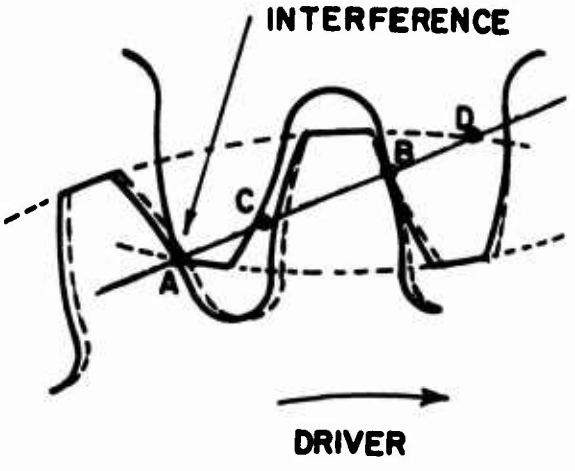

Figure 4. Tooth interference due to bending

where W_i = normal contact load at any arbitrary point i of double tooth contact, lb

W = total normal load, lb

δ_i = total tooth deflection at i, in.

δ_j = total tooth deflection at j, one base pitch from i, in.

Δ_i = modification of driven tooth at i, in.

Δ_j = modification of driver tooth at j, in.

For contact between B and D, at a point j one base pitch along the line of contact AD from point i, the normal load is

$$W_j = W - W_i \tag{13}$$

where W_j = normal contact load at j of double tooth contact, one base pitch from i, lb

For single tooth contact between C and B, the normal load is constant, as for example at an arbitrary point k,

$$W_k = W \tag{14}$$

where W_k = normal contact load at any arbitrary point k of single tooth contact, lb.

Equations (12), (13), and (14), when applied to points along the path of contact, define the load sharing pattern through the mesh cycle of spur gears with a contact ratio between 1 and 2. This fairly laborious calculation can easily be performed by means of a computer program, as is done in the current work (App. H). If such a computer program is not available, an approximate load sharing pattern, such as that used in the AGMA gear scoring design guide,[3] is often used in practice. The AGMA load sharing pattern is fixed, and is independent of the load level. However, in view of its approximate nature, this objection is mainly academic.

Spur gears with contact ratios greater than 2 are fairly rare; but are gaining in popularity for aircraft power gears. The impact of high contact ratio on spur gear performance has been discussed recently by Staph.[49] If the contact ratio is between 2 and 3, then 3 pairs of teeth share the load at the beginning, middle, and end of the mesh cycle; while only 2 pairs of teeth share the load during the remaining portions of the mesh cycle. The computation of the load sharing pattern for such gears can be done in a similar manner,[49] by using the Walker procedure. The AGMA load sharing pattern mentioned above does not apply to this case.

Tooth loads found by the above procedures are static loads, or those for very low-speed operation. Rigorous analysis of load sharing under dynamic conditions is currently not available. Gear-tooth dynamics can thus only be treated in an approximate manner, which will be discussed in the section which follows.

C. Spur Gear Dynamics

In the previous section, equations were given for finding the tooth loads between mating gear teeth for static or very low-speed operation. If the tooth profiles were perfectly designed, if the gears were perfectly manufactured and assembled, if the gears were operated at that unique load level for which the tooth profile modifications were designed, and if no other dynamic stimuli were present in the system, then these equations would also be valid for high-speed operation. Unfortunately, these conditions are never achievable in practice. Because of these deviations from the ideal, the actual tooth loads are higher than those calculated from the static load equations.

Dynamic loads result when, for one reason or another, the gear teeth undergo an angular speed change in the meshing process. For example, in a gear set in which the pinion is the driver, if the gear tooth just ready to engage the pinion tooth is too thick (a manufacturing tolerance problem), contact between the teeth will not occur on the line of action; but somewhere ahead of and off the line. The action will not be conjugate. The teeth will deflect to some small extent under load, lessening the shock of the sudden loading; but the main result will be an acceleration of the gear or a deceleration of the pinion, each in an effort to bring the point of contact, now off the line of contact, back onto the line. This acceleration or deceleration gives rise to an overload, or a dynamic load increment. The static load plus the dynamic increment is the dynamic load.

Although the previous example illustrates the dynamic load as being produced by the velocity change occurring at the first point of contact, in fact no such limitation exists. At any time during the nominal engagement of a pair of teeth whose profiles are such that contact moves off the theoretical line of action, a velocity change will occur to the pinion and the gear, producing a dynamic load. Generally speaking, however, the velocity change at the initial point of contact is the greatest and hence produces the largest dynamic loading in the cycle.

All gear pairs experience dynamic loads to some degree since gear perfection is not a reality. For high-precision gears operating at moderate speeds and loads, the dynamic loads are not very high and they do not cause serious problems.[4-6] On the other hand, highly-loaded gears and very high-speed gears, even lightly-loaded, may experience dynamic loads sufficiently high to cause concern. This is particularly true where a gear pair is designed for the ultimate in power-to-weight ratio such as aircraft gearing.

Of particular concern are gear systems which operate at speeds near the natural frequency of the gear mass/tooth spring system. At resonance the dynamic increment can equal the load due to the input power.[53-55] Some evidence exists which shows even higher dynamic increments if the damping in the system is less than about 7 percent of critical.[53-55] Fortunately, most combinations of material, lubricant, and gear blank design will provide this value of damping.

Dynamic loads may result from manufacturing tolerances in the pitch, pressure angle, tooth thickness, tooth profile, and lead, or from misalignment or tooth deflection, or anything which causes the gears to deviate dimensionally or operationally from perfection. Likewise, dynamic loads may arise from the operation of modified profile gears at loads other than that for which the modification was based, since the effect is the same as tooth mesh errors due to manufacturing tolerances.

From a practical standpoint, dynamic loads may be related to tooth deflection, δ, pitch error, e, and profile modification, Δ. Table 2 shows the relationships involved for several combinations of pitch error, deflection, and profile modification. The pitch error is the sum of the allowable pitch tolerances of each gear. Pitch tolerances are found in the AGMA Gear Handbook[56] for the class of gear under consideration. The total tooth deflection δ is the deflection at the point B (Fig. 2), since it is this deflection that affects the mesh at A.

TABLE 2. EFFECTIVE TOOTH ERRORS

Case	Pitch error, e	Total tooth deflection, δ	Effective pitch error, e_f	Profile modification, Δ	Effective error, e_e
a	0	0	0	0	0
b	e	0	e	0	e
c	e	δ	$e + \delta$	0	$e+\delta$
d	e	δ	$e + \delta$	$-\delta$	e
e	e	δ	$e + \delta$	$-\Delta$	$e+\delta-\Delta$

The effective pitch error, e_f, is the algebraic sum of e and δ.

The profile modification Δ is the sum of the tip modification of the driven gear and the root modification (if any) of the mating driving gear. Normally, profile modification tolerances are positive (i.e., removal of material), reducing the effective error and are thus not considered. Note in Table 2 for case d, the modification is equal to the total tooth deflection, thus negating the effect of the deflection at engagement.

The effective error, that error which the teeth "see" as they engage, is the algebraic sum of e_f and Δ. It is this error, regardless of its source or makeup, that will cause the dynamic load.

Gear-tooth dynamics has been a subject of considerable study from both theoretical and experimental standpoints; and the complexity of the problem is well illustrated by some of the references cited herein.[53-55, 57-65] Among the works that are fairly typical of the state of the art, the Seireg and Houser method[61, 62] represents a combined theoretical and experimental approach but is rather difficult to apply, while the Tuplin method[63] is based on a simple theoretical approach but is easier to use in practice.

It should be emphasized that the subject of gear-tooth dynamics is exceedingly complex. It involves by necessity not only the dynamic behavior of the gear teeth themselves, but also of the other components in the system which participate in governing the dynamic behavior of the gear teeth. The displacement, elastic, damping, and inertia characteristics of all these participating components are difficult to define and account for; and how well the currently available approaches actually work out in practice remains intriguing. In view of this situation, only the relatively simple Tuplin's method[63] will be discussed herein and employed in the computer program in this report (App. H). In addition to the Tuplin method, the empirical and even simpler AGMA approach[4-6] will also be mentioned.

A convenient way to account for the dynamic effect is to introduce a dynamic factor, K_v, defined as

$$K_v = \frac{\text{static load}}{\text{dynamic load}}$$

$$= \frac{\text{static load}}{\text{static load + dynamic increment}} \qquad (15)$$

The static load is computed by the procedure outlined in the preceding section. The dynamic load is then the static load divided by the dynamic factor.

Tuplin's Method. In order to apply the Tuplin method,[63] it is necessary to calculate the period of the natural frequency of the gear mass/tooth spring system. It may be calculated by any convenient method, as for example, the Holzer method, or by the following approximation:

$$T_n = 2\pi \sqrt{\frac{m_e}{k_\ell}} \tag{16}$$

where T_n = period of natural frequency of gear mass/tooth spring system, sec

m_e = equivalent mass of pinion and gear, lb-sec^2/in.

k_ℓ = spring rate of a pair of mating spur gear teeth, lb/in.

The spring rate of a pair of mating teeth is approximately constant through the mesh; thus a fair approximation to the spring rate may be found by considering a cantilever beam loaded with a uniform load across the tip. This gives

$$k_\ell = \frac{F E p^3}{32 (D_o - D)^3} \tag{17}$$

where F = face width, in.

E = Young's modulus, psi

p = circular pitch, in.

D_o = gear outside diameter, in.

D = gear pitch diameter, in.

If the gear drives, the equivalent pinion diameters should be used for D_o and D.

The time for the tooth error to be applied is assumed to be the time for the gears to turn through one circular pitch, or

$$t_e = \frac{p}{V_t} \tag{18}$$

where t_e = time for tooth error to be applied, sec

V_t = pitchline velocity, ips.

The ratio t_e/T_n is used in Figure 5 to determine the value of e_a/e_e. With e_e obtained from Table 2, the apparent tooth error, e_a, is calculated; and the dynamic increment is then

$$F_i = k_l e_a \tag{19}$$

where F_i = dynamic increment, lb

e_a = apparent error, in. (from Fig. 5)

The dynamic factor, K_v, may then be calculated from Equation (15).

If the gear train operates at speeds near the resonant frequency of the gear mass/tooth spring system, it may be shown that the critical value of t_e/T_n is given by the reciprocal of the number of pinion teeth.[63] Assuming a minimum number of pinion teeth as being 12, the critical value of t_e/T_n is 0.083, and $e_a/e_e = 0.96$ from Figure 5. From Equation (19),

$$F_i = k_l \left(\frac{e_a}{e_e}\right) e_e = 0.96\, k_l e_e \sim k_l e_e$$

In other words, the dynamic increment is nearly equal to the static load, or K_v is nearly 0.5, a result suggested earlier.

AGMA Method. The AGMA method[4] is extremely simple to apply in practice; but its use requires much experience and judgment.

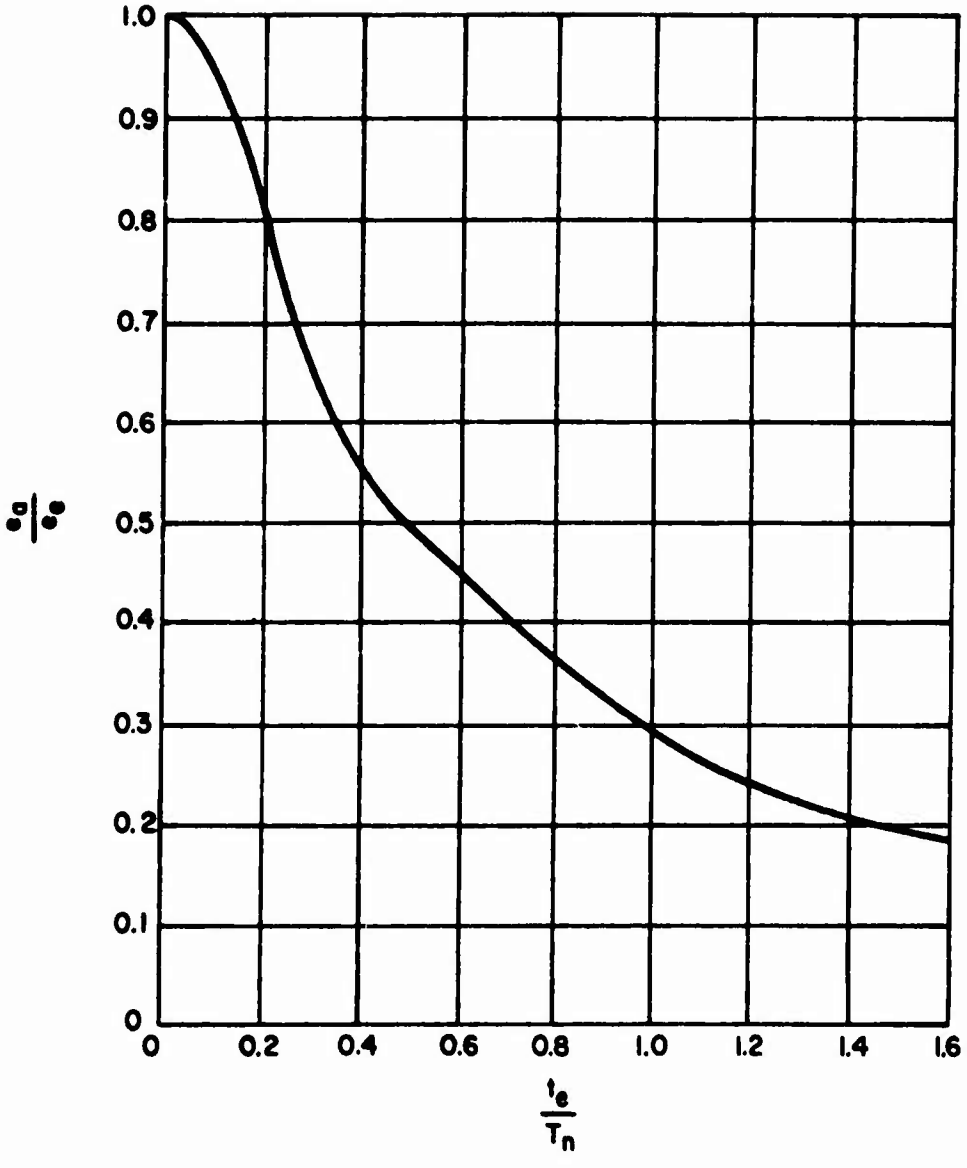

Figure 5. e_a/e_e vs. t_e/T_n for Tuplin's method

This method states that the dynamic factor, K_v, depends on: "(a) effect of tooth spacing and profile errors, (b) effect of pitchline and rotational speeds, (c) inertia and stiffness of all rotating elements, (d) transmitted load per inch of face, and (e) tooth stiffness." It then furnishes three simple equations for the dynamic factor, herein designated as K_{v1}, K_{v2}, and K_{v3} for convenience, for the following three situations:

For "high-precision" gears when the effect of the items listed above are such that "no appreciable dynamic load is developed,"

$$K_{v1} = 1 \tag{20}$$

For "high-precision" gears when the items listed above "can develop a dynamic load,"

$$K_{v2} = \sqrt{\frac{78}{78 + \sqrt{V_t}}} \tag{21}$$

For less precise gears,

$$K_{v3} = \frac{50}{50 + \sqrt{V_t}} \tag{22}$$

In Equations (21) and (22), V_t is the pitchline velocity, fpm.

The AGMA equations can of course be faulted for their lack of sophistication. However, in view of the complexity of the total gear-tooth dynamics problem and the difficulty of handling the problem in a rigorous but realistic manner, they do provide some easy and practical means of accounting for the dynamic effect if caution is exercised.

Further discussion of the dynamic factor as applied to practical prediction of the scoring-limited performance of gears will be deferred until Chapter VII.

CHAPTER IV
HELICAL GEAR MECHANICS

A. Helical Gear Kinematics

If a spur gear were sliced transversely into a number of thin plates, and each plate were displaced through a small positive angle with respect to the preceding one, the result would be a stepped gear. To carry the process further, the plates could become infinitesimal in thickness and infinite in number, then the result would be a helical gear. Consequently, the tooth profiles in any transverse plane of a helical gear are identical, but are shifted through an angle proportional to the axial displacement. The intersection of the tooth surface with the pitch cylinder is a helix.

The contact in a pair of uncrowned helical gears on parallel axes is approximately a rectangle. In actual practice, the contact may not be like this if misalignment is present, but may be more nearly a distorted ellipse.

Two helical gears viewed in the transverse plane (normal to the axes of rotation) are shown in Figure 6. The plane of action is projected above the gears. The slant lines in the plane of action are the lines of contact of the contacting tooth pairs. There are, in this case, two pairs of teeth simultaneously in contact, spaced one normal base pitch apart. Contact between a pair of teeth starts at point A and sweeps across the plane of action to end at point D'.

The geometry at an arbitrary point H on a line of contact may be found by determining the point's projection H' in the transverse plane. Then methods of analysis similar to those for spur gears may be used to determine tooth geometry at H'. The base helix angle, ψ_b, may be taken into account to translate the results back into the normal plane.

The projected radii of curvature at H' in the transverse plane are

$$\rho_p = VH'$$

$$\rho_g = WH'$$

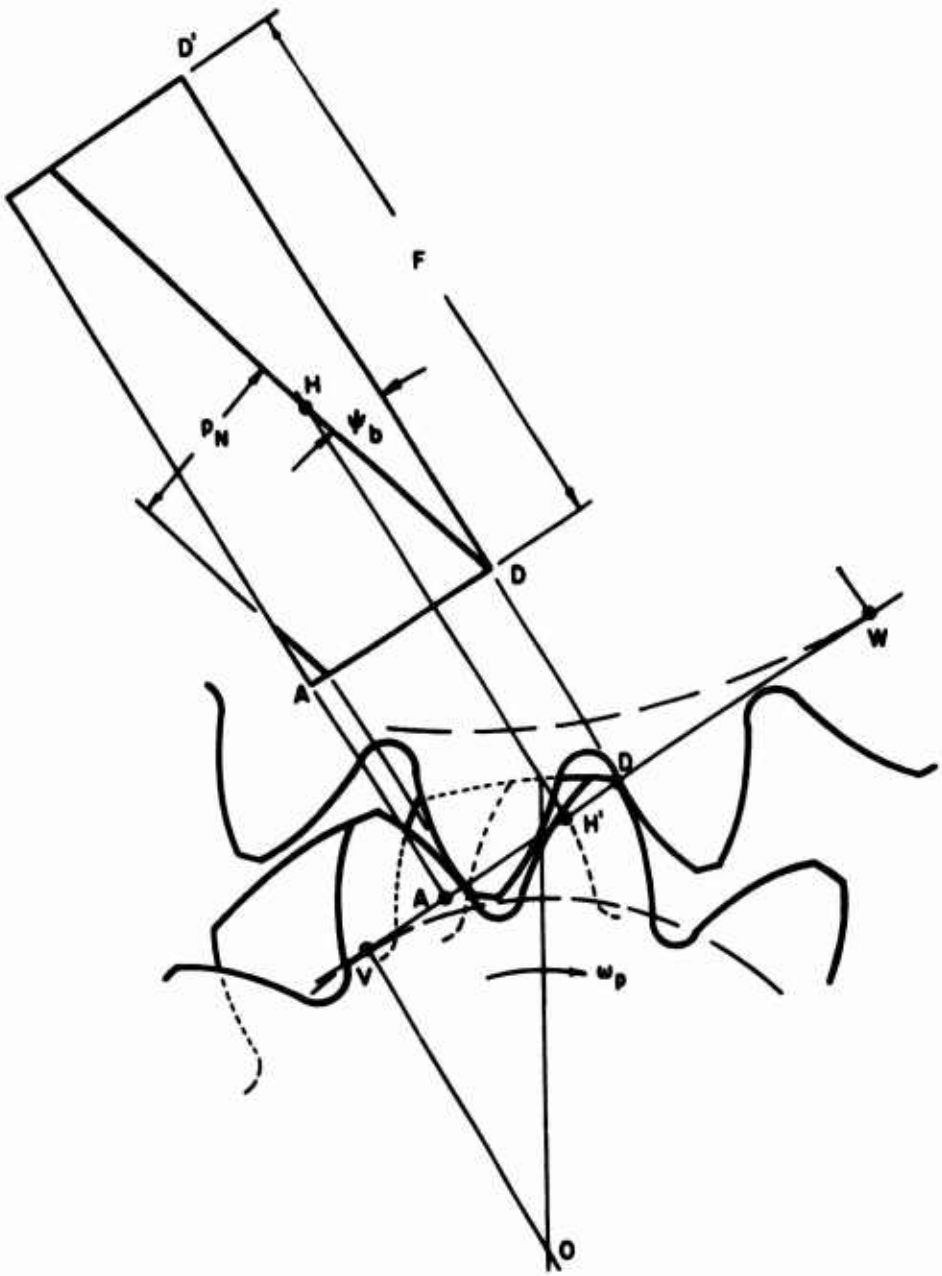

Figure 6. Helical gear geometry and kinematics

These radii may be translated back to the point H in the normal plane by taking into account the base helix angle, ψ_b, thus

$$\rho_{pn} = VH' \sec \psi_b$$

$$\rho_{gn} = WH' \sec \psi_b$$

Using these radii in the normal plane, the instantaneous sliding and sum velocities at the point H are

$$V_s = (\rho_{pn}\omega_p - \rho_{gn}\omega_g) \cos \psi_b \qquad (23)$$

$$V_t = (\rho_{pn}\omega_p + \rho_{gn}\omega_g) \cos \psi_b \qquad (24)$$

where ρ_{pn} = radius of curvature of pinion in normal plane, in.

ρ_{gn} = radius of curvature of gear in normal plane, in.

ω_p = angular velocity of pinion, rad/sec

ω_g = angular velocity of gear, rad/sec

ψ_b = base helical angle, deg.

B. Helical Gear Statics

As illustrated in Figure 6, two pairs of teeth are simultaneously in contact at the instant shown. This set of gears will always have two pair of teeth in contact at any one time, since as the leading line of contact nears point D', a new line enters at point A. Properly designed helical gears will always have at least two and often more pairs of teeth in contact at any one time. Because several pairs of teeth are in contact at one time, helical gears operate more quietly than spur gears, and with less shock at tooth engagement.

Like spur gears, a measure of the load sharing between pairs of teeth simultaneously in contact is the contact ratio. However, since contact in the plane of action of helical gears is in two dimensions, there are two contact ratios. The face contact ratio is that due to the

helical nature of the tooth elements that cause overlap between pairs of teeth. In terms of gear parameters, it is

$$m_f = \frac{F \tan \psi}{p} \tag{25}$$

where m_f = face contact ratio

F = face width, in.

ψ = helix angle, deg.

p = transverse circular pitch, in.

The transverse contact ratio is that due to load sharing in the transverse plane and is identical in nature to the contact ratio in spur gears, or

$$m_c = \frac{AD}{p_b} \tag{26}$$

where p_b is the transverse base pitch, in.

The total contact ratio is the sum of the face and transverse contact ratios, or

$$m_t = m_c + m_f \tag{27}$$

Because the load extends from the tip, diagonally across the gear face, to the root of a tooth, the tooth deflection is a complex function of tooth form and helix angle. No rational method is available for determining the tooth deflection. However, the flexibility of the tooth loaded near the tip, and the rigidity of the same tooth simultaneously loaded near the root, together with the several teeth in contact at one time, tend to distribute the load more evenly over the instantaneous lines of contact for uncrowned helical gears. This approximation is implied in the AGMA standard for rating the strength of helical and herringbone gear teeth[5] in the calculation of the load sharing ratio

$$m_N = \frac{F}{L} \tag{28}$$

where m_N = load sharing ratio

L = total length of lines of contact for all tooth pairs simultaneously in contact, in.

This equation implies that the fraction of the total normal load carried at any instant by any tooth is proportional to the ratio of the length of the instantaneous line of contact on that tooth to the total length of all instantaneous lines of contact on all teeth.

Figure 7 is a view of the plane of action of a pair of helical gears. Three pairs of teeth are in simultaneous contact in this illustration. The position of a line of contact from the time it starts at point A until it exits at point D' is determined by the parameter f, measured normally to the lines of contact. There may be, as shown in Figure 7, lines of contact ahead of and behind this line at a distance of p_N, the normal base pitch, apart.

The line of contact at distance f may be divided into a number of equal divisions and each such division may be treated for purposes of analysis as an elemental spur gear tooth having a width in the normal plane equal to the length of the division. The load is assumed constant over the length of the division, so that

$$W_i = W\ell / L \qquad (29)$$

where W_i = normal load on the elemental gear, lb

W = total normal load, lb

ℓ = length of a division, in.

The instantaneous sliding and sum velocities in the normal plane at the point of contact in the middle of the division, as for example at point M, are used as being representative of the conditions on the elemental gear.

C. Helical Gear Dynamics

Dynamic loads in helical gears arise from the same causes as they do in spur gears; namely, manufacturing tolerances, tooth

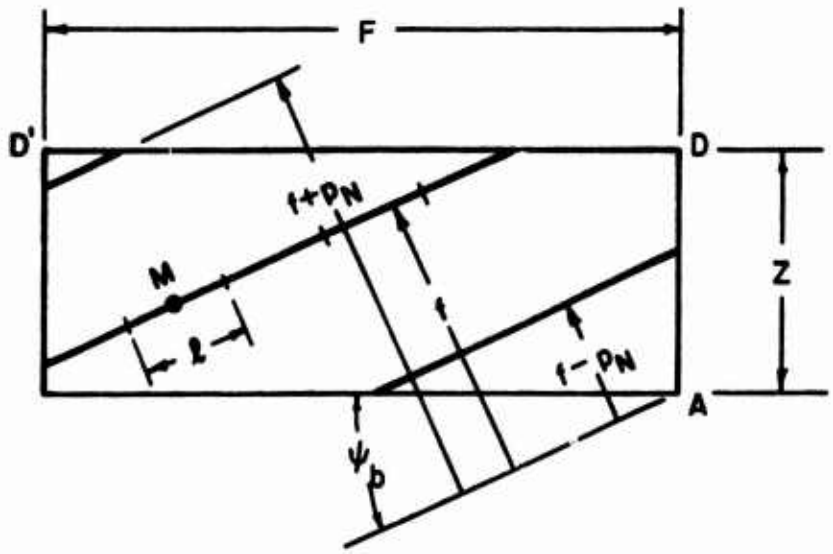

Figure 7. Helical gear contact condition

deflections, system dynamics, or anything that results in a change in the angular speeds of the teeth in action. However, since the load on helical gear teeth is applied diagonally across the tooth face, and because at least two and usually more teeth are simultaneously in contact, the tooth deflections are not as severe as they are in spur gears. Consequently, dynamic loads are, on the whole, somewhat less for helical gears than they are for spur gears. With only minor changes, the methods for determining the dynamic factors described previously for spur gears may be applied to helical gears.

Tuplin's Method. The dynamic factor for helical gears may be computed by the same equations presented in the preceding section for spur gears, with one exception. This exception relates to the tooth spring rate, k_l. Equation (17) previously given applies to spur gears. For helical gears, the approximate equation is

$$k_l = \frac{\pi E (p \cos \psi)^3}{96 (D_o - D)^2} \qquad (30)$$

where k_l = tooth spring rate for helical gears, lb/in.

E = Young's modulus, psi

p = transverse circular pitch, in.

ψ = helix angle, deg

D_o = gear outside diameter, in.

D = gear pitch diameter, in.

Note that the quantity p in Equation (18) should be the transverse circular pitch, since it and not the normal circular pitch governs the distance moved by points on the pitchline of the rotating gear.

AGMA Method. The AGMA method for estimating the dynamic factor of helical gears is also basically identical to that for spur gears. For helical gears, the AGMA procedure specifies two dynamic factors, K_{v1} and K_{v2}, exactly as in Equations (20) and (21), respectively. The third dynamic factor, K_{v3}, is not used for helical gears.

CHAPTER V
SPIRAL BEVEL GEAR MECHANICS

A. Spiral Bevel Gear Kinematics

Spiral bevel gears are related to straight bevel gears in much the same manner as helical gears are related to spur gears. That is to say, the element of a spiral bevel gear tooth forms a spiral helix about the pitch cone, whereas the element of a helical gear tooth forms a cylindrical helix about the pitch cylinder. Many of the advantages and disadvantages of helical gears, such as multiple tooth contact and thrust loading, are present in spiral bevel gears.

The bases of spiral bevel gears are pitch cones which intersect at a common point. The axial plane contains the gear axes. Figure 8, looking normal to the axial plane, shows some of the parts of a pair of spiral bevel gears. The pitch plane is seen as the line PO, and the pitch point is point P.

Figure 9 looks at the pitch cone normal to the pitch plane. Elements of a tooth make an angle ψ with the cone element midway of the face width. This is the spiral angle, and it is equivalent to the helix angle in helical gears with the exception that, due to the taper of the pitch cone, the value of the spiral angle is not constant but depends upon where along the cone element it is measured.

A section of the tooth on the normal plane is also shown in Figure 9. The pressure angle, ϕ_n, is specified in this plane. The most common spiral angle is 35°; the usual pressure angle is 20°. The tangent plane is also shown in Figure 9.

Since the plane of action shows the contact on all teeth in action simultaneously, it is more convenient to use the plane of action for study than to use the tooth surface. Accordingly, Figure 10 shows the plane of action bounded by the pairs of curved and tapering lines. To simplify the analysis, the plane of action is assumed to be rectangular with width F and length Z as shown in Figure 10.

The three diagonal lines in the plane of action represent the contact between three pairs of teeth which at the instant are sharing the load. These lines are actually the major axes of contact ellipses. The ellipse passing through the ends of the instantaneous lines of contact represents the limits of contact. If it were not for mismatch of

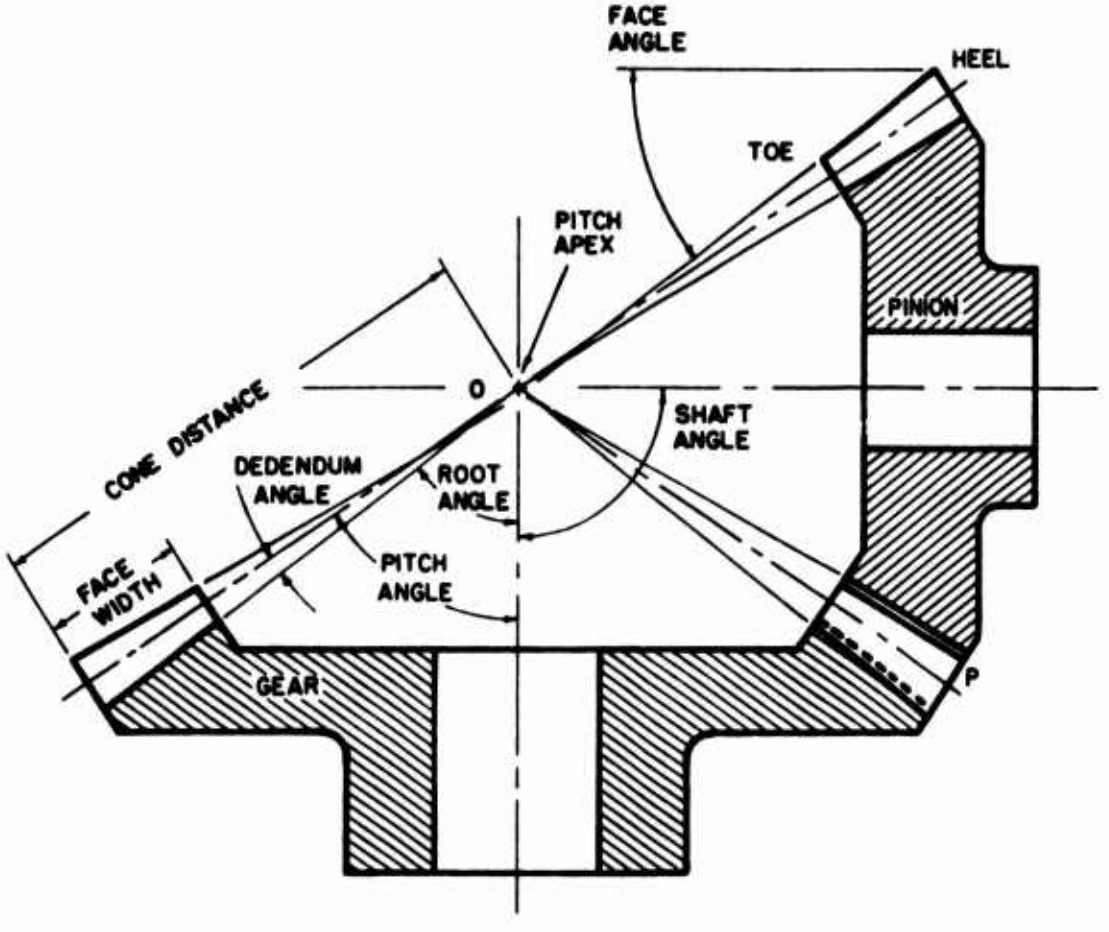

Figure 8. Spiral bevel gear geometry

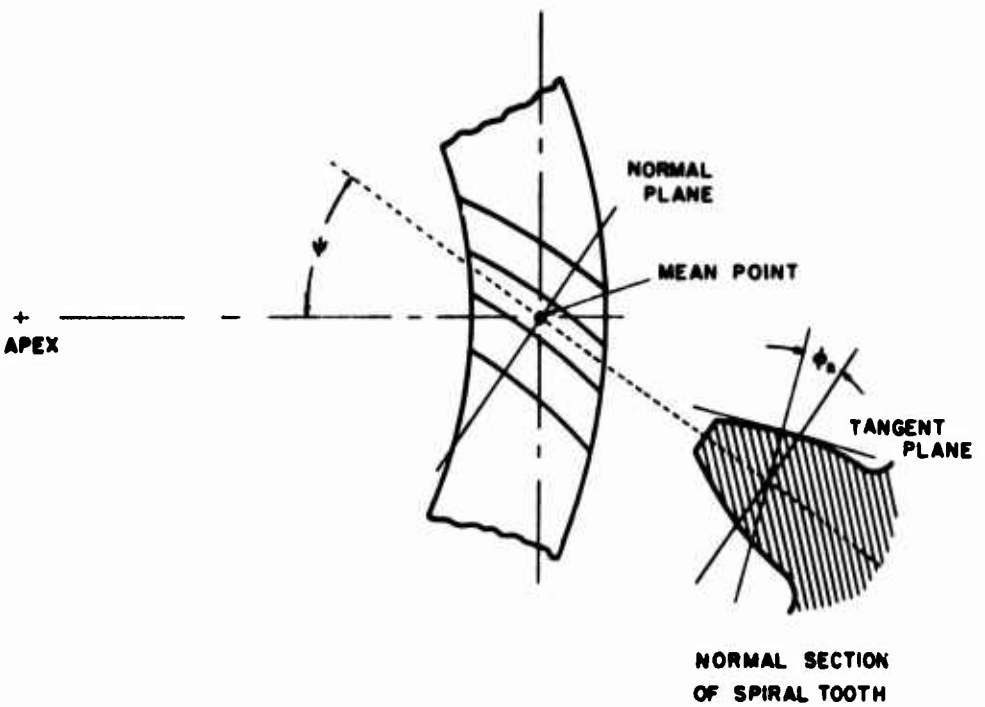

Figure 9. View normal to pitch plane

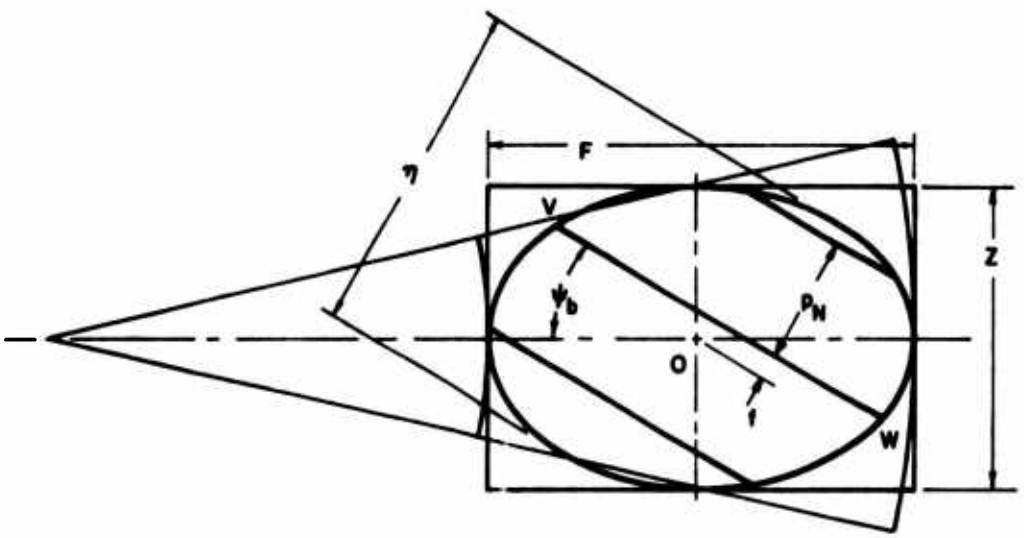

Figure 10. Spiral bevel gear contact condition

the teeth (to be discussed more fully later), the lines of contact would extend theoretically to the edges of the rectangle. Because the plane of action is tangent to the base cone, the lines of contact are inclined to the cone element by the angle ψ_b, instead of ψ as in Figure 9.

Because contact in the plane of action of spiral bevel gear teeth is in two dimensions, there are, as in helical gears, two contact ratios. These ratios are calculated from Equations (25) and (26) for helical gears, but they are combined differently to give a modified contact ratio as

$$m_o = \sqrt{m_f^2 + m_c^2} \tag{31}$$

where m_o = modified contact ratio

m_f = face contact ratio

m_c = transverse contact ratio

Sliding and sum velocities between tooth contact points midway of the line of contact VW are found by determining the components of the absolute velocities of the contact points on the pinion and gear in the tangent plane.

It may be shown[66] that the component of the velocity of the point of contact of the pinion tooth in the direction along the tooth element is

$$V_{Fp} = V_n\left[\tan\psi + |Z_o| \sin\phi_n \frac{\tan\psi}{A \tan\gamma} - |Z_o| \cos\phi_n \frac{1}{A \cos\psi}\right] \tag{32}$$

where V_{Fp} = component of velocity in the tangent plane of contact point on pinion along tooth element, ips

V_n = normal component of pitch point velocity in the pitch plane, ips

ψ = mean spiral angle (i.e., spiral angle at mean point, Fig. 9), deg.

Z_o = distance in the plane of action from center of contact to projection of contact point in mean normal section, in.

ϕ_n = pressure angle in normal plane, deg.

A = mean cone distance, in.

γ = pinion pitch angle, deg.

The component of the velocity of the point of contact of the pinion tooth in the profile direction is

$$V_{Pp} = V_n \left[\sin \phi_n + Z_o \frac{1}{A \tan \gamma} \right] \quad (33)$$

where V_{Pp} = component of velocity in the tangent plane of contact point on pinion in the profile direction, ips

Similar equations may be written for the corresponding contact point on the gear, in the tangent plane, as

$$V_{Fg} = V_n \left[\tan \psi - |Z_o| \sin \phi_n \frac{\tan \psi}{A \tan \Gamma} - |Z_o| \cos \phi_n \frac{1}{A \cos \Gamma} \right] \quad (34)$$

$$V_{Pg} = V_n \left[\sin \phi_n - Z_o \frac{1}{A \tan \Gamma} \right] \quad (35)$$

where V_{Fg} = component of velocity in tangent plane of contact point on gear along tooth element, ips

Γ = gear pitch angle, deg.

V_{Pg} = component of velocity in tangent plane of contact point on gear in the profile direction, ips

The difference and the sum of the components of the velocities in the two directions give the sliding and sum velocity components in

the direction along a tooth element and in the profile direction. Since these directions are orthogonal, these resulting components may be combined to give the sliding and sum velocities as

$$V_s = \sqrt{(V_{Fp} - V_{Fg})^2 + (V_{Pp} - V_{Pg})^2} \qquad (36)$$

$$V_t = \sqrt{(V_{Fp} + V_{Fg})^2 + (V_{Pp} + V_{Pg})^2} \qquad (37)$$

In order to apply Blok's conjunction temperature rise equation, it is necessary to determine the time for a contact point on each of a pair of sliding surfaces to cross the heat zone, the area of contact between the two surfaces. This requires a knowledge of the distance across the contact area. In spur and helical gears, this distance is the same for the point of contact of the pinion and gear. Because the axes of spiral bevel gears are not parallel, the corresponding contact points on the pinion and on the gear move across the area of contact in different directions.

Figure 11 shows a typical instantaneous contact area in the tangent plane of a pair of spiral bevel gears. V_p and V_g are the vector sums of the velocity components V_{Fp} and V_{Pp} for the pinion, and V_{Fg} V_{Pg} for the gear, respectively. The distance that the contact point on the pinion travels as it sweeps across the contact area is d_p, in the direction of V_p. Similarly, the distance that the contact point on the gear travels as it sweeps across the contact area is d_g, in the direction of V_g. These distances are

$$d_p = 2\sqrt{\frac{a^2b^2}{a^2\sin^2(\alpha_p + \omega) + b^2\cos^2(\alpha_p + \omega)}} \qquad (38)$$

$$d_g = 2\sqrt{\frac{a^2b^2}{a^2\sin^2(\alpha_g + \omega) + b^2\cos^2(\alpha_g + \omega)}} \qquad (39)$$

where d_p = instantaneous sliding distance of the pinion across the contact area, in.

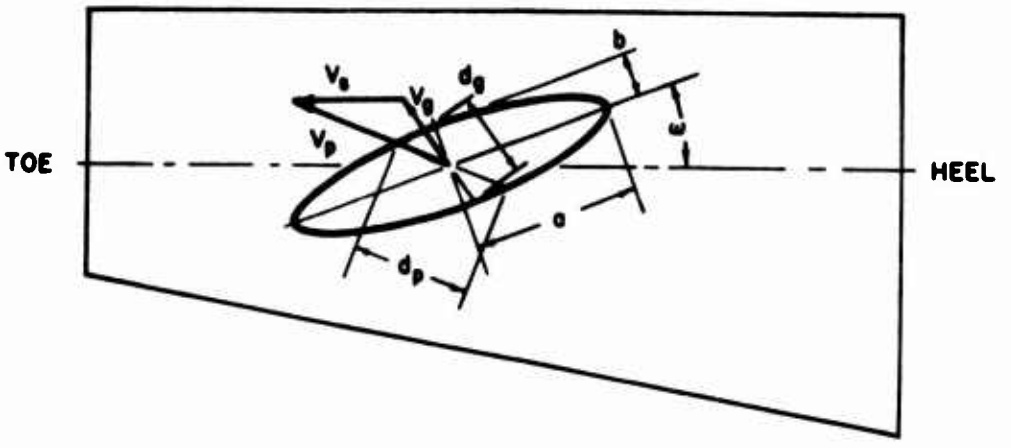

Figure 11. Spiral bevel gear kinematics

d_g = instantaneous sliding distance of the gear across the contact area, in.

a = major semiwidth of the contact ellipse, in.

b = minor semiwidth of the contact ellipse, in.

α_p = angle the resultant pinion velocity vector makes with pitchline, deg.

α_g = angle the resultant gear velocity vector makes with the pitchline, deg.

ω = angle of inclination of the line of contact with the pitchline, deg.

B. Spiral Bevel Gear Statics

In this section, an equation for the tooth contact stress will be developed. The method follows that of Reference 66 to which the reader is referred for more details. Other helpful references are References 67 and 68.

Theoretically, spiral bevel gear teeth should operate with conjugate motion. Contact would be along a line extending diagonally across the tooth surface, and moving generally from the heel to the toe (or reverse). However, because of their sensitivity to the effect of manufacturing and assembly tolerances, and deflection under loading, spiral bevel gear teeth do not operate with conjugate motion. Instead, contact shifts to the edge and load concentrations occur. To counteract this shifting of load, the tooth profiles are modified to produce "mismatch." This mismatch causes the point of contact to move back onto the tooth face and, although the mating surfaces are no longer conjugate, the resulting action is smoother and far better than that produced by the theoretical conjugate motion. The contact, with mismatch, is theoretically a point, but local yielding of the surface results in an elliptical contact zone (Fig. 11). Reference 69 gives an excellent review of mismatch techniques used in industry.

Since the mating surfaces of spiral bevel gear teeth are no longer conjugate, the classical Hertz contact stresses between cylinders do not apply. Reference 66 uses a combination of experimental results and approximations to the Hertz theory to obtain the tooth contact stress.

Referring to Figure 10, the variable f measures the displacement of the line of contact VW from the center of the surface of action. In the load analysis to be presented the line of contact VW is swept across the surface of action by varying f until the point is reached where the load on VW is a maximum.

From Reference 67, the load sharing ratio, the ratio of the load carried on the line VW to the total load is

$$m_N = \frac{\eta_1^3}{\eta_1^3 + A + B} \tag{40}$$

where m_N = load sharing ratio

η_1 = a function of variable dimension f

and

$$A = \sum_{k=1}^{n} \sqrt{\left[\eta_1^2 - 4kp_N(kp_N + 2f)\right]^3} \tag{41}$$

$$B = \sum_{k=1}^{n} \sqrt{\left[\eta_1^2 - 4kp_N(kp_N - 2f)\right]^3} \tag{42}$$

and p_N = mean normal base pitch, in.

f = a variable dimension locating the line of contact VW with respect to the center of the surface of action, in.

k = a positive integer which takes on successive values from 1 to n, generating all real terms in the series

The dimension f in Figure 10 is varied from $-\eta/2$ to $+\eta/2$ until maximum m_N is obtained. It is at this point that the scoring potential will be the greatest.

The length of the contact line VW is given by[67]

$$S_G = \frac{FZ\eta_1}{\eta^2} \tag{43}$$

where S_G = length of the contact line VW, in.

F = face width, in.

Z = mean length of path of contact in transverse plane, in.

η = length of contact normal to lines of contact, in.

The normal load on the line of contact VW is

$$W_j = W m_N \tag{44}$$

where W_j = normal load on line of contact VW, lb

W = total normal load, lb

consequently,

$$W_j = \frac{W_t m_N}{\cos \phi \cos \psi} \tag{45}$$

where W_t = tangential load at pitch point, lb

ϕ = pressure angle, deg.

ψ = mean spiral angle, deg.

C. Spiral Bevel Gear Dynamics

The actual tooth load or dynamic load is greater than the static load for exactly the same reasons as for spur and helical gears. The dynamic load is caused by manufacturing inaccuracies, tooth deflections, and system dynamics.

The Tuplin method for determining the dynamic factor for spur and helical gears is not applicable to spiral bevel gears. The dynamic load is, instead, evaluated by the use of factors relating to the type of dynamic load-producing function.[66]

The dynamic load on spiral bevel gears is obtained from

$$W_d = W \frac{K_i}{K_v} \tag{46}$$

where W_d = dynamic load, lb

K_i = inertia factor

K_v = dynamic factor

The inertia factor is related to the modified contact ratio, m_o. Because there are normally several pairs of teeth in contact simultaneously, load transfer is smooth and the inertia factor is customarily taken as unity.[66-68] However, if m_o is less than 2, load transfer is no longer smooth, the rotating velocities are variable, and gear inertia becomes a factor in the dynamic load. For a modified contact ratio of less than 2, the inertia factor is taken as $K_i = 2/m_o$.

The dynamic factor[6] is defined by the same AGMA formulas for K_{v1} and K_{v2}, i.e., Equations (20) and (21), respectively. As in the case of helical gears, the factor K_{v3} is not used for spiral bevel gears.

CHAPTER VI
BASIC SCORING PREDICTIVE DATA

A. Disk Test Program

As mentioned in Chapter I, the prediction of the scoring-limited performance of gears at the design stage is a far more difficult task than the mere avoidance of gear scoring by design without regard to the performance penalty to be paid. In order to make such a prediction, it is necessary to devise a suitable predictive scheme and to develop certain quantitative data that are required in the predictive process.

The formulation of the predictive scheme can be approached essentially in three ways. One way is to lay out a scheme that is as completely rational as possible, regardless of how complex it is. However, for reasons enumerated in Chapters II through V, the current state of the art does not permit this level of sophistication without a great deal of further work on the basic mechanism of scoring, the thermal behavior involved, as well as the influence of gear mechanics. The second way is to approach the problem in a primarily empirical manner, such as the current AGMA gear scoring design guide,[3] which involves assumptions that are basically arbitrary. The third alternative is to devise an interim scheme which recognizes the importance of the above-mentioned basic problems, but accepts approximations without waiting for definitive answers to these basic problems. One of the requirements of this program is that the predictive scheme to be developed should be simple enough for the practical engineers to use without having to resort to elaborate computer programs; but yet represent a tangible advance beyond the current state of the art. The third alternative is believed to satisfy this requirement best, and is therefore the one adopted herein.

The proposed predictive procedure entails two basic steps. The first step is to estimate the ideal scoring-limited power-transmitting capacity for a gear set assuming no tooth misalignment and dynamic load. The second step is to apply corrections for the misalignment and dynamic effects, thus enabling an estimate to be made of the actual scoring-limited power-transmitting capacity when misalignment and dynamic load are inevitably present. This chapter of the report will be concerned with the development of the basic data for predicting the ideal scoring-limited power-transmitting capacity. The prediction of the actual scoring-limited power-transmitting capacity will be taken up in the next chapter.

The data to be presented in this chapter were generated from controlled sliding-rolling disk tests. The bulk of the basic information was deduced from 187 disk tests performed under this program, using a modified Caterpillar disk tester herein designated as SwRI disk tester A for convenience, carburized AISI 9310 steel test disks of 10 different surface characteristics, a MIL-L-7808G synthetic oil (Oil F) and a MIL-L-23699 synthetic oil (Oil E), under a variety of test conditions.

The 10 disk types of different surface characteristics are herein referred to, for the sake of brevity, as follows:

Type 1 — Soft circumferentially-ground, plain
Type 1A — Soft circumferentially-ground, oxided

Type 3 — Rough circumferentially-ground, plain
Type 3A — Rough circumferentially-ground, oxided

Type 5 — Honed, plain
Type 5A — Honed, oxided

Type 7 — Rough cross-ground, plain
Type 7A — Rough cross-ground, oxided

Type 9 — Smooth circumferentially-ground, plain
Type 9A — Smooth circumferentially-ground, oxided

The "plain" disks are those which were not surface-treated after the grinding or honing process. The "oxided" disks were treated with a black oxide by a proprietary process after grinding or honing (App. D). The average surface characteristics of each type of test disk pairs are given in Table D-1. The properties of the test steel and test oils are given in Appendixes A and B.

Some of the test results from the above disk test program, as well as some other results obtained from SwRI disk tester A have been reported earlier in the literature.[25, 28] For the purpose of this report, supplementary information was also extracted from tests performed on an AFAPL disk tester[26, 32] herein designated as SwRI disk tester B for convenience; published results from a Thornton disk tester;[24, 29] as well as other unpublished results of disk tests conducted in the authors' laboratory.

A brief description of SwRI disk tester A, test conditions and

procedure, and a summary of the test results from this program are presented in Appendix D. These results, together with the results from other sources as mentioned above, will be examined at some length in the subsequent sections of this chapter. However, some cursory remarks of a general character appear pertinent at this juncture.

Of the 187 tests reported in Appendix D, 133 tests were performed with Oil F (MIL-L-7808G) and 54 tests with Oil E (MIL-L-23699). Viewed in another way, 98 tests were performed with the plain disks, while 89 tests were performed with the oxided disks. It is of interest to inquire how the test oil and the surface treatment influence the scoring-limited performance under otherwise comparable conditions.

In attempting to answer the above question, it should be recognized that scoring is a highly scattered phenomenon, and the scoring loads observed in even the best controlled, replicate disk tests may vary in the range of 3 to 1 or more under ostensibly identical test conditions.[20-32] Consequently, in order to answer the above question with real confidence, a large number of replicate tests must be performed for each disk-oil combination and each set of test conditions; and the results must be analyzed statistically. The performance of a large number of replicate tests was not feasible in a program of limited size when so many variables must be varied. It was therefore necessary to conduct the disk tests based partially on prior experience as to the relative importance of the many variables involved, and partially on the major emphasis of the overall program. The number of tests conducted for each disk-oil combination, covering all sets of test conditions, is presented in Table D-2. For each disk-oil combination, the number of tests conducted for each set of test conditions may be deduced from Tables D-3 to D-23, which also present the results at scoring or at test termination for each test.

In Tables D-3 to D-23, a quantity of special interest, i.e., the critical temperature, T_{cr}, for each set of replicate tests is derived by the Weibull analysis.[70] However, for the sake of convenience, the normal load reached at scoring, W, is reported only in terms of an algebraic average.

Effect of Test Oil. Figure 12 compares the average scoring load, W_f (i.e., the average W in Tables D-3 to D-23), of Oil E with that of Oil F, for those disk-oil-test variable combinations where

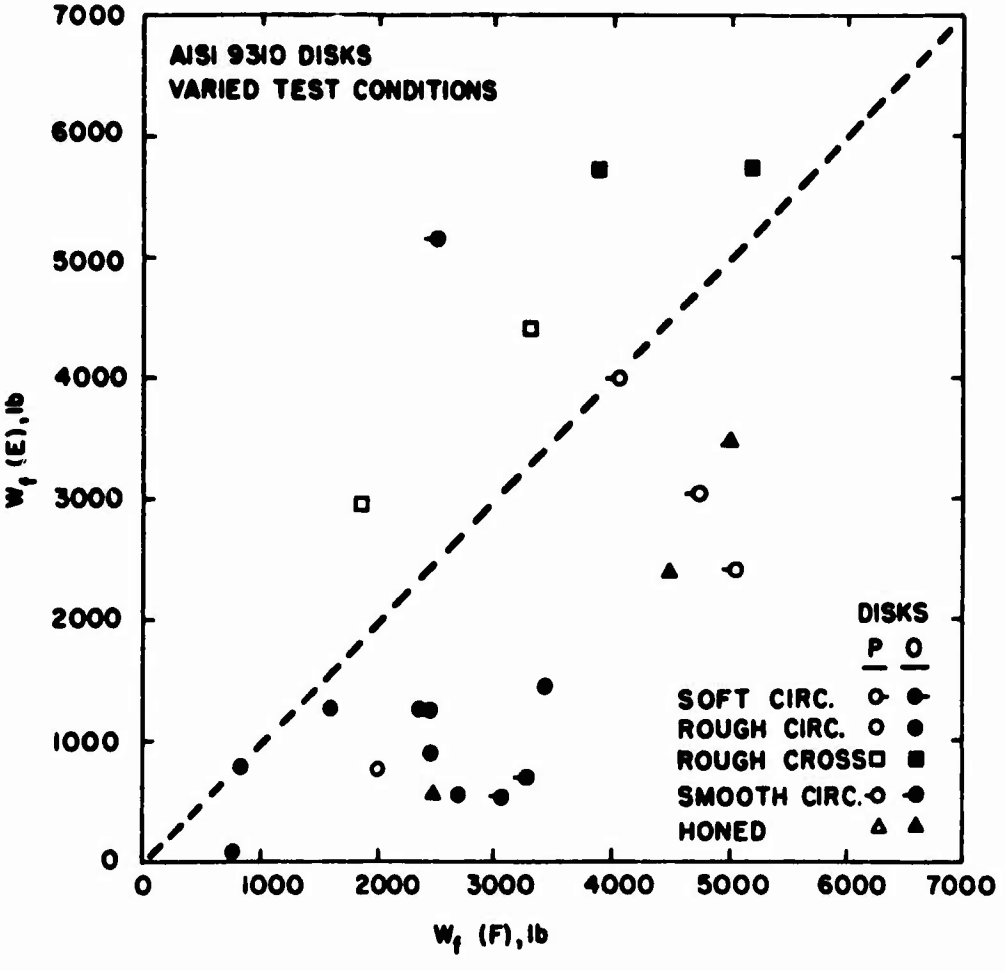

Figure 12. Effect of test oil on average scoring load

comparative results are available. In this figure, the results from the different disk types are represented by different symbols, using the hollow symbols for the plain disks and the solid symbols for the oxided disks. Although the test conditions are not shown in the figure, nor is this information necessary for the present comparison, each plotted point gives the W_f of Oil E as ordinate vs. the corresponding W_f of Oil F as abscissa. It is obvious that if the two oils should give equal performance, then regardless of the disk type and test conditions, all plotted points would lie on the diagonal line shown.

The fact that these points show a great deal of scatter is largely a matter of statistics. As mentioned earlier, only relatively few tests could be run for each disk-oil-test variable combination. As a matter of fact, of the 5 points that lie above the diagonal line, 4 had only one test conducted on Oil E while the remaining point had only 2 replicate tests. Since the range of scatter of the scoring load can be as large as 3 to 1 or more as mentioned before, not much confidence should be attached to these points. Thus, taken as a whole, the figure suggests that the scoring load of Oil E is lower than that of Oil F, despite the fact that Oil E has a higher viscosity than Oil F. A similar result was also observed in tests conducted with SwRI disk tester B using different-size test disks, with Oils E and F and another straight mineral oil of still higher viscosity.[26] It was found that the scoring load was actually highest with Oil F, intermediate with Oil E, and lowest with the straight mineral oil, under otherwise identical test conditions. The fact that oil viscosity as such affects the scoring load the "wrong" way is clear indication that elastohydrodynamic lubrication is not meaningful in controlling scoring as previously stated in Chapter II. Indeed, examination of Tables D-3 to D-23 will show that the computed EHD film thickness ratio, Λ, for all except a very few tests was substantially less than unity. The ratio Λ reported in these tables was based on the computed h_m by Equation (4) without applying side flow and inlet shear thermal corrections, and the composite surface roughness of the disk pair at scoring as defined by Equation (B-2) in Appendix B. The few instances with $\Lambda > 1$ all occurred at $V_t \geq 1080$ ips, when the inlet shear thermal correction would be expected to be more significant. Moreover, the effect of inlet starvation, even if small in the disk tests, was not, nor could it be, accounted for. Besides, it was very difficult to measure accurately the surface roughness of the disks after they had scored. Finally, the definition of the composite surface roughness of the disk pair is, after all, quite arbitrary in this or any other work, so that Λ is normally expected to be greater than unity when full, classical elastohydrodynamic lubrication ceases to exist. Considering all these factors, as well as the preponderance of the $\Lambda < 1$ values

obtained in all other tests, there can be little doubt that scoring occurred in the boundary lubrication regime as emphasized from the theoretical standpoint in Chapter II.

The fact that Oil E gave less scoring protection than Oil F, despite its higher viscosity, emphasizes the importance of surface chemistry in controlling scoring—a boundary lubrication phenomenon. No attempt has been made to draw a "weighted" curve in Figure 12 for the $W_f(E)$ vs. $W_f(F)$ results, because their relationsip is not simple, but depends on the operating conditions. This fact will be obvious from the subsequent sections of this chapter.

Effect of Surface Treatment. The effect of surface treatment is presented in Figure 13, in a similar manner. As in the preceding case, there is a great deal of scatter in the results, and the statistics are generally weak. Nevertheless, if more weight is given to those points with greater number of tests for both the plain and oxided cases, one must conclude that the W_f with the oxided disks is generally lower than the W_f with the plain disks. Again, the reason will be obvious later.

The use of black oxide surface treatment appears to be detrimental from the scoring standpoint, except with cross-ground disks to be discussed later. However, this detrimental effect is, in all likelihood, not significant in actual gears, because the practical limit of scoring for actual gears is generally more advanced than in the disk tests where the "true" incipient scoring can more readily be detected and identified. At a more severe level of scoring, the thin black oxide layer is apt to be worn off, so that the actual gears, whether oxided or not, are apt to behave as if there were no black oxide present so far as scoring is concerned. The practical advantages of the black oxide treatment are apparently that it serves as a rust preservative in storage, and that it is a very useful aid in checking the accuracy of gear manufacture or assembly. If the gear alignment is poor, or if the surface contour is not correct, the wearing off of the black oxide layer provides a convenient visual indication.

Effect of Surface Texture. Before leaving Figures 12 and 13, it is of interest to note that, despite their statistical weakness, there appears to be a tendency for the cross-ground disks to behave better when a black oxide layer is present. It is speculated that if the black oxide should offer any advantage, it would be more apt to show up with cross-ground disks because the grinding grooves, which are normal to the sliding motion, tend to retain the black oxide better. Apart

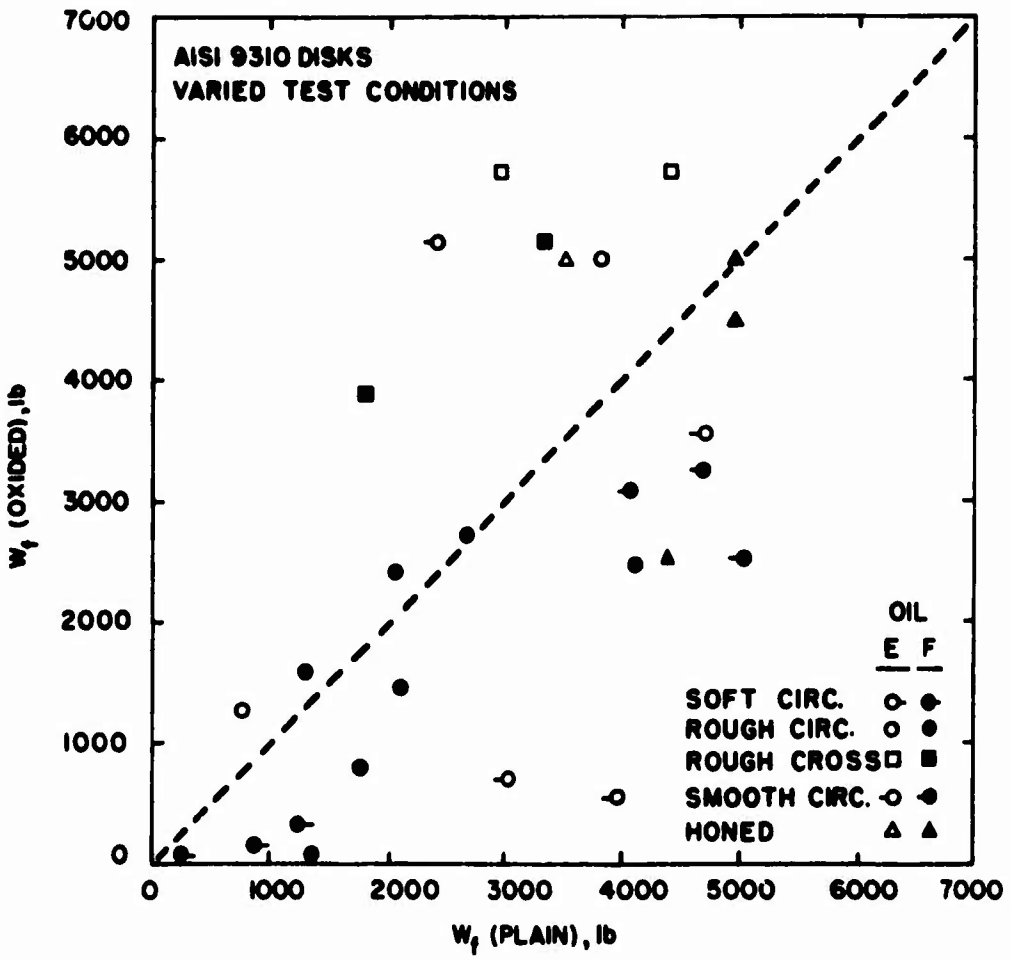

Figure 13. Effect of black oxide surface treatment on average scoring load

from this, it will be seen later that cross-ground disks give a lower coefficient of friction than circumferentially-ground disks of equal composite surface roughness even without a black oxide treatment, possibly due to micro-EHD action.[40-42] This is of course beneficial from the scoring viewpoint,[25] and by inference from the viewpoint of rubbing wear also. There is also evidence that the presence of the micro-EHD film is beneficial from the viewpoint of pitting as well.[71]

Now, since sliding in gears usually takes place normal to or nearly normal to the grinding grooves, the possible advantage suggested by the cross-ground disks, particularly in the presence of a black oxide treatment, is certainly worth investigating. Unfortunately, due to cost and disk delivery considerations, only very few tests were run with cross-ground disks in this program.

B. Critical Temperature

As originally postulated by Blok,[16,17] and subsequently defended by him,[23,27] the critical temperature, i.e., the maximum instantaneous surface temperature in a sliding-rolling conjunction for scoring to occur, is a function of the metal-oil combination but independent of the surface characteristics and operating conditions. On the other hand, there is a large volume of experimental disk test data[9,10,20-22,24-26,28-30] to show that Blok's constant critical temperature hypothesis is not strictly true. This controversy cannot be resolved on theoretical ground. However, as a practical design index, much depends upon how much accuracy or statistical confidence one wishes to attach to the scoring prediction. It is the authors' current thinking that elaborate refinements on the critical temperature is justified in the scoring prediction of sliding-rolling disks; but not for gears mainly because of the pronounced effects of tooth misalignment and dynamic load, the magnitudes of which, as will be seen in the next chapter, can only be reasonably well inferred, but not accurately established, at this time.

The authors have shown[25,26,28] that the effects of surface characteristics and operating variables on the critical temperature of a given metal-oil combination can be satisfactorily expressed by

$$T_{cr} = F(\zeta, M) \tag{47}$$

where F = an experimentally determined function, and

$$\zeta = \frac{\mu_o^2 V_s V_t}{R^2 \sigma_m^2} \tag{48}$$

$$M = \frac{V_s}{V_t} \tag{49}$$

where V_s = sliding velocity, ips

V_t = sum velocity, ips

ζ = a dimensionless parameter

M = sliding-to-sum velocity ratio

R = equivalent radius of curvature of the conjunction, in.

σ_m = maximum Hertz stress in the conjunction, psi

μ_o = oil viscosity at the conjunction inlet, lb-sec/in.^{2}

Equation (47) is extremely difficult to apply to practical gear design. This is partly because μ_o is very sensitive to the oil temperature at the conjunction inlet, T_o, and thus difficult to estimate accurately. Also, σ_m is difficult to estimate because misalignment and dynamic effects cannot be accurately quantified. Therefore, for the present purpose, a simpler approach which requires no estimates of these quantities, is being proposed.

Oil F. The critical temperature data for Oil F (MIL-L-7808G) in combination with AISI 9310 steel are presented in Tables D-3 to D-13 for the different disk types and operating conditions. Consider the plain, rough circumferentially-ground disks (Type 3) for the time being, the effects of V_s and V_t, at three constant M values, are presented in Figures 14 and 15, respectively.

In Tables D-3 to D-13, data for the scoring temperature, T_{cr}, for all individual sets of replicate tests, at 10-percent probability by Weibull analysis, are given, together with their 90-percent confidence limits. These are shown in the two figures by appropriate symbols and vertical bars, except that they are now designated as T_f as a matter of clarification. The symbol T_{cr} is now reserved to represent

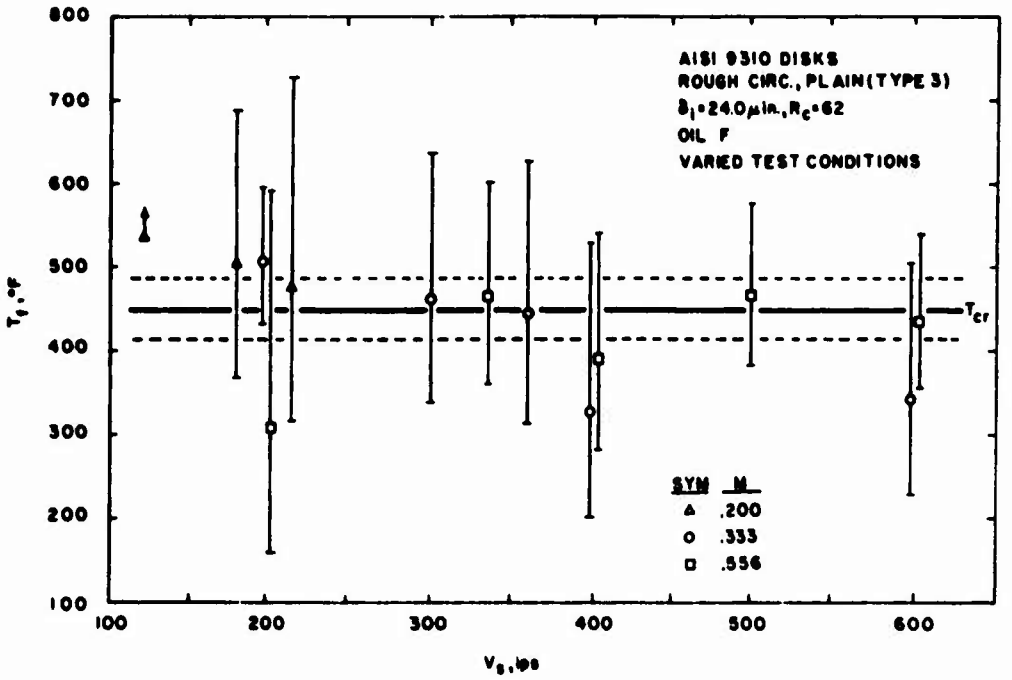

Figure 14. Effect of sliding velocity on critical temperature for Oil F and AISI 9310 steel

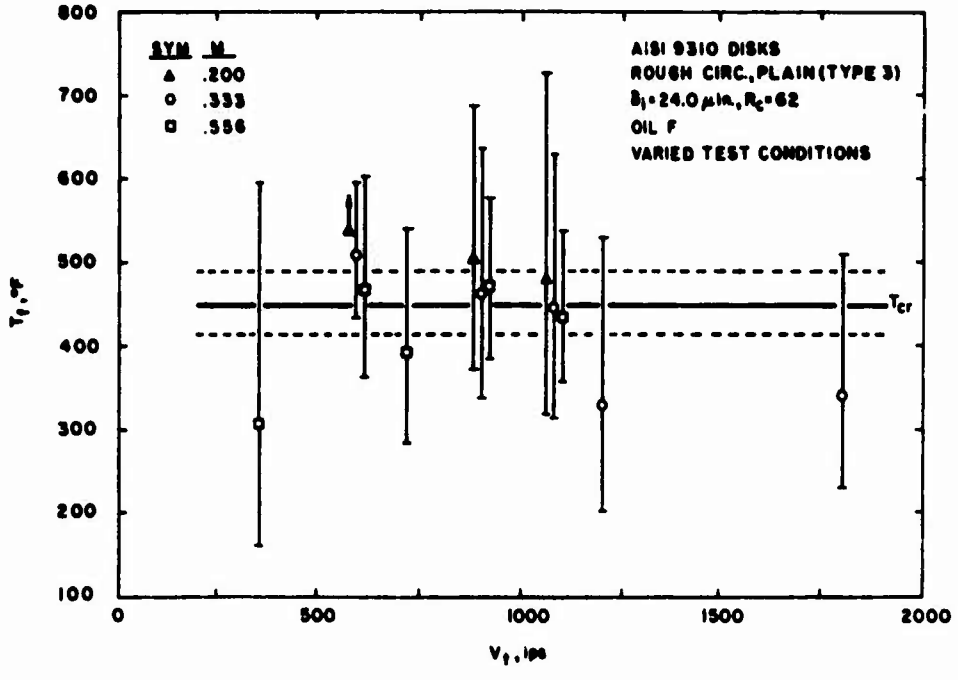

Figure 15. Effect of sum velocity on critical temperature for Oil F and AISI 9310 steel

a constant critical temperature by pooling all of the data on Oil F–Disk Type 3 combination together by a similar Weibull analysis. The point for V_s = 120 ips and M = 0.2 signifies that its T_f is higher than shown, since no scoring was obtained (Tests F130, F186, F187, Table D-5).

Close examination of the data presented in the two figures will show that T_f does indeed vary with V_s at constant V_t, and also with V_t at constant V_s, as previously reported.[25,26,29] However, it is evident that these variations are generally not significant when compared with the confidence limits involved. In view of this fact, the pooled result of all 61 tests for this particular metal-oil combination at 10-percent scoring probability can be regarded as constant and independent of operating conditions, defined herein as its critical temperature, T_{cr}. In this case, T_{cr} = 450°F and the lower and upper 90-percent confidence limits are 415°F and 488°F, respectively.

While the above analysis supports Blok's hypothesis on a statistical basis so far as the effect of operating variables are concerned, it has been found that the effect of surface roughness appears more significant and can, at any rate, be conveniently accounted for. This situation is summarized in Table 3, which includes data not only from this program; but also from other tests on similar metal-oil combinations performed in the authors' laboratory. Among these other tests, those on Type X disks (circumferentially-ground) were conducted also with SwRI disk tester A, while those on Type Y disks (honed) were conducted with SwRI disk tester B. Note that the number of tests included in the pooled Weibull analysis does not necessarily correspond with the number of scored tests given in Table D-2. This is because some of the unscored tests at high loads were treated in the Weibull analysis as suspended tests.

Figure 16 presents the above results in graphic form. Note that the critical temperature, T_{cr}, quite consistently decreases with increasing the initial composite surface roughness of the disk pair, δ_i; and is generally lower for the oxided disks than for the plain disks. Moreover, within the 90-percent confidence limits, neither the surface texture (i.e., whether the surfaces are circumferentially-ground, cross-ground, or honed) nor the small variation of surface hardness makes a significant difference. Accordingly, since more tests are available for the plain disks, its T_{cr} vs. δ_i line has been established by linear regression. The line for the oxided disks is then drawn parallel to that for the plain disks, giving some weight on the statistical distribution. The equations for the two straight lines are

TABLE 3. CRITICAL TEMPERATURE FOR OIL F AND AISI 9310 STEEL DISKS

Disk type	δ_i, μin.	R_c	M	No. of tests in analysis	T_{cr}, °F	Confidence limits, °F	
						Lower	Upper
Plain disks							
1	26.0	58	0.556	5	425	386	468
3	24.0	62	Mixed	61	450	415	488
7	23.5	62	0.556	6	480	402	574
X	15.2	62	0.333	5	408	345	483
9	9.5	62	0.556	3	530	362	775
Y	6.0	62	Mixed	86	490	458	524
5	5.5	62	0.556	3	560	532	590
Oxided disks							
1A	26.0	58	0.556	4	330	290	372
3A	24.0	62	Mixed	27	355	292	432
7A	23.5	62	0.556	4	445	393	504
9A	9.5	62	0.556	6	440	304	636
5A	5.5	62	0.556	5	500	403	620

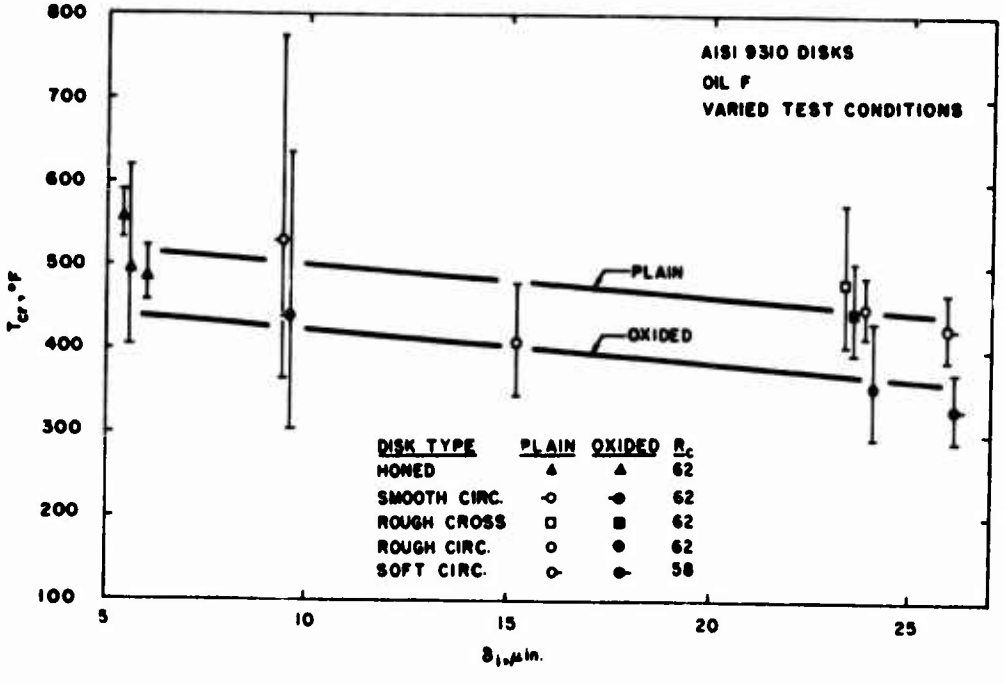

Figure 16. Effect of initial composite surface roughness on critical temperature for Oil F and AISI 9310 steel

Plain surfaces: $T_{cr} = 540 - 3.80\,\delta_i$ (50)

Oxided surfaces: $T_{cr} = 460 - 3.80\,\delta_i$ (51)

where T_{cr} = critical temperature for Oil F and AISI 9310 steel combination, °F

δ_i = initial composite surface roughness of the mating surfaces, μin. AA

The above equations can of course be criticized for not using the prevalent composite surface roughness at the moment of scoring. The reasons for using here the initial value, δ_i, are several. First, the prevalent surface roughness, though theoretically correct, is difficult to measure even on disks; and the after-scoring measurement is not necessarily the correct one since tests cannot be stopped instantaneously and some or severe surface deterioration inevitably occurs in the stopping process. Second, in practice, the initial surface roughness of gears can be measured; but the surface roughness in service depends on the length of service and operating conditions, and is thus a nebulous quantity. Third, if the gears are properly broken in and put into service, the surfaces generally become smoother. Thus, scoring is most prone to occur when the gear set is first run under the design conditions; and once this hurdle is crossed, scoring is not likely to occur unless the operating conditions are drastically made more severe. Considering these factors, it is felt that δ_i is more within the control of the designer and is usually the critical quantity to watch. Of course, if a prescribed break-in procedure is followed, the surface roughness after the break-in would be a better figure to use if it is measured, or it can be estimated if not measured such as by the relationship reported in Reference 25. In those instances where severe operating conditions are anticipated after extended service, it is certainly wise to measure the surface roughness before that occurs, and use what amounts to the δ_i for that new set of operating conditions.

Oil E. The critical temperature data for Oil E (MIL-L-23699) in combination with AISI 9310 steel, given in Tables D-14 to D-23 in Appendix D, may be treated similarly. Table 4 presents a summary of the data based on these results, plus data from Type Z disks (circumferentially-ground) of a similar metal-oil combination obtained also with SwRI disk tester A.

It should be noted that the data for Oil E are statistically much

TABLE 4. CRITICAL TEMPERATURE FOR OIL E AND AISI 9310 STEEL DISKS

Disk type	δ_i, μin.	R_C	M	No. of tests in analysis	T_{cr}, °F	Confidence limits, °F	
						Lower	Upper
Plain disks							
3	24.0	62	0.333	1	406	–	–
7	23.5	62	Mixed	6	573	479	685
Z	16.7	62	0.333	5	480	426	540
9	9.5	62	Mixed	5	572	516	634
5	5.5	62	0.333	3	440	413	468
Oxided disks							
3A	24.0	62	Mixed	18	340	276	419
9A	9.5	62	Mixed	7	380	309	468
5A	5.5	62	Mixed	8	345	252	473

weaker than for Oil F presented in Table 3. Consequently, some liberty must be taken in treating these data. The two straight lines drawn in Figure 17 are based on the assumption that the slope of the two lines is the same as that in Figure 16, while giving some weight to statistics. With this assumption, the equations for the two straight lines are

$$\text{Plain surfaces:} \quad T_{cr} = 515 - 3.80\,\delta_i \tag{52}$$

$$\text{Oxided surfaces:} \quad T_{cr} = 415 - 3.80\,\delta_i \tag{53}$$

where T_{cr} = critical temperature for Oil E and AISI 9310 steel combination, °F

δ_i = initial composite surface roughness of the mating surfaces, μin. AA

C. Coefficient of Friction

Apart from the critical temperature, the coefficient of friction is another primary parameter in controlling scoring. For general performance analysis, the friction behavior through the entire range of EHD to boundary lubrication is of interest. However, for scoring analysis, emphasis should clearly be on the boundary friction regime.

Attempts to generalize the friction behavior of sliding-rolling systems have not been fruitful.[9,10] This is because friction is not only exceedingly difficult to determine accurately by experiment, but also equally difficult to understand theoretically. Consequently, empirical approach has been necessary, and considerable uncertainties must be expected.

The authors have attempted to correlate the coefficient of friction of sliding-rolling disks with the dimensionless parameters ζ and M mentioned in the preceding section of this chapter. But due essentially to the same reasons, this method has been found to be most difficult to employ in practical gear design. Accordingly, a simpler correlation was proposed recently,[28] which will be used herein.

Oil F. Figures 18 and 19 for Oil F and plain, circumferentially-ground and cross-ground, AISI 9310 steel disks are taken from Reference 28 to illustrate the nature of the correlation. In these

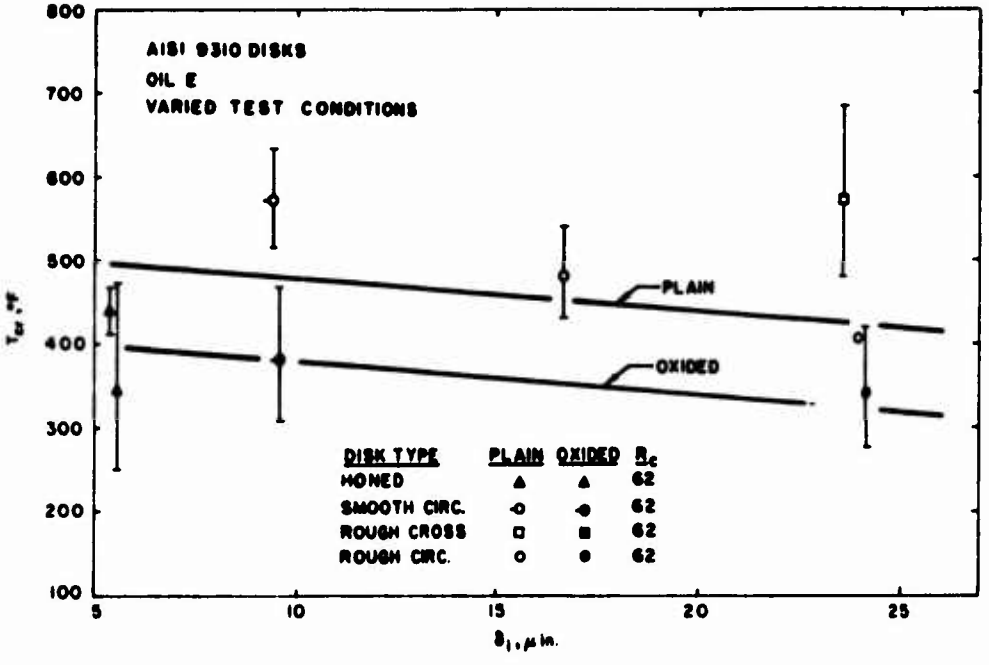

Figure 17. Effect of initial composite surface roughness on critical temperature for Oil E and AISI 9310 steel

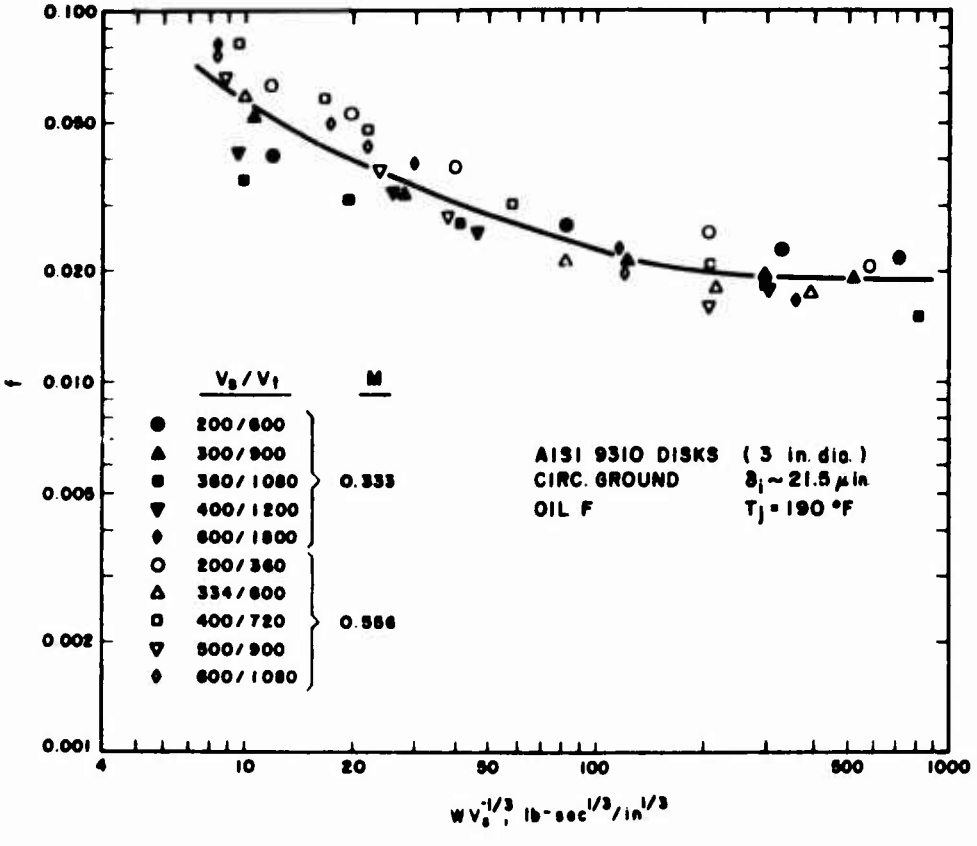

Figure 18. Friction behavior of plain circumferentially-ground AISI 9310 steel disks with Oil F

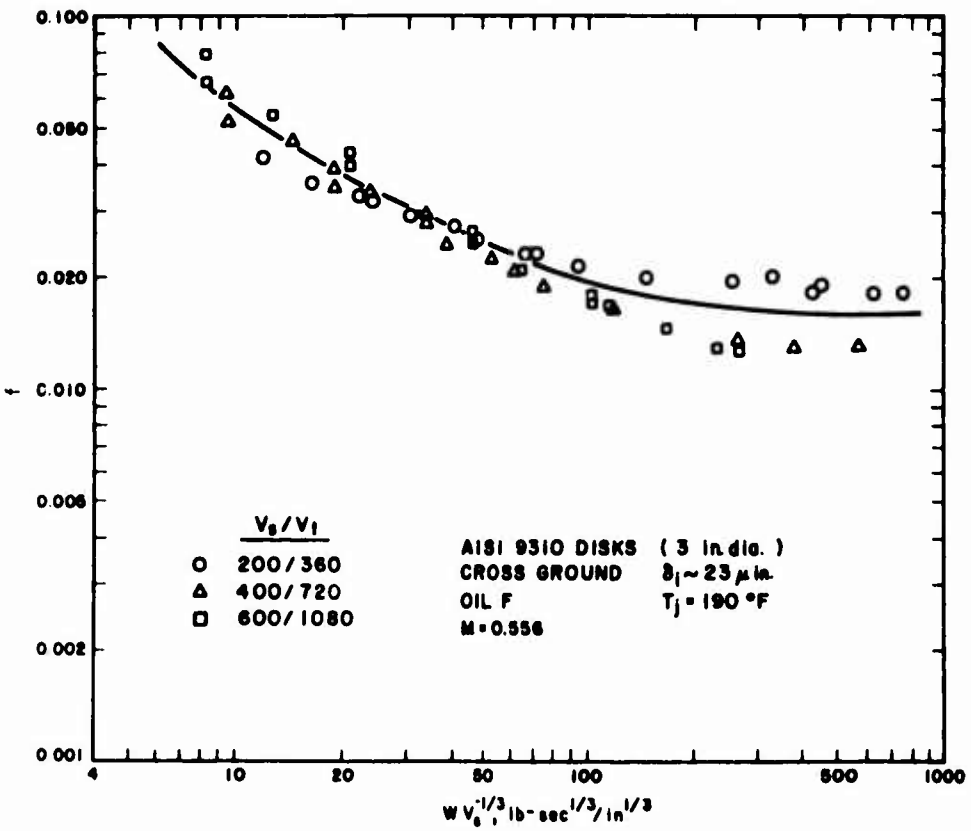

Figure 19. Friction behavior of plain cross-ground AiSI 9310 steel aisks with Oil F

figures, the coefficient of friction, f , is related to the quantity $WV_s^{-\frac{1}{3}}$, where W is the normal load, lb, and V_s is the sliding velocity, ips. It should be remarked that literally hundreds of data points are available not only from the disk scoring tests, but also from a great deal of additional friction measurements. However, for the sake of clarity, only very few "extreme values" are shown in the figures to indicate the scatter involved, which is about ±20 percent from the average curves at high values of $WV_s^{-\frac{1}{3}}$ (a range of greater interest in scoring prediction) and about ±40 percent at low values of $WV_s^{-\frac{1}{3}}$. Within this scatter range, it is seen that f bears an approximate relationship to $WV_3^{-\frac{1}{3}}$.

By comparing the two figures, it will be noted that at the same value of $WV_s^{-\frac{1}{3}}$, f is somewhat lower with the cross-ground disks than with the circumferentially-ground disks, even though the composite surface roughness of the cross-ground disks was slightly greater. This could be due to a micro-EHD effect.[25]

Figures 18 and 19 were based on partial data available in 1973. The more complete, updated results are now presented in Figure 20, for all 10 disk types investigated. For the sake of clarity, these updated results are presented herein merely as average curves, by omitting the data points. Note that with more data on the rough, circumferentially-ground disks (Type 3), the average δ_i is raised, as is the average f. Otherwise, the general trends and maximum scatter are about the same as in Figures 18 and 19.

Figure 20 reveals two items of major interest. First, with the exception of the cross-ground disks, the coefficient of friction is not measurably influenced by the black oxide surface treatment. The substantially lower f observed for the Type 7A (oxided, cross-ground) disks is based on data from only 4 scoring tests with Oil F (Table D-11). However, 2 other tests run on Type 7A disks with Oil E (Table D-21) gave similar results. These data are admittedly skimpy; but the enormous effect observed is certainly intriguing. As suggested in the preceding section, this effect could be due to the fact that the grinding grooves normal to the sliding direction tend to help retain the black oxide in the grooves. A similar mechanism is not present for all other surface textures.

The other item of interest is that the value of f on the flat portion of each curve, where f could be determined more accurately, generally increases with increasing the composite surface roughness of the disk pair. However, one wonders what effects the surface

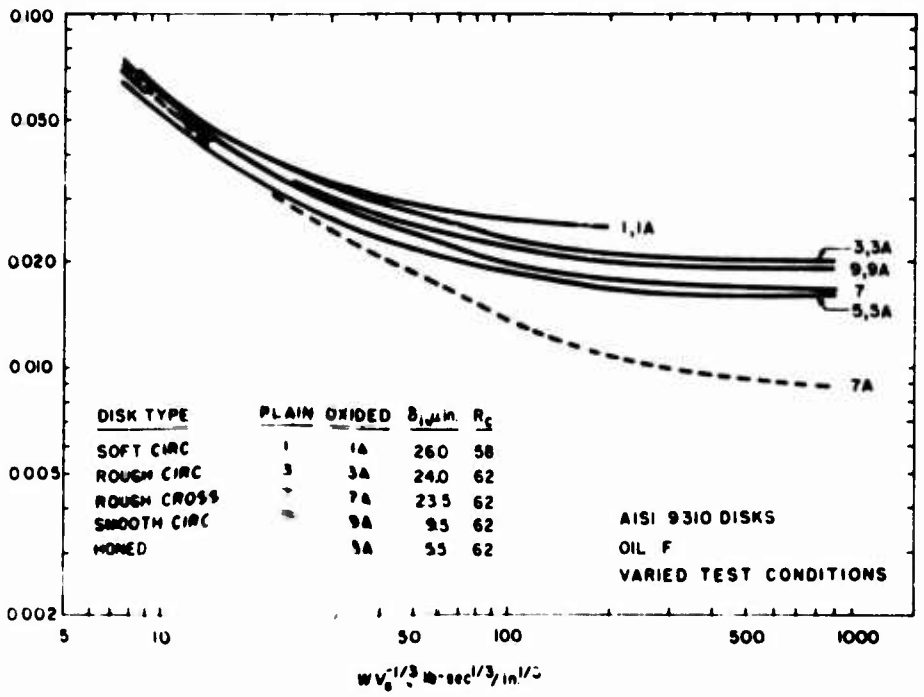

Figure 20. Friction behavior of ten types of AISI 9310 steel disks with Oil F

texture and hardness might have on the friction behavior. These latter effects will now be examined.

Figure 21 portrays the relationship between the flat-value f and δ_i, without including the data for Type 7A disks. In the absence of more data, it is believed logical to infer that the effect of δ_i on f is best represented by a straight line through the points for the smooth circumferentially-ground (Types 9 and 9A) and rough circumferentially-ground (Types 3 and 3A) disks. If this inference is correct, then the higher f for the soft circumferentially-ground disks (Types 1 and 1A) appears to be largely due to their lower case hardness. The lower f for the cross-ground disks (Type 7) then appears to be due to a micro-EHD effect suggested previously. Finally, the lower f for the honed disks (Types 5 and 5A) appears to be due to their "neutral texture," a surface texture which does not provide leakage paths for the oil in the conjunction as does the circumferentially-ground grooves.

It should be remarked that the general level of f shown here is much lower than that assumed in the AGMA gear scoring design guide,[3] and the effect of surface roughness on f is also less. A detailed comparison of the AGMA friction behavior with that observed here is presented in Appendix E for the sake of convenience. It is only necessary to state that the level and trend observed in this work are generally consistent with those obtained for the same and other oil-disk combinations on both SwRI disk testers A and B,[25, 26, 32] as well as those reported on mineral oils and different disks using the Thornton disk tester.[24, 29, 72]

In order to adapt the information presented in Figures 20 and 21 to computer programs, one way is to use first the data from Figure 20 recognizing that they apply only to the particular δ_i values specified, and then apply a correction for the effect of δ_i by assuming the same f vs. δ_i slope for all surface textures as that for the circumferentially-ground case shown in Figure 21. Another way is to approximate the curves in Figures 20 and 21 by straight lines, so that the variations can be written as equations for convenience.

For this approximation, it is assumed that each curve in Figure 20 may be represented by a horizontal line (i.e., constant f) for $WV_s^{-\frac{1}{3}} \geq 200$, and by an inclined straight line (i.e., an exponential variation of f with $WV_s^{-\frac{1}{3}}$) for $WV_s^{-\frac{1}{3}} < 200$ lb-sec$^{\frac{1}{3}}$/in.$^{\frac{1}{3}}$ The slope of the f vs. δ_i line in Figure 21 is 0.00007 per μin. AA. Using these values it can be readily shown that the friction equations for Oil F and

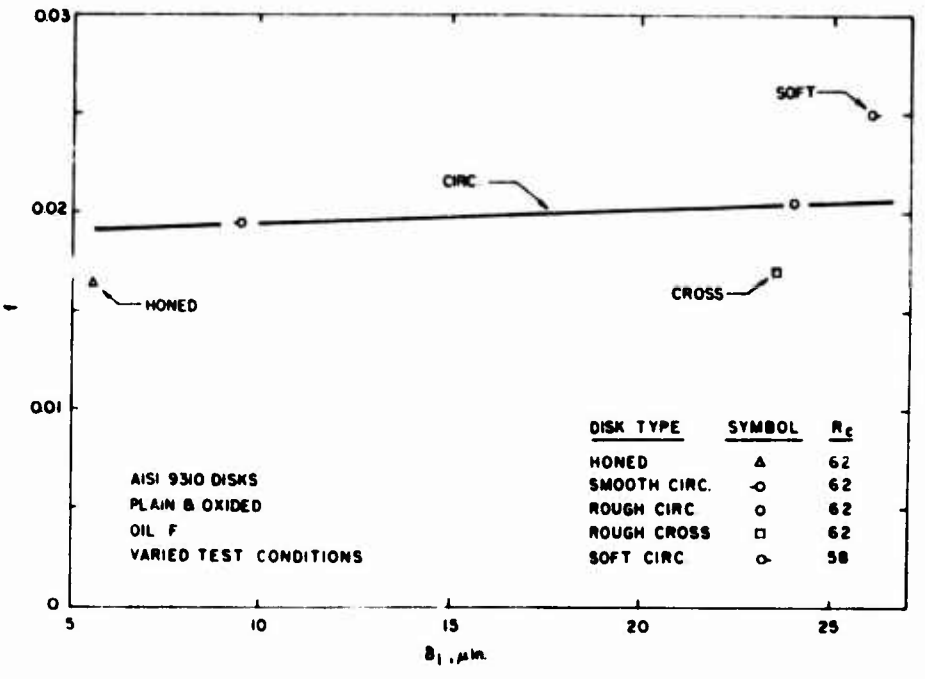

Figure 21. Effect of initial composite surface roughness on friction for Oil F and AISI 9310 steel

AISI 9310 steel combination are as follows.

For plain and oxided circumferentially-ground surfaces:

$$f = (0.0920 + 0.00034\,\delta_i)\,(WV_s^{-\frac{1}{3}})^{-0.3}$$

$$\text{at } WV_s^{-\frac{1}{3}} < 200 \tag{54}$$

$$f = 0.0188 + 0.00007\,\delta_i$$

$$\text{at } WV_s^{-\frac{1}{3}} \geq 200 \tag{55}$$

For plain cross-ground surfaces:

$$f = (0.0755 + 0.00034\,\delta_i)\,(WV_s^{-\frac{1}{3}})^{-0.3}$$

$$\text{at } WV_s^{-\frac{1}{3}} < 200 \tag{56}$$

$$f = 0.0154 + 0.00007\,\delta_i$$

$$\text{at } WV_s^{-\frac{1}{3}} \geq 200 \tag{57}$$

For oxided cross-ground surfaces:

$$f = (0.0407 + 0.00034\,\delta_i)\,(WV_s^{-\frac{1}{3}})^{-0.3}$$

$$\text{at } WV_s^{-\frac{1}{3}} < 200 \tag{58}$$

$$f = 0.0083 + 0.00007\,\delta_i$$

$$\text{at } WV_s^{-\frac{1}{3}} \geq 200 \tag{59}$$

For plain and oxided honed surfaces:

$$f = (0.0789 + 0.00034\,\delta_i)\,(WV_s^{-\frac{1}{3}})^{-0.3}$$

$$\text{at } WV_s^{-\frac{1}{3}} < 200 \tag{60}$$

$$f = 0.0161 + 0.00007\,\delta_i$$

$$\text{at } WV_s^{-\frac{1}{3}} \geq 200 \qquad (61)$$

In Equations (54) to (61), W = normal load, lb; V_s = sliding velocity, ips; and δ_i = initial composite surface roughness of the mating surfaces, μin. AA. The reasons for using the initial composite surface roughness were given in the preceding section.

Oil E. Within the precision of the friction measurements, the friction behavior of AISI 9310 steel disks is substantially the same with Oil E as with Oil F. Equations (54) to (61) are therefore also recommended for use with Oil E and AISI 9310 steel combination.

D. Surface Temperature

According to the critical temperature hypothesis (Chap. II, Sect. B), the scoring-limited power-transmitting capacity is controlled by the maximum rise of the instantaneous surface temperature in the conjunction, ΔT. Assuming that the critical temperature, T_{cr}, is known, it is then necessary to estimate the quasi-steady surface temperature, T_s, in order to arrive at an estimate for ΔT.

The value of T_s is determined by the frictional power loss in the conjunction and the heat loss to the environment by various heat transfer processes. The frictional power loss is defined as

$$\phi = f W V_s / 9336 \qquad (62)$$

where ϕ = frictional power loss, Btu/sec

f = coefficient of friction

W = normal load, lb

V_s = sliding velocity, ips

The heat transfer processes vary, of course, with the system configuration and operating conditions.

The authors showed in a recent publication[28] that for a specific system configuration and operating conditions, in steady operation, the following approximate relationship holds:

$$T_s - T_j = C\phi^n \qquad (63)$$

where T_j = oil jet temperature, °F

C, n = fitting constants

Figure 22 illustrates such a relationship[28] for SwRI disk tester A, using a "horn" to supply the test oil to the exit side of the conjunction and halfway around both disks (Fig. D-1, App. D). Plain, rough circumferentially-ground (Type 3) and cross-ground (Type 7) disks were used. The test oil was Oil F, the total oil flow rate was 20 gpm, and T_j was 140°F and 190°F. The operating conditions (i.e., V_s, V_t, and W) were varied over a wide range. For the sake of clarity, the plotted points do not include all available data; but they do portray the maximum scatter of the data, which are due largely to errors in the friction measurement as explained in the preceding section. Note that within the experimental scatter, the relationship is as shown by Equation (63); and this relationship is not systematically influenced by the disk type, the oil jet temperature, or the operating conditions.

Figure 23 presents the more complete data for SwRI disk tester A, using both Oil E and Oil F, supplied by the horn at 20 gpm total flow rate, at 140°F and 190°F jet temperatures, all 10 disk types investigated in this program; and with test conditions widely varied. Again, the plotted points indicate the maximum scatter observed. It is seen that, within the scatter range, the data exhibit an almost identical exponential relationship as that shown in Figure 22—a relationship essentially unaffected by the disk type or surface characteristics, the oil or the oil jet temperature, or the operating conditions.

Figure 24 shows the trends computed from data reported by Bell and Dyson,[24,29] using the Thornton disk tester. The test disks were straight cylindrical disks made of EN 34 steel, at two levels of surface finish, F. A straight mineral oil and the same oil with an EP additive were used. The oil was supplied by means of two jets, located on the inlet and exit sides of the conjunction. The tests covered two T_j and total oil flow rate combinations; and the test conditions were widely varied. It is seen that an exponential relationship

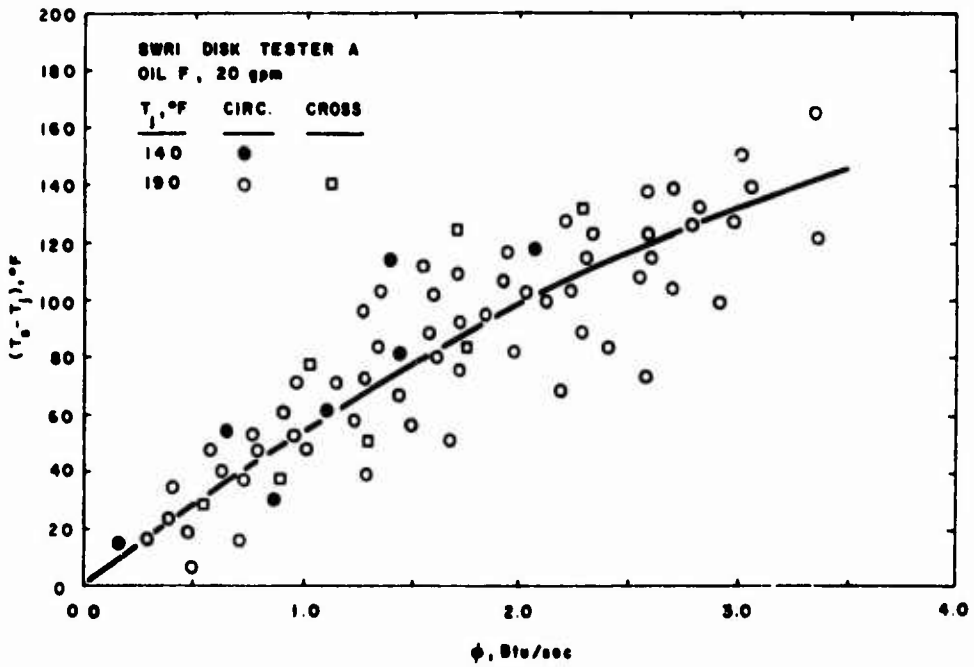

Figure 22. Variation of $(T_s - T_j)$ with ϕ for Oil F and two disk types

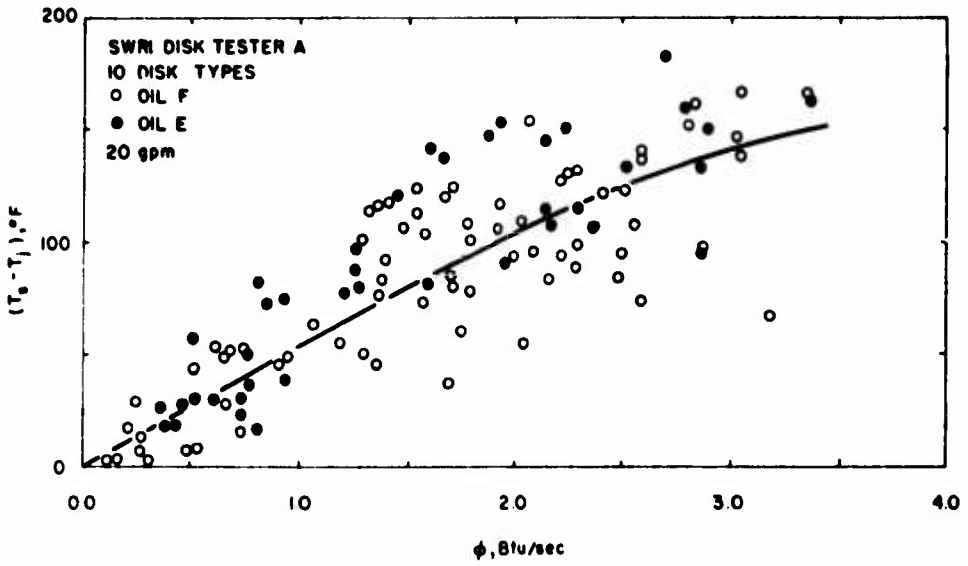

Figure 23. Variation of $(T_s - T_j)$ with ϕ for Oils E and F and ten disk types

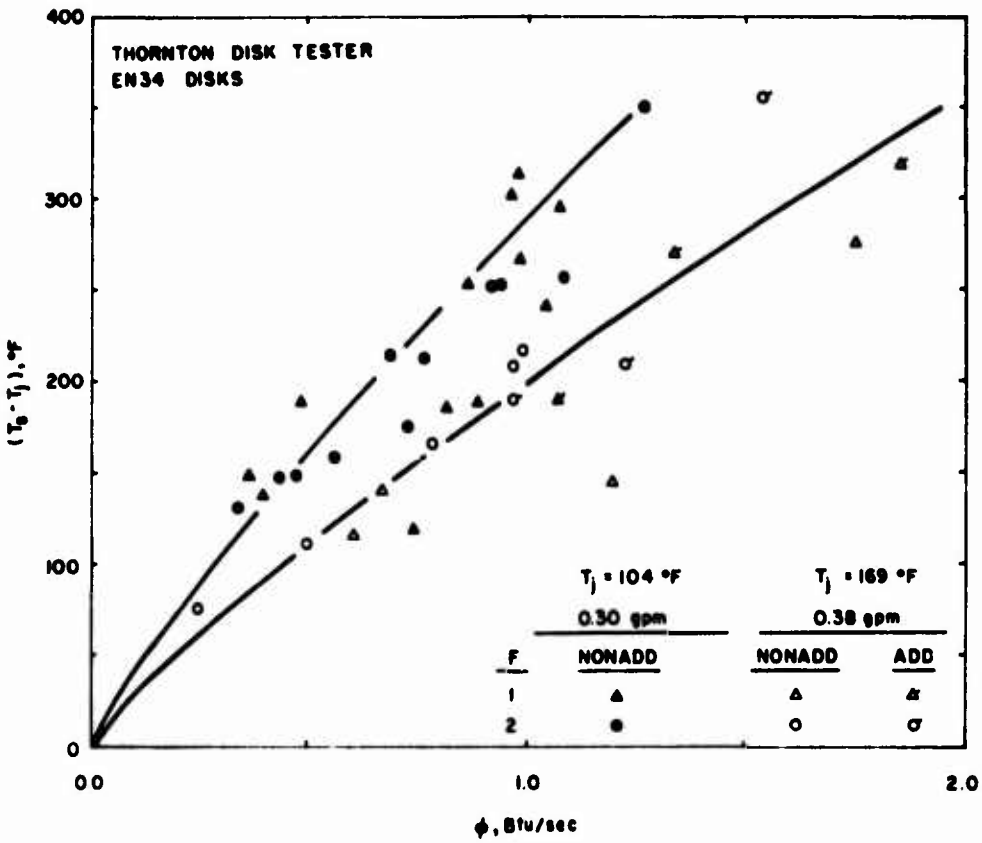

Figure 24. Variation of $(T_s - T_j)$ with ϕ based on the results of Bell and Dyson

also holds, one for each oil flow rate; and each such relationship is not significantly affected by the oil or the oil jet temperature, the surface finish of the disks, or the operating conditions.

The preceding figures serve to show that the $(T_s - T_j)$ vs. ϕ relationship is essentially exponential and not affected by the disk material, disk surface characteristics, and oil type; and, within the range of the investigation, not affected also by the oil jet temperature and operating conditions. In other words, while these factors are expected to affect the magnitude of friction, they do not appreciably affect the relationship between $(T_s - T_j)$ and ϕ since friction enters the makeup of both $(T_s - T_j)$ and ϕ almost similarly. On the other hand, the quantitative behavior is seen to be significantly influenced by the oil flow rate and, by implication, the disposition of the oil jet and the system design, i.e., by those considerations which control the overall heat transfer from the disks. This latter situation is well illustrated by Table 5.

In compiling the information presented in Table 5, it was found that the data shown in Figures 22, 23, and 24, as well as those to be discussed, all yield a value of n of about 0.80 in Equation (63); but the value of C depends on those factors which influence the overall heat transfer. In other words, Equation (63) may now be written as

$$T_s - T_j = C \phi^{0.80} \tag{64}$$

and the constant C is the sole parameter which reflects the system's thermal characteristics. For example, the data for SwRI disk tester A with the horn oil jet at a total oil flow rate of 20 gpm (i.e., Figs. 22 and 23) represent Case 10 in Table 5, and the corresponding value of C is 55. The data for the Thornton disk tester with inlet-exit oil jets (Fig. 24) yield C = 285 at a total oil flow rate of 0.30 gpm (Case 6), and C = 200 at a total oil flow rate of 0.38 gpm (Case 7).

The variation of C shown in Table 5 with the oil flow rate is presented in Figure 25. Note that the value of C is generally highest with the Thornton disk tester, intermediate with SwRI disk tester B, and lowest with SwRI disk tester A—reflecting the influence of design on system heat transfer. Note further that with the same SwRI disk tester B at two constant oil flow rates, the exit jet location gives a lower value of C, or more effective cooling, than the inlet jet location. While this latter effect is believed to be real and is apparently also

TABLE 5. VALUE OF C FROM THREE DISK TESTERS

Case	Disk tester	Oil jet type	Disk material	Disk type	Oil type	T_i, °F	Oil flow, gpm	C
1	SwRI B	Inlet	AISI 9310	Honed	Oil F	190	0.033	360
2	SwRI B	Inlet	AISI 9310	Honed	Oil F	190	0.25	180
3	SwRI B	Exit	AISI 9310	Honed	Oil F	190	0.033	260
4	SwRI B	Exit	AISI 9310	Honed	Oil F	190	0.25	130
5	SwRI A	Exit	SAE 8620	Circ.	Mineral	Varied	0.50	125
6	Thornton	In-exit	EN 34	Circ.	Mineral	104	0.30	285
7	Thornton	In-exit	EN 34	Circ.	Mineral	169	0.38	200
8	SwRI B	Horn	AISI 9310	Honed	Oil F	190	2.5	100
9	SwRI B	Horn	AISI 9310	Honed	Oil F	190	10	100
10	SwRI A	Horn	AISI 9310	Varied	E&F	Varied	20	55

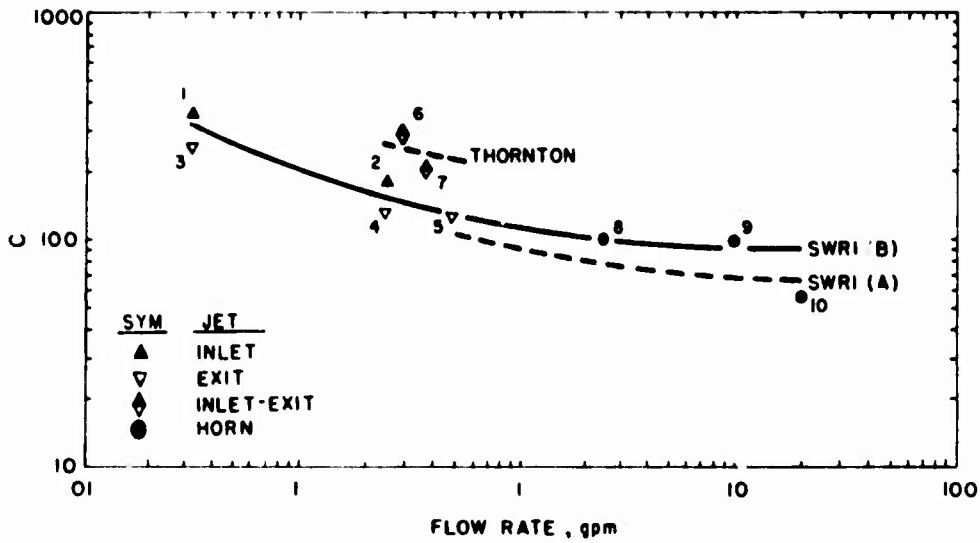

Figure 25. Variation of C with total oil flow rate and system design

experienced in gear operation, a single curve is herein drawn for SwRI disk tester B to emphasize the major trends, namely, the oil flow rate and the tester design. Finally, the effect of oil flow rate on C is quite marked at low flow rates, and generally tends to level off at high flow rates.

It is believed that Equation (64), with the value of C judiciously selected (such as from Fig. 25 or further refined data), gives a tangible basis for estimating the value of T_s. In the AGMA gear scoring design guide,[3] an implied assumption is that T_s is equal to T_j. It is obvious from the data presented herein that this assumption is far from being true.

E. Conjunction-Inlet Oil Temperature

The temperature of the oil at the conjunction inlet, T_o, is of interest mainly in elastohydrodynamic film thickness calculations (App. C). Although EHD film thickness will not receive emphasis in this report for reasons given in Chapter II, Section C, information for estimating T_o is presented for the sake of completeness.

Figure 26 shows the variation of $(T_o - T_j)$ with ϕ previously reported[28] for SwRI disk tester A, Types 3 and 7 disks, Oil F supplied by the horn at 20 gpm flow rate, at T_j = 140°F and 190°F. Figure 27 presents the more complete results for the same tester and horn, same T_j and oil flow rate, Oil E and Oil F, and the 10 disk types. Note that substantially the same exponential relationship is shown in these figures. This relationship may be represented by

$$T_o - T_j = C_o \phi^{0.80} \tag{65}$$

where T_o = conjunction-inlet oil temperature, °F

T_j = oil jet temperature, °F

ϕ = frictional power loss, Btu/sec

C_o = a fitting constant

By comparing Figures 26 and 27 for $(T_o - T_j)$ and Figures 22 and 23 for $(T_s - T_j)$, it will be found that

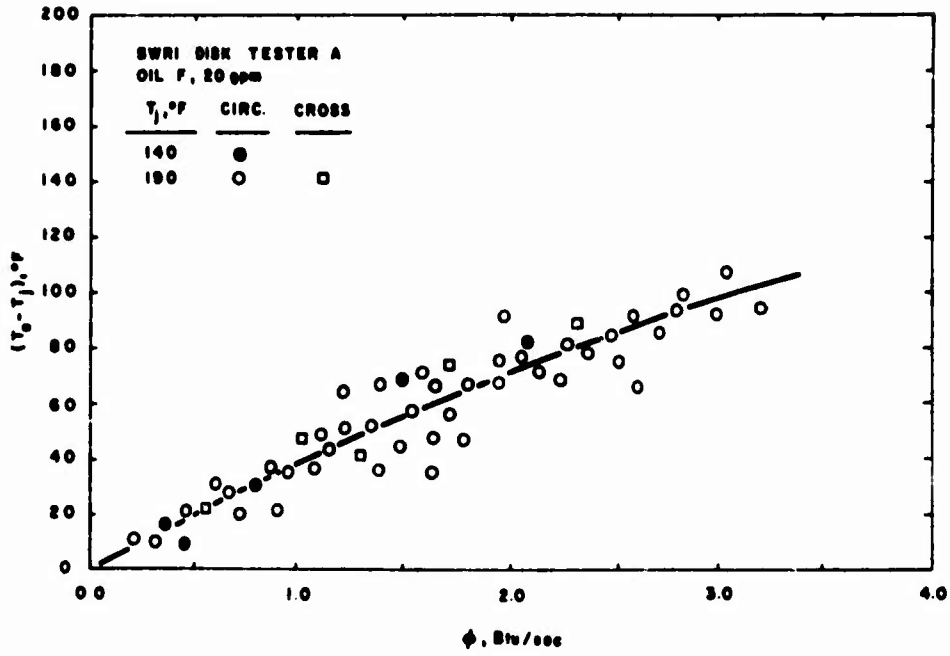

Figure 26. Variation of $(T_O - T_j)$ with ϕ for Oil F and two disk types

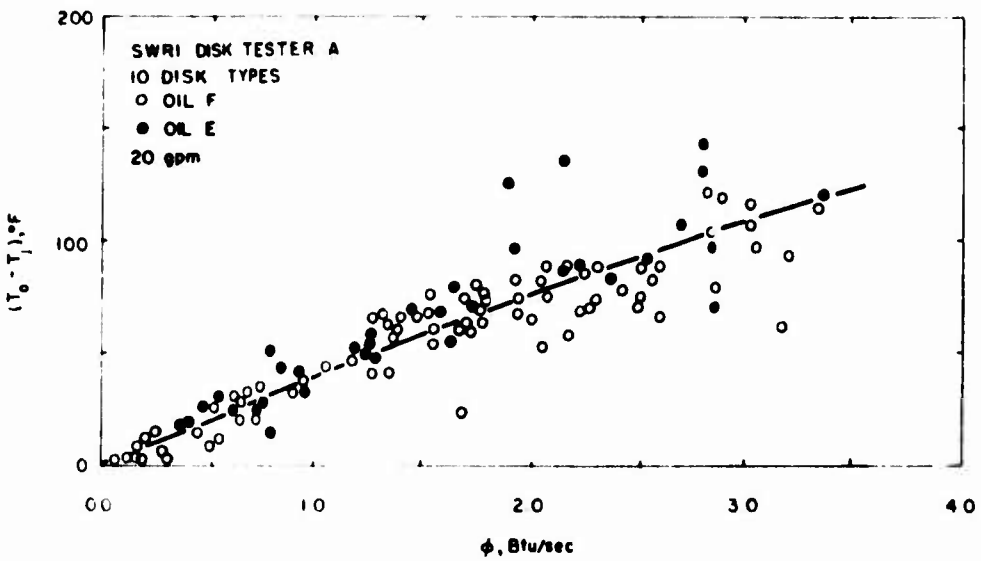

Figure 27. Variation of $(T_o - T_j)$ with ϕ for Oils E and F and ten disk types

$$C_o = 0.70\,C \qquad (66)$$

is a very good approximation over the range of variables investigated.

Equation (65) gives a tangible basis for estimating the value of T_o. It is seen from Equation (66) that the assumption of either $T_o = T_j$ or $T_o = T_s$, as commonly used, is not satisfactory.

CHAPTER VII
GEAR SCORING PREDICTION

A. Basic Procedure

It was noted in Chapter II, Section B, that the mechanism of scoring is still basically not understood. However, phenomenological observations to date suggest that it is probably triggered by a thermal interaction between the relatively moving surfaces; and that among the several thermal scoring models that have been proposed, the critical temperature model appears to be the most plausible and promising. It was also noted that apart from the need for establishing a meaningful critical temperature criterion, the prediction of the scoring-limited power-transmitting capacity of gears further requires a consideration of the important influences of gear mechanics—a subject whose complexity was broadly indicated in Chapter II, Section F, and further discussed in Chapters III, IV, and V.

In view of the aforementioned problems, it was concluded in Chapter VI, Section A, that a completely rational procedure for predicting the scoring-limited power-transmitting capacity of gears is not now possible. On the other hand, an essentially empirical procedure, such as the AGMA gear scoring design guide,[3] certainly leaves much to be desired. Accordingly, an interim predictive scheme, which recognizes the importance of the above-mentioned problems but accepts certain necessary approximations, appears to be the only viable approach.

The predictive scheme to be discussed herein can readily be applied to practical gear design. It is assumed that the scoring behavior of gear teeth follows the same phenomenological behavior of sliding-rolling disks, except for the effects of gear mechanics. This assumption implies that the basic data derived from steady-operating sliding-rolling disks (Chap. VI) may be applied to the transient process of the gear-tooth action, provided the effect of gear-tooth dynamics can be isolated and taken into account. Additionally, it is implied that the effect of gear-tooth misalignment can also be isolated and accounted for. These assumptions are difficult to defend from a rigorous theoretical standpoint, and as such they are "approximations" being forced upon the problem by the current state of the art. Refinements or revisions of the technique are naturally possible; nevertheless, the results thus far obtained appear quite plausible. The analysis also shows that thermal behavior, gear-tooth misalignment, and gear-tooth

dynamics exert major impacts on the scoring-limited power-transmitting capacity of gears.

The basic premise of the proposed gear scoring predictive method may be stated by the equation

$$P_A = P_I S_m S_d \tag{67}$$

where P_A = actual scoring-limited power-transmitting capacity, hp

P_I = ideal scoring-limited power-transmitting capacity, hp

S_m = misalignment factor

S_d = dynamic factor

In other words, the proposed predictive procedure entails, in effect, two basic steps. The first step is to estimate the ideal scoring-limited power-transmitting capacity of a gear set, by considering the thermal effect and assuming perfect tooth alignment and no dynamic load. The second step is to estimate the actual scoring-limited power-transmitting capacity, by applying corrections for the misalignment and dynamic effects. For the sake of convenience, the general features of this procedure will first be considered. Some specific details related to gear types will be discussed in the final sections of this chapter.

B. Ideal Scoring-Limited Power-Transmitting Capacity

The prediction of the ideal scoring-limited power-transmitting capacity, P_I, of a given gear set operating under specified conditions requires, in principle, successive comparisons of the ideal maximum instantaneous conjunction surface temperature, T_c, somewhere in the gear mesh, as the transmitted power is being progressively increased at the specified gear speed and operating conditions, with the critical temperature, T_{cr}, of the metal-surface-oil combination. The word "ideal" signifies that these comparisons are being made for the assumed case of perfect tooth alignment and static tooth load. From Equation (1) in Chapter II,

$$T_c = T_s + \Delta T \tag{68}$$

where T_C = maximum instantaneous surface temperature at any point in the gear mesh, °F

T_s = quasi-steady gear surface temperature, °F

ΔT = maximum instantaneous surface temperature rise at any point in the gear mesh, °F

Note that as the power level is increased at otherwise constant operating conditions, ΔT increases, and its magnitude varies through the gear mesh. At the same time, T_s also increases; but its magnitude remains constant with respect to time. Consequently, T_C also increases, and its magnitude varies through the gear mesh. When the maximum value of T_C somewhere in the gear mesh equals the critical temperature, T_{cr}, scoring occurs and the corresponding power transmitted is, by definition, the ideal scoring-limited power-transmitting capacity of the gear set under the specified operating conditions.

Outline of Predictive Process. The prediction of P_I then comprises the following steps:

1. An estimate of the critical temperature, T_{cr}.

2. At constant gear speed and operating conditions, calculate the quasi-steady surface temperature, T_s, by progressively increasing the power level, while assuming perfect tooth alignment and static tooth load.

3. Similarly, calculate the maximum instantaneous surface temperature rise, ΔT, through the gear mesh.

4. From Steps 2 and 3, calculate the maximum instantaneous conjunction surface temperature, T_C, through the gear mesh.

5. When the maximum value of T_C at some point in the gear mesh (from Step 4) equals the critical temperature, T_{cr} (from Step 1), the scoring criterion is met; hence the corresponding power transmitted is the ideal scoring-limited power-transmitting capacity of the gear set under the specified operating conditions.

Input Data. The prediction process as described can readily be carried out by means of a computer. The required equations and numerical constants or coefficients for each step will now be outlined.

1. As noted in Chapter VI, Section B, the statistically

defined critical temperature, T_{cr}, of a given metal-oil combination is a function of the composite surface roughness of the mating surfaces, but independent of the surface texture and operating conditions. Moreover, although the black oxide surface treatment was found to have a substantial effect on T_{cr} in the disk tests, the practical scoring level of gears, which is generally more severe, tends to permit removal of the thin black oxide layer so that its effect is apt to be essentially absent in practical gears. Therefore, if the gears are made of carburized AISI 9310 steel, whether or not surface-treated with black oxide, and if the oil is Oil F, then the critical temperature is given by Equation (50). For the same metal and Oil E, the critical temperature is given by Equation (52).

2. The quasi-steady surface temperature, T_s, is a time-averaged quantity, whose magnitude depends upon the frictional heat generated at the meshing surfaces and the heat removal from these surfaces by various means—principally by conduction and convection. In other words, T_s is highly dependent upon gear design, system design, and operating conditions; and its prediction requires a quantitative knowledge of the effects of these factors on both the frictional heat generation and the heat removal.

For the simple case of steady-operating sliding-rolling disk systems, it was shown in Chapter VI, Section D, that the frictional heat generated per unit time, or the frictional power loss, is

$$\phi = f W V_s / 9336$$

where ϕ = frictional power loss, Btu/sec

f = coefficient of friction

W = normal load, lb

V_s = sliding velocity, ips

and the relation between T_s and ϕ may be approximated by the equation

$$T_s - T_j = C\phi^{0.80}$$

where T_j = oil jet temperature, °F

C = a fitting constant for sliding-rolling disk systems

The constant C in the above equation was found to depend quite markedly on the rate at which the oil supplied by the jet (or jets, or horn) impinges on the sliding-rolling disk surfaces and also the disk system design.

When applied to gears, the quantities V_s, W, and f generally all vary through the gear mesh, or with respect to time. Accordingly, ϕ also varies with respect to time; and it is the time-averaged ϕ that controls the quasi-steady surface temperature. In other words, the quasi-steady surface temperature of gears is expected to be governed by the equation

$$T_s - T_j = C'\phi_{av}^{0.80} \tag{69}$$

where ϕ_{av} = average frictional power loss, Btu/sec

C' = a fitting constant for gear systems

The solution to Equation (69) requires the assignment of the magnitude of the constant C' and the evaluation of the quantity ϕ_{av}. As will be seen presently, the selection of the value of C' is very difficult basically because little is known about the heat transfer processes involved in gear operation. However, the calculation of ϕ_{av} can readily be accomplished by an integration process which accounts for the variations of V_s, W, and f in the gear mesh. Depending upon the gear type, the instantaneous sliding velocity, V_s, may be deduced from kinematic analysis (Sect. A of Chaps. III, IV, V). The instantaneous static normal load, W, may be obtained from static load analysis (Sect. B of Chaps. III, IV, V). The instantaneous coefficient of friction, f, is a function of $WV_s^{-\frac{1}{3}}$ and the oil and surface characteristics (Chap. VI, Sect. C).

In Chapter VI, Section C, it was found that with AISI 9310 steel, Oils E and F gave substantially the same friction behavior. For practical gear scoring predictions, the effect of black oxide surface treatment on friction will be ignored, as suggested in Step 1. Accordingly, the relationship between f and $WV_s^{-\frac{1}{3}}$ and composite surface roughness, for carburized AISI 9310 steel with either Oil E or Oil F, may be approximated by Equations (54) and (55), or Equations (56) and (57), or Equations (60) and (61), as applicable. With honed surfaces, the use of Equations (60) and (61) presents no complication. With ground surfaces, the rather significant effect of the sliding

direction with respect to the grinding grooves should be noted. For example, with ground spur gears, the sliding motion is usually normal to the grinding grooves; thus Equations (56) and (57) for cross-ground surfaces should be used. On the other hand, with helical and spiral bevel gears, the sliding motion is usually at an angle to the grinding grooves; thus an interpolation between Equations (56) and (57) for cross-ground surfaces and Equations (54) and (55) for circumferentially ground surfaces is required. The interpolation procedure will be explained in Sections C and D of Chapter VIII, by reference to specific examples of helical and spiral bevel gears.

3. The calculation of the maximum instantaneous surface temperature rise, ΔT, through the gear mesh utilizes basically Equation (3), repeated herein for convenience:

$$\Delta T = \frac{1.11\, f w \left| \sqrt{V_1} - \sqrt{V_2} \right|}{\beta \sqrt{B}} \qquad (70)$$

In applying this equation, Blok's thermal coefficient, β, is a property of the gear steel (App. A). The instantaneous surface velocities, V_1 and V_2, may be deduced from kinematic analysis. The equation applies directly to spur gears with perfect alignment, which give an instantaneous rectangular contact so that w is simply the instantaneous unit static normal load. With helical gears, the equation applies to an elemental instantaneous contact area, which may be treated as a rectangle. With spiral bevel gears, the instantaneous contact area is an ellipse; thus application of Equation (70) will require an approximation. This is customarily done, as first suggested by Kelley,[18] by replacing the ellipse with an equivalent rectangle of the same major and minor widths as the ellipse and the same maximum Hertz stress at the center. In that case, the quantity w will be replaced by an "equivalent unit load," which is equal to 3w/4.

Calculation of ϕ_{av} of Gears. In calculating the average frictional power loss, ϕ_{av}, in Equation (69), it should be borne in mind that both the sliding velocity, V_s, and the normal load, W, change cyclically through the mesh; and, by Equations (54) to (61), the coefficient of friction, f, also changes cyclically through the mesh. Consider, for example, a set of gears with a contact ratio less than 2, as illustrated in Figure 2. In the course of a mesh cycle, as any one tooth experiences its double-tooth contact in approach from point A to point C, its preceding tooth simultaneously experiences its double-tooth

contact in recess from point B to point D. Following this, the tooth which has reached point C experiences its single-tooth contact from point C to point B. After this, the next mesh cycle begins, with the tooth which is now at point B completing its double-tooth contact in recess from point B to point D, while at the same time a new tooth goes through its double-tooth contact in approach from point A to point C; and the process repeats.

The total frictional heat generated in each mesh cycle is thus

$$\int_A^C \phi(t)\,dt \quad + \quad \int_B^D \phi(t)\,dt \quad + \quad \int_C^B \phi(t)\,dt$$

$$= \left[\int_A^C \phi'(\epsilon)\,d\epsilon \quad + \quad \int_B^D \phi'(\epsilon)\,d\epsilon \quad + \quad \int_C^B \phi'(\epsilon)\,d\epsilon \right] \frac{dt}{d\epsilon}$$

$$= \left[\int_A^C \phi'(\epsilon)\,d\epsilon \quad + \quad \int_B^D \phi'(\epsilon)\,d\epsilon \quad + \quad \int_C^B \phi'(\epsilon)\,d\epsilon \right] \frac{1}{6n_p}$$

where $\phi(t)$ = instantaneous frictional power loss expressed as a function of time, Btu/sec

$\phi'(\epsilon)$ = instantaneous frictional power loss expressed as a function of pinion roll angle, Btu/sec

n_p = rotative speed of pinion, rpm

and the degrees of pinion roll angle per second is

$$\frac{d\epsilon}{dt} = \frac{360\,n_p}{60} = 6n_p$$

Now, in each pinion revolution, as many mesh cycles take place as there are the number of pinion teeth. Moreover, the number of pinion revolutions per second is $n_p/60$. Therefore, the number of mesh cycles per second is equal to $N_p\,(n_p/60)$. Accordingly, the average frictional power loss for the gear set is

$$\phi_{av} = \left[\int_A^C \phi'(\epsilon)\, d\epsilon + \int_C^B \phi'(\epsilon)\, d\epsilon + \int_B^D \phi'(\epsilon) \right] \left(\frac{N_p}{6n_p} \right) \left(\frac{n_p}{60} \right)$$

or

$$\phi_{av} = \left[\int_A^C \phi'(\epsilon)\, d\epsilon + \int_C^B \phi'(\epsilon)\, d\epsilon + \int_B^D \phi'(\epsilon)\, d\epsilon \right] \frac{N_p}{360} \qquad (71)$$

where ϕ_{av} = average frictional power loss of the gear set, Btu/sec

N_p = number of pinion teeth

Equation (71) was derived for a gear set with a contact ratio between 1 and 2. If the contact ratio is greater than 2, a similar reasoning yields

$$\phi_{av} = \left[\sum' \int \phi'(\epsilon)\, d\epsilon \right] \frac{N_p}{360} \qquad (72)$$

For a contact ratio between 2 and 3, the expression in the brackets contains 5 terms, to be integrated over the first triple-tooth contact, the first double-tooth contact, the second triple-tooth contact, the second double-tooth contact, and the third triple-tooth contact.[49] Similarly, for still higher contact ratios, the number of terms in the brackets must be correspondingly increased.

Equation (72) is generally applicable to any gear type at any contact ratio, provided it is noted that the expression for $\phi'(\epsilon)$ must consider the effect of gear type on f, W, and V_s, and provided the number of terms in the brackets is set conmensurate with the contact ratio. The procedure for solving Equation (72) is therefore dependent on the gear design, as will be explained in Sections D, E, and F of this chapter, and also by reference to specific examples in Sections B, C, and D of Chapter VIII.

Selection of C' of Gears. The way Equation (69) is set up, the constant C' is the sole parameter which defines the heat removal characteristics of the gear system. The value of C' is dependent on the heat transfer processes involved, particularly conduction and convection from the meshing gear surfaces; and these processes are

expected to be influenced by gear design, system design, and operating conditions. Confident assessment of the value of C' requires a detailed analysis of the heat transfer processes; and in view of the direct dependence of $(T_s - T_j)$ on C' in Equation (69), it is clear that each case should be examined individually and "rules of thumb" are difficult to apply. Unfortunately, no rational analysis of the heat transfer behavior of gears, or of any rotating lubricated machine elements, is known to have been made to date.[10] Therefore, for the purpose at hand, a tentative guideline, however crude, is required.

The basis of this tentative guideline is the variation of the constant C for sliding-rolling disk systems presented in Figure 25, to which a "correction" is applied to obtain the corresponding value of C' for gear systems. As seen in Figure 25, the value of C for a disk system is markedly influenced by the rate at which the oil supplied by the jet (or jets, or horn) impinges on the meshing surfaces, as well as the system design as it affects heat convection and conduction from the meshing surfaces. For the present purpose, the curve for SwRI disk tester B in Figure 25 will be taken as the basis for estimating purposes. It will be assumed that the value of C' for any gear system is related to the value of C for SwRI disk tester B, at the same oil flow rate, as follows:

$$C' = KC \tag{73}$$

where the factor K accounts for the difference in heat transfer behaviors between the gear system and the reference disk system. The value of K is expected to depend on the gear design, system design, and operating conditions. In general, the oil which is supplied by the jet (or jets, or horn) impinges directly on the meshing surfaces of the disks where frictional heat is generated, and thus performs the best job of removing the frictional heat by convection. This is not so with gears, because the oil jetted toward the gears usually cannot penetrate deep into the gear mesh and tends to break up or atomize due to gear rotation. Moreover, the gear type would be expected to exert a considerable influence on this behavior, with the influence being smaller for spur gears due to their "open" configuration, and greater for helical and spiral bevel gears due to their less "open" configuration.

In addition to heat convection, the effect of heat conduction along the gear shafts is also important. In the disk systems referred to in Figure 25, the disks were straddle-mounted so that there were two

paths to remove the heat by conduction from the disks. With gears that are straddle-mounted, it is clear that there are likewise two heat conduction paths. On the other hand, with overhung gears, heat conduction can take place only along one end of the shafts, so that the heat removal rate is expected to be greatly reduced.

While the general heat transfer behavior described above is believed to be qualitatively correct, the assignment of the quantitative value of K in Equation (73) for different gear types and gear mounting arrangements is of course very difficult. As said before, the authors are not aware of any available information of this kind. In the absence of such information, the following tentative values of K are assumed:

$$K = 1.5 \text{ for straddle-mounted spur gears} \tag{74}$$

$$K = 3.0 \text{ for overhung spur gears} \tag{75}$$

$$K = 2.5 \text{ for straddle-mounted helical and spiral bevel gears} \tag{76}$$

$$K = 5.0 \text{ for overhung helical and spiral bevel gears} \tag{77}$$

The K values given above are admittedly very arbitrary; but no viable and more precise alternative appears possible at this time. They serve at least as a tentative element in the overall predictive framework, until more refined solution to the problem becomes available.

C. Actual Scoring-Limited Power-Transmitting Capacity

It is clear from Equation (67) that in order to predict the actual scoring-limited power-transmitting capacity of the gear set, it is necessary to estimate the misalignment factor, S_m, and the dynamic factor, S_d. Confident assessment of S_m and S_d is, as indicated in Chapters II to V, exceedingly difficult. Empirical correlations are likewise difficult, because even if P_A for a gear set is known by test and the corresponding P_I is obtained from the preceding analysis, one only knows the magnitude of the product $S_m S_d$, but not the individual magnitudes of S_m and S_d. An attempt will be made presently to deduce the probable magnitudes of these two factors, based upon some spur gear scoring test results furnished by AGMA. However, before doing so, an overview of the problem appears in order.

Misalignment Factor. The effect of angular misalignment on

the strength-related failures of spur gear teeth was first examined by Van Zandt,[73] then applied to helical gears by Wellauer,[74] and later adopted for use in the AGMA strength design standards for spur[4] and helical gears.[5] The effect of tooth misalignment on the scoring-limited power-transmitting capacity of spur gears was emphasized by Kelley and Lemanski.[22] The procedure of calculation has been outlined in References 4 and 5.

Using the above-mentioned procedure, the effect of angular misalignment on the value of S_m of spur and helical gears has been calculated and is presented in Figure 28. In this figure, w_t denotes a fictitious unit tangential tooth load, which gives a measure of the so-called load-carrying capacity; e is the angular misalignment; and F is the effective face width. Note that at any value of w_t and F, S_m reduces markedly with increasing e. Note further that, due to elastic deformation across the tooth face, the misalignment effect is substantially reduced with narrow gears and with increased torque or w_t. These latter effects are illustrated in Figure 29 for an angular misalignment of 0.001 rad.

The misalignment problem is considerably more difficult to handle for spiral bevel gears, mainly because the gear surfaces are curved three-dimensionally and therefore misalignment will produce a very complex tooth contact condition. The problem was discussed by Coleman,[75] who stated that aircraft spiral bevel gears frequently require a load distribution factor of 1.4 or more. In the AGMA strength design standard for spiral bevel gears,[6] the load distribution factor is taken as 1.10 to 1.40 for straddle-mounted aircraft-type spiral bevel gears, and 1.25 to 1.50 for overhung-mounted aircraft-type spiral bevel gears. The misalignment factor, S_m, as employed herein, is the reciprocal of the AGMA load distribution factor. Therefore, accepting the AGMA values as being representative, the misalignment factor, S_m, for aircraft-type spiral bevel gears is then in the range of 0.71 to 0.91 if straddle-mounted, and in the range of 0.67 to 0.80 if overhung-mounted.

It is seen that the effect of tooth misalignment in reducing the scoring-limited power-transmitting capacity from the ideal case of perfect alignment is very powerful. A particularly disturbing aspect of the problem is that the misalignment in actual gears can be caused by manufacturing errors, tolerance stackup in the assembly process, support bearing misalignment, shaft deflections under load, and differential thermal expansions of the housing and related components. The situation is so involved, particularly with the more complex gear

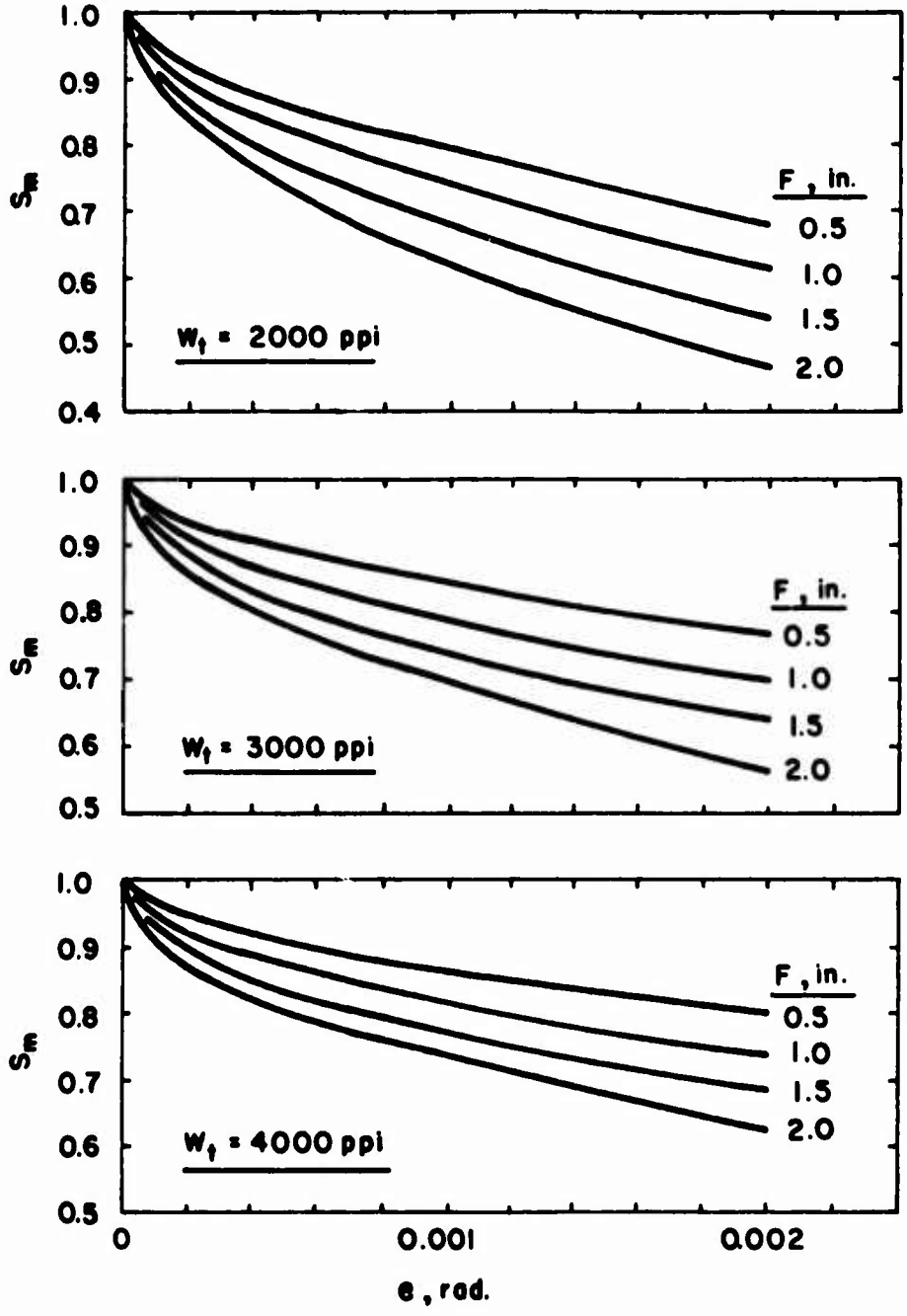

Figure 28. Misalignment factor for spur and helical gears vs. angular misalignment

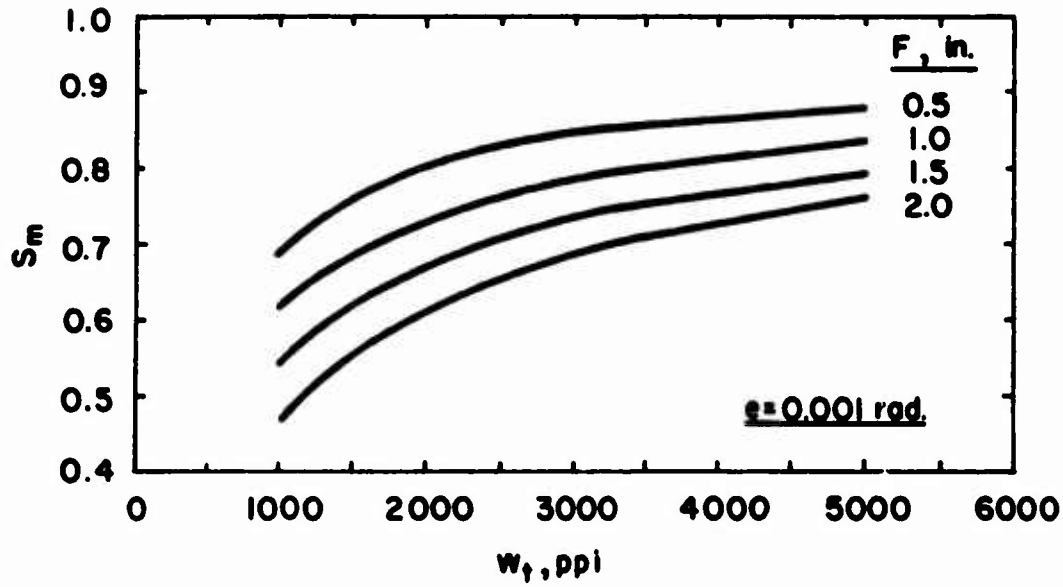

Figure 29. Misalignment factor for spur and helical gears at constant angular misalignment

types, that the net value of e cannot be realistically predicted or controlled in the design process. Measurement of e in an assembled gear set requires extreme accuracy, because S_m is so sensitive to e, especially in the range of low e which is of major interest. Finally, examination of the "contact pattern" across the tooth face can be quite misleading, because "full contact" can be expected unless gross misalignment is present. For example, with spur and helical gears, "full contact" would prevail for any value of S_m of 0.5 or greater, regardless of the combination of F and w_t. In other words, "full contact" would be observed for all values of F up to 1.5 in. shown in Figure 28; but yet the misalignment may be very much in excess of 0.002 rad.

For aircraft power gears, which are designed, manufactured, and assembled with care, it is felt that an angular misalignment of 0.001 rad. may very likely be a realistic optimal limit—an amount significant enough in reducing the power-transmitting capacity from perfect alignment; but small enough so that it could easily escape notice in practice. Thus, in the absence of specific information to the contrary, it is believed that e = 0.001 rad. is probably a fairly reasonable value to use in aircraft-type spur and helical gear design, and Figure 29 can be used to estimate the value of S_m. For aircraft-type spiral bevel gears, an assumed value of S_m of 0.75 for straddle-mounted gears, or 0.70 for overhung gears, is believed to be realistically optimal. If the actual value of S_m should be found to be substantially lower than these target values, more stringent control in design, manufacture, and assembly would appear warranted.

Dynamic Factor. It should be clear from Chapter II, Section F, and Chapters III to V that the dynamic factor is another extremely difficult quantity to handle, both theoretically and practically. However, its pronounced effect in reducing the actual gear performance from ideal can readily be seen from Figure 30.

Figure 30 plots the dynamic factor, S_d, as a function of the pitchline velocity, V_t. The horizontal line designated as K_{v1} and the curves designated as K_{v2} and K_{v3} are taken from the AGMA strength design standard for spur gears.[4] The AGMA strength design standards for helical gears[5] and spiral bevel gears[6] use the same K_{v1} and K_{v2}; but not K_{v3} due essentially to the greater degree of load sharing and hence smoother load transfer in these gear types.

The equations for these AGMA K_v values were given in Chapter III, Section C, but are repeated below for convenience:

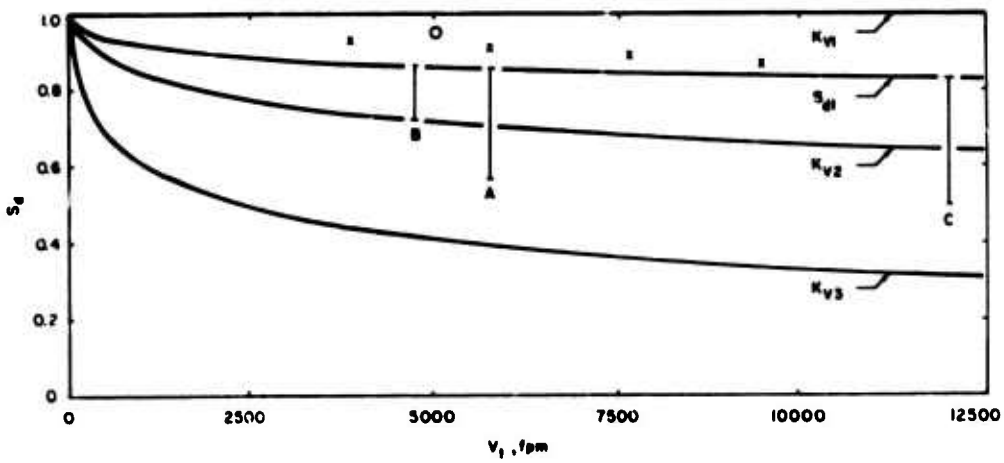

Figure 30. Dynamic factor vs. pitchline velocity

$$K_{v1} = 1 \tag{78}$$

$$K_{v2} = \sqrt{\frac{78}{78 + \sqrt{V_t}}} \tag{79}$$

$$K_{v3} = \frac{50}{50 + \sqrt{V_t}} \tag{80}$$

These equations are empirical and do not explicitly account for the effects of gear and system design, manufacturing errors, and operating variables as discussed, for example, in Chapter III, Section C. It is clear that K_{v1} is in reality a definition of the static load, which is not strictly achievable even for "high precision" gears in theory or practice. At the other extreme, K_{v3} would appear to be rather pessimistic for aircraft-quality spur gears and too pessimistic for aircraft-quality helical and spur gears. In order to provide some measure of flexibility for the purposes of design and performance analysis when no reliable estimate of the system dynamic behavior is available, another empirical dynamic factor, defined as

$$S_{d1} = \frac{K_{v1} + K_{v2}}{2} \tag{81}$$

has been found to be quite helpful.

Figure 30 compares the four curves with the dynamic factors calculated by Tuplin's method (Sect. C, Chaps. III and IV) for an aircraft-type spur gear set at four pitchline velocities (shown by the crosses) and for an aircraft-type helical gear set at one pitchline velocity (shown by a circle), as well as the dynamic factors deduced from the test results for several aircraft-type spur gear sets furnished by AGMA (shown by vertical bars A, B, and C). The deduction of the AGMA data will be discussed presently. It is seen that, if these data are indicative of what may happen in practice, then K_{v2} appears to be a fairly typical average for aircraft-type spur gears, with an uncertainty range as high as S_{d1} and as low as halfway between K_{v2} and K_{v3}.

In view of the enormous complexity of the problem and a lack of other specific information at present, it is suggested that K_{v2} be taken as a reasonable dynamic factor for aircraft spur gears, and S_{d1} as a reasonable dynamic factor for aircraft helical and spiral bevel gears, provided no unusual system dynamic stimulus is present. If substantially lower dynamic factors are suspected in practice, a review of the details of design, manufacture, and system dynamics would seem to be indicated.

AGMA Spur Gear Test Results. As an aid to evaluating the scoring-limited performance of typical aircraft power gears, 13 sets of full-scale spur gear scoring test results were supplied to this program by the Tribology Division, AGMA Aerospace Gearing Committee. Only 5 sets of such data, from tests employing AISI 9310 steel gears and MIL-L-7808 or MIL-L-23699 oils that went far enough to reach scoring, were analyzed and made use of herein in an attempt to deduce the probable values of the misalignment and dynamic factors.

A description of the five AGMA test series, their experimentally determined P_A, and their estimated P_I by the procedure outlined in the preceding section, are detailed in Appendix E. It will be noted that, in each cited case, only one test was available for scoring analysis. Since there is no statistical basis for a single test, it was not thought necessary to estimate the P_I for each case by a full computer program. Rather, making use of the AGMA computer printouts, their results were converted by simple mathematical manipulations, which are identical to the procedure outlined in the preceding section in all respects, except by assuming a different but constant f in each case. The assumption of a constant f for each test is not a drastic one, because scoring generally occurs in the fairly flat region of the f vs. $WV_s^{-\frac{1}{3}}$ curve (Fig. 20). But this assumption greatly simplifies the computations, so that they could easily be handled manually. These rather simple manipulations are explained in detail in Appendix E.

Table E-7 compares the actual and ideal performance of the cases examined. The quantity of special interest here is the ratio of P_A to P_I, which, from Equation (67), is the product of S_m and S_d in each case.

In an effort to estimate the individual values of S_m and S_d for each case when their product is known, it is necessary to assume some value for S_m or S_d and examine whether the resulting S_d or S_m would appear plausible. The process is then repeated until plausible answers are obtained. Table 6 summarizes the results of this type of analysis.

TABLE 6. ESTIMATES FOR MISALIGNMENT AND DYNAMIC FACTORS FOR AGMA SPUR GEAR TESTS

	Series B (Test 272)	Series B (Test 273)	Series A1 (Test 87)	Series A2 (Test 118)	Series A3 (Test 110)	Series C (Test 10)
F, in.	1.55	1.55	0.50	0.50	0.50	0.25
δ_i, μin. AA	15.0	15.0	12.8	30.0	39.0	18.0
V_t, fpm	4760	4760	5749	5749	5749	11968
w_t, ppi	2308	3078	4160	2398	1956	2800
$S_m S_d$	0.71	0.76	0.37	0.32	0.34	0.31
Assume $S_d = S_{d1}$						
S_d	0.87	0.87	0.86	0.86	0.86	0.83
S_m	0.82	0.87	0.43	0.37	0.40	0.37
e, rad.	0.0003	0.0002	0.0104	0.0073	0.0054	0.0120
Assume $S_d = K_{v2}$						
S_d	0.72	(0.76)*	0.71	0.71	0.71	0.64
S_m	0.99	1.00	0.52	0.45	0.48	0.48
e, rad.	~0	0	0.0077	0.0057	0.0042	0.0075
Assume e = 0.005 rad.						
S_m	-	-	0.65	0.50	0.45	0.62
S_d	-	-	0.57	0.64	0.76	0.50

* In this case, a maximum value of $S_m = 1.00$ is assumed. Thus $S_d = 0.76$, which is greater than $K_{v2} = 0.72$.

Table 6 lists the effective face width, F; initial composite surface roughness, δ_i; pitchline velocity, V_t; unit tangential load at scoring, w_t ; and $S_m S_d$ product for the six tests in which scoring was obtained. The values of the $S_m S_d$ product are taken directly from Table E-7 for Series A1, A2, A3, and C. For each of the two tests in Series B, the two $S_m S_d$ products deduced for two assumed oil jet temperatures in Table E-7 are averaged to give a single value listed in Table 6.

Let it first be assumed that the dynamic factor, S_d, in each test is as high as S_{d1} at that particular V_t. Figure 30 or Equation (81) then gives the tabulated value of S_d for the test. Since $S_m = (S_m S_d / S_d)$, then the corresponding value of S_m for the test can be calculated. Knowing this S_m and given F and w_t, the appropriate value of e for the test can be read off Figure 28 by interpolation, or calculated by the AGMA method[4] if e is greater than 0.002 rad. Note from Table 6 that the values of e for the two Series B tests are very small, indicating good alignment in these tests. On the other hand, the values of e for the other four tests appear to be excessive. This is because at values of S_m less than 0.5, less than "full contact" across the tooth face would be expected, and this condition would probably have been noticed by an alert test operator.

Let it now be assumed that the dynamic factor, S_d, in these tests is equal to K_{v2}; then similar calculations will yield the values of S_m and e shown next in Table 6. It is seen that Test B272 would indicate almost perfect tooth alignment. As to Test B273, even the assumption of a perfect tooth alignment would yield $S_d = 0.76/1.00 = 0.76$, which is greater than the assumed $S_d = 0.72$ for Test B272. If it is then assumed that Test B272 also has $S_d = 0.76$, the corresponding misalignment factor would be $S_m = 0.71/0.76 = 0.93$, which gives e = 0.0001 rad., or still an extremely good tooth alignment.

The assumption of $S_d = K_{v2}$ gives significantly more plausible results for the Series A and Series C tests. Note from Table 6 that the values of e are considerably reduced as compared with the case of $S_d = S_{d1}$. Further, the values of S_m are now all close enough to 0.5 so that "full contact" across the tooth face might have resulted, and the presence of the misalignment could have escaped notice.

Finally, if it is assumed that e = 0.005 rad. in the Series A and Series C tests, then the resulting values of S_m, and the corresponding values of S_d, would be as shown at the bottom of Table 6. These S_m values appear, on the whole, to be even more plausible than those given

by the assumption of $S_d = K_{v2}$. However, with the assumed e = 0.005 rad., the S_d values would all be less than K_{v2}.

In reviewing the various values of S_m and S_d presented above, it should be kept in mind that only single tests are involved, so the results should be interpreted with caution. It would appear that perfect tooth alignment would be more likely accidental than realistically achievable; but a misalignment in excess of, say, 0.005 rad. should have been detected by alert test personnel. Thus, selecting only those values of S_d in Table 6 that lie within these misalignment limits, then the probable range of S_d for these tests would be as shown by the vertical bars in Figure 30.

In other words, depending upon what sort of tooth misalignment was assumed for these AGMA spur gear tests, the dynamic factor, S_d, could be as portrayed by the vertical bars shown in Figure 30, giving a rather good average corresponding to K_{v2} but with a large range of uncertainty. This exercise shows clearly that more definitive data on both misalignment and dynamic effects are urgently needed. It also shows that while both factors are important, poor misalignment can easily mask the probable effect of the dynamic load.

In the prediction of the actual scoring-limited power-transmitting capacity of gears, careful assessment of the probable misalignment and dynamic effects is desirable but obviously not easy. In the absence of specific information, performance predictions based on an assumed angular misalignment of 0.001 rad., and an assumed dynamic factor equal to K_{v2} for spur gears or S_{d1} for helical and spiral bevel gears, would appear to be reasonable, though perhaps somewhat optimistic, for aircraft power gear practice.

D. Spur Gear Scoring Prediction

The preceding sections have dealt with the prediction of the ideal and actual scoring-limited power-transmitting capacities of gears in detail, except for those items related to specific gear types. This section will be concerned with those aspects of the predictive procedure dealing specifically with spur gears. The next two sections will deal with helical and spiral bevel gears.

Instantaneous Coefficient of Friction. The quantity f is required in calculating T_s and ΔT, and thus in the prediction of the ideal scoring-limited power-transmitting capacity. As noted in Section B of this chapter, the selection of the proper equations for f for spur gears is

straightforward. Specific examples will be given in Section B of the next chapter.

Quasi-Steady Surface Temperature. The quantity T_s is calculated by Equation (69), and the procedures for calculating ϕ_{av} and assigning the value of the constant C' have been explained in Section B of this chapter.

In calculating ϕ_{av} by Equation (72), note that the instantaneous frictional power loss, ϕ', expressed as a function of the pinion roll angle, ϵ, is given in the computer printout (App. H). With this information, Equation (72) may be solved graphically by plotting ϕ' vs. ϵ and measuring the areas under the curve. However, numerical integration by the computer is by far the easier, as will be explained in Section B of the next chapter. A specific example will be given in Appendix K.

Maximum Instantaneous Surface Temperature Rise. The quantity ΔT is also required in the prediction of the ideal scoring-limited power-transmitting capacity. The basic equation for ΔT is given by Equation (70). For spur gears,

$$B = (32\, w R/\pi \overset{*}{E})^{\frac{1}{2}}$$

$$V_1 = 2\pi \rho_p n_p/60$$

$$V_2 = 2\pi \rho_g n_g/60$$

Substituting the above expressions into Equation (70), and taking $\overset{*}{E} = 33 \times 10^6$ psi, one obtains

$$\Delta T = \frac{15.23\, f w^{\frac{3}{4}} \left| \sqrt{\rho_p n_p} - \sqrt{\rho_g n_g} \right|}{\beta R^{\frac{1}{4}}} \qquad (82)$$

where β is given in Appendix A for AISI 9310 steel.

Critical Temperature. The quantity T_{cr} is required to establish the scoring condition and obtain the ideal scoring-limited power-transmitting capacity. This quantity was dealt with in Section B of this chapter.

Misalignment and Dynamic Factors. The misalignment factor, S_m, and dynamic factor, S_d, are required in the prediction of the actual scoring-limited power-transmitting capacity by Equation (67). If no other specific information is available at the design stage, it is recommended that S_m be based on an assumed angular misalignment of 0.001 rad., and S_d be assumed to be equal to K_{v2}.

E. Helical Gear Scoring Prediction

The prediction of the scoring-limited power-transmitting capacity of helical gears is basically similar to that of spur gears. However, on account of the high contact ratios normally used in helical gears, the load sharing problem is far more complex (Chap. IV, Sect. B). The customary, approximate way to handle the problem has been illustrated in Figure 7. At any instant in the mesh cycle, several pairs of teeth are sharing the total normal tooth load; and the fraction of this load carried by any tooth pair is assumed to be proportional to the ratio of the length of the line of contact on that tooth pair to the total length of lines of contact on all contacting tooth pairs. This is tantamount to assuming that the instantaneous unit static normal load at any point on all lines of contact of all simultaneously contacting teeth at that instant is constant and equal to

$$w = W/L \tag{83}$$

and the instantaneous static normal load carried by any elemental gear tooth with midpoint at M (Fig. 7) is

$$W_i = w\ell = W\ell/L \tag{84}$$

where w = instantaneous unit static load, ppi

W = total static normal load, lb

W_i = instantaneous static normal load on an elemental tooth, lb

L = total length of instantaneous lines of contact on all simultaneously contacting tooth pairs, in.

ℓ = length of line of contact on an elemental tooth, in.

Note that although w is constant at any given instant in the mesh, it is not constant throughout the mesh cycle because L is not constant throughout the mesh cycle. Also, since ℓ is chosen to be an integral divider of the length of the particular instantaneous line of contact on which it lies, it is generally not the same on all simultaneous lines of contact. Accordingly, W_i is generally not constant at any instant spatially and not constant through the mesh cycle.

Instantaneous Coefficient of Friction. As noted in Section B of this chapter, the sliding motion in the helical gear mesh is inclined at an angle to the orientation of the grinding grooves. This orientation effect is taken as a function of the helix angle, and should be accounted for in writing the equations for f. A specific example will be given in Section C of the next chapter.

Quasi-Steady Surface Temperature. The quantity T_s is calculated by Equation (69), and the procedure for assigning the value of the constant C' needs no further comment. The quantity ϕ_{av} is calculated basically by Equation (72) which is general for all gear types. However, some additional manipulations are required due to the manner in which the helical gear analysis is made.

In calculating ϕ_{av} for helical gears, it is first necessary to calculate the elemental contribution $\Delta\phi = \Delta(f W V_s)$ at any arbitrary point M on an instantaneous line of contact (Fig. 7), and to obtain the total instantaneous ϕ along this line by summing all of the elemental contributions over this line. This summation is comparable to ϕ' in Equation (72). If this summation were expressed as a function of the pinion roll angle at the line of contact under consideration, then the successive values of $\phi'(\epsilon)$ obtained as contact progressed over the plane of action could be applied directly to Equation (72).

However, for the sake of convenience, the computer program (App. I) is written with successive lines of contact spaced equal distances apart as a function of their distance f from the initial contact point A, as shown in Figure 7. Since ϕ is thus a function of the linear distance f and not the pinion roll angle ϵ, Equation (72) must be transformed to read

$$\phi_{av} = \left[\frac{\int \phi''(f)\, df}{f_{D'}} \right] \Delta\epsilon \left(\frac{N_p}{360} \right) \qquad (85)$$

where $\phi''(f)$ = instantaneous frictional power loss expressed as a function of parameter f, Btu/sec

$f_{D'}$ = normal distance from the first point of contact A to the final point of contact D' (Fig. 7)

$\Delta\epsilon$ = angle the pinion turns through from the first point of contact A to the final point of contact D', deg

N_p = number of pinion teeth

Note that the integration is performed over the distance f, normal to the instantaneous lines of contact. The bracketed term in Equation (85) represents the average ϕ'' over the plane of action.

The value of $\Delta\epsilon$ is found from the length of the path of contact in the transverse plane as

$$\Delta\epsilon = \frac{2Z}{d_b} \cdot \frac{180}{\pi} \tag{86}$$

where Z = length of path of contact in transverse plane, in.

d_b = base diameter of pinion, in.

The ratio $180/\pi$ converts the expression to angular degrees.

Maximum Instantaneous Surface Temperature Rise. The quantity ΔT at any point M in Figure 7 is obtained by substituting W_i/ℓ for w in Equation (82), thus:

$$\Delta T = \frac{15.23\, f\, (W_i/\ell)^{\frac{3}{4}} \left| \sqrt{\rho_p n_p} - \sqrt{\rho_g n_g} \right|}{\beta R^{\frac{1}{4}}} \tag{87}$$

where all quantities except β, n_p and n_g are the instantaneous values at point M.

Critical Temperature. The quantity T_{cr} was dealt with in Section B of this chapter.

Misalignment and Dynamic Factors. If no other specific information is available at the design stage, it is recommended that the misalignment factor, S_m, be based on an assumed angular misalignment of 0.001 rad.; and the dynamic factor, S_d, be assumed to be equal to S_{d1}.

F. Spiral Bevel Gear Scoring Predictions

The prediction of the scoring-limited power-transmitting capacity of spiral bevel gears is similar in principle to that of helical gears, but with the added complications of the cross-axes arrangement and the varying spiral angle. For the present purpose, the approximate kinematic and static load analyses, due largely to Coleman[66,67] and briefly covered in Chapter V, will be adapted for use.

Instantaneous Coefficient of Friction. As in the case of helical gears, the sliding motion in the spiral bevel gear mesh is also inclined at an angle to the orientation of the grinding grooves. This orientation effect is taken as a function of the spiral angle, and should be accounted for in writing the equations for f. A specific example will be given in Section D of the next chapter.

Quasi-Steady Surface Temperature. The calculation of T_s for spiral bevel gears is similar to that for helical gears, except that the quantity ϕ'' for any instantaneous line of contact is directly calculated (App. J), and a summation along the line is thus not required.

The contact condition in a pair of spiral bevel gears is shown in Figure 10. Motion sweeps across the plane of action in the axial as well as the transverse directions, much as in the helical gear. However, unlike the uniform contact assumed along a contact line in helical gears, the contact in spiral bevel gears is assumed concentrated at the middle of the contact line. Thus to estimate T_s, it is only necessary to integrate over the diagonal length of action, η, the instantaneous values of ϕ'' for a large number of contact lines uniformly spaced over the contact ellipse in the plane of action.

Using an expression similar to Equation (85), ϕ_{av} is then

$$\phi_{av} = \left[\frac{\int \phi''(f)\, df}{\eta}\right] \Delta\epsilon \left(\frac{N_p}{360}\right) \tag{88}$$

where $\phi''(f)$ = instantaneous frictional power loss expressed as a function of parameter f, Btu/sec

f = distance from the center of contact area to a line of contact (Fig. 10), in.

η = length of contact normal to lines of contact, in.

$\Delta\epsilon$ = angle through which the pinion turns from initial contact to final contact, deg.

N_p = number of pinion teeth

The value of $\Delta\epsilon$ in this case is

$$\Delta\epsilon = \frac{Z}{A \sin \gamma} \cdot \frac{180}{\pi} \tag{89}$$

where Z = length of contact in transverse plane, in.

A = mean cone distance, in.

γ = pitch angle of pinion, deg.

Maximum Instantaneous Surface Temperature Rise. In Coleman's analysis,[66] the quantity ΔT at the midpoint on any instantaneous line of contact (Fig. 10) was expressed in terms of the maximum Hertz stress, q_o, at that point. He used basically Kelley's approximation[18] to enter Equation (70). Coleman's expression for ΔT may then be shown to be

$$\Delta T = \frac{\sqrt{\pi}\ f\ q_o\ V_s}{2\beta\left(\sqrt{V_p/d_p} + \sqrt{V_g/d_g}\right)} \tag{90}$$

with

$$q_o = C_p\sqrt{\frac{W_j}{S_G R}} \tag{91}$$

and

$$C_p = \sqrt{\frac{3\overset{*}{E}}{4\pi}} \tag{92}$$

Substituting Equations (91) and (92) into Equation (90), and taking $\overset{*}{E} = 33 \times 10^6$ psi, one obtains

$$\Delta T = \frac{2487\, f\, \sqrt{W_j}\, V_s}{\beta \sqrt{S_G R}\left(\sqrt{V_p/d_p} + \sqrt{V_g/d_g}\right)} \tag{93}$$

In Equations (90) and (93), the kinematic relationships have been dealt with in Chapter V, Section A, while the static load relationships have been dealt with in Chapter V, Section B. Thus, V_s is given by Equation (36), and d_p and d_g by Equations (38) and (39), respectively. V_p and V_g, not previously given, are

$$V_p = \sqrt{V_{Fp}^2 + V_{Pp}^2} \tag{94}$$

$$V_g = \sqrt{V_{Fg}^2 + V_{Pg}^2} \tag{95}$$

where V_{Fp}, V_{Pp}, V_{Fg}, and V_{Pg} are given by Equations (32), (33), (34), and (35), respectively. S_G is given by Equation (43). W_j is given by Equation (45). Note that except for β and $\overset{*}{E}$, which are properties of the gear steel, all other quantities entering Equation (90) or Equation (93) are not constant either spatially or through the mesh cycle.

Critical Temperature. The quantity T_{cr} was dealt with in Section B of this chapter.

Misalignment and Dynamic Factors. If no other specific information is available at the design stage, it is recommended that the misalignment factor, S_m, be taken as 0.75 for straddle-mounted spiral bevel gears and 0.70 for overhung spiral bevel gears, and that the dynamic factor, S_d, be assumed to be equal to S_{d1}.

CHAPTER VIII
GEAR SCORING TEST PROGRAM

A. General

In order to evaluate the validity of the gear scoring prediction method outlined in the preceding chapter, the plan was to select or design typical aircraft-type spur, helical, and spiral bevel gears, and to predict their probable scoring-limited power-transmitting capacities under specified operating conditions. Concurrently, these selected or designed gears were to be procured or manufactured, and then tested under the specified operating conditions to determine their actual scoring-limited power-transmitting capacities. The predicted and the experimentally-determined values were then to be compared.

Recommendations on the specific gear designs and test plans were made with the aid of Bell Helicopter Company (subcontractor) and submitted to the Eustis Directorate, U.S. Army Air Mobility Research and Development Laboratory for prior approval. After USAAMRDL approval was received, the procurement and manufacture of the gears were handled by BHC. Testing of these gears was subsequently performed by BHC under SwRI supervision.

The gear test program originally called for a total of 30 tests, comprising 10 tests each on spur, helical, and spiral bevel gears. The 10 tests on each gear type were further divided into two sets of 5 tests each, with some design feature or test condition varied. All gears were to be made of AISI 9310 CEVM steel, carburized to give an effective case thickness of 0.030-0.040 in., a case hardness of 60-63 R_C, a core hardness of 33-41 R_C, and surface-treated with black oxide as per BHC Specification BPSFW 4084—essentially the same as the test disks used in the disk tests (Chap. VI and App. D). The test oil was to be Oil F (App. A), the same MIL-L-7808G oil used in the disk tests.

The other gear and test details will be given later in Sections B, C, and D of this chapter and in Appendixes F and G. However, the gear test program had undergone certain changes as it developed, and these changes will now be reviewed.

Spur Gears. All spur gears were to be 31 x 76 teeth, with a diametral pitch of 8.5 $in.^{-1}$ Five sets of these gears were to be ground to about 17 μin. AA surface finish and 5 sets honed to about 7 μin. AA surface finish. All tests were to be run at a pinion speed of 8,000 rpm, at an oil jet temperature of 190°F.

As it turned out, the gears received from the vendor were found to be much smoother than specified; but it was decided to proceed with the testing in order to expedite the program. It was also found that the torque capacity of the test rig available at BHC was not enough to score the gears at 190°F oil jet temperature and 8,000 rpm pinion speed. It was felt that increasing the test speed at maximum rig torque capacity was risky. Accordingly, the test plan was modified to test all spur gears at an oil jet temperature of 250°F.

Helical Gears. The helical gears were to be 31 x 138 teeth, with a diametral pitch of 8.5 $in.^{-1}$ and a helix angle of 18.3°. Five sets of these gears were to be tested at 5,000 rpm, and 5 sets at 25,000 rpm. The oil jet temperature was to be 190°F.

As it happened, manufacturing problems were encountered by the vendor, and delivery of the helical gears was repeatedly delayed. It became necessary to modify the program to delete testing of the helical gears entirely.

Spiral Bevel Gears. It was planned to test 5 sets each of two spiral bevel gear designs. One design was to be 22 x 23 teeth, with a diametral pitch of 6.11 $in.^{-1}$, and a spiral angle of 35°. These 5 sets were duly tested at the planned pinion speed of 4,500 rpm and the planned oil jet temperature of 190°F.

The other design was to be 19 x 62 teeth, with a diametral pitch of 6.33 $in.^{-1}$, and a spiral angle of 35°. These 5 sets were to be tested at a pinion speed of 6,000 rpm and an oil jet temperature of 190°F. Due to scheduling problems of the available test rig at BHC, it was not possible to conduct these tests expeditiously. Accordingly, the program was modified to delete the 5 tests on the 19 x 62 spiral bevel gears.

In summary, due to various difficulties encountered, the originally scheduled 30 gear tests were not all run. Rather, only 15 tests were performed, 5 each on the ground spur gears, the honed spur gears, and the 22 x 23 spiral bevel gears.

The subsequent sections of this chapter will first present the predicted scoring-limited power-transmitting capacities of the gear sets, and then compare these with the experimentally-determined values. For the sake of convenience, sample runs of the computer programs are presented in Appendixes H, I, and J for the three gear types. Likewise, summaries of the spur gear and spiral bevel gear

test data are presented in Appendixes F and G, respectively.

B. Spur Gear Test Program

The spur gear test program consisted of replicate tests on 5 sets of ground spur gears and 5 sets of honed spur gears of same design and material, tested for scoring at the same speed and oil jet temperature. Details of the test equipment, test procedure, and results are summarized in Appendix F.

The test gears were made of AISI 9310 CEVM steel, carburized to a case thickness of 0.030-0.040 in., a case hardness of 60-63 R_C, a core hardness of 33-41 R_C, and surface-treated with a black oxide. The dimensions of the pinions and gears are given in Table 7. The measured surface roughnesses in the profile and lead directions of the pinions and gears are presented in Appendix F, where it is estimated that the average initial composite surface, δ_i, was 13.7 μin. AA for the 5 sets of ground gears, and 15.8 μin. AA for the 5 sets of honed gears.

The test oil was Oil F, a MIL-L-7808G synthetic oil.

The tests were conducted at a pinion speed of 8,000 rpm, with the pinion as the driver. The corresponding pitchline velocity was 7,638 fpm. The gears were mounted on vertical shafts, and were lubricated by cascading oil and by an oil jet directed into the mesh. Flow through the oil jet was 0.28 gpm and the oil jet temperature was 250°F. The cascading oil flow rate and temperature were not measured.

Dimensional inspection of the test section housing and bearings revealed that the test rig had an assembled misalignment of 0.0007 rad., with the lower end of the teeth (i.e., the S/N end in Fig. F-2) being more heavily loaded than the upper end. Apart from this, tooth misalignment also resulted from the lead errors on the pinion and gear teeth. An attempt was made to balance the lead errors on the mating pairs of pinions and gears. As shown in Appendix F, the best estimate for the average resultant tooth misalignment was 0.00076 rad. for the ground gear sets, and 0.00084 rad. for the honed gear sets.

Ideal Scoring Power of Ground Spur Gears. The ideal scoring limited power-transmitting capacity of the ground spur gears was estimated by the procedure outlined in Chapter VII. For reasons given in Chapter VII, the critical temperature, T_{cr}, and the coefficient of

TABLE 7. SPUR GEAR DESIGN DATA

	Pinion (Driver)	Gear (Driven)
Number of teeth	31	76
Diametral pitch, in.$^{-1}$	8.5	8.5
Pitch diameter, in.	3.6471	8.9412
Face width, in.	1.375	1.250
Pressure angle, deg	22.0	22.0
Outside diameter, in.	3.907	9.184
Root diameter, in.	3.354	8.632
Mean circular tooth thickness, in.	0.1848	0.1768
Start of tip modification, deg roll	27.49	25.00
End of tip modification, deg roll	32.15	26.89
Nominal slope of tip modification line, in.	-0.00035	-0.00045
Nominal slope of profile slope line, in.	0	0
Nominal slope of tooth slope line, in.	0	0
Maximum allowable errors:		
Tooth to tooth spacing, in.	0.0002	0.0002
Accumulated spacing, in.	0.0006	0.0006
Slope of tip modification line, in.	±0.00015	±0.00015
Slope of profile line, in.	±0.0001	±0.0001
Slope of tooth slope line, in.	±0.00025	±0.00025
Material and surface:		
Material, AISI	9310	9310
Case thickness, in.	0.030-0.040	0.030-0.040
Case hardness, R_C	60-63	60-63
Core hardness, R_C	33-41	33-41
Surface finish, μin. AA	See text	See text

friction, f, are assumed to be those of the plain surfaces, i.e., surfaces as if there were no black oxide surface treatment. In other words, noting that $\delta_i = 13.7$ μin. AA for the ground spur gears, then the critical temperature, from Equation (50), is

$$T_{cr} = 540 - 3.80\,\delta_i = 488°F \tag{96}$$

and the coefficient of friction, from Equations (56) and (57), is

$$f = (0.0755 + 0.00034\,\delta_i)(WV_s^{-\frac{1}{3}})^{-0.3}$$

$$= 0.0802\,(WV_s^{-\frac{1}{3}})^{-0.3}$$

$$\text{at } WV_s^{-\frac{1}{3}} < 200 \tag{97}$$

$$f = 0.0154 + 0.00007\,\delta_i = 0.0164$$

$$\text{at } WV_s^{-\frac{1}{3}} \geq 200 \tag{98}$$

The quasi-steady surface temperature, T_s, is given by Equation (69), which at $T_j = 250°F$ reads

$$T_s = T_j + C'\phi_{av}^{0.80} = 250 + 225\phi_{av}^{0.80} \tag{99}$$

where ϕ_{av} is defined by Equation (72). In estimating the value of C' in Equation (99), the cascading oil is assumed to contribute negligibly toward the cooling of the gear meshing surfaces, since this oil from the upper support bearings is immediately flung off as it falls on the top sides of the gears, and thus has little chance of entering the gear mesh. Accordingly, at an oil jet flow rate of 0.28 gpm, Figure 25 gives C = 150; and C' = 1.5 x 150 = 225 by Equation (74).

The calculation of ϕ_{av} by Equation (72) is straightforward since $\phi'(\epsilon)$ is known from the computer program (App. H) from the

kinematic and static load analyses. The numerical integration process to obtain ϕ_{av} is also written into the computer program. However, to illustrate how this is done, a numerical example will be given in Appendix K.

The maximum instantaneous surface temperature rise, ΔT, is given by Equation (82), with β taken as 42.15 lb/°F-in.sec$^{\frac{1}{2}}$ (App. A). In other words,

$$\Delta T = \frac{0.361\, f\, w^{\frac{3}{4}} \left| \sqrt{\rho_p n_p} - \sqrt{\rho_g n_g} \right|}{R^{\frac{1}{4}}} \qquad (100)$$

The maximum instantaneous surface temperature, T_c, is then

$$T_c = T_s + \Delta T \qquad (101)$$

Equations (97), (98), (99), (72), (100), and (101) are then employed to compute the instantaneous values of T_c in the gear mesh at different power levels. The computer program is presented in Appendix H, along with a sample run at 600 hp. The major computer results at 600 hp and several additional power levels are summarized in Table 8. In this table, P is the power transmitted; W is the normal tooth load, which depends only on P; T_s is the quasi-steady surface temperature, which depends only on P; ΔT is the maximum instantaneous surface temperature rise somewhere in the gear mesh, which depends on both P and mesh position; T_c is the maximum instantaneous surface temperature, which also depends on both P and mesh position; and the critical temperature is constant for the problem.

It will be recalled from Equation (96) that T_{cr} = 488°F in this case. Thus, from Table 8, the ideal scoring-limited power-transmitting capacity, P_I, is expected to be between 900 and 1000 hp. A graphical way to determine the value of P_I is shown in Figure 31, by plotting the tabulated values of T_c vs. P. The intersection of this curve with T_{cr} = 488°F yields P_I equal to 957 hp for the ground spur gears.

Ideal Scoring Power of Honed Spur Gears. With the honed spur gears, the initial composite surface roughness, δ_i, is 15.8 μin.

TABLE 8. IDEAL SPUR GEAR PERFORMANCE SUMMARY

P, hp	W, lb	ϕ_{av}, Btu/sec	T_s, °F	ΔT, °F	T_c, °F	T_{cr}, °F
Ground gears (δ_i = 13.7 μin. AA)						
600	2795.7	0.5763	394.7	18.6	413.4	488
700	3261.7	0.6688	413.1	21.5	434.6	488
800	3727.6	0.7631	431.2	24.2	455.5	488
900	4193.6	0.8595	449.3	26.7	476.0	488
1000	4659.6	0.9583	467.5	28.8	496.3	488
Honed gears (δ_i = 15.8 μin. AA)						
600	2795.7	0.6048	400.5	19.6	420.1	480
700	3261.7	0.7018	419.5	22.6	442.1	480
800	3727.6	0.8005	438.3	25.5	463.8	480
900	4193.6	0.9015	457.1	28.0	485.1	480
1000	4659.6	1.0052	475.9	30.3	506.2	480

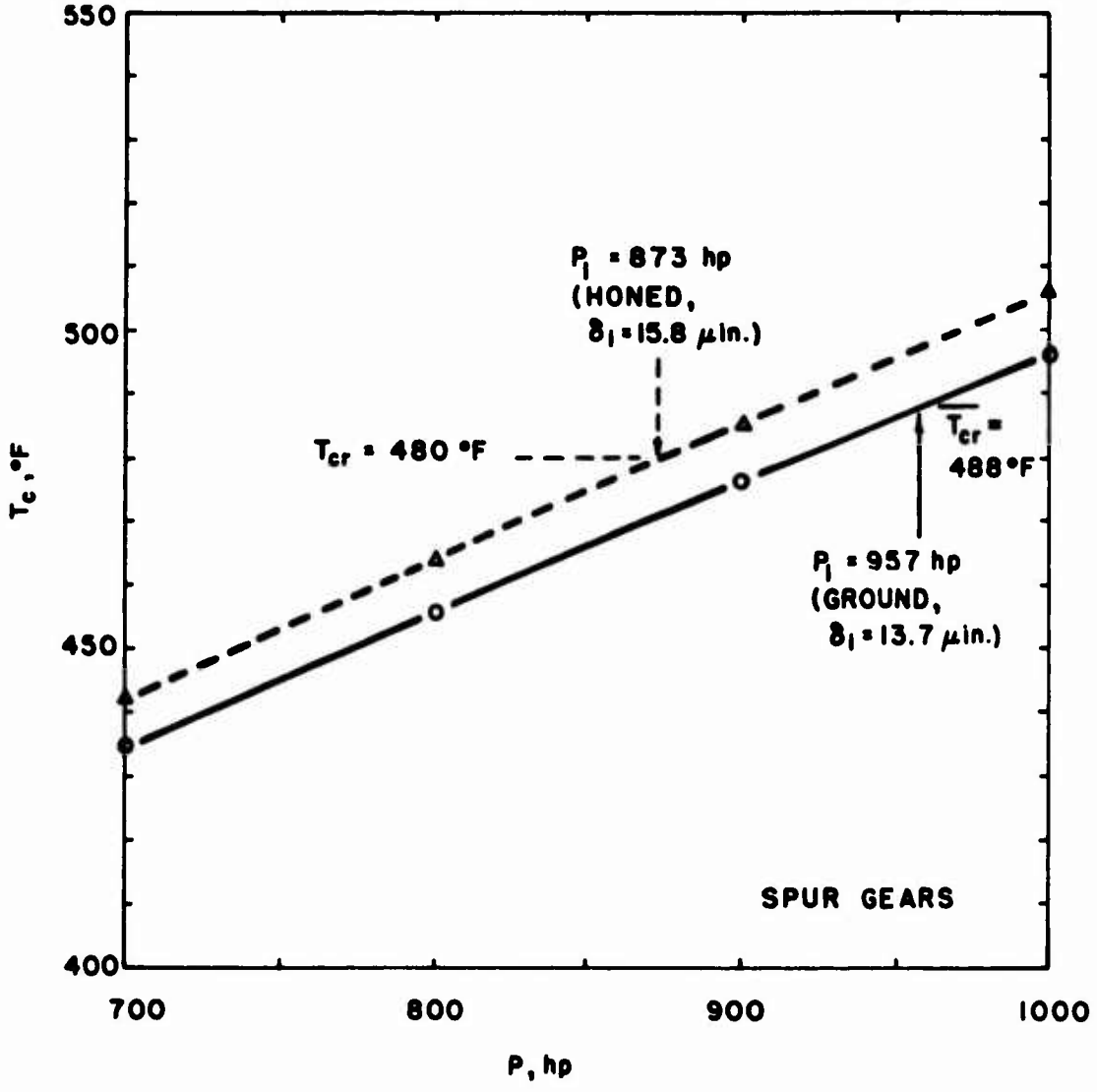

Figure 31. Determination of ideal scoring power of ground and honed spur gears

AA. Accordingly, Equation (50) gives

$$T_{cr} = 540 - 3.80\,\delta_i = 480°F \qquad (102)$$

and Equations (60) and (61) give

$$f = (0.0789 + 0.00034\,\delta_i)(WV_s^{-\frac{1}{3}})^{-0.30}$$

$$= 0.0842\ (WV_s^{-\frac{1}{3}})^{-0.30}$$

$$\text{at } WV_s^{-\frac{1}{3}} < 200 \qquad (103)$$

$$f = 0.0161 + 0.00007\,\delta_i = 0.0172$$

$$\text{at } WV_s^{-\frac{1}{3}} \geq 200 \qquad (104)$$

It is clear that Equations (99), (100), and (101) apply equally to this case, by noting that f will now be defined by Equations (103) and (104).

Equations (99), (72), (100), (101), (103), and (104) are now employed in the computer program in the same manner as in the preceding case. A summary of the major computer results is presented in Table 8. A plot of T_C vs. P for this case is shown dashed in Figure 31. The ideal scoring-limited power-transmitting capacity, P_I, is then equal to 873 hp for the honed spur gears.

Actual Scoring Power of Ground Spur Gears. In order to predict the actual scoring-limited power-transmitting capacity, it is necessary to estimate the misalignment factor, S_m, and the dynamic factor, S_d, and then apply Equation (67).

In order to estimate S_m, both the angular misalignment, e, and the unit tangential tooth load, w_t, are required. The unit tangential tooth load for any gear set is

$$w_t = \frac{126050\,P}{n_p\,d\,F} \qquad (105)$$

where w_t = unit tangential tooth load, ppi

P = power transmitted, hp

n_p = pinion speed, rpm

d = pitch diameter of pinion, in.

F = effective face width, in.

For the ground gear sets, the average tooth misalignment, e, was, as stated previously, estimated to be 0.00076 rad. At P_I = 957 hp, the unit tangential tooth load, w_t, is (126050 x 957)/(8000 x 3.6471 x 1.25) = 3308 ppi. Accordingly, with e = 0.00076 rad. and w_t = 3308 ppi, Figure 28 gives S_m = 0.80 by interpolation.

To estimate the dynamic factor, it is assumed that $S_d = K_{v2}$ (Chap. VII, Sect. D). The pitchline velocity is V_t = 7638 fpm. At this V_t, Figure 30 gives $S_d = K_{v2}$ = 0.68.

Having thus estimated the values of S_m and S_d, Equation (67) then gives a predicted actual scoring-limited power-transmitting capacity of

$$P_A = P_I S_m S_d$$

$$= 957 \times 0.80 \times 0.68 = 521 \text{ hp}$$

This predicted P_A may be compared with the experimentally determined P_A given in Appendix F. If the comparison is made with the average experimentally determined P_A of >679 hp, then the prediction is at least 23 percent too low. Such a comparison is, however, not correct because the average P_A has no statistical meaning. The proper basis of comparison should be the statistically deduced, experimentally determined P_A of 507 hp. On this basis, the prediction is seen to be only 3 percent too high.

Actual Scoring Power of Honed Spur Gears. As stated earlier, the average tooth misalignment for the honed spur gears was 0.00084

rad. At P_I = 873 hp, w_t = (126050 x 873)/(8000 x 3.6471 x 1.25) = 3017 ppi. At e = 0.00084 and w_t = 3017 ppi, Figure 28 gives S_m = 0.78.

Let it be assumed again that $S_d = K_{v2} = 0.68$ at V_t = 7638 fpm. Then the predicted P_A is

$$P_A = 873 \times 0.78 \times 0.68 = 463 \text{ hp}$$

Appendix F shows that the average experimentally determined P_A is 606 hp, and the statistically deduced, experimentally determined P_A is 425 hp. As argued earlier, the proper basis of comparison is the statistically deduced P_A of 425 hp. On this basis, it is seen that the predicted P_A is 9 percent too high.

C. Helical Gear Test Program

As mentioned earlier, the helical gear test program was not run. However, a computer program for helical gears has been written (App. I), the basis for which will be explained.

The test gears intended for the test program were to be made of AISI 9310 CEVM steel, carburized and surface-treated with a black oxide as shown in Table 9, which also presents the design data. The surface finish on both pinion and gear was specified to be 22 μin. AA maximum. If the gears were produced to this maximum surface finish, then, by Equation (B-4) in Appendix B, the initial composite surface roughness of a gear set would be $\delta_i = 3\,(22 + 22)/4 = 33$ μin. AA.

The test oil was to be Oil F, a MIL-L-7808G synthetic oil.

The tests were to be run at a pinion speed of 5,000 rpm, with the pinion as the driver. The corresponding pitchline velocity is 5,028 fpm. The oil jet temperature was to be 190°F.

Ideal Scoring Power of Helical Gears. For reasons given in Chapter VII, the critical temperature, T_{cr}, and the coefficient of friction, f, are herein assumed to be those of the plain surfaces, i.e., surfaces as if no black oxide were present. Therefore, at the assumed value of δ_i = 33 μin. AA, Equation (50) gives

$$T_{cr} = 540 - 3.80\,\delta_i = 415°F \qquad (106)$$

TABLE 9. HELICAL GEAR DESIGN DATA

	Pinion (Driver)	Gear (Driven)
Number of teeth	31	138
Diametral pitch (normal plane), in.$^{-1}$	8.5	8.5
Pitch diameter, in.	3.8413	17.6998
Face width, in.	2.500	2.380
Pressure angle (normal plane), deg	22.0	22.0
Outside diameter, in.	4.032	17.290
Root diameter, in.	3.528	16.786
Mean circular tooth thickness (normal plane), in.	0.1782	0.1782
Helix angle, deg	18.2966	18.2966
Lead of helix, in.	36.5000	162.4681
Hand of helix	LH	RH
Start of tip modification, deg roll	26.88	25.18
End of tip modification, deg roll	30.74	25.95
Nominal slope of tip modification line, in.	0.00008	0.00008
Nominal slope of profile slope line, in.	0	0
Nominal slope of tooth slope line, in.	0	0
Maximum allowable errors:		
Tooth to tooth spacing, in.	0.0002	0.0003
Accumulated spacing, in.	0.0006	0.0010
Slope of tip modification line, in.	±0.00008	±0.00008
Slope of profile slope line, in.	±0.0002	±0.0002
Slope of tooth slope line, in.	±0.0015	±0.0002
Material and surface:		
Material, AISI	9310	9310
Case thickness, in.	0.030-0.040	0.030-0.040
Case hardness, R_C	60-63	60-63
Core hardness, R_C	33-41	33-41
Surface finish, μin. AA max.	22	22

To calculate the coefficient of friction, note that the direction of sliding in helical gears is not normal, but inclined, to the orientation of the grinding grooves. In this case, the helix angle of the gear set is $\psi = 18.2966°$, so the direction of sliding makes an angle of $90 - 18.2966 = 71.7034°$ to the grinding grooves; and $\cot(71.7034°) = 0.33065$. An approximate way to account for this orientation effect is to interpolate between Equations (56) and (57) for the cross-ground situation and Equations (54) and (55) for the circumferentially-ground situation. The equations for f are then approximately

$$f = \left[0.0755 + 0.33065\,(0.0920 - 0.0755) + 0.00034\,\delta_i\right](WV_s^{-\frac{1}{3}})^{-0.30}$$

$$= (0.0810 + 0.00034\,\delta_i)(WV_s^{-\frac{1}{3}})^{-0.30}$$

$$= 0.0922\,(WV_s^{-\frac{1}{3}})^{-0.30} \qquad \text{at } WV_s^{-\frac{1}{3}} < 200 \qquad (107)$$

$$f = 0.0154 + 0.33065\,(0.0188 - 0.0154) + 0.00007\,\delta_i$$

$$= 0.0165 + 0.00007\,\delta_i = 0.0188 \qquad \text{at } WV_s^{-\frac{1}{3}} \geq 200 \qquad (108)$$

The quasi-steady surface temperature, T_s, is given by Equation (69), thus:

$$T_s = T_j + C'\phi_{av}^{0.80} = 190 + 312.5\,\phi_{av}^{0.80} \qquad (109)$$

where ϕ_{av} is now defined by Equation (85). In assigning the value of

C', it is assumed that the oil jet flow rate is 0.60 gpm. Then Figure 25 gives C = 125, and Equation (76) yields C' = 2.5 x 125 = 312.5.

The computation of ϕ_{av} by Equation (85) is accomplished by the computer program (App. I) as explained in Chapter VII, Section E. A numerical example for this computation will be given in Appendix K.

The maximum instantaneous surface temperature rise, ΔT, is given by Equation (87), with β = 42.15 lb/°F-in.sec$^{\frac{1}{2}}$.

The maximum instantaneous surface temperature, T_c, is thus given by Equation (101).

Equations (107), (108), (109), (85), (87), and (101) are then employed in the computer program to compute the instantaneous values of T_c at various points on various instantaneous lines of contact in the gear mesh, at different power levels. The computer program is presented in Appendix I, along with a sample run at 600 hp. The major computer results at 600 hp and several additional power levels are summarized in Table 10. The symbols in Table 10 are defined the same way as in Table 9, except that ΔT and thus T_c are the maximas somewhere on one of the instantaneous lines of contact somewhere in the mesh.

Figure 32 presents a plot of T_c vs. P given in Table 10. At the assumed T_j = 190°F, the figure yields a predicted ideal scoring-limited power-transmitting capacity, P_I, of 1210 hp.

As a matter of interest, Figure 32 also shows the ideal performance for an assumed T_j = 250°F, the same oil jet temperature at which the spur gears were tested. For this case, Equation (109) should be changed to read $T_s = 250 + 312.5\,\phi_{av}^{0.80}$, with all other equations remaining the same. The corresponding performance is shown dashed in Figure 32, and the corresponding predicted P_I is 796 hp.

Actual Scoring Power of Helical Gears. In the absence of other specific information, let it be assumed that the gear misalignment is e = 0.001 rad. The procedure for estimating the misalignment factor, S_m, of spur gears will be employed for helical gears as well. The procedure will yield S_m = 0.68 for the case of T_j = 190°F, and S_m = 0.61 for the case of T_j = 250°F.

In estimating the dynamic factor, S_d, it will be assumed, in

TABLE 10. IDEAL HELICAL GEAR PERFORMANCE SUMMARY

P, hp	W, lb	ϕ_{av}, Btu/sec	T_s, °F	ΔT, °F	T_c, °F	T_{cr}, °F
T_j = 190°F						
600	4471.4	0.2690	299.3	26.1	325.4	415
700	5216.6	0.3115	312.9	27.9	340.8	415
800	5961.9	0.3541	326.2	29.7	355.9	415
900	6707.1	0.3973	339.3	31.3	370.6	415
1000	7452.3	0.4404	352.2	32.8	385.0	415
1100	8197.4	0.4835	364.7	34.3	399.0	415
1200	8942.8	0.5265	377.1	36.6	413.6	415
1300	9688.0	0.5695	389.2	38.8	428.0	415
1400	10433.2	0.6124	401.1	41.1	442.2	415
T_j = 250°F						
600	4471.4	0.2690	359.3	26.1	385.4	415
700	5216.6	0.3115	372.9	27.9	400.8	415
800	5961.9	0.3541	386.2	29.7	415.9	415
900	6707.1	0.3973	399.3	31.3	430.6	415
1000	7452.3	0.4404	412.2	32.8	445.0	415
1100	8197.4	0.4835	424.7	34.3	459.0	415
1200	8942.8	0.5265	437.1	36.6	473.6	415
1300	9688.0	0.5965	449.2	38.8	488.0	415
1400	10433.2	0.6124	461.1	41.1	500.2	415

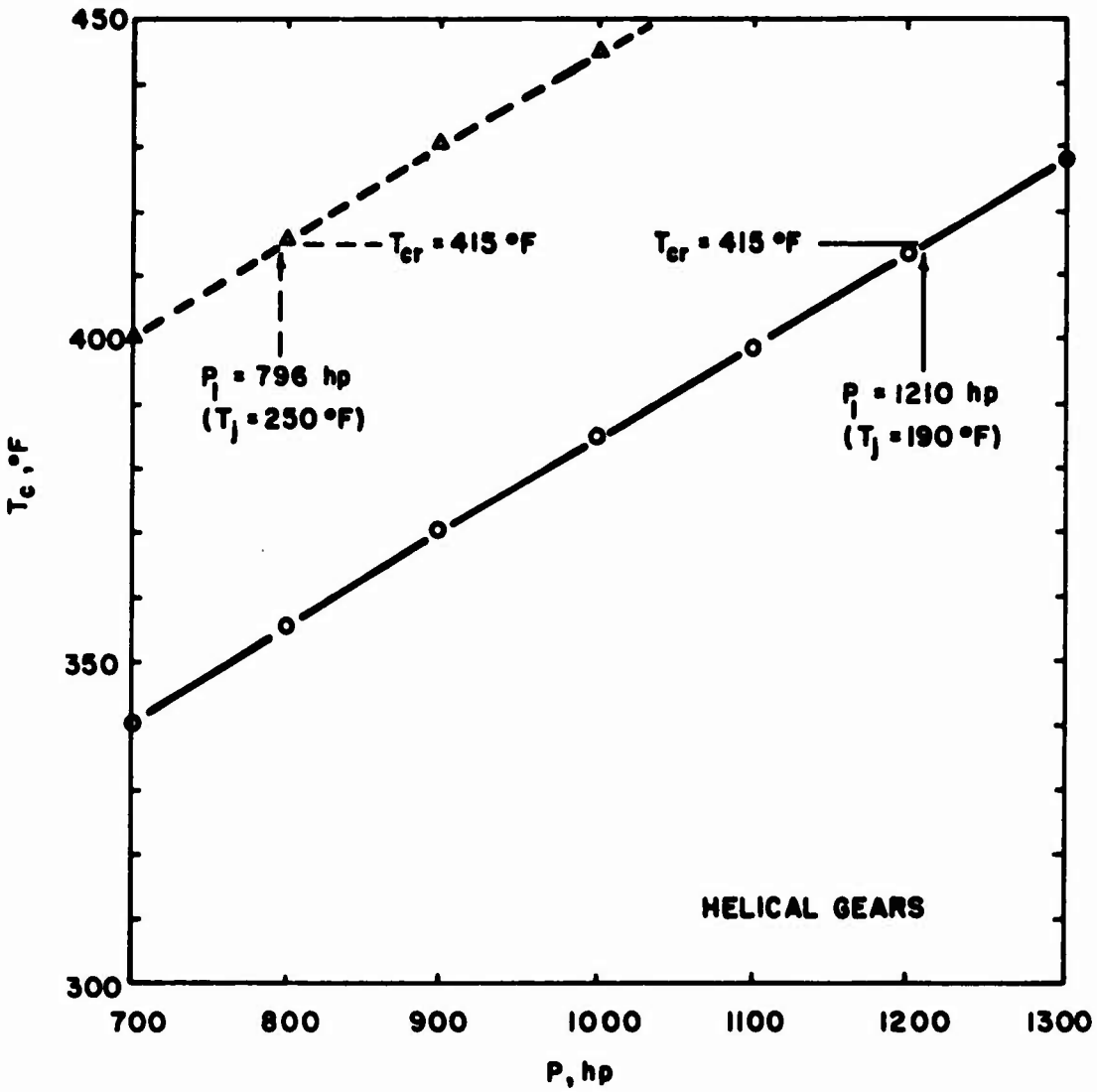

Figure 32. Determination of ideal scoring power of helical gears

the absence of other specific information, that $S_d = S_{dl}$ for helical gears. At $V_t = 5028$ fpm, Figure 30 gives $S_d = S_{dl} = 0.86$.

From Equation (67), the predicted actual scoring-limited power-transmitting capacity is thus $P_A = 708$ hp for the case of $T_j = 190°F$, and $P = 418$ hp for the case of $T_j = 250°F$. The powerful influence of the oil jet temperature on scoring-limited power-transmitting capacity is clearly indicated.

The quality of the above predictions is not known, since no tests were actually conducted.

D. Spiral Bevel Gear Test Program

As mentioned earlier, only one design of spiral bevel gears was tested. The predicted performance and experimentally determined performance of these gears will now be compared.

The spiral bevel gears in question were made of AISI 9310 CEVM steel, carburized and surface-treated with a black oxide as shown in Table 11, which also presents the design data. As in the case of the helical gears, the surface finish of the spiral bevel gears was specified to be 22 μin. AA maximum. Attempts were made to measure the actual surface roughness of these gears, but without success (App. G). Accordingly, for the present estimating purposes, a surface finish of 22 μin. AA on both pinion and gear is assumed. The corresponding initial composite surface roughness of the gear set is then $\delta_i = 3(22 + 22)/4 = 33$ μin. AA by Equation (B-4) in Appendix B.

The test oil was Oil F, a MIL-L-7808G synthetic oil.

The tests were conducted at a pinion speed of 4,500 rpm, with the pinion as the driver. The corresponding pitchline velocity is 4,241 fpm. The oil jet temperature was 190°F. The oil jet flow rate was 0.45 gpm.

Ideal Scoring Power of Spiral Bevel Gears. For reasons given in Chapter VII, the critical temperature, T_{cr}, and the coefficient of friction, f, are assumed to be those of the plain surfaces, i.e., surfaces as if no black oxide were present. Consequently, at the assumed value of $\delta_i = 33$ μin. AA, Equation (50) gives

$$T_{cr} = 540 - 3.80\,\delta_i = 415°F \qquad (110)$$

TABLE 11. SPIRAL BEVEL GEAR DESIGN DATA

	Pinion (Driver)	Gear (Driven)
Number of teeth	22	23
Diametral pitch, $in.^{-1}$	6.111	6.111
Pitch diameter, in.	3.6000	3.7637
Face width, in.	0.871	0.871
Pressure angle, deg	22.5	22.5
Outside diameter, in.	3.794	3.935
Mean circular tooth thickness, in.	0.213	0.208
Outer cone distance, in.	2.604	2.604
Mean cone distance, in.	2.171	2.171
Working depth, in.	0.258	0.258
Whole depth, in.	0.289	0.289
Addendum, in.	0.134	0.124
Dedendum, in.	0.155	0.165
Pitch apex to crown, in.	1.789	1.710
Outer normal top land, in.	0.073	0.058
Mean normal top land, in.	0.073	0.077
Inner normal top land, in.	0.074	0.062
Outer normal backlash, in.	0.004	0.006
Pitch angle, deg	43.727	46.273
Face angle to flank, deg	46.244	48.556
Root angle, deg	41.444	43.756
Dedendum angle, deg	2.283	2.517
Outer spiral angle, deg	44.835	44.835
Mean spiral angle, deg	35.000	35.000
Inner spiral angle, deg	25.990	25.990
Hand of spiral	LH	RH
Material, AISI	9310	9310
Case thickness, in.	0.030-0.040	0.030-0.040
Case hardness, R_C	60-63	60-63
Core hardness, R_C	33-41	33-41
Surface finish, μin. AA max.	22	22

In calculating the coefficient of friction, f, it is noted that the mean spiral angle of the gear set is $\psi = 35°$. Thus, the sliding motion makes an angle of $90 - 35 = 65°$ to the grinding grooves. Thus, using the same procedure as for the helical gears, and noting that $\cot 65° = 0.70021$, the approximate equations for f are

$$f = \left[0.0755 + 070021\ (0.0920 - 0.0755) + 0.00034\ \delta_i \right] (WV_s^{-\frac{1}{3}})^{-0.30}$$

$$= (0.0871 + 0.00034\ \delta_i)\ (WV_s^{-\frac{1}{3}})^{-0.30}$$

$$= 0.0983\ (WV_s^{-\frac{1}{3}})^{-0.30}$$

$$\text{at } WV_s^{-\frac{1}{3}} < 200 \qquad (111)$$

$$f = 0.0154 + 0.70021\ (0.0188 - 0.0154) + 0.00007\ \delta_i$$

$$= 0.0178 + 0.00007\ \delta_i = 0.0201 \qquad (112)$$

The quasi-steady surface temperature, T_s, is again given by Equation (69), so

$$T_s = T_j + C'\phi_{av}^{0.80} = 190 + 675\ \phi_{av}^{0.80} \qquad (113)$$

where ϕ_{av} is defined by Equation (88). In this case, at an oil jet flow rate of 0.45 gpm, C = 135 from Figure 25, and $C' = 5 \times 135 = 675$ from Equation (77).

The computation of ϕ_{av} by Equation (88) is accomplished by the computer program (App. J), as explained in Chapter VII, Section F. A numerical example of this computation will be given in Appendix K.

The maximum instantaneous surface temperature rise, ΔT, is

given by Equation (90), with β = 42.15 lb/°F-in.-sec$^{\frac{1}{2}}$.

The maximum instantaneous surface temperature, T_C, is given by Equation (101).

Equations (111), (112), (113), (88), (90), and (101) are then employed in the computer program to compute the maximum instantaneous values of T_C through the mesh at different power levels. The computer program is presented in Appendix J, along with a sample run at 600 hp. The major computer results at 600 hp and several additional power levels are summarized in Table 12. In this table, W_t is the tangential tooth load, and ΔT and T_C are the maximas on an instantaneous line of contact somewhere in the mesh.

Figure 33 presents a plot of T_C vs. P given in Table 12. At T_j = 190°F, the predicted ideal scoring-limited power-transmitting capacity is seen to be P_I = 627 hp.

Figure 33 also presents a plot of T_C vs. P for T_j = 250°F. By increasing T_j to 250°F, it is seen that P_I is reduced to 420 hp.

Actual Scoring Power of Spiral Bevel Gears. In the absence of other specific information, the misalignment factor for the overhung spiral bevel gear set is taken as S_m = 0.70, in accordance with the recommendation made in Chapter VII, Section F. The pitchline velocity is V_t = 4241 fpm. Thus, from Figure 30, $S_d = S_{dl}$ = 0.87.

Applying Equation (67), the predicted actual scoring-limited power-transmitting capacity is then

$$P_A = 627 \times 0.70 \times 0.87 = 382 \text{ hp}$$

for the case of T_j = 190°F. From Appendix G, the average experimentally-determined P_A at T_j = 190°F is 367 hp, and the statistically deduced, experimentally determined P_A is 346 hp. The latter value, which is statistically more meaningful, should be used as the basis for comparison. It is seen that the predicted P_A is 10 percent too high.

The predicted actual scoring-limited power-transmitting capacity of the same gears, if operated at an oil jet temperature of 250°F, is

$$P_A = 420 \times 0.70 \times 0.87 = 256 \text{ hp}$$

TABLE 12. IDEAL SPIRAL BEVEL GEAR PERFORMANCE SUMMARY

P, hp	W_t, lb	ϕ_{av}, Btu/sec	T_s, °F	ΔT, °F	T_c, °F	T_{cr}, °F
T_j = 190°F						
300	2333.3	0.1013	298.1	20.5	318.7	415
400	3111.1	0.1333	324.7	24.2	348.9	415
500	3888.8	0.1651	349.8	28.6	378.4	415
600	4666.6	0.1975	374.4	32.8	407.3	415
700	5444.3	0.2299	398.3	36.9	435.1	415
800	6222.1	0.2623	421.4	40.7	462.1	415
T_j = 250°F						
300	2333.3	0.1029	358.1	20.5	378.7	415
400	3111.1	0.1353	384.7	24.2	408.9	415
500	3888.8	0.1676	409.8	28.6	438.4	415
600	4666.6	0.2005	434.4	32.8	467.3	415
700	5444.3	0.2334	458.3	36.9	495.1	415
800	6222.1	0.2662	481.4	40.7	522.1	415

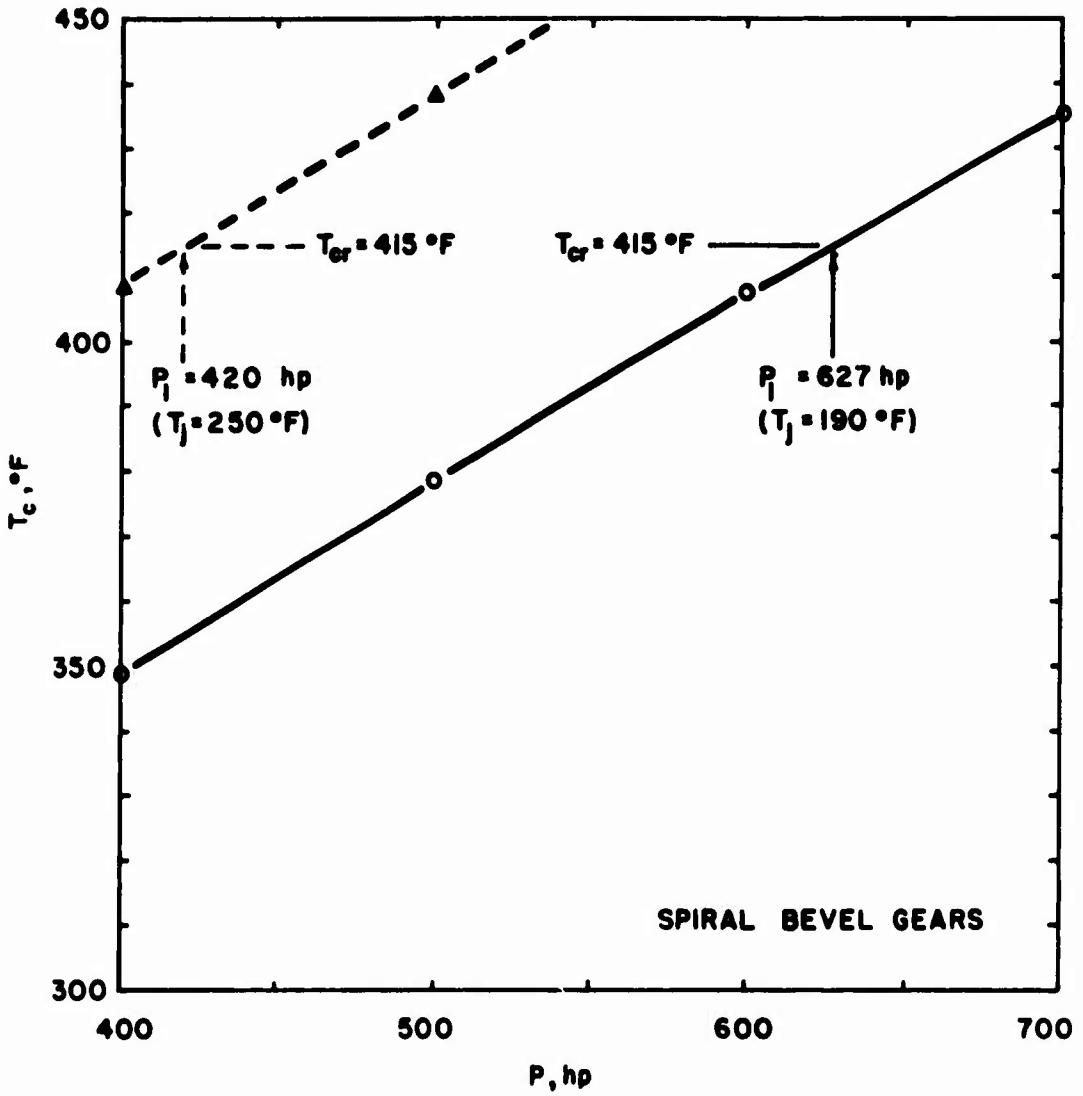

Figure 33. Determination of ideal scoring power of spiral bevel gears

which is much lower than that predicted for T_j = 190°F. However, no test data are available for comparison in this instance.

CHAPTER IX
CONCLUSIONS AND RECOMMENDATIONS

A. Conclusions

A method has been devised for predicting the scoring potential and scoring-limited power-transmitting capacity of spur, helical, and spiral bevel gears. Computer programs for making such predictions for the three gear types have been written and are presented herein.

In order to evaluate the quality of the predictions made, full-scale scoring tests have been performed on typical aircraft-quality gears by Bell Helicopter Company, the subcontractor. The predicted scoring-limited power-transmitting capacities have been found to be within 10 percent of the statistically deduced test results from two series of tests on spur gears and one series of tests on spiral bevel gears. Helical gears were not tested in this program, due to difficulties encountered by the subcontractor in the scheduling of gear manufacturing and testing.

The predictive scheme comprises basically two steps. The first step involves the prediction of the ideal scoring-limited power-transmitting capacity, assuming perfect tooth alignment and no dynamic tooth load. The probable, actual scoring-limited power-transmitting capacity is then deduced from the ideal scoring-limited power-transmitting capacity by applying corrections for the misalignment and dynamic effects.

Due to the current lack of a fundamental understanding of the mechanism of scoring, the thermal behavior involved, and the detailed effects of gear mechanics, a completely rational approach in gear scoring prediction is deemed impossible at this time. On the other hand, a basically empirical procedure, such as the current AGMA gear scoring design guide,[3] leaves much to be desired. The proposed scheme is accordingly in the nature of an engineering compromise, which recognizes the importance of the above-mentioned basic problems but accepts certain approximations imposed by the current state of the art.

The key assumption involved in the methodology presented herein is that the effects of tooth misalignment and dynamic tooth load can be isolated in the prediction of the ideal scoring-limited power-transmitting capacity, and later separately accounted for in the

assessment of the actual scoring-limited power-transmitting capacity. Once this assumption is accepted, the entire predictive scheme is relatively straightforward; and the only tasks that remain are those of establishing the various functional relationships and the magnitudes of the several constants and coefficients involved.

In the prediction of the ideal scoring-limited power-transmitting capacity, Blok's well-known critical temperature hypothesis[16, 19, 23] has been modified in several respects, including quantitative descriptions of the critical temperature and the coefficient of tooth friction, based on data derived from steady-operating sliding-rolling disk tests. Perhaps the most important advance that has been made here is a technique for estimating the quasi-steady surface temperature of gears, which has been a totally neglected subject so far. However, due to a lack of information on the heat transfer behavior of gear systems, the quantitative magnitude of the constant C' in Equation (69) had to be assigned rather arbitrarily.

In the prediction of the actual scoring-limited power-transmitting capacity, the major tasks have been assigning the quantitative magnitudes of the misalignment factor and dynamic factor. The approach employed herein follows basically the AGMA procedure for rating the strength of gear teeth.[4-6] The numerical constants have been deduced from five sets of spur gear scoring test results made available to this program by AGMA.

It goes without saying that the basic equations and particularly the numerical constants and coefficients used herein are tentative, since they were deduced from a rather limited data base. Refinements or improvements are to be expected as additional disk and gear test results become available.

B. Recommendations

The mechanism of scoring has been a subject of serious research for almost 40 years, since Blok published his first paper in 1937.[16] Any refinements on this hypothesis that have been introduced since that time have been relatively minor. The general concept of a critical temperature for scoring can neither be defended nor be refuted on strictly theoretical ground. It appears that further understanding of the mechanism of scoring will require a fundamental approach backed up by detailed, combined theoretical analysis and sophisticated experimental observations.

Granting the tentative nature of the predictive scheme presented herein, the results clearly emphasize the importance of the thermal behavior of the gear system in affecting the quasi-steady gear surface temperature, and of the effects of misalignment and dynamic load on transient tooth action and hence on scoring. A definitive understanding of these three facets of gear performance is sorely needed, either to improve the predictive methodology as proposed herein, or hopefully to enable the development of a completely rational scheme of gear scoring prediction.

REFERENCES

1. "Gear Nomenclature—Terms, Definitions, and Abbreviations," AGMA Standard 112.04, Aug. 1965.

2. "Nomenclature of Gear-Tooth Wear and Failure," AGMA Standard 110.03, Jan. 1962.

3. "Gear Scoring Design Guide for Aerospace Spur and Helical Power Gears," AGMA Information Sheet 217.01, Oct. 1965.

4. "Rating the Strength of Spur Gear Teeth," AGMA Standard 220.02, Aug. 1966.

5. "Rating the Strength of Helical and Herringbone Gear Teeth," AGMA Standard 221.02, Jul. 1965.

6. "Rating the Strength of Spiral Bevel Gear Teeth," AGMA Standard 223.01, Jan. 1964.

7. Rabinowicz, E., Friction and Wear Materials, John Wiley & Sons, New York, 1965.

8. Archard, J. F., "Wear," Interdisciplinary Approach to Friction and Wear, NASA Spec. Publ. 181, 1968.

9. Ku, P. M., "Tribology of Gears and Splines," Proc. Tribology Workshop, NSF, 1974.

10. Ku, P. M., "Gear Failure Modes—Importance of Lubrication and Mechanics," ASLE Annual Meeting, Atlanta, Ga., May 5-9, 1975.

11. Littmann, W. E., "The Mechanism of Contact Fatigue," Interdisciplinary Approach to the Lubrication of Concentrated Contacts, NASA Spec. Publ. 237, 1970.

12. Landen, E. W., "Slow-Speed Wear of Steel Surfaces Lubricated by Thin Oil Films," ASLE Trans., Vol. 11, 1968.

13. Buckingham, E., Analytical Mechanics of Gears, McGraw-Hill Book Co., New York, 1949.

14. Dudley, D. W., Practical Gear Design, McGraw-Hill Book Co., New York, 1954.

15. Merritt, H. E., Gears, Pitman & Sons, London, 1954.

16. Blok, H., "Les temperature des surface dans des condition de graissage sous pression extreme," Congr. mondial pétrole, 2 me Congr., Vol. 3, 1937.

17. Blok, H., "Theoretical Study of Temperature Rise at Surface of Actual Contact under Oiliness Lubricating Conditions," Proc. Gen. Disc. on Lubrication, IMechE, 1937.

18. Kelley, B. W., "A New Look at the Scoring Phenomena of Gears," SAE Trans., Vol. 61, 1953.

19. Blok, H., "Lubrication as a Gear Design Factor," Proc. Int. Conf. on Gearing, IMechE, 1958.

20. Leach, E. F., and Kelley, B. W., "Temperature—The Key to Lubricant Capacity," ASLE Trans., Vol. 8, 1965.

21. Matveevsky, R. M., "The Critical Temperature of Oil with Point and Line Contact Machines," Trans. ASME, Jour. Basic Engrg., Vol. 87D, 1965.

22. Kelley, B. W., and Lemanski, A. J., "Lubrication of Involute Gearing," Proc. IMechE, Vol. 182, Pt. 3A, 1967-68.

23. Blok, H., "The Postulate About the Constancy of Scoring Temperature," Interdisciplinary Approach to the Lubrication of Concentrated Contacts, NASA Spec. Publ. 237, 1970.

24. Bell, J. C., and Dyson, A., "The Effect of Some Operating Factors on the Scuffing of Hardened Steel Discs," Elastohydrodynamic Lubrication, 1972 Symposium, IMechE, 1972.

25. Staph, H. E., Ku, P. M., and Carper, H. J., "Effect of Surface Roughness and Surface Texture on Scuffing," Mechanism and Machine Theory, Vol. 8, 1973.

26. Carper, H. J., Ku, P. M., and Anderson, E. L., "Effect of Some Material and Operating Variables on Scuffing," Mechanism and Machine Theory, Vol. 8, 1973.

27. Blok, H., "Blitztemperatutheorie und Fresskriterion-Heute," Fressen an Zahnradern Stand der Berechnungsmethoden, Munich, Germany, Apr. 1973.

28. Carper, H. J., and Ku, P. M., "Thermal and Scuffing Behavior of Disks in Sliding-Rolling Contact," ASLE Trans., Vol. 17, 1975.

29. Bell, J. C., Dyson, A., and Hadley, J. W., "The Effects of Rolling and Sliding Speeds on the Scuffing of Lubricated Steel Discs," ASLE Trans., Vol. 17, 1975.

30. Dyson, A., "Gear Scuffing—A Review," Tribology International, Vol. 8, 1975.

31. Fowle, T. I., "Gear Lubrication: Relating Theory to Practice," ASLE Annual Meeting, Atlanta, Ga., May 5-9, 1975.

32. Carper, H. J., Anderson, E. L., and Ku, P. M., "An Investigation of Scuffing Conducted on the AFAPL Disk Tester," AFAPL Tech. Rept. 72-28, Jun. 1972.

33. Dowson, D., and Higginson, G. R., Elastohydrodynamic Lubrication, Pergamon Press, London, 1966.

34. Dowson, D., "Elastohydrodynamic Lubrication," Interdisciplinary Approach to the Lubrication of Concentrated Contacts, NASA Spec. Publ. 237, 1970.

35. Cheng, H. S., "A Numerical Solution of the Elastohydrodynamic Film Thickness in an Elliptic Contact," Trans. ASME, Jour. Lub. Tech., Vol. 92F, 1970.

36. Cheng, H. S., "Calculation of Elastohydrodynamic Film Thickness in High-Speed Rolling and Sliding Contacts," MTI Rept. 67-24, 1967.

37. Cheng, H. S., "Prediction of Film Thicknesses and Sliding Frictional Coefficient in Elastohydrodynamic Contacts," ASME Winter Annual Meeting, New York, Oct. 6-9, 1974.

38. Dyson, A., and Wilson, A. R., "Film Thicknesses in Elastohydrodynamic Lubrication at High Slide/Roll Ratios," Proc. IMechE, Vol. 183, Pt. 3P, 1968-9.

39. Turchina, V., Sanborn, D. M., and Winer, W. O., "Temperature Measurements in Sliding Elastohydrodynamic Point Contacts," Trans. ASME, Jour. Lub. Tech., Vol. 96F, 1974.

40. Fowles, P. E., "The Application of Elastohydrodynamic Film Thickness to Individual Asperity-Asperity Contacts," Trans. ASME, Jour. Lub. Tech., Vol. 91F, 1969.

41. Johnson, K. L., Greenwood, J. A., and Poon, S. Y., "A Simple Theory of Asperity Contact in Elastohydrodynamic Lubrication," Wear, Vol. 19, 1972.

42. Archard, J. F., "Elastohydrodynamic Lubrication of Real Surfaces," Tribology, Vol. 6, 1973.

43. Castle, P., and Dowson, D., "A Theoretical Analysis of the Starved Elastohydrodynamic Lubrication Problem for Cylinders in Line Contact," Elastohydrodynamic Lubrication, 1972 Symposium, IMechE, 1972.

44. Ku, P. M., editor, Interdisciplinary Approach to Friction and Wear, NASA Spec. Publ. 181, 1968.

45. Ling, F. F., Klaus, E. E., and Fein, R. S., editors, Boundary Lubrication—An Appraisal of World Literature, ASME, 1969.

46. Ku, P. M., editor, Interdisciplinary Approach to the Lubrication of Concentrated Contacts, NASA Spec. Publ. 237, 1970.

47. Ku, P. M., editor, Interdisciplinary Approach to Liquid Lubricant Technology, NASA Spec. Publ. 318, 1972.

48. Dyson, A., General Theory of Kinematics and Geometry of Gears in Three Dimensions, Oxford Univ. Press, London, 1969.

49. Staph, H. E., "A Parametric Analysis of High-Contact-Ratio Spur Gears," ASLE Annual Meeting, Atlanta, Ga., May 5-9, 1975.

50. Walker, H., "Gear Tooth Deflection and Profile Modification, I," The Engineer, Vol. 166, 1938.

51. Walker, H., "Gear Tooth Deflection and Profile Modification, II," The Engineer, Vol. 166, 1938.

52. Walker, H., "Gear Tooth Deflection and Profile Modification, III," The Engineer, Vol. 170, 1940.

53. Harris, S. L., "Dynamic Loads on the Teeth of Spur Gears," Proc. IMechE, Vol. 172, 1958.

54. Reswick, J. B., "Dynamic Loads in Spur and Helical Gear Teeth," Trans. ASME, Vol. 77, 1955.

55. Utagawa, M., and Harada, T., "Dynamic Loads on Spur Gear Teeth at High Speeds," Bull. JSME, Vol. 4, 1961.

56. AGMA Gear Handbook, Vol. I, AGMA Standard 390.03, 1971.

57. Remmers, E. P., "The Dynamics of Gear Pair Systems," ASME Paper 71-DE-23, 1971.

58. Attia, A. Y., "Dynamic Loading of Spur Gear Teeth," Trans. ASME, Jour. Engrg. for Industry, Vol. 81, 1959.

59. Utagawa, M., "Dynamic Loads on Spur Gear Teeth," Bull. JSME, Vol. 1, 1958.

60. Kasuba, R., "Dynamic Loads on Spur Gear Teeth by Analog Computation," ASME Paper 71-DE-26, 1971.

61. Houser, D. R., and Seireg, A., "An Experimental Investigation of Dynamic Factors in Spur and Helical Gears," Trans. ASME, Jour. Engrg. for Industry, Vol. 92, 1970.

62. Seireg, A., and Houser, D. R., "Evaluation of Dynamic Factors for Spur and Helical Gears," Trans. ASME, Jour. Engrg. for Industry, Vol. 92, 1970.

63. Tuplin, W. A., "Dynamic Loads on Gear Teeth," Machine Design, Vol. 25, 1953.

64. Tuplin, W. A., Gear Load Capacity, John Wiley & Sons, New York, 1961.

65. Utagawa, M., and Harada, T., "Dynamic Loads on Spur Gear Teeth Having Pitch Errors at High Speed," Bull. JSME, Vol. 5, 1963.

66. Coleman, W., "A Scoring Formula for Bevel and Hypoid Gears," Trans. ASME, Jour. Lub. Tech., Vol. 89F, 1967.

67. Coleman, W., "Pitting Resistance of Bevel and Hypoid Gears," AGMA Paper 229.05, Oct. 1960.

68. "Surface Durability (Pitting) Formulas for Spiral Bevel Gear Teeth," AGMA Standard 216.01, Jan. 1964.

69. Baxter, M. L., "Effect of Misalignment on Tooth Action of Bevel and Hypoid Gears," ASME Paper 61-MD-20, 1961.

70. Johnson, L. G., Statistical Treatment of Fatigue Experiments, Elsevier Publishing Co., New York, 1964.

71. Onion, R. A., and Archard, J. F., "The Pitting of Gears and Discs," private communication (to be published).

72. Bell, J. C., and Dyson, A., "Mixed Friction in an Elastohydrodynamic System," Elastohydrodynamic Lubrication, 1972 Symposium, IMechE, 1972.

73. Van Zandt, R. P., "Contact Length and Bending Stress Conditions between Two Non-Parallel Contacting Spur Gear Teeth," AGMA Gear Rating Coordinating Report, Oct. 1951.

74. Wellauer, E. J., "Strength Rating of Helical Gears," AGMA Paper 229.04, 1960.

75. Coleman, W., "Pitting Resistance of Bevel and Hypoid Gear Teeth," AGMA Paper 229.05, 1960.

APPENDIX A
PROPERTIES OF TEST STEEL AND TEST OILS

Test Steel

All test disks and test gears employed in this program were made of AISI 9310 CEVM steel, carburized to give a specified case thickness, case hardness, and core hardness.

The bulk properties of the AISI 9310 steel are taken as follows:

Quantity	Symbol	Unit	Value	Remarks
Young's modulus	E	psi	30×10^6	
Poisson's ratio	ν	-	0.30	
Equivalent Young's modulus	$\overset{*}{E}$	psi	33×10^6	$\overset{*}{E} = E/(1-\nu^2)$
Density	ρ	$lb/in.^3$	0.283	
Specific heat	c	in./°F	1075	
Thermal conductivity	k	lb/°F-sec	5.84	
Blok's thermal coefficient	β	$lb/°F\text{-}in.sec^{\frac{1}{2}}$	42.15	$\beta = (\rho\, c\, k)^{\frac{1}{2}}$

Test Oils

Two synthetic aviation gas turbine lubricants, a MIL-L-7808G lubricant herein designated as Oil F and a MIL-L-23699 lubricant herein designated as Oil E, were employed in the program. Adequate quantities of these oils, each from a single production batch, were supplied for use in both the disk tests and the gear tests by the USAF Aero Propulsion Laboratory, under the code designations of O-67-23 for Oil F and O-64-2 for Oil E.

The measured properties of these two oils at atmospheric pressure are as follows:

Quantity	Symbol	Unit	Oil F	Oil E
Specification MIL-L-	-	-	7808G	23699
Density at 60°F	ρ_{60}	g/ml	0.953	1.007
Kin. viscosity at 100°F	ν_o	cs	13.4	27.5
Kin. viscosity at 210°F	ν_o	cs	3.23	5.07
Sp. ht. at 300°F	c	Btu/lb-°F	0.541	0.541
Th. cond. at 300°F	k	Btu/ft-°F-sec	0.0841	0.0703
Neutralization no.	-	mg KOH/g	0.2	0.2

The oil properties at any temperature and pressure may be calculated by the following expressions:

$$\rho = \rho_{60} - G(T - 60)$$

$$\text{loglog}\,(\nu_o + 0.60) = A - B \log (T + 460)$$

$$\mu_o = \nu_o \rho_o$$

$$\mu = \mu_o e^{\alpha p}$$

$$\alpha_o = \frac{K}{T\beta}$$

where T = temperature, °F

p = pressure, psig

ρ_o = density at atmospheric pressure and temperature T, g/ml

ρ_{60} = density at atmospheric pressure and 60°F, g/ml

ν_o = kinematic viscosity at atmospheric pressure and temperature T, cs

μ_o = absolute viscosity at atmospheric pressure and temperature T, cp

μ = absolute viscosity at pressure p and temperature T, cp

α = pressure-viscosity coefficient at pressure p and temperature T, psi^{-1}

α_o = pressure-viscosity coefficient at atmospheric pressure and temperature T, psi^{-1}

B, A, B, K, β = fitting constants which are functions of the oil in question

The various fitting constants to be used in the preceding equations are as follows:

	$G \times 10^4$	A	B	$K \times 10^4$	β
Oil F	3.94	11.75543	4.24477	12.717	0.566
Oil E	4.14	11.16683	3.99787	9.496	0.492

APPENDIX B
COMPOSITE SURFACE ROUGHNESS

Surface roughness has been found to have a significant effect on the lubrication-related failures.[9, 10, 24-26] In order to relate the lubrication and failure behaviors to surface roughness, some way of quantitatively describing the "composite surface roughness" of two interacting surfaces is required. The method employed herein is given below.

Composite Surface Roughness of a Single Surface

The composite surface roughness of a single surface is herein defined as

$$\delta = (\delta_x + \delta_y)/2 \qquad \text{(B-1)}$$

where δ = composite surface roughness of a single surface, μin. AA

δ_x = surface roughness in one direction (usually the direction of sliding), μin. AA

δ_y = surface roughness in the perpendicular direction, μin. AA

Composite Surface Roughness of a Pair of Surfaces

The composite surface roughness of a pair of interacting surfaces is herein defined as

$$\delta_c = \delta_1 + \delta_2 \qquad \text{(B-2)}$$

where δ_c = composite surface roughness of a pair of surfaces, μin. AA

δ_1 = composite surface roughness of surface 1, μin. AA

δ_2 = composite surface roughness of surface 2, μin. AA

Approximate Procedure

In general, it is good practice to measure the surface roughnesses of both surfaces in two directions, and then calculate the composite surface roughness of each surface by Equation (B-1) and that of the pair by Equation (B-2). However, in many practical cases, the surface roughness is usually measured in only one direction. In such cases, the surface roughness in the normal direction has to be assumed.

With ground surfaces, it has been found from measurements on both the test disks and test gears, as well as a large volume of additional data on hand in the authors' laboratory, that the ratio of the surface roughness across the grinding marks to that in the direction of grinding is generally quite close to 2. In other words, if δ_x is the surface roughness across the grinding marks, then $\delta_y \sim \delta_x/2$ with good approximation. It then follows from Equation (B-1) that

$$\delta \sim 3\delta_x/4 \tag{B-3}$$

and from Equation (B-2) that

$$\delta_c \sim 3(\delta_{x1} + \delta_{x2})/4 \tag{B-4}$$

With honed surfaces, δ_x and δ_y are usually nearly equal. Thus

$$\delta \sim \delta_x \tag{B-5}$$

and

$$\delta_c \sim \delta_x + \delta_y \tag{B-6}$$

APPENDIX C
ELASTOHYDRODYNAMIC FILM THICKNESS

As explained in Chapter II, Section C, EHD film thickness calculations will not be given emphasis in this report. However, as a matter of general interest, the procedure for such calculations will be given below.

Sliding-Rolling Disks

The minimum oil film thickness developed by EHD action in a flooded, elliptic conjunction of perfectly smooth surfaces, in steady operation, is given by Equation (5) and repeated below:

$$h'_m = 26.5 \frac{\alpha_o^{0.54}(\mu_o V_t)^{0.70} R^{0.43} \phi_s \phi_t}{w^{0.13} \overset{*}{E}^{0.03}} \qquad (C\text{-}1)$$

where h'_m = minimum oil film thickness, μin.

α_o = pressure-viscosity coefficient of oil at conjunction-inlet temperature and near-atmospheric pressure, psi^{-1}

μ_o = absolute viscosity of oil at conjunction-inlet temperature and near-atmospheric pressure, cp

$\overset{*}{E}$ = equivalent Young's modulus of material, psi

R = equivalent radius of curvature at the conjunction, in.

w = unit normal load, ppi

V_t = sum velocity, ips

ϕ_s = side flow correction factor

ϕ_t = inlet-shear thermal correction factor

In EHD oil film thickness analysis, the controlling oil properties are those prevalent at the conjunction inlet, i.e., at the

conjunction-inlet oil temperature, T_o, and near-atmospheric pressure. If T_o is known, the appropriate values of α_o and μ_o may be calculated, as recommended in Appendix A.

In general, T_o is higher than the oil jet temperature, T_j, and lower than the quasi-steady surface temperature, T_s. For a sliding-rolling disk system in steady operation, T_o can easily be measured by means of a thermocouple. In case T_o is not known, then it may be estimated, as shown in Chapter VI, Section E, as follows:

$$T_o - T_j = C_o \phi^{0.80} \qquad \text{(C-2)}$$

where C_o = a fitting constant, and ϕ = frictional power loss, Btu/sec.

For sliding-rolling disks, C_o may be estimated as given in Chapter VI, Section E; and ϕ is given by

$$\phi = f W V_s / 9336 \qquad \text{(C-3)}$$

where ϕ = frictional power loss, Btu/sec

f = coefficient of friction

W = normal load, lb

V_s = sliding velocity, ips

The values of R, w, ϕ_s, and ϕ_t may be obtained by the procedure outlined by Cheng.[37]

Gears

To compute h'_m at any point in a gear mesh, the effect of gear mechanics on quantities entering Equation (C-1) must be taken into account. This matter is considered in Chapters III, IV, and V for spur, helical, and spiral bevel gears, respectively.

In order to estimate T_o for gears, it should be recognized that ϕ in Equation (C-2) varies cyclically through a mesh cycle. Thus

Equation (C-2) should be modified to read

$$T_o - T_j = C'_o \phi_{av}^{0.80} \qquad \text{(C-4)}$$

where ϕ_{av} = average frictional power loss, Btu/sec, and $C'_o = 0.70\,C'$ by applying Equation (66). The estimation of C' and the calculation of ϕ_{av} for gears are given in Chapter VII, Section B.

EHD Film Thickness Ratio

As explained in Chapter II, Section C, there is at present no viable way to account for the effect of surface roughness and surface texture on the EHD film thickness. However, an empirical parameter is often used in practice to indicate, in a very approximate way, whether or not the operation is in the EHD regime, or how deeply the operation is in the boundary lubrication regime. This parameter is defined as

$$\Lambda = \frac{h'_m}{\delta_c} \qquad \text{(C-5)}$$

where Λ = EHD film thickness ratio

h'_m = minimum oil film thickness, μin., as given by Equation (C-1)

δ_c = composite surface roughness of a pair of surfaces, as given in Appendix B.

APPENDIX D
SUMMARY OF DISK TEST DATA

Test Equipment

The basic equipment employed in the work reported herein is the Caterpillar disk tester,[20] which has, however, been rather substantially modified in the authors' laboratory.[25] This tester employs two identical test disks of 3 in. diameter and 14 in. crown radius, whose material and surface characteristics may be varied. Crowned disks are used to minimize misalignment problems.

Figure D-1 shows the general arrangement of the test disks and some major instrumentation used. The two test disks are mounted on parallel shafts and a normal load, W, is applied between them. The lower shaft is driven by a variable-speed hydraulic motor through pulleys and timing belt. The upper shaft is driven off the lower shaft by means of one of several sets of phase gears of different speed ratios. The surface velocities of the two disks are V_1 and V_2, thus the sliding velocity is $V_s = V_1 - V_2$, the sum velocity is $V_t = V_1 + V_2$, and the sliding-to-sum velocity ratio is $M = V_s/V_t$.

The test oil, at temperature T_j, is jetted toward the center of the conjunction in the center plane of the disks. The disks are cooled largely by impinging jets of the test oil supplied by a horn which envelopes halves of the disks. The oil pressure is maintained at 40 psig, and the total oil flow rate is approximately 20 gpm. The oil temperature at the conjunction inlet, T_o, is measured by a thermocouple probe placed in the center plane of the disks, 0.250 in. ahead of the conjunction center, and riding with a slight pressure on one of the disks. The quasi-steady surface temperature of the disks, T_s, is estimated from T_o by means of a relationship established by a separate calibration employing thermocouples embedded in the disks and operating the disks with V_1, V_2, W, T_j and the oil systematically varied.

The upper shaft of the Caterpillar tester is so instrumented that the reaction torque on this shaft can be measured. The disk friction torque, T_f, is then the difference between the reaction torque and the machine-loss torque, the latter being due principally to losses in the upper-shaft support bearings. The machine-loss torque is derived from a separate calibration involving operating the disks in both normal and reverse directions of rotation with the same

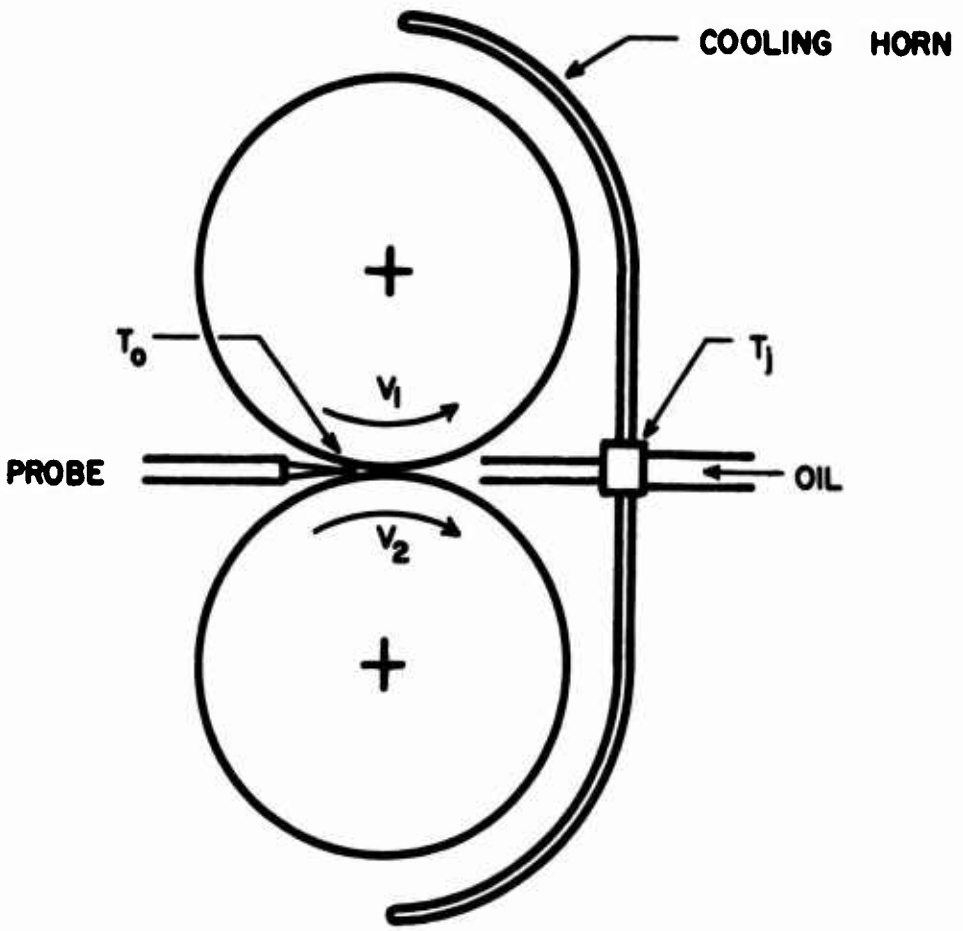

Figure D-1. Arrangement of test disks and instrumentation for SwRI disk tester A

V_1, V_2, W, T_j and oil; and with these variables varied systematically. The disk coefficient of friction is simply $f = T_f/rW$, where $r = 1.5$ in. is the disk radius.

The occurrence of metallic contact between the disks is observed by the instantaneous contact resistance technique. With straight mineral oils, reduction of the contact resistance to near zero is a good indication of metallic contact and usually of scoring when the test conditions are such that scoring occurs. With reactive oils, the contact resistance often collapses only partially due to the presence of a reactive surface film, so that the technique provides no reliable indication of asperity contact. A slight but abrupt increase in the reaction torque is usually the best indication of scoring under these circumstances. In all cases, actual scoring is always verified by visual examination.

Test Disks

The test disks employed in this program were all fabricated by the Bell Helicopter Company. They were all 3 in. in diameter and had a crown radius of 14 in. They were made of AISI 9310 CEVM steel, carburized to give a case thickness of 0.045-0.053 in., a case hardness as given in Table D-1, and a core hardness of 36-41 R_C.

As shown in Table D-1, 10 different types of test disks were used, consisting of 5 types of surface finishes and 2 types of surface treatments. The "plain" disks were not surface-treated, i.e., they were as ground or honed. The "oxided" disks were surface-treated with a black oxide after grinding or honing. The black oxide was applied in accordance with BHC Specification BPSFW 4084, to a nominal thickness of "less than 100 μin." However, measurements made at SwRI showed virtually no effect on the surface roughness by the black oxide treatment. The symbol δ_i denotes the initial composite surface roughness of the disk pairs.

Disk Test Program

The 10 types of disks were tested with 2 test oils, over a range of sliding and sum velocities to be detailed later. Most of the tests were conducted at an oil jet temperature of 190°F, with some at 140°F. As shown in Table D-2, 187 tests were performed, 160 of which resulted in scoring failure.

TABLE D-1. AVERAGE PROPERTIES OF TEST DISK PAIRS

Disk type	Surface finish	Surface treatment	Case hardness, R_C	δ_i, μin. AA
1	Soft circ. ground	Plain	58 ± 1	26 ± 2
1A	Soft circ. ground	Oxided	58 ± 1	26 ± 2
3	Rough circ. ground	Plain	62 ± 1	24 ± 2
3A	Rough circ. ground	Oxided	62 ± 1	24 ± 2
5	Honed	Plain	62 ± 1	5.5 ± 1
5A	Honed	Oxided	62 ± 1	5.5 ± 1
7	Rough cross ground	Plain	62 ± 1	23.5 ± 1
7A	Rough cross ground	Oxided	62 ± 1	23.5 ± 1
9	Smooth circ. ground	Plain	62 ± 1	9.5 ± 1
9A	Smooth circ. ground	Oxided	62 ± 1	9.5 ± 1

TABLE D-2. NUMBER OF DISK TESTS PERFORMED AND SCORED

Oil code	T_j, °F	Disk type	No. of tests Total	No. of tests Scored	Disk type	No. of tests Total	No. of tests Scored
F	190	1	5	5	1A	5	5
F	190	3	65	58	3A	24	20
	140	3	-	-	3A	7	7
F	190	5	3	3	5A	5	4
F	190	7	6	6	7A	4	3
F	190	9	3	2	9A	6	5
Total for Oil F			82	74		51	44
E	190	3	1	1	3A	12	12
	140	3	-	-	3A	6	6
E	190	5	3	3	5A	8	5
E	190	7	4	3	7A	2	0
	140	7	2	2	7A	-	-
E	190	9	6	4	9A	10	6
Total for Oil E			16	13		38	29
Grand total			98	87		89	73

Note further from Table D-2 that the number of tests performed with Oil F was 82 with plain disks and 51 with oxided disks, or a total of 133. The number of tests performed with Oil E was 16 with plain disks and 38 with oxided disks, or a total of 54. Viewed in another way, 98 tests were performed with the plain disks, while 89 tests were performed with the oxided disks.

Further, most of the tests were performed with Types 3 and 3A disks (a total of 109 tests for both oils), mainly due to the customary use of circumferentially-ground disks in disk testing and also cost considerations. As it turned out, it was found that, at about the same initial composite surface roughness (Table D-1), Types 7 and 7A disks gave substantially different results from Types 3 and 3A disks (Chap. VI). Since spur gears generally slide normal to the grinding marks, and the helical and spiral bevel gears approximate this condition, it would have been more desirable to run more tests with the cross-ground disks. Unfortunately, this could not be done in the program, as the disks had to be ordered and fabricated in advance, and the program could not be modified by the time this effect was noted.

Disk Test Procedure

The test disks were examined for nicks, scratches, rust spots, etc., and wiped dry; after which they were inspected for case hardness and transverse and circumferential surface roughnesses. Then they were covered with a straight mineral oil and placed in storage. Just prior to testing, they were cleaned with trisolvent, wiped dry with a clean cloth, and assembled on the shafts to check the runout.

The break-in of the test disks was performed using the desired test oil at T_j = 90°F, V_s = 23.6 ips, and V_t = 70.8 ips. The load schedule comprised 4 equal increments of 500 lb of 15 min duration each, which gave a maximum break-in load of 2000 lb. This break-in procedure was used regardless of the test conditions to be employed later. Following the break-in, the disks were removed from the shafts for inspection and surface roughness measurement, and then reinstalled for subsequent testing.

The testing was performed using the desired T_j at an initial load of 70 lb, with V_s and V_t brought up to the desired values. Subsequent to this, the load was increased in equal increments of 35 lb

of 3 min duration each, until scoring failure occurred or until the machine capacity (about 6000 lb) was reached. Upon conclusion of the test, the disks were removed for inspection and surface roughness measurement.

When changing from an oil to one of another type, the following procedure was used: The used test oil was first drained from the system. The system was flushed completely with a clean trisolvent (equal parts of reagent grade acetone, benzene, and isopropyl alchohol), which was drained and discarded. This was followed by two more flushings with the clean solvent. The system was then charged with new test oil. This oil was circulated for 30 min, then drained and discarded. A second charge of test oil was handled likewise. After this oil was drained, the sump was filled with its normal charge of test oil. When testing for extended periods with the same oil, samples were periodically drawn and checked for viscosity and neutralization number changes, and the oil was replaced as necessary by draining and one flushing with new oil. The criteria for oil change were a viscosity increase of 5 percent, or a neutralization increase of 0.2 mg KOH/g. These conditions were, however, never reached in the tests reported herein.

The surface roughnesses of the disks were measured at the end of each break-in and also at the end of each test, from which the corresponding composite surface roughnesses of the disk pairs were calculated by the procedure given in Appendix B. For the break-in and test procedures used herein, it was found that the composite surface roughness of the disk pairs was generally reduced about 20 percent after break-in and about 30 percent after test.[25,26] These values did not vary much when all tests were taken as a whole. Therefore, for the sake of brevity, these composite surface roughness values are not included in the data tabulation in this report.

Summary of Disk Test Results

The summaries of all disk test results are given in Tables D-3 to D-23. Each table presents the conditions reached at scoring in each test for a given test disk and test oil combination, at a given test oil jet temperature. Replicate tests were run in most cases, sometimes to as many as 5 to 6 tests.

The nomenclature and symbols used in these tables have mostly been introduced earlier, and also given in the List of Symbols at the end of this report. The only necessary explanations are given

below.

The "mode" of scoring failure is identified as follows: The symbol "CR" represents that scoring was detected by a collapse of the instantaneous contact resistance and subsequently verified by visual inspection. The symbol "TO" represents that scoring was detected by a torque increase and subsequently verified by visual inspection. The symbol "PS" represents premature scoring, i.e., scoring occurring during the first load step (W = 70 lb) and in most instances before the conditions stabilized. The symbol "No" represents that no scoring was obtained at the reported highest load, at which time the test was terminated.

Except as noted below, the quantities W, f, T_o, and T_s are measured quantities. The quantity ΔT was computed by Equation (3) in Chapter II, by using Kelley's equivalent unit load[18] since the test disks are crowned. T_c is as defined by Equation (1) in Chapter II.

The minimum oil film thickness, h_m, was computed by Equation (C-1) in Appendix C, by taking $\phi_s\phi_t = 1$. The EHD film thickness ratio, Λ, was calculated by Equation (C-5) in Appendix C, based on h_m as computed above and the composite surface roughness of each disk pair at the end of the test.

For each set of replicate tests, the scoring load or the highest test load, W, for each test is tabulated. The average scoring load, Avg. W, for the replicate tests is given immediately below the tabulated values of W.

For each set of replicate tests, the conjunction temperature, T_c, for each test at scoring is tabulated. The critical temperature, T_{cr}, is computed by Weibull analysis from the individual values of T_c for the replicate tests, at 10-percent probability. This T_{cr} value is given immediately below the tabulated T_c values. The values given in the parenthesis immediately after the T_{cr} value are the lower and upper limits of T_{cr} at 90-percent confidence.

In performing the Weibull analysis, all T_c values for the prematurely scored tests were treated as if these tests actually scored at the initial load of 70 lb, and the coefficient of friction at scoring was estimated from the f vs. W history of the other tests in the same set. From these f and W values, the approximate values of T_o, T_s, ΔT, and T_c were computed. For tests with no scoring, the tabulated values of T_c were treated as suspensions, and included in

the Weibull analysis.

These results are discussed in Chapter VI, along with other available data.

TABLE D-3. SCORING RESULTS FOR TYPE I DISKS AND OIL F (T_j = 190°F)

Test no.	V_s, ips	V_t, ips	M	Mode	W, lb	f	T_o, °F	T_s, °F	ΔT, °F	T_c, °F	h_m, μin.	Λ
F122	200	360	0.556	CR	977	0.0248	217	233	202	435	2.8	0.19
F125				CR	1077	0.0282	220	240	241	481	2.8	0.21
				Avg. W =	1027					T_{cr} = 390 (300/508)		
F105	400	720	0.556	TO	1073	0.0199	223	235	240	475	4.4	0.36
F128				CR	657	0.0229	211	218	216	435	5.0	0.38
				Avg. W =	865					T_{cr} = 395 (322/485)		
F106	600	1080	0.556	CR	273	0.0304	201	199	226	426	7.8	0.56

TABLE D-4. SCORING RESULTS FOR TYPE IA DISKS AND OIL F (T_j = 190°F)

Test no.	V_s, ips	V_t, ips	M	Mode	W, lb	f	T_o, °F	T_s, °F	ΔT, °F	T_c, °F	h_m, μin.	Λ
F121	200	360	0.556	CR	355	0.0296	202	208	145	353	3.5	0.26
F124				CR	312	0.0	199	202	139	341	3.6	0.30
				Avg. W =	334					T_{cr} = 330 (302/360)		
F107	400	720	0.556	CR	212	0.0321	197	197	172	369	6.2	0.36
F126				PS	-70	-0.0596	-191	-191	-184	-374	-	-
				Avg. W =	141					T_{cr} = 362 (341/384)		
F108	600	1080	0.556	PS	-70	-	-	-	-	-	-	-

TABLE D-5. SCORING RESULTS FOR TYPE 3 DISKS AND OIL F (T_j = 190°F)

Test no.	V_s, ips	V_t, ips	M	Mode	W, lb	f	T_o, °F	T_s, °F	ΔT, °F	T_c, °F	h_m, μin.	A
F82	200	360	0.556	CR	2816	0.0211	246	286	297	578	2.1	0.15
F104				CR	3076	0.0214	255	298	309	607	2.0	0.14
F163				CR	3400	0.0209	257	204	317	621	1.9	0.15
F168				TO	3240	0.0199	258	306	295	601	1.9	0.13
F176				PS	-70	-0.0518	-193	-193	-113	-306	-	-
F194				TO	3446	0.0209	259	303	319	622	1.9	0.15
				Avg. W =	2675					T_{cr} = 307 (160/592)		
F130	120	600	0.200	No	>6373	<0.0272	-258	-284	>253	>538	-2.6	-0.19
F186				No	>5353	<0.0281	-258	-297	>239	>536	-2.6	-0.19
F187				No	>5924	<0.0258	-281	-307	>231	>538	-2.3	-0.16
				Avg. W	>5883					T_{cr} >537		
F83	200	600	0.333	CR	3406	0.0236	242	265	269	534	3.0	0.18
F133				TO	4144	0.0219	258	289	276	565	2.7	0.14
F145				TO	5306	0.0228	278	331	325	656	2.3	0.14
F155				CR	3316	0.0220	251	294	248	542	2.9	0.23
F171				CR	4475	0.0207	264	302	271	573	2.6	0.19
				Avg. W =	4129					T_{cr} = 508 (434/596)		
F142	334	600	0.556	CR	2705	0.0173	265	310	302	612	2.7	0.20
F160				CR	2470	0.0198	254	278	331	610	2.9	0.23
F165				CR	1893	0.0199	242	274	290	565	3.2	0.25
F172				CR	905	0.0211	223	242	213	455	3.9	0.27
F180				CR	2504	0.0188	257	293	316	609	2.8	0.23
				Avg. W =	2095					T_{cr} = 467 (361/604)		
F80	400	720	0.556	CR	2855	0.0159	266	307	313	620	3.0	0.24
F102				CR	1848	0.0176	239	258	280	437	3.7	0.26
F164				CR	1509	0.0207	238	260	295	556	3.8	0.27
F169				TO	3328	0.0144	267	298	305	604	3.0	0.24
F177				PS	-70	-0.0670	-193	-193	-207	-399	-	-
F193				CR	1031	0.0199	227	242	235	478	4.3	0.32
				Avg. W =	1774					T_{cr} = 392 (284/541)		

TABLE D-5. SCORING RESULTS FOR TYPE 3 DISKS AND OIL F (T_j = 190°F) (Cont'd)

Test no.	V_s, ips	V_t, ips	M	Mode	W, lb	f	T_o, °F	T_s, °F	ΔT, °F	T_c, °F	h, μin.	Λ
F131	180	900	0.200	No	>6392	<0.0243	-282	-316	>277	>593	-3.0	-0.22
F188				No	>5950	<0.0245	-284	-316	>269	>586	-3.0	-0.18
F189				TO	5906	0.0266	298	335	292	627	2.8	0.19
F195				TO	4900	0.0243	262	379	243	522	3.4	0.24
				Avg. W =	5787					T_{cr} = 505 (370/688)		
F134	300	900	0.333	No	>3468	<0.0190	-264	-295	>269	>564	-3.5	-0.24
F146				TO	4167	0.0194	281	327	300	626	3.1	0.22
F156				CR	1596	0.0207	235	253	198	451	4.5	0.32
F173				CR	3897	0.0188	275	313	282	595	3.2	0.21
F181				CR	4099	0.0184	261	274	282	556	3.5	0.27
				Avg. W =	3445					T_{cr} = 465 (339/637)		
F143	500	900	0.556	TO	1646	0.0164	242	257	274	531	4.3	0.35
F161				CR	2709	0.0153	277	317	329	646	3.3	0.25
F166				CR	1198	0.0192	231	248	274	523	4.8	0.34
F174				CR	666	0.0244	224	237	259	496	5.3	0.34
F182				PS	-70	-0.0852	-192	-192	-294	-486	-	-
F192				CR	1164	0.0222	234	246	312	557	4.7	0.34
				Avg. W =	1242					T_{cr} = 470 (384/577)		
F132	216	1080	0.200	No	>6031	<0.0243	-283	-311	>294	>605	-3.4	-0.23
F190				TO	5654	0.0234	287	329	274	603	3.3	0.22
F191				TO	5776	0.0192	272	297	228	525	3.6	0.29
				Avg. W =	5820					T_{cr} = 480 (318/726)		
F141	360	1080	0.333	TO	5758	0.0151	305	355	301	656	3.0	0.25
F147				CR	3689	0.0186	286	326	296	622	3.5	0.26
F157				CR	1152	0.0213	228	239	190	429	5.6	0.44
F175				CR	3706	0.0182	278	307	290	597	3.6	0.28
F183				CR	4244	0.0173	287	323	296	619	3.4	0.33
				Avg. W =	3710					T_{cr} = 446 (316/629)		

TABLE D-5. SCORING RESULTS FOR TYPE 3 DISKS AND OIL F (T_j = 190°F)(Cont'd)

Test no.	V_s, ips	V_t, ips	M	Mode	W, lb	f	T_o, °F	T_s, °F	ΔT, °F	T_c, °F	h_m, μin.	A
F81	600	1080	0.556	CR	1030	0.0174	235	253	252	505	5.3	0.45
F103				CR	202	0.0388	200	197	248	445	8.1	0.56
F129				CR	981	0.0184	229	243	260	503	5.6	0.43
F144				CR	1019	0.0199	234	247	287	534	5.4	0.37
F162				CR	2196	0.0161	258	268	340	608	4.3	0.34
F167				CR	2861	0.0141	255	263	341	604	4.3	0.33
				Avg. W =	1382					T_{cr} = 438 (356/539)		
F84	400	1200	0.333	CR	817	0.0180	214	217	142	359	6.9	0.44
F128				CR	710	0.0249	214	218	184	402	7.0	0.49
F158				CR	2219	0.0177	241	242	231	473	5.2	0.43
F178				TO	3327	0.0176	278	312	282	594	3.9	0.35
F184				CR	2956	0.0187	267	288	281	569	4.2	0.32
				Avg. W =	2006					T_{cr} = 329 (204/530)		
F127	600	1800	0.333	CR	547	0.0207	210	206	164	371	9.7	0.63
F159				CR	1023	0.0228	231	240	247	487	7.8	0.53
F170				CR	818	0.0183	226	230	177	407	8.3	0.60
F179				CR	1302	0.0195	226	244	238	482	8.0	0.67
F185				CR	2993	0.0167	284	298	310	608	5.1	0.39
				Avg. W =	1337					T_{cr} = 340 (229/506)		

TABLE D-6. SCORING RESULTS FOR TYPE 3A DISKS AND OIL F (T_j = 190°F)

Test no.	V_s, ips	V_t, ips	M	Mode	W, lb	f	T_o, °F	T_s, °F	ΔT, °F	T_c, °F	h_m, μin.	A
F74	200	360	0.556	CR	2798	0.0236	256	308	325	634	2.0	0.13
F78				CR	2627	0.0240	254	306	320	627	2.0	0.15
				Avg. W =	2712					T_{cr} = 615 (583/648)		
F135	120	600	0.200	No	>6384	<0.0295	~269	~312	>274	>586	~2.4	~0.16
F136				No	>6392	<0.0258	~264	~307	>240	>547	~2.5	~0.18
F152				No	>6419	<0.0255	~268	~310	>238	>548	~2.4	~0.19
F154				No	>6434	<0.0273	~275	~320	>255	>575	~2.3	~0.16
				Avg. W	>6407					T_{cr} >564		
F62	200	[illegible]	[illegible]	CR	2649	0.0245	241	277	247	524	3.1	0.18
F63				CR	945	0.0276	214	231	166	397	4.2	0.22
F64				CR	127	0.0472	193	192	104	296	5.9	0.32
F137				TO	5188	0.0199	272	321	280	601	2.4	0.17
F138				CR	3567	0.0233	258	299	273	572	2.7	0.17
F148				CR	2394	0.0211	231	244	202	446	3.4	0.21
				Avg. W =	2478					T_{cr} = 290 (165/510)		
F139	334	600	0.556	CR	1315	0.0263	244	277	322	599	3.3	0.27
F140				CR	2652	0.0188	268	315	325	640	2.6	0.20
F149				CR	932	0.0226	226	244	232	475	3.8	0.28
F150				CR	1084	0.0218	242	272	242	513	3.4	0.24
F151				CR	1247	0.0212	235	264	252	516	3.5	0.26
				Avg. W =	1446					T_{cr} = 435 (322/574)		
F75	400	720	0.556	CR	1511	0.0206	251	291	295	585	3.5	0.31
F77				PS	~70	~0.0574	~194	~194	~177	~373	-	-
				Avg. W =	791					T_{cr} = 245 (74/806)		
F76	600	1080	0.556	PS	~70	~0.660	~202	~209	~248	~457	-	-
F61	400	1200	0.333	CR	2720	0.0172	256	283	249	532	4.6	0.30
F65				CR	2087	0.0175	243	264	222	486	5.1	0.39
				Avg. W =	2404					T_{cr} = 450 (358/565)		
F66	600	1800	0.333	CR	1190	0.0178	231	236	208	443	7.7	0.58
F67				CR	2009	0.0162	265	285	246	530	5.9	0.40
				Avg. W =	1600					T = 375 (234/601)		

TABLE D-7. SCORING RESULTS FOR TYPE 3A DISKS AND OIL F (T_j = 140°F)

Test no.	V_s, ips	V_t, ips	M	Mode	W, lb	f	T_o, °F	T_s, °F	ΔT, °F	T_c, °F	h_m, μin.	Λ
F68	200	360	0.556	CR	561	0.0210	156	170	130	299	6.4	-
F79				CR	1056	0.0271	172	194	229	423	5.1	0.35
				Avg. W =	809					T_{cr} = 215 (87/531)		
F72	200	600	0.333	CR	3443	0.0181	206	254	208	462	4.4	0.28
F69	400	720	0.556	CR	2464	0.0146	216	264	268	531	4.6	0.32
F70	600	1080	0.556	CR	1390	0.0144	206	240	242	482	7.0	0.46
F71	400	1200	0.333	CR	2984	0.0151	223	258	228	486	6.4	0.37
F73	600	1800	0.333	CR	1159	0.0160	186	195	184	380	13.1	0.68

TABLE D-8. SCORING RESULTS FOR TYPE 5 DISKS AND OIL F (T_j = 190°F)

Test no.	V_s, ips	V_t, ips	M	Mode	W, lb	f	T_o, °F	T_s, °F	ΔT, °F	T_c, °F	h_m, μin.	Λ
F96	200	360	0.556	CR	4975	0.0166	259	292	306	597	1.8	0.39
F94	400	720	0.556	CR	4972	0.0117	260	274	304	578	3.0	0.63
F95	600	1080	0.556	CR	4402	0.0102	269	285	304	589	3.8	1.05

TABLE D-9. SCORING RESULTS FOR TYPE 5A DISKS AND OIL F (T_j = 190°F)

Test no.	V_s, ips	V_t, ips	M	Mode	W, lb	f	T_o, °F	T_s, °F	ΔT, °F	T_c, °F	h_m, μin.	A
F99	200	360	0.556	No	>4979	<0.0169	-264	-303	>310	>613	-1.8	-0.24
F97	400	720	0.556	CR	4733	0.0123	265	286	313	598	2.9	0.39
F100				CR	4260	0.0127	265	290	305	594	2.9	0.41
				Avg. W =	4496					T_{cr} = 594		
F98	600	1080	0.556	CR	2499	0.0128	242	246	289	534	4.7	0.76
F101				CR	2507	0.0130	247	274	239	513	3.4	0.44
				Avg. W =	2503					T_{cr} = 500 (403/620)		

TABLE D-10. SCORING RESULTS FOR TYPE 7 DISKS AND OIL F (T_j = 190°F)

Test no.	V_s, ips	V_t, ips	M	Mode	W, lb	f	T_o, °F	T_s, °F	ΔT, °F	T_c, °F	h_m, μin.	A
F111	200	360	0.556	CR	4000	0.0174	256	298	287	585	1.9	0.12
F114				CR	4417	0.0180	264	315	312	626	1.8	0.10
				Avg. W =	4208					T_{cr} = 560 (490/641)		
F109	400	720	0.556	CR	2507	0.0130	247	274	239	513	3.4	0.20
F112				CR	4161	0.0129	278	322	307	629	2.7	0.12
				Avg. W =	3334					T_{cr} = 430 (261/709)		
F110	600	1080	0.556	CR	2222	0.0122	251	274	259	534	4.5	0.25
F113				CR	1404	0.0143	231	241	242	483	5.3	0.36
				Avg. W =	1813					T_{cr} = 450 (360/562)		

TABLE D-11. SCORING RESULTS FOR TYPE 7A DISKS AND OIL F (T_j = 190°F)

Test no.	V_s, ips	V_t, ips	M	Mode	W, lb	f	T_o, °F	T_s, °F	ΔT, °F	T_c, °F	h_m, μin.	Λ
F115	400	720	0.556	No	>5068	<0.0084	-260	-291	>219	>510	-3.6	-0.26
F118				CR	5260	0.0078	251	270	208	478	3.8	0.32
				Avg. W =	>5164					T_{cr} = 440 (358/540)		
F116	600	1080	0.556	CR	3424	0.0078	254	275	205	480	5.1	0.30
F117				CR	4356	0.0073	273	299	218	517	4.5	0.25
				Avg. W =	3890					T_{cr} = 450 (366/553)		

TABLE D-12. SCORING RESULTS FOR TYPE 9 DISKS AND OIL F (T_j = 190°F)

Test no.	V_s, ips	V_t, ips	M	Mode	W, lb	f	T_o, °F	T_s, °F	ΔT, °F	T_c, °F	h_m, μin.	Λ
F93	200	360	0.556	No	>5050	<0.0201	-267	-302	>372	>674	-1.8	-0.26
F91	400	720	0.556	CR	4705	0.0141	294	351	356	707	2.4	0.35
F92	600	1080	0.556	CR	4072	0.0122	25	257	350	607	4.2	0.58

TABLE D-13. SCORING RESULTS FOR TYPE 9A DISKS AND OIL F (T_j = 190°F)

Test no.	V_s, ips	V_t, ips	M	Mode	W, lb	f	T_o, °F	T_s, °F	ΔT, °F	T_c, °F	h_m, μin.	A
F87	200	360	0.556	No	>4996	<0.0194	~278	~343	>357	>700	~1.6	~0.17
F90				PS	~70	~0.0490	~192	~192	~107	~298	-	-
				Avg. W =	2533							
F85	400	720	0.556	CR	4755	0.0138	292	341	351	692	2.5	0.24
F88				CR	1742	0.0188	250	282	290	572	3.5	0.27
				Avg. W =	3249					T_{cr} = 485 (301/782)		
F86	600	1080	0.556	CR	4477	0.0105	306	356	318	674	3.1	0.34
F89				CR	1671	0.0160	251	271	294	565	3.6	0.39
				Avg. W =	3074					T_{cr} = 465 (288/750)		

TABLE D-14. SCORING RESULTS FOR TYPE 3 DISKS AND OIL E (T_j = 190°F)

Test no.	V_s, ips	V_t, ips	M	Mode	W, lb	f	T_o, °F	T_s, °F	ΔT, °F	T_c, °F	h_m, μin.	A
E19	400	1200	0.333	CR	781	0.0231	220	228	179	406	9.3	0.53

TABLE D-15. SCORING RESULTS FOR TYPE 3A DISKS AND OIL E (T_j = 190°F)

Test no.	V_s, ips	V_t, ips	M	Mode	W, lb	f	T_o, °F	T_s, °F	ΔT, °F	T_c, °F	h_m, μin.	Λ
E24	200	360	0.556	PS	-70	-0.1154	-195	-195	-252	-447	-	-
E25				CR	2080	0.0281	240	278	334	612	3.1	0.20
E29				PS	-70	-0.1154	-195	-195	-252	-447	-	-
E30				PS	-70	-0.1154	-195	-195	-252	-447	-	-
				Avg. W =	572					T_{cr} = 400 (295/542)		
E14	200	600	0.333	CR	764	0.0227	207	216	123	340	6.4	0.43
E16				CR	1030	0.0179	208	217	113	330	6.2	0.41
				Avg. W =	897					T_{cr} = 320 (301/343)		
E39	400	720	0.556	PS	-70	-0.0574	-194	-194	-177	-373	-	-
E15	400	1200	0.333	CR	2595	0.0123	249	266	173	439	6.6	0.46
E17				CR	550	0.0812	212	218	527	725	10.2	0.78
E18				CR	657	0.0258	214	220	183	404	9.9	0.63
				Avg. W =	1267					T_{cr} = 235 (67/693)		
E21	600	1800	0.333	TO	710	0.0207	225	230	187	417	11.9	0.80
E22				CR	1831	0.0185	279	297	269	566	7.4	0.48
				Avg. W =	1270					T_{cr} = 325 (154/687)		

TABLE D-16. SCORING RESULTS FOR TYPE 3A DISKS AND OIL E (T_j = 140°F)

Test no.	V_s, ips	V_t, ips	M	Mode	W, lb	f	T_o, °F	T_s, °F	ΔT, °F	T_c, °F	h_m, μin.	Λ
E26	200	360	0.556	CR	781	0.0280	166	188	204	392	6.9	0.44
E37	200	600	0.333	CR	1457	0.0273	185	213	204	417	7.6	0.49
E27	400	720	0.556	CR	1279	0.0222	192	218	292	510	8.0	0.61

TABLE D-16. SCORING RESULTS FOR TYPE 3A DISKS AND OIL E (T_j = 140°F) (Cont'd)

Test no.	V_s, ips	V_t, ips	M	Mode	W, lb	f	T_o, °F	T_s, °F	ΔT, °F	T_c, °F	h_m, μin.	Λ
E31	600	1080	0.556	CR	234	0.0536	105	157	369	526	19.0	1.26
E36	400	1200	0.333	CR	1333	0.0225	200	220	227	448	10.6	0.63
E38	600	1800	0.333	CR	2311	0.0190	261	285	310	595	8.1	0.56

TABLE D-17. SCORING RESULTS FOR TYPE 5 DISKS AND OIL E (T_j = 190°F)

Test no.	V_s, ips	V_t, ips	M	Mode	W, lb	f	T_o, °F	T_s, °F	ΔT, °F	T_c, °F	h_m, μin.	Λ
E3	200	600	0.333	CR	4054	0.0149	289	268	186	455	4.2	0.85
E1	400	1200	0.333	CR	3549	0.0105	253	272	173	446	6.3	1.14
E2	600	1800	0.333	CR	3289	0.0092	268	281	180	461	7.5	1.20

TABLE D-18. SCORING RESULTS FOR TYPE 5A DISKS AND OIL E (T_j = 190°F)

Test no.	V_s, ips	V_t, ips	M	Mode	W, lb	f	T_o, °F	T_s, °F	ΔT, °F	T_c, °F	h_m, μin.	Λ
E20-2	200	360	0.556	No	>4000	<0.0170	~258	~310	>280	>590	~2.6	~0.27
E23				No	>4972	<0.0156	~268	~327	>287	>614	~2.3	~0.37
E28				CR	1564	0.0156	222	248	161	409	3.7	0.53
				Avg. W	>3512					T_{cr} = 340 (162/713)		

TABLE D-18. SCORING RESULTS FOR TYPE 5A DISKS AND OIL E (T_j = 190°F)(Cont'd)

Test no.	V_s, ips	V_t, ips	M	Mode	W, lb	f	T_o, °F	T_s, °F	ΔT, °F	T_c, °F	h_m, μin.	Λ
E47	400	720	0.556	CR	3243	0.0115	279	331	242	573	3.7	0.68
E50				CR	1528	0.0124	241	272	179	451	5.2	0.83
				Avg. W =	2386					T_{cr} = 360 (191/677)		
E48	600	1080	0.556	CR	764	0.0124	216	221	155	375	9.0	1.40
E49				CR	422	0.0151	206	208	140	348	10.3	1.67
				Avg. W =	593					T_{cr} = 317 (254/395)		
E20-1	400	1200	0.333	No	>4986	<0.0112	274	296	218	515	5.2	0.61

TABLE D-19. SCORING RESULTS FOR TYPE 7 DISKS AND OIL E (T_j = 190°F)

Test no.	V_s, ips	V_t, ips	M	Mode	W, lb	f	T_o, °F	T_s, °F	ΔT, °F	T_c, °F	h_m, μin.	Λ
E33	200	360	0.556	CR	7035	0.0149	279	341	325	666	2.1	0.15
E35	400	720	0.556	CR	4417	0.0134	283	322	328	650	3.5	0.20
E34	600	1080	0.556	CR	2951	0.0114	275	297	278	575	5.0	0.28
E32	400	1200	0.333	No	>3997	<0.0126	~280	~302	>221	>524	~5.1	~0.25

TABLE D-20. SCORING RESULTS FOR TYPE 7 DISKS AND OIL E (T_j = 140°F)

Test no.	V_s, ips	V_t, ips	M	Mode	W, lb	f	T_o, °F	T_s, °F	ΔT, °F	T_c, °F	h_m, μin.	Λ
E52	400	720	0.556	TO	6241	0.0112	322	356	325	681	9.9	0.64
E53	600	1080	0.556	CR	4296	0.0123	335	351	365	715	12.6	0.51

TABLE D-21. SCORING RESULTS FOR TYPE 7A DISKS AND OIL E (T_j = 190°F)

Test no.	V_s, ips	V_t, ips	M	Mode	W, lb	f	T_o, °F	T_s, °F	ΔT, °F	T_c, °F	h_m, μin.	Λ
E55	400	720	0.556	No	5768	0.0077	315	337	214	551	10.4	0.76
E56	600	1080	0.556	No	5754	0.0058	326	335	199	534	13.0	0.90

TABLE D-22. SCORING RESULTS FOR TYPE 9 DISKS AND OIL E (T_j = 190°F)

Test no.	V_s, ips	V_t, ips	M	Mode	W, lb	f	T_o, °F	T_s, °F	ΔT, °F	T_c, °F	h_m, μin.	Λ
E12	200	360	0.556	CR	2418	0.0244	243	288	313	600	3.0	0.39
E45	400	720	0.556	CR	3047	0.0148	287	342	300	643	3.5	0.38
E46	600	1080	0.556	No	>3993	<0.0109	~332	~405	>312	>717	~3.5	~0.52
E6	400	1200	0.333	CR	4410	0.0152	288	323	279	603	4.8	0.60
E9				No	>4996	<0.0158	~310	~354	>309	>662	4.2	0.49
				Avg. W = 4703						T_{cr} = 565 (458/697)		
E7	600	1800	0.333	TO	3840	0.0118	310	341	248	589	5.7	0.50

TABLE D-23. SCORING RESULTS FOR TYPE 9A DISKS AND OIL E (T_j = 190°F)

Test no.	V_s, ips	V_t, ips	M	Mode	W, lb	f	T_o, °F	T_s, °F	ΔT, °F	T_c, °F	h_m, μin.	A
E13	200	360	0.556	No	>7967	<0.0159	-298	-372	>369	>742	-1.9	-0.29
E10-2				CR	2346	0.0187	465	265	236	502	3.3	0.31
				Avg. W =	5156					T_{cr} = 360 (131/989)		
E4	200	600	0.333	No	>3965	<0.0193	-245	-278	>239	>517	-4.0	-0.43
E10-1				No	>5043	<0.0214	-263	-305	>298	>603	-3.5	-0.30
				Avg. W	>4504					T_{cr} >560		
E41	400	720	0.556	CR	774	0.0232	223	242	238	480	6.3	0.82
E42				CR	636	0.0192	215	220	178	399	7.0	0.93
				Avg. W =	705					T_{cr} = 330 (197/554)		
E43	600	1080	0.556	CR	347	0.0196	206	208	165	374	10.5	1.35
E44				CR	749	0.0155	224	234	191	425	8.4	1.00
				Avg. W =	548					T_{cr} = 330 (229/475)		
E5	400	1200	0.333	CR	3556	0.0115	260	284	190	474	5.9	0.55
E11	600	1800	0.333	No	>4979	<0.0088	-643	-349	>210	>559	-5.2	-0.57

APPENDIX E
ANALYSIS OF AGMA SPUR GEAR TEST DATA

As an aid to evaluating the scoring-limited performance of typical aerospace power gears, 13 sets of full-scale spur gear scoring test results, collected by the Tribilogy Division, AGMA Aerospace Gearing Committee, were supplied to this program. Only five sets of such data, from tests employing AISI 9310 steel gears and MIL-L-7808 or MIL-L-23699 oils that went far enough to reach scoring, were analyzed and made use of herein.

A brief description of the five test series selected for analysis is given in Table E-1. Note that Series A1, A2, and A3 were identical except for the surface roughness of the test gears. Other than Series B, all tests were performed at an oil jet temperature of 200°F at an unreported oil flow rate, and the gear surface temperature was not measured. Series B was performed at an unreported oil jet temperature with the oil flow rate varied but not reported; however, the gear surface temperature was measured and reported.

The tests were generally performed under the stated conditions by progressively increasing applied load (Series A1, A2, A3, and C) or by progressively decreasing the oil flow rate (Series B), until scoring was obtained.

Basis of AGMA Reported Data

The AGMA test results are reported in form of computer printouts for each test, listing, among other items, the values of the maximum conjunction-surface temperature rise, ΔT, vs. the roll angle, based on the AGMA gear scoring design guide.[3] This ΔT herein designated as $\Delta T(AGMA)$ for clarity, is given for 21 values of roll angle through the mesh, and also for the pitch point and for the lowest and highest points of single tooth contact. The equation for $\Delta T(AGMA)$ is, by simple algebraic manipulation of the expression given in the AGMA design guide,

$$\Delta T(AGMA) = 0.0175 \left(\frac{50}{50-S}\right) \frac{w^{\frac{3}{4}} \left|\sqrt{\rho_p n_p} - \sqrt{\rho_g n_g}\right|}{R^{\frac{1}{4}}} \qquad (E\text{-}1)$$

TABLE E-1. DESCRIPTION OF AGMA SPUR GEAR TESTS

	Series A1	Series A2	Series A3	Series B	Series C
Test gear material, AISI	9310	9310	9310	9310	9310
Driver (pinion):					
N_p, no. of teeth	30	30	30	28	32
d, pitch diameter, in.	6.000	6.000	6.000	5.600	2.286
S', surface finish, μin. AA	8	20	25	10	12
Driven (gears):					
N_g, no. of teeth	30	30	30	39	64
D, pitch diameter, in.	6.000	6.000	6.000	7.800	4.572
S', surface finish, μin. AA	9	20	27	10	12
Other gear characteristics:					
ϕ, pressure angle, deg	25	25	25	25	20
F, effective face width, in.	0.500	0.500	0.500	1.550	0.250
m_c, contact ratio	1.47	1.47	1.47	1.48	1.78
Test oil, MIL-L-	7808D	7808D	7808D	7808G	23699
Test conditions:					
n_p, driver speed, rpm	3660	3660	3660	3247	20000
n_g, driven speed, rpm	3660	3660	3660	2311	10000
V_t, pitchline velocity, fpm	5749	5749	5749	4760	11948
T_j, oil jet temperature, °F	200	200	200	—	200
Oil flow rate, gpm	—	—	—	—	—

where the various quantities are defined in the List of Symbols. Note that S = surface roughness in the profile direction (after break-in), μin. rms.

The critical temperature hypothesis (Chap. II, Sect. B) states that

$$T_c = T_s + \Delta T \qquad \text{(E-2)}$$

and that scoring occurs when T_c reaches the critical temperature, T_{cr}, for the metal-oil combination concerned. Thus, the AGMA design guide gives

$$T_{cr}(\text{AGMA}) = T_s(\text{AGMA}) + \Delta T(\text{AGMA}) \qquad \text{(E-3)}$$

where $T_{cr}(\text{AGMA}) = T_{cr}$ by the AGMA procedure, °F

$T_s(\text{AGMA})$ = "initial temperature," °F ("may be oil inlet")

$\Delta T(\text{AGMA})$ = as defined by Equation (E-1)

Note that in the AGMA design guide, $\Delta T(\text{AGMA})$ is calculated from the actual scoring-limited power, and as such it includes the effects of gear-tooth misalignment and dynamic load. Since these effects vary for different gear sets and for different operating conditions, the $\Delta T(\text{AGMA})$ thus computed as well as the resulting $T_{cr}(\text{AGMA})$ are not basic quantities. This is one of the reasons for introducing in Chapter VII the concept of the ideal scoring-limited power-transmitting capacity, to which corrections are applied for misalignment and dynamic load in order to arrive at the actual scoring-limited power-transmitting capacity.

Another source of error in the AGMA design guide is the assumption that $T_s(\text{AGMA})$ may be taken as the oil inlet temperature, T_j. This has not been found to be true as discussed in Chapters VI and VII.

Finally, the $\Delta T(\text{AGMA})$ equation, i.e., Equation (E-1), entails certain assumptions principally related to the coefficient of friction. This matter will now be examined.

Comparison of AGMA and True ΔT

As derived by Blok (Chap. II, Sect. B), the basic equation for ΔT is

$$\Delta T = \frac{1.11\, f w \left| \sqrt{V_1} - \sqrt{V_2} \right|}{\beta \sqrt{B}} \qquad \text{(E-4)}$$

For spur gears, it can be shown that

$$B = (32\, w R / \pi E^*)^{\frac{1}{2}}$$

$$V_1 = 2\pi \rho_p n_p / 60$$

$$V_2 = 2\pi \rho_g n_g / 60$$

where all the quantities are defined in the List of Symbols.

Substituting the above expressions into Equation (E-4), and taking $E^* = 33 \times 10^6$ psi, one obtains

$$\Delta T = \frac{15.23\, f w^{\frac{3}{4}} \left| \sqrt{\rho_p n_p} - \sqrt{\rho_g n_g} \right|}{\beta R^{\frac{1}{4}}} \qquad \text{(E-5)}$$

Accordingly, if Equation (E-1) were to be equal to Equation (E-5), then the coefficient of friction implicit in Equation (E-1) must conform to

$$0.0175 \left(\frac{50}{50-S} \right) = 15.23 \frac{f(AGMA)}{\beta}$$

Taking $\beta = 42.15$ lb/°F-in.-sec$^{\frac{1}{2}}$, then

$$f(AGMA) = 0.04843 \left(\frac{50}{50-S} \right) \qquad \text{(E-6)}$$

which is equivalent to assuming that f(AGMA) = 0.060 at S ~ 10 μin. rms.

The value of f(AGMA) as given by Equation (E-6) is, in general, much higher than the value of f derived from the sliding-rolling disk tests (Chap. VI, Sect. C). Their ratio is, from Equation (E-6),

$$\frac{f}{f(AGMA)} = 20.65\, f\,(1 - 0.02\,S) \qquad (E\text{-}7)$$

and consequently

$$\frac{\Delta T}{\Delta T(AGMA)} = 20.65\, f\,(1 - 0.02\,S) \qquad (E\text{-}8)$$

where f is, in general, a variable depending upon the metal-oil combination and operating conditions. Since f is usually lower than f(AGMA), it follows from Equation (E-8) that the true ΔT must be smaller than ΔT(AGMA).

Calculation of T_s

As mentioned earlier, the AGMA design procedure does not provide a specific guideline for assigning the value of T_s. In practical gear scoring analysis, either T_s is taken as T_j as implied by the AGMA design guide, or else some sort of estimate must be made.

In calculating T_s, use will be made of the method outlined in Chapter VII, Section B, i.e., by the relation

$$T_s - T_j = C'\phi_{av}^{0.80} \qquad (E\text{-}9)$$

where ϕ_{av} = average frictional power loss, Btu/sec

C' = a fitting constant for gear systems

The selection of C' and the calculation of ϕ_{av} were discussed in Chapter VII, Section B.

Conversion of AGMA Test Data

In order to obtain the values of T_s, ΔT, and T_c for the AGMA tests, one alternative is to assign appropriate values of f and C' andto calculate the values of ϕ_{av} by a computer program. However, inasmuch as the AGMA computer printouts have already furnished key numerical results on the basis of the AGMA procedure, these results can readily be converted without using a computer. This latter alternative is explained below for the Series A1 tests.

Composite Surface Roughness. From Table E-1, the surface roughnesses of the pinion and gear in the profile direction for Series A1 are 8 and 9 μin. AA, respectively. Thus, by Equation (B-4) in Appendix B, the initial composite surface roughness of the pinion and gear surfaces is

$$\delta_i = 3(8 + 9)/4 = 12.8\ \mu\text{in. AA}$$

Coefficient of Friction. It was shown in Chapter VI, Section C, that f is a function of $WV_s^{-\frac{1}{3}}$, but that f is nearly constant when $WV_s^{-\frac{1}{3}}$ is greater than 200. For the sake of convenience, this constant value of f is used in the present data conversion. For AISI 9310 steel gears and MIL-L-7808 oil (Oil F), this is, by Equation (57)

$$f = 0.0154 + 0.00007\,\delta_i = 0.0163$$

Average Friction Power Loss. The average frictional power loss is given by Equation (72) as follows:

$$\phi_{av} = \left[\sum \int \phi'(\epsilon)\, d\epsilon\right] \frac{N_p}{360} \qquad \text{(E-10)}$$

where ϕ_{av} = average frictional power loss, Btu/sec

ϕ' = $f W V_s/9336$, Btu/sec

N_p = number of pinion teeth

In this conversion process, f is taken as constant; thus ϕ_{av} becomes a function of $\int d(WV_s)$ only. Accordingly, the values of W and V_s can be readily deduced from the AGMA printouts and plotted vs. the roll angle. The areas under the curve for the single and double tooth contact regions are then measured by means of a planimeter.

Applying the above equation and with proper units, then for Series A1

$$\phi_{av} = 0.001324\,P$$

where P = power transmitted, hp.

Quasi-Steady Surface Temperature. The quantity $(T_s - T_j)$ is then computed from Equation (E-9) by taking C' = 173. This is equivalent to assuming that the oil flow rate jetted toward the gear mesh is 1.0 gpm. At this flow rate, C = 115 from Figure 25; and applying Equation (74), C' = 1.5 x 115 = 173. In other words,

$$T_s - T_j = 173\,\phi_{av}^{0.80}$$

Since T_j = 200°F for Series A1, then

$$T_s = 200 + 173\,\phi_{av}^{0.80}$$

Conjunction Surface Temperature Rise. The quantity ΔT is given by Equation (E-8), where S is expressed in μin. rms by the AGMA procedure. In these tests, S' in μin. AA was given. By taking S = 0.9S', then Equation (E-8) becomes

$$\frac{\Delta T}{\Delta T(AGMA)} = 20.65\,f\,(1 - 0.018S')$$

For Series A1, S' = (8 + 9)/2 = 8.5 μin. AA, and f = 0.0163 as given earlier. Thus

$$\Delta T = 0.285\,\Delta T(AGMA)$$

Critical Scoring Point. The ΔT of special interest in gear scoring analysis is that which has the highest value in the mesh cycle. The AGMA computer printouts tabulate all ΔT(AGMA) values vs. the roll angle, and the highest ΔT(AGMA) values are attained approximately midway on the recess portion of double tooth contact. These values are therefore extracted from the AGMA computer printouts, and the revised ΔT is calculated by the preceding equation.

Revised Data for AGMA Tests

Series A1. Using the above procedure, the revised data for Series A1 at critical scoring point are calculated, and are tabulated in Table E-2. Note that scoring first occurred in Test 87 at 362 hp. At this power level, $T_s = 296°F$, $\Delta T = 38°F$, and $T_c = 334°F$. By the AGMA rationale, the critical temperature would have to be 334°F. Yet, from Equation (50), the true critical temperature in this case is

$$T_{cr} = 540 - 3.80\,\delta_i = 491°F$$

Thus assuming no tooth misalignment and dynamic tooth load, the ideal scoring-limited power-transmitting capacity must be considerably greater than 362 hp. An estimate for the ideal power-transmitting capacity for this case will be given later. It is only necessary to emphasize here that the difference between the actual and ideal power-transmitting capacity must be due to misalignment and dynamic effects.

Series A2. Series A2 differs from Series A1 only in that the test gears have rougher surfaces. Following the same procedure as illustrated above, the revised data for Series A2 tests are presented in Table E-3. Scoring first occurred in Test 118 at 209 hp, at which time $T_s = 265°F$, $\Delta T = 28°F$, and $T_c = 293°F$. Yet, the true critical temperature in this case is

$$T_{cr} = 540 - 3.80\,\delta_i = 426°F$$

which is considerably higher than 293°F.

Series A3. Series A3 differs from Series A1 and A2 in that the test gears have even rougher surfaces. Following the same procedure as illustrated above, the revised data for Series A3 tests are given in Table E-4. Scoring first occurred in Test 110 at 170 hp, at which time $T_s = 257°F$, $\Delta T = 26°F$, and $T_c = 283°F$. The true critical temperature in this case is

TABLE E-2. REVISED DATA FOR SERIES A1 TESTS

Test no.	P, hp	ϕ_{av}, Btu/sec	T_j, °F	T_s, °F	$\Delta T(AGMA)$, °F	ΔT, °F	T_c, °F	Remarks
82	329	0.4356	200	289	125	36	325	
96	348	0.4608	200	293	131	37	330	
92	355	0.4700	200	294	133	38	332	
101	361	0.4780	200	295	135	38	333	
87	362	0.4793	200	296	135	38	334	Scored
80	377	0.4991	200	299	139	40	339	Scored
102	384	0.5084	200	300	141	40	340	
97	391	0.5177	200	302	143	41	343	
106	393	0.5203	200	302	143	41	343	Scored
107	436	0.5773	200	311	155	44	355	Scored
103	438	0.5799	200	312	155	44	356	Scored
104	465	0.6157	200	317	163	46	363	Scored
105	474	0.6276	200	319	165	47	366	Scored

Conversion equations

$$\delta_i = 3(8 + 9)/4 = 12.8\ \mu\text{in. AA}$$

$$f = 0.0154 + 0.00007\,\delta_i = 0.0163$$

$$\phi_{av} = 0.001324\,P$$

$$T_s = T_j + 173\,\phi_{av}^{0.80}$$

$$\Delta T = 20.65\,f\,(1 - 0.018\,S')\,\Delta T(AGMA)$$

$$= 0.285\,\Delta T(AGMA)$$

$$T_{cr} = 540 - 3.80\,\delta_i = 491\,°F$$

TABLE E-3. REVISED DATA FOR SERIES A2 TESTS

Test no.	P, hp	ϕ_{av}, Btu/sec	T_j, °F	T_s, °F	ΔT(AGMA), °F	ΔT, °F	T_c, °F	Remarks
115	193	0.2794	200	261	117	27	288	
113	201	0.2858	200	263	120	27	290	
118	209	0.2972	200	265	123	28	293	Scored
119	223	0.3171	200	269	130	30	299	Scored
116	232	0.3299	200	271	134	31	301	
120	239	0.3399	200	273	136	31	304	Scored
114	270	0.3839	200	280	150	35	315	Scored
117	271	0.3854	200	280	150	35	315	Scored

Conversion equations

$$\delta_i = 3\,(20 + 20)/4 = 30.0\ \mu\text{in. AA}$$

$$f = 0.0154 + 0.00007\,\delta_i = 0.0175$$

$$\phi_{av} = 0.001422\,P$$

$$T_s = T_j + 173\,\phi_{av}^{0.80}$$

$$\Delta T = 20.65\,f\,(1 - 0.018\,S')\,\Delta T(\text{AGMA})$$

$$= 0.231\,\Delta T(\text{AGMA})$$

$$T_{cr} = 540 - 3.80\,\delta_i = 426°\text{F}$$

TABLE E-4. REVISED DATA FOR SERIES A3 TESTS

Test no.	P, hp	ϕ_{av}, Btu/sec	T_j, °F	T_s, °F	ΔT(AGMA), °F	ΔT, °F	T_c, °F	Remarks
110	170	0.2501	200	257	132	26	283	Scored
111	199	0.2927	200	265	149	30	295	Scored
108	207	0.3045	200	267	153	30	297	Scored
109	207	0.3045	200	267	153	30	297	Scored
112	217	0.3192	200	269	159	32	301	Scored

Conversion equations

$$\delta_i = 3(25 + 27)/4 = 39.0\ \mu\text{in. AA}$$

$$f = 0.0154 + 0.00007\,\delta_i = 0.0181$$

$$\phi_{av} = 0.001471\,P$$

$$T_s = T_j + 173\,\phi_{av}^{0.80}$$

$$\Delta T = 20.65\,f\,(1 - 0.018\,S')\,\Delta T(\text{AGMA})$$

$$= 0.199\,\Delta T(\text{AGMA})$$

$$T_{cr} = 540 - 3.80\,\delta_i = 392°\text{F}$$

$$T_{cr} = 540 - 3.80\,\delta_i = 392°F$$

which is again considerably higher than 283°F.

Series B. Series B tests were conducted at 3 different power levels, with the oil flow rate reduced to approach scoring. Neither the oil jet temperature nor the oil flow rate was reported. However, T_s was measured and reported. Since T_s is known in this case, all that is needed is to revise the ΔT, in order to obtain T_c. The revised results are presented in Table E-5.

Note that scoring occurred in Test 272 at 516 hp, at which time $T_s = 402°F$, $\Delta T = 20°F$, and $T_c = 422°F$; and also in Test 273 at 688 hp, $T_s = 409°F$, $\Delta T = 24°F$, and $T_c = 433°F$. The true critical temperature in this case is

$$T_{cr} = 540 - 3.80\,\delta_i = 483°F$$

which is considerably higher than either 422°F or 433°F.

The quantity ϕ_{av} is not required in the data conversion, but it will be required in the estimate of the ideal scoring-limited power-transmitting capacity. This quantity is thus also furnished in Table E-5.

Series C. Series C was conducted with AISI 9310 steel gears and MIL-L-23699 oil (Oil E), in a similar manner as Series A1, A2, and A3. Hence a similar data conversion process may be used.

It was noted in Chapter VI, Section B, that the coefficient of friction for AISI 9310 steel disks was nearly the same with Oil E and Oil F, thus the same f equation is used in this case as before. The other data manipulations require no further comments. The revised results are presented in Table E-6.

Note that scoring first occurred in Test 10 at 254 hp, T_s 261°F, $\Delta T = 38°F$, and $T_c = 299°F$. This is considerably lower than the true critical temperature for this metal-oil combination, which, from Equation (52), is

$$T_{cr} = 515 - 3.80\,\delta_i = 447°F$$

TABLE E-5. REVISED DATA FOR SERIES B TESTS

Test no.	P, hp	ϕ_{av}, Btu/sec	T_j, °F	T_s, °F	ΔT(AGMA), °F	ΔT, °F	T_c, °F	Remarks
265	344	0.4259	—	171	52	15	186	
268	344	0.4259	—	280	52	15	295	
271	344	0.4259	—	398	52	15	413	
266	516	0.6388	—	171	70	20	191	
269	516	0.6388	—	305	70	20	325	
272	516	0.6388	—	402	70	20	422	Scored
267	688	0.8517	—	187	87	24	211	
264	688	0.8517	—	195	87	24	219	
270	688	0.8517	—	303	87	24	327	
273	688	0.8517	—	409	87	24	433	Scored

Conversion equations

$$\delta_i = 3(10 + 10)/4 = 15.0\ \mu\text{in. AA}$$

$$f = 0.0154 + 0.00007\,\delta_i = 0.0165$$

$$\phi_{av} = 0.001238\,P$$

$$T_s = \text{measured}$$

$$\Delta T = 20.65\,f\,(1 - 0.018\,S')\,\Delta T(\text{AGMA})$$

$$= 0.279\,\Delta T(\text{AGMA})$$

$$T_{cr} = 540 - 3.80\,\delta_i = 483°\text{F}$$

TABLE E-6. REVISED DATA FOR SERIES C TESTS

Test no.	P, hp	ϕ_{av}, Btu/sec	T_j, °F	T_s, °F	ΔT(AGMA), °F	ΔT, °F	T_c, °F	Remarks
1	63	0.0673	200	220	50	14	234	
4	190	0.2031	200	248	114	31	279	
7	222	0.2373	200	255	128	35	290	
10	254	0.2715	200	261	141	38	299	Scored
13	286	0.3057	200	267	154	42	309	Scored
16	317	0.3389	200	273	167	45	318	Scored
18	349	0.3731	200	278	179	48	326	Scored
20	381	0.4073	200	284	191	52	336	Scored

Conversion equations

$$\delta_i = 3(12 + 12)/4 = 18.0\ \mu\text{in. AA}$$

$$f = 0.0154 + 0.00007\,\delta_i = 0.0167$$

$$\phi_{av} = 0.001069\,P$$

$$T_s = T_j + 173\,\phi_{av}^{0.80}$$

$$\Delta T = 20.65\,f\,(1 - 0.018S')\,\Delta T(AGMA)$$

$$= 0.270\,\Delta T(AGMA)$$

$$T_{cr} = 515 - 3.80\,\delta_i = 447°F$$

Estimation of Ideal Scoring-Limited Power Capacity

As defined in Chapter VII, Section A, the ideal scoring-limited power-transmitting capacity, P_I, of a set of gears is that for the ideal case in the absence of tooth misalignment and dynamic load. This quantity may be predicted for the cases examined by the computer, as explained in Chapter VII, Section B. However, it can also be done by relatively simple calculations as illustrated below.

Series A1. At constant speed and constant T_j, Table E-2 gives

$$T_s = 200 + 173\,\phi_{av}^{0.80}$$

Table E-2 also gives $T_{cr} = 491°F$. Thus the general expression for ΔT is

$$\Delta T = 491 - T_s = 291 - 173\,\phi_{av}^{0.80} \qquad \text{(E-11)}$$

Now, at constant speed and constant f, Equation (E-5) states that ΔT must also be proportional to $w^{0.75}$ or $P^{0.75}$. Take Test 87 in Table E-2, $\Delta T = 38°F$ at $P = 362$ hp. Thus

$$\Delta T = 38\left(\frac{P}{362}\right)^{0.75} \qquad \text{(E-12)}$$

By the critical temperature hypothesis, scoring would occur when ΔT from Equation (E-11) equals ΔT from Equation (E-12). To obtain this ΔT, the two ΔT curves from the two above equations may be easily calculated, and plotted vs. P. The intersection of these two curves then gives P_I on the abscissa and the corresponding ΔT on the ordinate. From Equation (E-11), the corresponding T_s is simply $T_s = 491 - \Delta T$.

Using the above procedure, it can be shown that, for Series A1 conditions,

$$P_I = 973 \text{ hp}$$

$$\Delta T = 80°F$$

$$T_s = 411°F$$

These results are tabulated in Table E-7, along with other pertinent data.

Series A2, A3, and C. An identical procedure may be used for these test series. The results obtained are presented in Table E-7 for comparison.

Series B. Series B requires a different treatment, since T_j in this case is not known. It is proposed to estimate the ideal performance for this case at two assumed values of T_j, and examine the results.

Consider Test 272 in Table E-5, which scored at 516 hp, at measured $T_s = 402°F$. The value of T_j is not known. Moreover, scoring was obtained by reducing the oil flow rate, which is also not known. In the absence of such information, let it first be assumed that $T_j = 200°F$. This then permits an estimate for the value of C' in Equation (E-10), thus:

$$C' = (T_s - T_j) \Big/ \phi_{av}^{0.80}$$

$$= (402 - 200) / (0.6388)^{0.80} = 289.1$$

Then under the assumed conditions

$$T_s - 200 = 289.1\, \phi_{av}^{0.80}$$

Since $T_{cr} = 483°F$, therefore

$$\Delta T = 483 - T_s = 283 - 289.1\, \phi_{av}^{0.80} \qquad \text{(E-13)}$$

The other ΔT expression is

$$\Delta T = 20 \left(\frac{P}{516}\right)^{0.75} \qquad \text{(E-14)}$$

TABLE E-7. COMPARISON OF ACTUAL AND IDEAL PERFORMANCE

	Series B (Test 272)		Series B (Test 273)		Series A1	Series A2	Series A3	Series C
	Case I	Case II	Case III	Case IV	(Test 87)	(Test 118)	(Test 110)	(Test 10)
δ_i, μin.	15.0	15.0	15.0	15.0	12.8	30.0	39.0	18.0
T_j, °F	200	250	200	250	200	200	200	200
V_t, fpm	4760	4760	4760	4760	5749	5749	5749	11968
f	0.0165	0.0165	0.0165	0.0165	0.0163	0.0175	0.0181	0.0167
Actual Performance								
T_s, °F	402	402	409	409	296	265	257	261
ΔT, °F	20	20	24	24	38	28	26	38
T_c, °F	422	422	433	433	334	293	283	299
P_A, hp	516	516	688	688	362	209	170	254
Ideal Performance								
T_s, °F	458	456	454	453	411	361	334	355
ΔT, °F	25	27	29	30	80	65	58	92
T_{cr}, °F	483	483	483	483	491	426	392	447
P_I, hp	700	756	879	933	973	644	496	821
Comparison								
P_A/P_I	0.74	0.68	0.78	0.74	0.37	0.32	0.34	0.31

Solving Equations (E-13) and (E-14) simultaneously as before, one obtains

$$P_I = 700 \text{ hp}$$

$$\Delta T = 25°F$$

$$T_s = 458°F$$

These values are tabulated in Table E-7 as Case I.

For Case II, it is assumed that $T_j = 250°F$. In that case

$$C' = (402 - 250)/(0.6388)^{0.80} = 217.5$$

Thus, similar to the above,

$$\Delta T = 483 - T_s = 233 - 217.5\,\phi_{av}^{0.80} \qquad \text{(E-15)}$$

and Equation (E-14) remains applicable in this case.

Solving Equations (E-14) and (E-15) simultaneously as before, then

$$P_I = 756 \text{ hp}$$

$$\Delta T = 27°F$$

$$T_s = 456°F$$

as tabulated in Table E-7 as Case II.

Note from Table E-5 that scoring was also obtained in Test 273 at 688 hp, at measured $T_s = 409°F$. By similar calculations, the ideal performance based on Test 273 at $T_j = 200°F$ and $250°F$ can also be estimated. These results are presented in Table E-7 as Case III and Case IV, respectively.

Comparison of Actual and Ideal Performance

Table E-7 compares the actual performance with the ideal

performance for the 5 test series examined. A quantity of key interest is the ratio of the actual to ideal scoring-limited power-transmitting capacity, P_A/P_I, which is given on the last line of the table.

Note for Series B that the value of P_A/P_I for Cases I, II, III, and IV, based upon two different tests each with two assumed T_j values, do not vary greatly. The average of this ratio for Series B is 0.74; the standard deviation is 0.04, or only 5.5 percent.

As defined in Chapter VII, Section A, the fact that P_A/P_I is less than unity is due to the effects of tooth misalignment and dynamic load. The deduced data so far do not directly provide an indication of the relative contributions of the misalignment and dynamic effects. However, the influence of dynamic effect is unmistakenly reflected by the steady decrease of P_A/P_I in Table E-7 as the pitchline velocity, V_t, is increased. An attempt to separate the misalignment and dynamic effects is presented in Chapter VII, Section C.

APPENDIX F
SUMMARY OF SPUR GEAR TEST DATA

The spur gear test program consisted of replicate tests on five sets of ground spur gears and five sets of honed spur gears of same design and material, tested for scoring at the same speed and oil jet temperature. These tests were performed at BHC under subcontract to SwRI. BHC Report 299-097-005, "Results of Gear Tooth Scoring Investigation Conducted on 31 x 76 Spur Gears" by R. Battles, R. T. Jenkins, and C. E. Braddock, dated October 24, 1974, was submitted to SwRI on December 2, 1974. Copies of the full report are on file at USAAMRDL, BHC, and SwRI. The following is an abstract of the report, plus analysis and interpretations made by SwRI personnel.

Test Gears

A description of the spur gears is given in Table 7 in Chapter VIII, Section B. Briefly, the pinion had 31 teeth, a pitch diameter of 3.4671 in., and a face width of 1.375 in.; and the gear had 76 teeth, a pitch diameter of 8.9412 in., and a face width of 1.250 in. The diametral pitch was 8.5 $in.^{-1}$, and the pressure angle was 22.0°. The gears were made of AISI 9310 CEVM steel, carburized to a case thickness of 0.030-0.040 in., a case hardness of 60-63 R_C, and a core hardness of 33-41 R_C—essentially the same as the test disks employed in the disk test program (App. D).

The surface finishes of the gears were originally specified as about 17 μin. AA for the ground gears and about 7 μin. AA for the honed gears. However, the gears as received from the vendor were found to be considerably smoother. In order to expedite the test program, five sets of ground spur gears as received were selected for the spur gear test program, and the remaining five sets were rehoned at BHC.

The surface finishes of all pinions and gears were measured by BHC in both profile and lead directions before break-in, after break-in, and after test termination. These measurements were made on two teeth by three instruments at different times; but not by the same instrument at all times. In order to facilitate comparisons on the same basis, the reported measurements by BHC were converted to one instrument base by a constant multiplier. The revised initial surface roughness values for the gears are presented in Table F-1. The revised surface roughness values after break-in are presented in

TABLE F-1. INITIAL SURFACE ROUGHNESS OF SPUR GEARS

Test no.	Pinion, μin. AA			Gear, μin. AA			δ_i, μin. AA (Pinion & gear)
	Profile	Lead	Composite	Profile	Lead	Composite	
Ground gears							
G1	10.1	4.5	7.3	7.6	4.2	5.9	13.2
G2	9.7	3.5	6.6	9.0	3.2	6.1	12.7
G3	8.8	4.9	6.9	8.8	2.8	5.8	12.7
G4	9.8	4.2	7.0	9.1	5.6	7.4	14.4
G5	9.8	3.9	6.9	9.8	7.7	8.7	15.6
Avg.	9.6	4.2	6.9	8.9	4.7	6.8	13.7
Honed gears							
H1	6.8	7.0	6.9	9.0	10.0	9.5	16.4
H2	7.0	6.5	6.8	8.5	9.0	8.8	15.6
H3	7.0	7.5	7.3	8.5	8.0	8.3	15.6
H4	7.0	7.3	7.2	9.5	10.5	10.0	17.2
H5	7.0	6.3	6.7	7.5	7.5	7.5	14.2
Avg.	7.0	6.9	7.0	8.6	9.0	8.8	15.8

Table F-2. Surface roughness values after test termination, being generally very high and erratic and not pertinent to this study, are not presented herein.

In Tables F-1 and F-2, the test numbers with prefix "G" refer to the ground gear sets, while those with prefix "H" refer to the honed gear sets. Each tabulated surface roughness value in the profile or lead direction is the revised value of the average of the two readings taken on the two teeth. The composite surface roughness of either the pinion or gear is calculated by using Equation (B-1) in Appendix B. The composite surface roughness of the gear set is then calculated by using Equation (B-2).

Referring now to the data for the ground gears shown in Table F-1, it will be noted that the initial composite surface roughness of the gear set, δ_i, varied from 12.7 μin. AA to 15.6 μin. AA, with an average of 13.7 μin. AA. Note further that the ratio of surface roughness in the profile direction to that in the lead direction is fairly close to 2, which is characteristic of most ground surfaces (App. B). The initial composite surface roughness, δ_i, of the honed gear sets varied from 14.2 μin. AA to 17.2 μin. AA, with an average of 15.8 μin. AA.

Table F-2 shows similar surface roughness data after break-in. Note that the break-in process reduced the average composite surface roughness of the ground gear sets by about 21 percent and that of the honed gear sets by about 27 percent—generally in line with the trends previously reported for sliding-rolling disks.[25]

Test Oil

The test oil used was Oil F, the same MIL-L-7808G oil used in the disk test program (App. D).

Test Equipment

A 4-square regenerative test rig shown in Figure F-1 was used in testing. Note that the test gears were mounted on vertical shafts, with the gear as the driver. In addition to the conventional measurements of gear speed, gear torque, and oil jet temperature, temperature measurements were also made on the test pinion by means of four welded thermocouples at locations shown in Figure F-2.

Dimensional inspection of the test section housing, support bearings, and bearing retainers revealed a basic rig misalignment of

TABLE F-2. SURFACE ROUGHNESS OF SPUR GEARS AFTER BREAK-IN

Test no.	Pinion, μin. AA			Gear, μin. AA			δ_i, μin. AA (Pinion & gear)
	Profile	Lead	Composite	Profile	Lead	Composite	
Ground gears							
G1	7.0	5.0	6.0	5.6	5.0	5.3	11.3
G2	6.0	3.2	4.6	5.6	2.8	4.2	8.8
G3	6.7	4.2	5.5	8.3	5.6	7.0	12.5
G4	7.4	4.2	5.8	8.7	3.5	6.1	11.9
G5	5.6	2.5	4.1	6.3	4.6	5.5	9.6
Avg.	6.5	3.8	5.2	6.9	4.3	5.6	10.8
Honed gears							
H1	5.0	5.5	5.3	4.5	6.8	5.7	11.0
H2	5.3	5.5	5.4	5.5	6.5	6.0	11.4
H3	4.8	6.5	5.7	7.0	8.0	7.5	13.2
H4	2.5	5.0	3.8	6.5	7.0	6.8	10.6
H5	4.8	5.5	5.2	6.0	6.8	6.4	11.6
Avg.	4.5	5.6	5.1	5.9	7.0	6.5	11.6

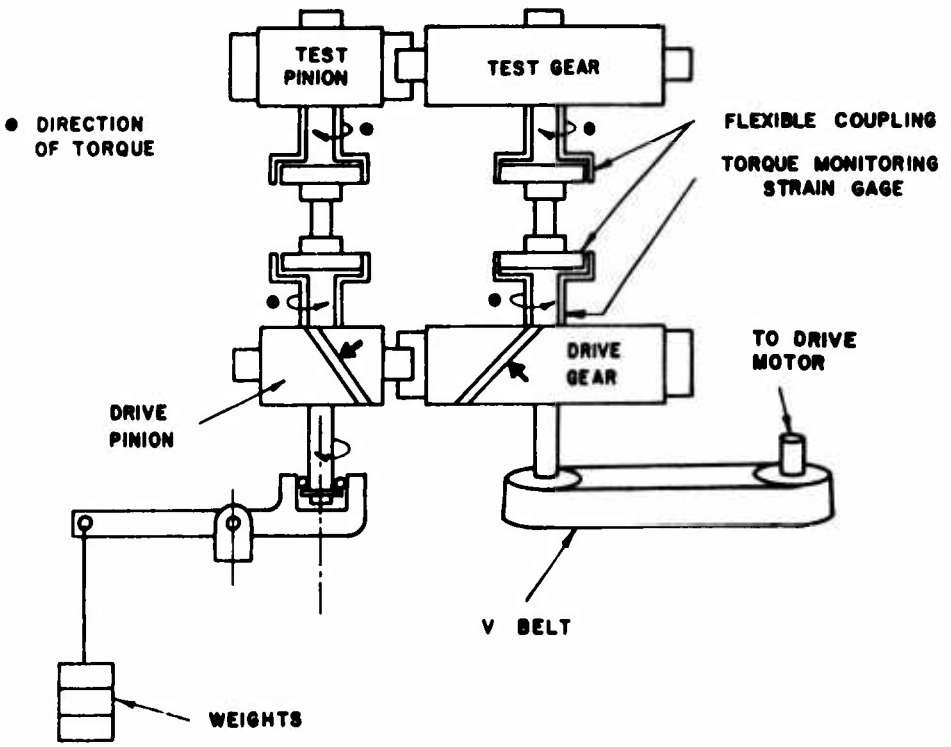

Figure F-1. Schematic of spur gear test rig

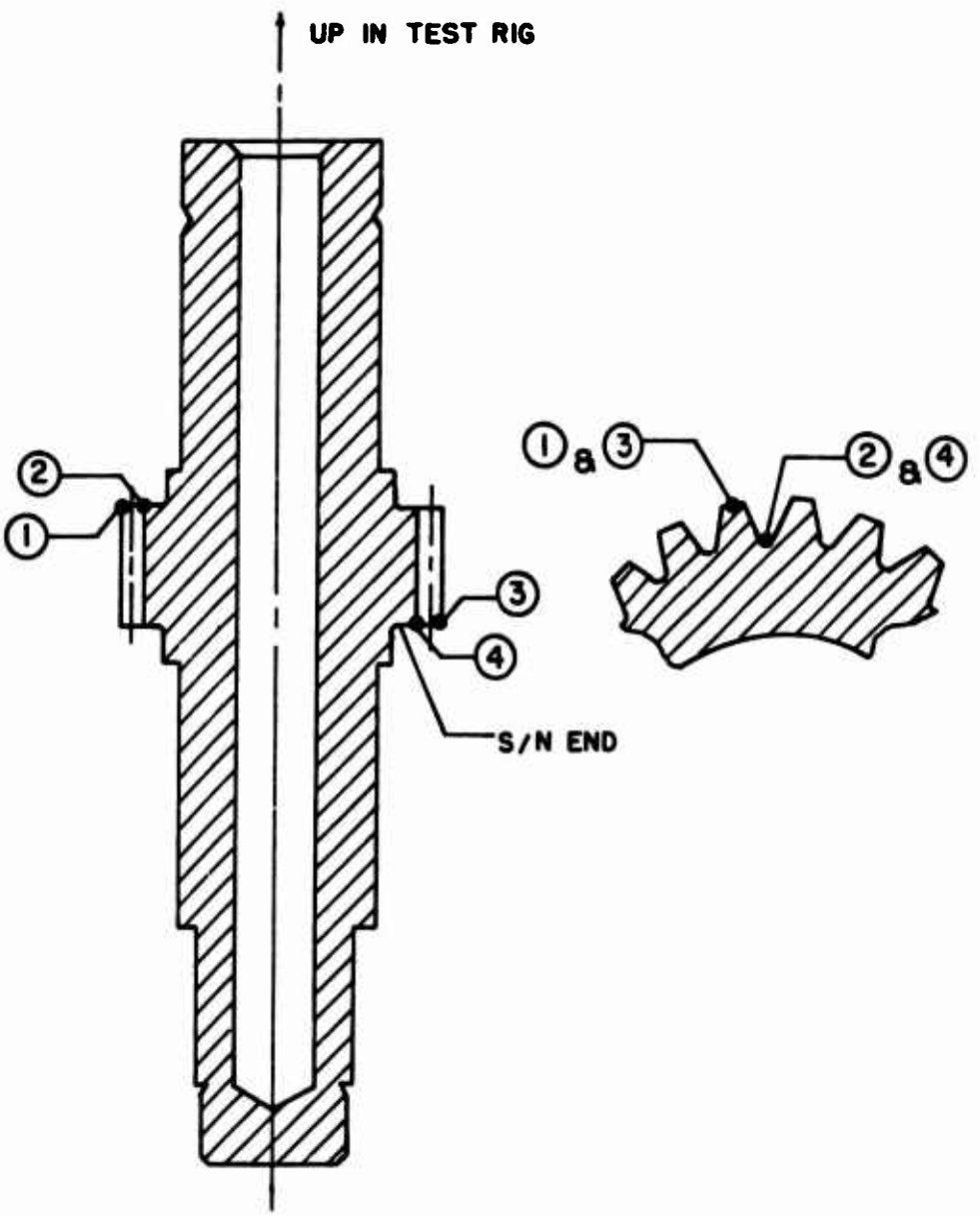

Figure F-2. Thermocouple locations on spur gear pinion

0.0007 rad. between the pinion and gear, with the lower end of the tooth (the S/N end, Fig. F-2) being the more heavily loaded than the upper end.

It was also found that the pinions and gears themselves had some lead errors. An attempt was made to match the pinion and gear in each set to compensate for the lead errors as much as possible. The net lead errors on the five sets of ground gears averaged 0.00006 rad. The net lead errors on the five sets of honed gears averaged 0.00014 rad. The variations from these average values from one matched set to another was less than 0.00008 rad. standard deviation.

The total misalignment of the gear teeth is the sum of the misalignments in the test rig and the gear sets. The total misalignment thus averaged 0.00076 rad. for the ground gear sets, and 0.00084 rad. for the honed gear sets.

Test Procedure

The gear sets were broken in by the following schedule: First, at an oil jet temperature of 120°F and a pinion speed of 4,385 rpm (55% of test speed), each gear set was operated for 30 min. at each of four load levels, viz., 500, 1000, 1500, and 2000 ppi. The oil jet temperature was then raised to 190°F, and each gear set was operated for 30 min. at each of two load levels, viz., 1000 and 2000 ppi.

The scoring test was conducted at an oil jet temperature of 250°F and a pinion speed of 7,992 rpm. The tooth load was increased from an initial value of 1000 ppi, in 150-ppi steps of 10 min. each, until either scoring was obtained or the test rig capacity (2950 ppi) was reached. After each load step, the rig was stopped and a visual inspection made to detect scoring. Following the inspection, the previous load step was repeated before proceeding to the next load step.

The test gears were lubricated by cascading oil and by an oil jet directed into the gear mesh. During the scoring test sequence, the oil jet temperature was 250°F and the flow rate was 0.28 gpm. Neither the temperature nor the flow rate of the cascading oil was measured. However, the cascading oil temperature was estimated by BHC to be close to 250°F, since the oil was drawn from the same heated reservoir as that supplied to the oil jet. The cascading oil flow rate was estimated by BHC to be about 2-3 times the oil jet flow rate, or about $2.5 \times 0.28 = 0.7$ gpm.

Scoring-Limited Power-Transmitting Capacity

The test results on the 10 spur gear sets are summarized in Table F-3.

With the ground gears, two of the tests did not result in scoring at the maximum rig capacity of 791 hp. The average scoring power was therefore in excess of 679 hp by an unknown margin. A statistically more meaningful scoring power, deduced from Weibull analysis at 10-percent scoring probability, is 507 hp, and its 90-percent confidence limits are 334 and 770 hp.

With the honed gears, all 5 tests produced scoring. The average scoring power was 606 hp. A statistically more meaningful scoring power, deduced from Weibull analysis at 10-percent scoring probability, is 425 hp, and its 90-percent confidence limits are 270 and 688 hp.

It is interesting to note that the ground gears were smoother than the honed gears, hence the ground gears would be expected to score at a higher power level than the honed gears. This trend is indeed reflected by both the average and statistically-deduced scoring power. However, the statistically-deduced values are more meaningful. The poor confidence limits were due to the inherent scatter of the scoring phenomenon and the very few tests performed.

Pinion Surface Temperature

The pinion surface temperature was measured by means of welded thermocouples at four locations as shown in Figure F-2. The readings at scoring or at test termination (i.e., at 791 hp) are presented in Table F-3. Note that the temperature at the upper end of the pinion was much lower than that at the lower end. Much of this difference was of course due to the effect of tooth misalignment discussed earlier, which placed less load on the upper end of the gear teeth than on the lower end. The other reason might be that the cascading oil, which must go through the cooler upper support bearing, was actually at a lower temperature than 250° F as it hit the upper gear surfaces, and became heated as it progressed downward. On the other hand, temperature measurements of this kind are difficult to make at best; and it is suspected that all reported pinion surface temperature readings are probably on the low side. There is presently no realistic way to evaluate the overall flow and heat transfer effects being encountered.

TABLE F-3. SUMMARY OF SPUR GEAR TEST RESULTS

Test no.	Scoring load, ppi	Scoring torque, in.-lb	Scoring power, hp	Pinion surface temperature, °F			
				Upper end		Lower end	
				Tooth tip	Tooth root	Tooth tip	Tooth root
Ground gears							
G1	2050	10622	550	219	234	285	278
G2	>2950	>15285	>791	>227	>245	>269	>264
G3	2650	13731	711	235	246	280	275
G4	2050	10622	550	231	244	256	255
G5	>2950	>15285	>791	>237	>251	>270	>271
Honed gears							
H1	2800	14508	751	245	240	300	285
H2	2500	12954	671	236	245	312	299
H3	1900	9845	510	237	239	278	-
H4	2350	12176	630	246	251	283	282
H5	1750	9067	469	228	235	263	267

APPENDIX G
SUMMARY OF SPIRAL BEVEL GEAR TEST DATA

The spiral bevel gear test program consisted of five replicate tests on a specific design of spiral bevel gears. BHC Report 299-097-004, "Results of Gear Tooth Scoring Investigation Conducted on 22 x 23 Spiral Bevel Gears" by R. Battles, R. T. Jenkins, and C. E. Braddock, dated June 27, 1974, was submitted to SwRI on October 31, 1974. Copies of the full report are on file at USAAMRDL, BHC, and SwRI. The following is an abstract of the report, plus analysis and interpretations made by SwRI personnel.

Test Gears

A description of the spiral bevel gears tested in this program is given in Table 11 in Chapter VIII, Section D. Briefly, the pinion had 22 teeth, a pitch diameter of 3.6000 in., and a face width of 0.866 in.; and the gear had 23 teeth, a pitch diameter of 3.7637 in., and a face width of 0.866 in. The diametral pitch was 6.111 $in.^{-1}$, the pressure angle was 22.5°, and the spiral angle was 35.0°. The gears were made of AISI 9310 CEVM steel, carburized to a case thickness of 0.030-0.040 in., a case hardness of 60-63 R_C, and a core hardness of 33-41 R_C—essentially the same as the test disks employed in the disk test program (App. D).

The surface finish of the gears was specified as 22 μin. AA maximum. Attempts were made at BHC to measure the surface roughnesses of the pinions and gears; but without success. Therefore, no surface roughness readings were reported.

Test Oil

The test oil used was Oil F, the same MIL-L-7808G oil used in the disk test program (App. D).

Test Equipment

A standard transmission test stand available at BHC was modified for use in testing. As shown in Figure G-1, an electric motor was connected to a variable-speed magnetic coupling driving a speed-up gearbox, which drove the test gears via a slave transmission. To simplify the operation of the test stand, the main rotor mast was removed, and a water brake was used for power absorption.

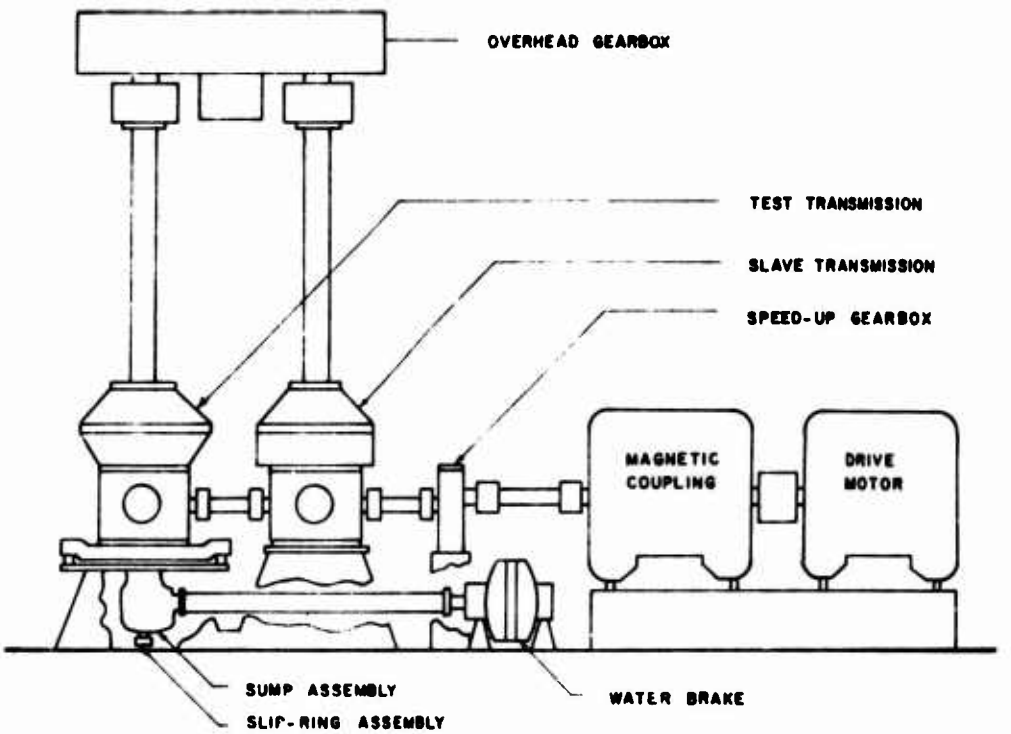

Figure G-1. Schematic of spiral bevel gear test rig

The test gears were installed in an overhung mounting with each gear supported by a duplex ball bearing and a roller bearing. The pinion was the driver.

In addition to the conventional measurements of gear speed, gear torque, and oil jet temperature, temperature measurements were also made on the test pinion by means of five imbedded or welded thermocouples at locations shown in Figure G-2.

No information on possible test gear misalignment was available.

Test Procedure

The gear sets were broken in by the following schedule: First, at an oil jet temperature of 120°F and a pinion speed of 2,700 rpm (60% of test speed), each gear set was operated for 30 min. at each of three load levels, viz., 517, 1035, and 1551 ppi. The oil jet temperature was then raised to 190°F, and each gear set was operated for 30 min. at each of two load levels, viz., 1035 and 2070 ppi.

The scoring test was conducted at an oil jet temperature of 190°F and a pinion speed of 4,500 rpm. The tooth load was increased from an initial value of 2070 ppi, in 207-ppi steps of 10 min. each, until scoring was obtained. After each load step, the rig was stopped for visual inspection of scoring. Following the inspection, the previous load step was repeated before proceeding to the next load step.

The test gears were lubricated by cascading oil and by an oil jet directed into the mesh. During the scoring test sequence, the oil jet temperature was 190°F and the flow rate was 0.45 gpm. Neither the temperature nor the flow rate of the cascading oil was measured. However, as in the case of spur gear tests (App. F), it is estimated that the cascading oil temperature was close to 190°F and the flow rate was probably on the order of 1.1 gpm.

Scoring-Limited Power-Transmitting Capacity

Six tests were run on the spiral bevel gears. However, one test was aborted because the test oil pump was inadvertently not turned on. The results of the five remaining valid tests are summarized in Table G-1. The average scoring power was 367 hp. A statistically more meaningful scoring power, derived from Weibull analysis at 10-percent scoring probability, is 346 hp, and its 90-percent confidence limits are 320 and 374 hp.

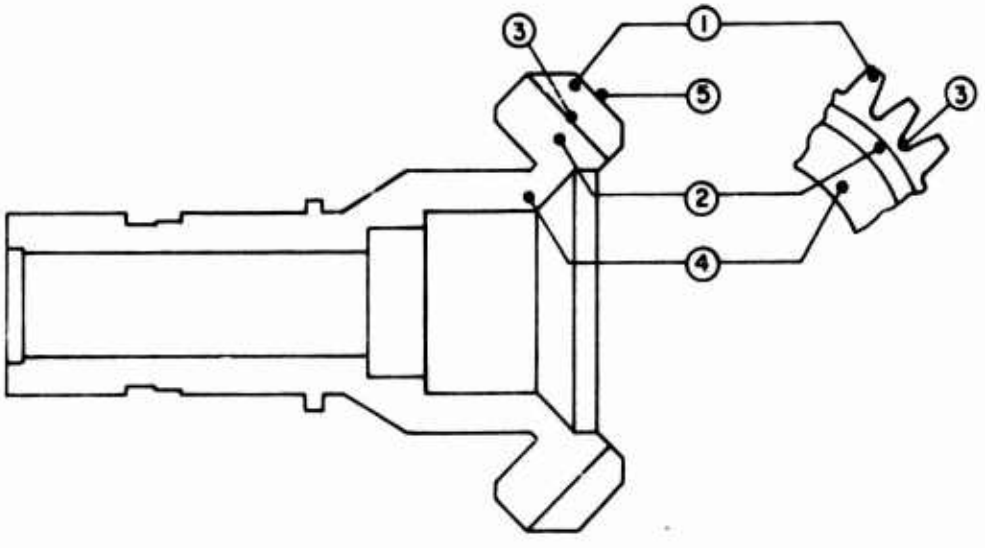

Figure G-2. Thermocouple locations on spiral bevel gear pinion

TABLE G-1. SUMMARY OF SPIRAL BEVEL GEAR TEST RESULTS

Test no.	Scoring load, ppi	Scoring torque, in.-lb	Scoring power, hp	Pinion surface temperature, °F			Pinion blank temperature, °F	
				Tooth tip	Tooth root	Top land	Web	Hub
1	4140	5222	357	200	187	–	169	185
2	4347	5483	374	–	190*	–	–	–
3	4554	5744	392	–	213*	220	–	–
4	4140	5222	357	–	224*	275	–	–
5	4140	5222	357	–	217	235	–	–

* Average of readings from three equally spaced thermocouples in position 3 (Fig. G-2).

Pinion Surface and Blank Temperatures

The pinion surface temperature was measured by means of imbedded or welded thermocouples at three locations shown in Figure G-2. The temperatures reached at scoring are presented in Table G-1. In Tests 2, 3, and 4, the reported temperatures at the tooth root were the averages of readings from three equally-spaced thermocouples in position 3 shown in Figure G-2. The individual thermocouple readings in each case differed from the reported average by about ±10°F. Note that the tooth tip and top land temperatures were generally higher than the tooth root temperature, due apparently to the fact that the spiral bevel gear teeth were not modified and therefore carried more load at the tooth tip.

The pinion blank temperature was measured by means of imbedded thermocouples at two locations shown in Figure G-2. As seen in Table G-1, only one set of pinion blank temperatures was taken (Test 1). Note that the blank temperature was considerably lower than the surface temperature, and is therefore not a realistic quantity to use in critical temperature calculations.

APPENDIX H
SPUR GEAR COMPUTER PROGRAM

Program Goal

This program evaluates the scoring potential of spur gears. Pertinent gear data are entered into the program, and data relating to contact geometry, tooth contact loads, friction, instantaneous surface temperature, and instantaneous frictional power loss are determined for approximately 21 points in the mesh. Contact loads are determined from quasi-static conditions, considering the effect of tooth deflections by Walker's method.[50-52] A dynamic factor by Tuplin's method[63] is also calculated.

Program Language and Computer Type

The program is written in FORTRAN IV language for a CDC 6000 Series computer, using RUN compiler and SCOPE 3.4 system.

Input Cards

There are 11 data cards per set of data. Up to 4 additional cards may be used to study the effect of modifications other than the designed profile modification.

Data are entered according to the gear's function, driver or driven, instead of the more common but less descriptive appellation of pinion and gear.

Input data are entered on each card. In most cases up to 10 characters may be entered. All data are in inches unless noted otherwise. Card data and necessary explanations follow:

Word	Column	Symbol	Description
Input Card 1			
1	1-5	KARC	Use: 0 - if Columns 61 through 80 on Card 4 and Columns 1 through 20 on Card 5 are arc tooth thickness 1 - if Columns 61 through 80 on Card 4 and Columns 1 through 20 on Card 5 are chordal tooth thickness

Word	Column	Symbol	Description
Input Card 2	(PRELIMINARY INPUT DATA)		
1	1-10	ANP	Number of driver teeth
2	11-20	ANG	Number of driven teeth
3	21-30	BP	Thermal constant (driver), $lb/°F\text{-}in.\text{-}sec^{\frac{1}{2}}$
4	31-40	BG	Thermal constant (driven), $lb/°F\text{-}in.\text{-}sec^{\frac{1}{2}}$
5	41-50	BRKP	Tip break radius, maximum (driver)
6	51-60	BRKG	Tip break radius, maximum (driven)
7	61-70	DOPMA	Outside diameter, maximum (driver)
8	71-80	DOGMA	Outside diameter, maximum (driven)
Input Card 3			
1	1-10	DOPMI	Outside diameter, minimum (driver)
2	11-20	DOGMI	Outside diameter, minimum (driven)
3	21-30	DRPMA	Root diameter, maximum (driver)
4	31-40	DRGMA	Root diameter, maximum (driven)
5	41-50	DRPMI	Root diameter, minimum (driver)
6	51-60	DRGMI	Root diameter, minimum (driven)
7	61-70	EP	Young's modulus (driver)
8	71-80	EG	Young's modulus (driven)

Word	Column	Symbol	Description
Input Card 4			
1	1-10	FMINP	Face width, minimum (driver)
2	11-20	FMING	Face width, minimum (driven)
3	21-30	PRP	Poisson's ratio (driver)
4	31-40	PRG	Poisson's ratio (driven)
5	41-50	RFMIP	Root fillet radius, minimum (driver)
6	51-60	RFMIG	Root fillet radius, minimum (driven)
7	61-70	TPMAS	Arc or chordal tooth thickness at standard pitch diameter, maximum (driver)
8	71-80	TGMAS	Arc or chordal tooth thickness at standard pitch diameter, maximum (driven)
Input Card 5			
1	1-10	TPMIS	Arc or chordal tooth thickness at standard pitch diameter, minimum (driver)
2	11-20	TGMIS	Arc or chordal tooth thickness at standard pitch diameter, minimum (driven)
3	21-30	BMIN	Backlash, minimum
4	31-40	BMAX	Backlash, maximum
5	41-50	CNSTD	Use: 0 - if gears operate on standard centers Value - if gears operate on non-standard centers

Word	Column	Symbol	Description
Input Card 5 (Cont'd)			
6	51-60	PHIN	Pressure angle, deg.
7	61-70	PND	Diametral pitch
Input Card 6	(RPM AND HORSEPOWER LOOP)		
1	1-10	RPMP	Rpm of driver, initial
2	11-20	RINC	Rpm increment. Blank if only one rpm
3	21-30	RPMX	Rpm maximum. Blank if only one rpm The effect of several driver speeds on the gear set may be studied by using this loop. There are no limits on the number of times the speed is incremented, so long as the maximum rpm does not exceed 10 digits
4	31-40	HORSES	Horsepower, initial
5	41-50	DHP	Horsepower increment. Blank if only one horsepower
6	51-60	HMP	Horsepower maximum. Blank if only one horsepower The effect of the application of several power levels for the gear set may be studied using this loop. Since this horsepower loop is inside the rpm loop, the program will analyze the complete range of horsepower for each rpm before moving on to the next rpm

Word	Column	Symbol	Description
Input Card 7	(PROFILE MODIFICATIONS)		
1	1-10	MOD	Use: 0 - if profiles are not modified 1 - if pinion and gear tips are modified 2 - if pinion tip and root are modified 3 - if gear tip and root are modified
2	11-20	P1	Modification at break diameter for modified profiles in engagement from A to C If MOD = 0, leave blank If MOD = 1 or 3, this is gear tip modification If MOD = 2, this is pinion root modification
3	21-30	P2	Modification at break diameter for modified profiles in engagement from B to D If MOD = 0, leave blank If MOD = 1 or 2, this is pinion tip modification If MOD = 3, this is gear root modification
4	31-40	E1	Roll angle, deg., where modification ends If MOD = 0, leave blank

Word	Column	Symbol	Description
Input Card 7 (Cont'd)			
			If MOD = 1 or 3, this is gear roll angle If MOD = 2, this is pinion roll angle
5	41-50	E2	Roll angle, deg., where modification ends If MOD = 0, leave blank If MOD = 1 or 2, this is pinion roll angle If MOD = 3, this is gear roll angle
6	51-60	RDMORE	Use: 0 - if this is last modification card 1 - if another modification card follows A separate card is used for each set of modifications, up to a total of 5 cards. Each card may use a different MOD so that the effect of various types of modification may be studied, as well as the effect of different amounts of modification. The program assumes a linear modification from the break radius to a radius having a roll angle of E1 or E2
Input Card 8 (METHOD CARD)			
1	1-10	METH	If only static conditions are to be obtained, leave blank; otherwise put a 1 in Col. 10 to calculate a dynamic factor

Word	Column	Symbol	Description
Input Card 9			If METH is blank, omit this card; otherwise:
1	1-10	AP	Thickness of driver gear rim below the root. If gear is solid, this dimension will be the height the driver extends above the shaft surface.
2	11-20	AG	Thickness of driven gear rim below the root. If gear is solid, this dimension will be the height the driven gear extends above the shaft surface.
3	21-30	PEP	Pitch or spacing error (driver)
4	31-40	PEG	Pitch or spacing error (driven)
5	41-50	PMI	Mass moment of inertia (driver), $lb\text{-}sec^2\text{-}in.$
6	51-60	PMG	Mass moment of inertia (driven), $lb\text{-}sec^2\text{-}in.$
Input Card 10			If METH is blank, omit this card. If METH is 1 and values are unknown from other sources, leave card blank; otherwise:
1	1-10	NAT(1)	Lowest natural frequency of gear system, rpm
2	11-20	NAT(2)	Highest natural frequency of gear system, rpm
3	21-30	NAT(3)	Natural frequency of teeth acting as a spring, rpm

Word	Column	Symbol	Description
Input Card 10 (Cont'd)			
			These natural frequencies are those for a system consisting of the two gears under analysis, and the gears (or loads) on the ends of their shafts. These frequencies may be found by the Holzer method. If none of these frequencies are available for input, the program will calculate NAT(3) from the simple system consisting of the two gear blanks as masses and the contacting teeth as springs.
Input Card 11	(FRICTION AND TEMPERATURE)		
1	1-10	FR1	Friction factor from Eq. (55), (57), (59), or (61)
2	11-20	FR2	Friction factor from Eq. (54), (56), (58), or (60)
3	21-30	TCON	Temperature difference factor from Eq. (69)
4	31-40	TEMP	Oil jet temperature, °F

A sample set of data cards for the ground spur gear design and operating conditions given in Chapter VIII, Section B, is shown in Figure H-1.

Since the tooth thickness is given as arc length on Cards 4 and 5, Card 1 contains a zero in Column 5. The pinion was the driver in this example, so pinion data were entered in the driver parts of the appropriate cards. From Card 6, it is noted that the effect of one speed level was studied at six power levels, 100 hp apart. The involute profiles of the pinion and gear were modified on the tips; hence Card 7 contains a 1 in Column 10 for MOD. Since only one set of modifications was considered, Column 60 for RDMORE is blank. Card 8 has a 1 in Column 10 indicating that a dynamic factor was calculated. Since a dynamic factor was calculated, Card 9 contains data. No vibration data were available; hence Card 10 is blank. Card 11

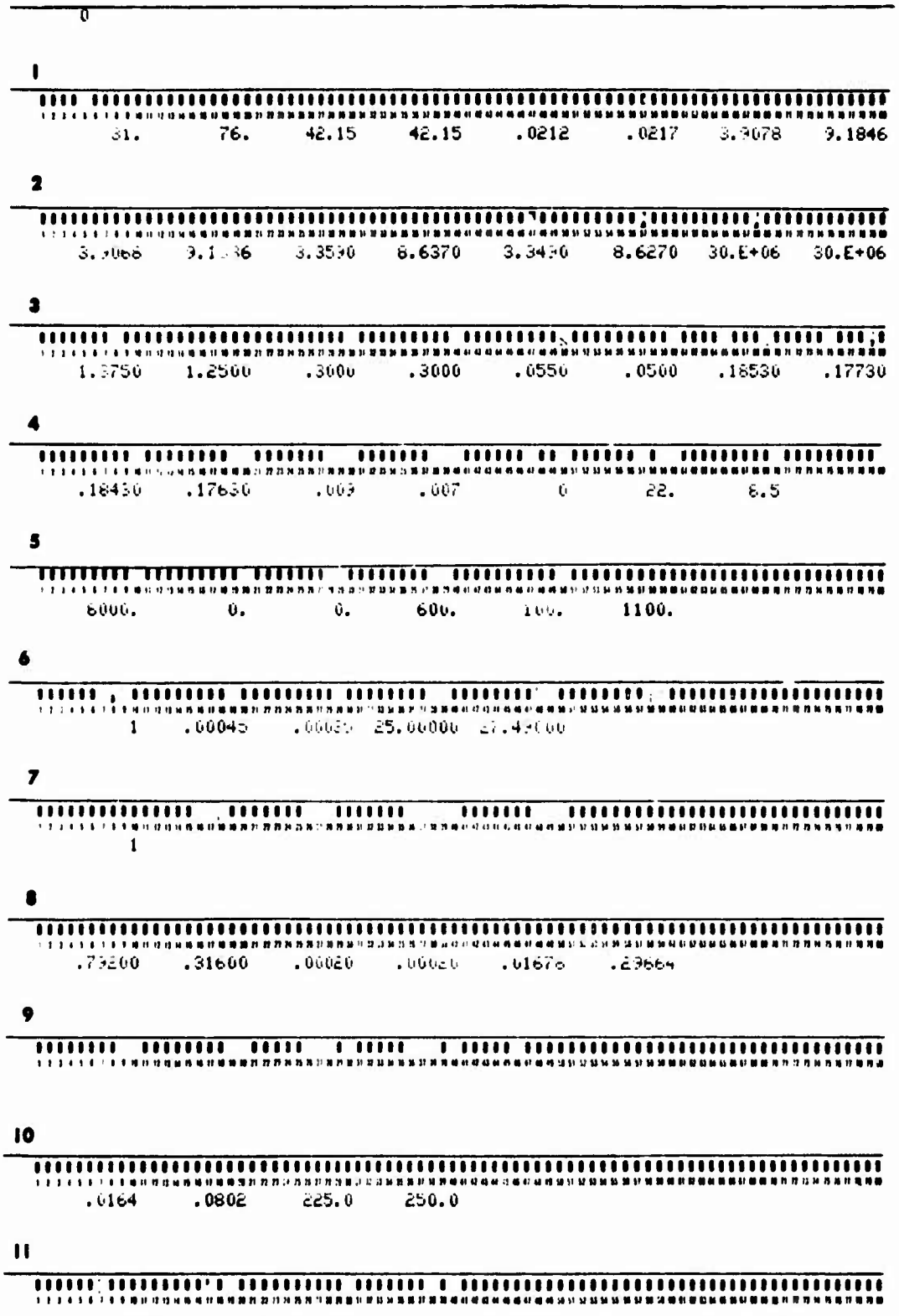

Figure H-1. Sample ground spur gear computer program data cards

contains friction factors calculated for plain cross-ground surfaces with a composite surface roughness of 13.7 μin. AA, using Equations (56) and (57).

Computer Program

Figure H-2 shows the listing of the computer program. Control cards are not included.

Sample Printout

Figure H-3 gives the data printout for the input data of Figure H-1. Results are shown for 600 hp only.

The first page of the printout lists the input data for reference purposes, plus miscellaneous geometric parameters. The second page provides additional input data listing.

The third page is the ROLL ANGLE SECTION in which roll angles are given for both the pinion and gear for the start and end of contact, and for the lowest point of single tooth contact (LPSTC) and the highest point of single tooth contact (HPSTC).

Two contact ratios are given. The larger represents the maximum attainable, ignoring tip rounding. The smaller value is the actual contact ratio, taking the rounding into account.

The body of the figure gives, for corresponding pinion and gear roll angles, the radii of curvature and the instantaneous sliding and sum velocity for several points throughout the mesh.

The next page is a continuation of the ROLL ANGLE SECTION, listing the dimensions of the uniform stress parabola inscribed within the tooth outline.

The fifth page is the LOAD FORCE SECTION, in which the quasi-static loads are determined as a function of the tooth deflections and the profile modifications at several points in the mesh cycle.

Roll angles at positions 7 and 8 and also positions 17 and 18 are duplicated. Positions 7 and 8 represent the point where double-tooth contact starts (LPSTC), and positions 17 and 18 represent the point where double-tooth contact ends (HPSTC). Two positions are needed to define conditions at each of these points, because as the gear

teeth go from double-tooth to single-tooth contact, or the reverse, the load theoretically changes instantaneously.

The last page is the FLASH TEMPERATURE SECTION where, for points throughout the mesh cycle, the parameters related to the operational behavior of the gears are given. The dynamic increment and corresponding dynamic factor are given at the bottom of the page.

The program enters the rpm loop first, then the hp loop, and finally the modification loop. Thus the program will perform all of the calculations in the LOAD FORCE SECTION and the FLASH TEMPERATURE SECTION for each set of modifications specified in the modification loop at the initial values of hp and rpm. When the modification loop has been completed, the hp will be incremented and the modification loop repeated.

```
      PROGRAM SPURGR (INPUT,OUTPUT,TAPE5=INPUT,TAPE6=OUTPUT)                SPGR0010*0001
C                     *  EXTERNAL SPUR GEARS - FOR  *                     SPGR0020*0002
C                     *  EVALUATING DESIGN PARA-    *                     SPGR0030*0003
C                     *  METERS, PROGRAMMED BY-     *                     SPGR0040*0004
C                     *        MARY CARTER  SWRI    *                     SPGR0050*0005
C                     * * * * * * * * * * * * * * * *                     SPGR0060*0006
C                                                                          SPGR0070*0007
      REAL MAT,MATFO                                                       SPGR0080*0008
      INTEGER ROWORE                                                       SPGR0090*0009
      DIMENSION  ID(2),ID1(6),                    IMD(5),IMD1(9),IMD2(5)SPGR0100*0010
     *,          IMD3(7) , IM(9),IM1(6),IM2(3), IP(2), AMOD(5,9),        SPGR0110*0011
     *           FP(90),FG(90), FPCO(90),FGCO(90), MP(90),MG(90), MOD(5)SPGR0120*0012
     *,                  MAT(3), OFSP(90), DECP(90),DECG(90), RMOP(90),SPGR0130*0013
     *           RMOG(90),  ROLLRAY(90,2),  VS(90),VT(90), OFSG(90),    SPGR0140*0014
     *           FRIC(90), PME(90), TP(90),TG(90), XDIMP(90),XDIMG(90)  SPGR0150*0015
     *,          WXFO(90,2)                                               SPGR0160*0016
      DATA ID/10H FORCE  = /,                                              SPGR0170*0017
     *    ID1/10H LOAD FORC,10HFACTOR BY ,10HTUPLIN MET,                   SPGR0180*0018
     *       10HE         ,10H          ,10HHOD       /                   SPGR0190*0019
      DATA IMD /10H  SECTION ,10HVARIABLES ,10HUSED IN,...,10H LOOP     ,SPGR0210*0020
     *          10H CALCS,   /,                                          SPGR0220*0021
     *    IMD1 /10H  NORMAL  ,10HHORSEPOWER,10H MODIF,   ,10H METHOD   /SPGR0230*0022
     *,   IMD2 /10H   ROLL   ,10H  LOAD    ,10HDYNAMIC   ,10H HERTZ    ,SPGR0240*0023
     *          10H  FLASH   /                                           SPGR0250*0024
     *,   IMD3 /10H  ANGLES  ,10H FORCE    ,10HFRICTION  ,10H STRESS   ,SPGR0260*0025
     *          10H  TEMP F  ,10H CTEMP    ,10H PME      /              SPGR0270*0026
      COMMON JA,JB,JC,JD,KAMP,PI,RN,WN,RPMP,LOU,LIN,ANP,ANG,DRP,DBG,     SPGR0280*0027
     *   DDBG,CNSTD,PEP,PEG,ALPHA,DPA,P1,P2,IXT,BET                      SPGR0290*0028
C          LIN  -- INPUT LOGICAL UNIT NUMBER                             SPGR0300*0029
C          LOU  -- OUTPUT LOGICAL UNIT NUMBER                            SPGR0310*0030
C          KRW  -- NO. OF ROWS OF STORAGE ARRAY...(ROLLRAY)              SPGR0320*0031
C          RN   -- CONVERT FROM DEGREES TO RADIANS                       SPGR0330*0032
C          DEGR -- CONVERT FROM RADIANS TO DEGREES                       SPGR0340*0033
C                                                                        SPGR0350*0034
      KRW=90                                                             SPGR0360*0035
      LIN=5                                                              SPGR0370*0036
      LOU=6                                                              SPGR0380*0037
      RN=.01745329                                                       SPGR0390*0038
      DEGR=57.29577951                                                   SPGR0400*0039
      PI=3.141592653589                                                  SPGR0410*0040
C                                                                        SPGR0420*0041
C     INPUT DATA SECTION                                                 SPGR0430*0042
C                                                                        SPGR0440*0043
    5 READ   (LIN,1000) KARC                                             SPGR0450*0044
      IF (EOF,LIN) 200,10                                                SPGR0460*0045
   10 WRITE (LOU,1100)                                                   SPGR0470*0046
      READ (LIN,1020)  ANP,ANG,BP,BG,BRKP,BRKG,DOPMA,DOGMA,              SPGR0480*0047
     *                 DOPMI,DOGMI,DRPMA,DRGMA,DRPMI,DRGMI,EP,EG,        SPGR0490*0048
     *                 FMINP,FMING,PRP,PRG,RFMIP,RFMIG,TPMAS,TGMAS,      SPGR0500*0049
     *                 TPMIS,TGMIS,BMIN,BMAX,CNSTD,PHIN,PND              SPGR0510*0050
      WRITE (LOU,1120) ANP,ANG,BP,BG,BRKP,BRKG,DOPMA,DOGMA,              SPGR0520*0051
     *                 DOPMI,DOGMI,DRPMA,DRGMA,DRPMI,DRGMI,EP,EG         SPGR0530*0052
      WRITE  (LOU,1126) FMINP,FMING,PRP,PRG,RFMIP,RFMIG,TPMAS,TGMAS,     SPGR0540*0053
     *                  TPMIS,TGMIS,BMIN,BMAX,CNSTD,PHIN,PND             SPGR0550*0054
C     PERFORM PRELIMINARY CALCULATIONS                                   SPGR0560*0055
      FNRA=PHIN*RN                                                       SPGR0570*0056
      FNSI=SIN(FNRA)                                                     SPGR0580*0057
      FNCO=COS(FNRA)                                                     SPGR0590*0058
      FNTA=FNSI/FNCO                                                     SPGR0600*0059
      CSTD=(ANP+ANG)/(2.*PND)                                            SPGR0610*0060
      IF (CNSTD)    110,109,110                                          SPGR0620*0061
  109 CNSTD=CSTD                                                         SPGR0630*0062
```

Figure H-2. Listing of ground spur gear computer program

```
  110 PDX=(ANP*ANG)/(2.*CNSTD)                                          SPGR0640*0063
      FX=(CSTD*FNCO)/CNSTD                                              SPGR0650*0064
      FXRA=ATAN(SQRT(1.-(FX)**2)/FX)                                    SPGR0660*0065
      FXSI=SIN(FXRA)                                                    SPGR0670*0066
      FXCO=COS(FXRA)                                                    SPGR0680*0067
      FXTA=FXSI/FXCO                                                    SPGR0690*0068
C                                                                       SPGR0700*0069
      ZFN=FNTA*FNRA                                                     SPGR0710*0070
      ZFX=FXTA*FXRA                                                     SPGR0720*0071
      ANG=ANG/ANP                                                       SPGR0730*0072
      RMG=ANP/ANG                                                       SPGR0740*0073
C                                                                       SPGR0750*0074
      DP=ANP/PND                                                        SPGR0760*0075
      DBP=DP*FNCO                                                       SPGR0770*0076
      DXP=ANP/PDX                                                       SPGR0780*0077
      DG=ANG/PND                                                        SPGR0790*0078
      DBG=DG*FNCO                                                       SPGR0800*0079
      DXG=ANG/PDX                                                       SPGR0810*0080
      DODBP=DOPMI*(2.*BRKP)                                             SPGR0820*0081
      DODBG=DOGMI*(2.*BRKG)                                             SPGR0830*0082
      ZA = .5*(SQRT((DODBG*DODBG)+(DNG*DBG))-SQRT((DXG*DXG)-(DBG*DBG))) SPGR0840*0083
      ZR = .5*(SQRT((DODBP*DODBP)+(DBP*DBP))-SQRT((DXP*DXP)-(DBP*DBP))) SPGR0850*0084
      VO = .5*SQRT((DXP*DXP)-(DBP*DBP))                                 SPGR0860*0085
      WO = .5*SQRT((DXG*DXG)-(DBG*DBG))                                 SPGR0870*0086
      VAB=VO-ZA                                                         SPGR0880*0087
      PB = PI*DBP / ANP                                                 SPGR0890*0088
      CPN=PI*DXP/ANP                                                    SPGR0900*0089
      ER = 1./(((1.-(PRP*PRP))/EP+((1.-(PRG*PRG))/EG))/2.)             SPGR0910*0090
      WDP= DOPMI*URPMA                                                  SPGR0920*0091
      WDG = DOGMI*DRGMA                                                 SPGR0930*0092
      ADP=(DODBP-DXP)/2.                                                SPGR0940*0093
      ADG=(DODBG-DXG)/2.                                                SPGR0950*0094
      FNRA=FNRA/RN                                                      SPGR0960*0095
      FXRA=FXRA/RN                                                      SPGR0970*0096
      WRITE  (LOU,1200) ADP,ADG,DBP,DBG,DODBP,DODWG,DP,DG,              SPGR0980*0097
     *                  DXP,DXG,WDP,WDG                                 SPGR0990*0098
      WRITE  (LOU,1201) ANG,CNSTD,CPN,FNRA,FXRA,ER,PB,                  SPGR1000*0099
     *                  PDX,RMG,VO,WO,ZA,ZFN,ZFX,ZR                     SPGR1010*0100
C                                                                       SPGR1020*0101
      FNRA=FNRA*RN                                                      SPGR1030*0102
      FXRA=FXRA*RN                                                      SPGR1040*0103
      IF (KARC.EQ.0) GO TO 116                                          SPGR1050*0104
C                                                                       SPGR1060*0105
C  CALCULATE ARC TOOTH THK, FROM CHORDAL THK.                           SPGR1070*0106
C                                                                       SPGR1080*0107
      AN=(.5*TPMIS)/(.5*DP)                                             SPGR1090*0108
      ANA=ATAN(AN/(SQRT(1.-(AN)**2)))                                   SPGR1100*0109
      TPMIS=ANA*DP                                                      SPGR1110*0110
      AN=(.5*TPMAS)/(.5*DP)                                             SPGR1120*0111
      ANA=ATAN(AN/(SQRT(1.-(AN)**2)))                                   SPGR1130*0112
      TPMAS=ANA*DP                                                      SPGR1140*0113
      AN=(.5*TGMIS)/(.5*DG)                                             SPGR1150*0114
      ANA=ATAN(AN/(SQRT(1.-(AN)**2)))                                   SPGR1160*0115
      TGMIS=ANA*DG                                                      SPGR1170*0116
      AN=(.5*TGMAS)/(.5*DG)                                             SPGR1180*0117
      ANA=ATAN(AN/(SQRT(1.-(AN)**2)))                                   SPGR1190*0118
      TGMAS=ANA*DG                                                      SPGR1200*0119
      WRITE  (LOU,1206) TPMAS,TGMAS,TPMIS,TGMIS                         SPGR1210*0120
C                                                                       SPGR1220*0121
C  CALCULATE ARC TOOTH THK, AT THE OPERATING PITCH DIA,  (DXP)          SPGR1230*0122
C                                                                       SPGR1240*0123
  116 TPMIN=DXP*(((TPMIS/DP)+ZFN)-ZFX)                                  SPGR1250*0124
```

Figure H-2. Listing of ground spur gear computer program (cont'd)

```
      TPMAX=DXP*(((TPMAS/DP)+ZFN)-ZFX)                                  SPGR1260-0125
      TGMIN=DXG*(((TGMIS/DG)+ZFN)-ZFX)                                  SPGR1270-0126
      TGMAX=DXG*(((TGMAS/DG)+ZFN)-ZFX)                                  SPGR1280-0127
      PK=(TPMIN/DXP)+ZFX                                                SPGR1290-0128
      GK=(TGMIN/DXG)+ZFX                                                SPGR1300-0129
      WRITE  (LOU,1206) TPMAX,TGMAX,TPMIN,TGMIN,PK,GK                   SPGR1310-0130
      READ (LIN,1040) RPMP,RINC,RPMX,HORSES,DHP,HPM                     SPGR1320-0131
 1040 FORMAT (6F10.2)                                                   SPGR1330-0132
      WRITE  (LOU,1127) RPMP                                            SPGR1340-0133
      IF (RINC.EQ.0.) GO TO 12                                          SPGR1350-0134
      WRITE  (LOU,1128) RINC,RPMX                                       SPGR1360-0135
C                                                                       SPGR1365-0136
C     READ VARIABLES FOR HORSEPOWER LOOP                                SPGR1370-0137
   12 WRITE  (LOU,1115) IMD(2),IMD(3),IMD1(2),IMD(4)                    SPGR1380-0138
      WRITE  (LOU,1140) HORSES                                          SPGR1390-0139
      IF (DHP.EQ.0) GO TO 24                                            SPGR1400-0140
      WRITE  (LOU,1141) DHP,HPM                                         SPGR1410-0141
C                                                                       SPGR1420-0142
   24 I=1                                                               SPGR1430-0143
   25 READ   (LIN,1046) MOD(I),(AMOD(I,J),J=1,4),RDMORE                SPGR1440-0144
      IF (MOD(I).EQ.0) GO TO 29                                         SPGR1450-0145
      IF (I.GT.1) GO TO 26                                              SPGR1460-0146
      WRITE  (LOU,1115) IMD(2),IMD(3),IMD1(3),IMD(4)                    SPGR1470-0147
   26 IM1=IM2(1)                                                        SPGR1480-0148
      IM2=IM2(2)                                                        SPGR1490-0149
      IF (MOD(I).GT.2) IM1=IM2(2)                                       SPGR1500-0150
      IF (MOD(I).GT.1) IM2=IM2(3)                                       SPGR1510-0151
   27 WRITE (LOU,1146) AMOD(I,1),AMOD(I,2)                              SPGR1520-0152
      WRITE (LOU,1147) AMOD(I,3),AMOD(I,4)                              SPGR1530-0153
   28 IF (RDMORE.EQ.0) GO TO 30                                         SPGR1540-0154
      I=I+1                                                             SPGR1550-0155
      GO TO 25                                                          SPGR1560-0156
   30 NMOD=I                                                            SPGR1570-0157
C                                                                       SPGR1580-0158
C        READ AND PRINT DATA FOR DFORCE SECTION                         SPGR1590-0159
C                                                                       SPGR1600-0160
      READ   (LIN,1050) METH                                            SPGR1610-0161
      WRITE(LOU,38)                                                     SPGR1620-0162
   38 FORMAT(///42H METHOD USED FOR CALCULATING NORMAL FORCE=/           SPGR1630-0163
     *      1X,29H1 NORMAL FORCE = STATIC FORCE)                        SPGR1640-0164
      IF(METH.NE.1) GO TO 41                                            SPGR1650-0165
      READ  (LIN,1055) AP,AG,PEP,PEG,PMI,GMI,NAT                        SPGR1660-0166
      WRITE(LOU,39)                                                     SPGR1670-0167
   39 FORMAT(1X,44H2 DYNAMIC FACTOR CALCULATED BY TUPLIN METHOD)        SPGR1680-0168
      WRITE  (LOU,1155) AP,AG,PEP,PEG,PMI,GMI,NAT                       SPGR1770-0169
C                                                                       SPGR1780-0170
C        READ AND PRINT DATA FOR FLASH TEMP SECTION                     SPGR1790-0171
   41 READ   (LIN,1060) FR1,FR2,TCON,TEMP                               SPGR1800-0172
      WRITE  (LOU,1110) IMD(2),IMD(3),IMD2(3),IMD3(3),IMD(1)            SPGR1810-0173
   45 WRITE  (LOU,1160) FR1,FR2,TCON,TEMP                               SPGR1820-0174
C                                                                       SPGR1830-0175
C                                                                       SPGR1840-0176
  100 IPMI=PMIN                                                         SPGR1850-0177
C                                                                       SPGR1860-0178
      FW=FMINP                                                          SPGR1870-0179
      IF (FMING.LT.FMINP) FW=FMING                                      SPGR1880-0180
C                                                                       SPGR1890-0181
C     BEGIN RPM LOOP                                                    SPGR1900-0182
C                                                                       SPGR1910-0183
      HP1=HORSES                                                        SPGR1920-0184
   90 HORSES=HP1                                                        SPGR1930-0185
      IRECAL=1                                                          SPGR1940-0186
```

Figure H-2. Listing of ground spur gear computer program (cont'd)

```
  130 TQP = (63025.*HORSES)/RPMP                                        SPGR1950*0187
      WTP = (2.*TQP)/DXP                                                SPGR1960*0188
      RPMG=RPMP*RMG                                                     SPGR1970*0189
      TQG=(63025.*HORSES)/RPMG                                          SPGR1980*0190
      WTG=(2.*TQG)/DXG                                                  SPGR1990*0191
      WN  = WTP/FX                                                      SPGR2000*0192
      MM=1                                                              SPGR2010*0193
      KAMP=1                                                            SPGR2020*0194
      IF (IRECAL.EQ.0) GO TO 135                                        SPGR2030*0195
  161 IRECAL=0                                                          SPGR2040*0196
C                                                                       SPGR2050*0197
C     ROLLANGLE SECTION                                                 SPGR2060*0198
C                                                                       SPGR2070*0199
  150 WRITE  (LOU,1210) IMD2(1),IMD3(1),IMD(1)                          SPGR2080*0200
      CALL ROLLANG        (VO,ZA,ZR,WO,DOPMA,DOGMA,PB,FXTA              SPGR2090*0201
     *                    ,ROLLRAY,RMOP,RMOG,DECP,DECG,VS,VT            SPGR2100*0202
     *                    ,EBCP,EECP,MARK1,MARK3,KRW)                   SPGR2110*0203
      CALL PHI        (DECP,FP   ,MP,TP,XDIMP,DFSP,DXP,DBP,DRPMI,PK,ANP,  SPGR2120*0204
     *  RPMIP,EP,PI,RN,JD,PMINP,FPCO,KRW)                               SPGR2130*0205
      CALL PHI        (DECG,FG   ,MG,TG,XDIMG,DFSG,DXG,DBG,DRGMI,GK,ANG,  SPGR2140*0206
     *  RPMIG,EG,PI,RN,JD,PMING,FGCO,KRW)                               SPGR2150*0207
      WRITE (LOU,1215)                                                  SPGR2160*0208
      DO 155 I=1,JD                                                     SPGR2170*0209
      T1=TP(I)*2.                                                       SPGR2180*0210
      T2=TG(I)*2.                                                       SPGR2190*0211
      WRITE  (LOU,1220) MP(I),MG(I),T1,T2,FPCO(I),FGCO(I)               SPGR2200*0212
  155 CONTINUE                                                          SPGR2210*0213
C                                                                       SPGR2220*0214
C     LOAD SECTION                                                      SPGR2230*0215
C           BEGINNING OF MODIFICATION LOOP                              SPGR2240*0216
  135 IF (KAMP.EQ.2) GO TO 195                                          SPGR2250*0217
      IF (MOD(MM).EQ.0) GO TO 145                                       SPGR2260*0218
  140 P1=AMOD(MM,1)                                                     SPGR2270*0219
      P2=AMOD(MM,2)                                                     SPGR2280*0220
      E1=AMOD(MM,3)                                                     SPGR2290*0221
      E2=AMOD(MM,4)                                                     SPGR2300*0222
  145 WRITE  (LOU,1210) IMD2(2),IMD3(2), IMD(1),HORSES,RPMP,WN          SPGR2310*0223
      MD=MOD(MM)                                                        SPGR2320*0224
      CALL LDVROL (ROLLRAY,DFSP,DFSG,WXFO,MD,                           SPGR2330*0225
     *        E1,E2,MARK1,MARK3,EBCP,EECP,KRW,TDFES)                    SPGR2340*0226
      IF (KAMP.EQ.2) IRECAL=1                                           SPGR2350*0227
      GO TO (160,150) KAMP                                              SPGR2360*0228
C                                                                       SPGR2370*0229
C     WHEN KAMP=2  THE ROLL ANGLE AND LOAD CALCULATIONS ARE REPEATED    SPGR2380*0230
C                                                                       SPGR2390*0231
C     DYNAMIC FACTOR SECTION                                            SPGR2400*0232
C      MF,,,METHOD INDICATOR                                            SPGR2410*0233
C                        MF=1   NORMAL FORCE=LOAD FORCE FOR EACH        SPGR2420*0234
C                               ROLL ANGLES POSITION                    SPGR2430*0235
C                        MF=2   CALL SUBROUTINE FORCE  TO CALC.         SPGR2440*0236
C                               A DYNAMIC FACTOR                        SPGR2450*0237
C                                                                       SPGR2460*0238
C                                                                       SPGR2470*0239
  160 IMT=1                                                             SPGR2480*0240
      MF=1                                                              SPGR2490*0241
      L1=1                                                              SPGR2510*0242
      L2=4                                                              SPGR2520*0243
      DF=1                                                              SPGR2530*0244
      GO TO 210                                                         SPGR2540*0245
  165 IF (METH.EQ.0) GO TO 510                                          SPGR2550*0246
      MF=2                                                              SPGR2560*0247
      GO TO 180                                                         SPGR2570*0248
```

Figure H-2. Listing of ground spur gear computer program (cont'd)

```
  100 L1=2                                                                  SPGR2580+0249
      L2=NP+9                                                               SPGR2590+0250
      L3=NP+1                                                               SPGR2600+0251
      WRITE (LOU,1250) IHD2(3),ID1(2),ID1(L3),ID1(L2)                       SPGR2610+0252
      NATP=NAT(3)                                                           SPGR2615+0253
      CALL FORCE       (AP,AG,   CPN,DXP,DXG,EP,EG,FMINP,FMING,FNRA,        SPGR2620+0254
     *HORSES,NATP,PMI,GMI,PRP,PRG,TPMIS,TGMIS,VA,WDP,WDG,IMT,TDFES)         SPGR2630+0255
      GO TO 510                                                             SPGR2640+0256
C                                                                           SPGR2650+0257
C     FLASH TEMPERATURE SECTION                                             SPGR2660+0258
C                                                                           SPGR2670+0259
C    *FOR EACH ROLL ANGLE POSITION A FRICTION COEFFICIENT IS DETERMINED     SPGR2680+0260
C    *VALUES ARE THEN FOUND FOR FLASH TEMPERATURE.                          SPGR2690+0261
C                                                                           SPGR2710+0262
  210 CALL FRPHE          (TS,TEMP,WXPO,FRIC,PHE,KRW,JD,L1,VS,FN,ER,        SPGR2720+0263
     *  PHEAV,FR1,FR2,TCON,JS,JC,ROLLRAY,PMET,JA,RPMP,ANP)                 SPGR2730+0264
      WRITE  (LOU,1211) IHD2(5),IHD3(5),IHD(1),HORSES,RPMP,WN,TS,PHEAV      SPGR2740+0265
      WRITE  (LOU,1250) IHD1(1),ID(L1),ID1(MF),ID1(L2)                      SPGR2750+0266
      WRITE  (LOU,1230) IHD2(1),IHD2(2),(IHD2(N),N=4,5),(IHD3(M),M=1,7)     SPGR2760+0267
      DO 270 I=1,JD                                                         SPGR2770+0268
      DFORCE=WXFO(I,L1)                                                     SPGR2780+0269
      RHOE = (RHOP(I)*RHOG(I))/(RHOP(I)+RHOG(I))                            SPGR2790+0270
      IF (DFORCE.NE.0.) GO TO 215                                           SPGR2800+0271
      DT    =0.                                                             SPGR2810+0272
      HERTZ=0.                                                              SPGR2820+0273
      CTEMP=TS                                                              SPGR2830+0274
      GO TO 255                                                             SPGR2840+0275
  215 HERTZ=.3989*SQRT(ER/FN)*SQRT(DFORCE/RHOE)                             SPGR2850+0276
      DT=.201*(FRIC(I)*((DFORCE/FN)**(3./4.))*(ER**(1./4.))/(RHOE**(1./     SPGR2860+0277
     **.))*(ABS(RHOP(I)-(ANP/ANG*RHOG(I)))*SQRT(RPMP)/(SP*SQRT(RHOP(I))    SPGR2870+0278
     **(SG*SQRT(ANP/ANG*RHOG(I)))))                                         SPGR2880+0279
  225 CTEMP=TS+DT                                                           SPGR2890+0280
  255 WRITE  (LOU,1235) I,ROLLRAY(I,1),DFORCE,FRIC(I),HERTZ,DT,             SPGR2900+0281
     *            CTEMP,PHE(I)                                             SPGR2910+0282
  270 CONTINUE                                                              SPGR2920+0283
C     INCREMENT METHOD LOOP                                                 SPGR2930+0284
  500 GO TO (165,510) MF                                                    SPGR2940+0285
C                                                                           SPGR2950+0286
C     INCREMENT MODIFICATION LOOP                                           SPGR2960+0287
  510 IF (MM.EQ.NMOD) GO TO 520                                             SPGR2970+0288
      MM=MM+1                                                               SPGR2980+0289
      IF (IRECAL.EQ.1) GO TO 151                                            SPGR2990+0290
      GO TO 135                                                             SPGR3000+0291
C                                                                           SPGR3010+0292
C     INCREMENT HORSEPOWER LOOP                                             SPGR3020+0293
C                                                                           SPGR3030+0294
  520 IF (HORSES.GE.HPM) GO TO 600                                          SPGR3040+0295
  525 HORSES=HORSES+DHP                                                     SPGR3050+0296
      GO TO 130                                                             SPGR3060+0297
  600 IF (RPMP.GE.RPMX) GO TO 5                                             SPGR3070+0298
      RPMP=RPMP+RINC                                                        SPGR3080+0299
      GO TO 90                                                              SPGR3090+0300
C     INPUT FORMATS                                                         SPGR3100+0301
 1000 FORMAT (8I5)                                                          SPGR3110+0302
 1020 FORMAT (8F10.5/6F10.5,2E10.2/8F10.5/7F10.5)                           SPGR3120+0303
 1045 FORMAT (5X,I5,4F10.5,25X,I5)                                          SPGR3130+0304
 1050 FORMAT (I10)                                                          SPGR3140+0305
 1055 FORMAT (6F10.5/3F10.2)                                                SPGR3150+0306
 1060 FORMAT (2F10.4,2F10.1)                                                SPGR3160+0307
C     PRELIMINARY DATA OUTPUT FORMATS                                       SPGR3170+0308
 1100 FORMAT (1H1)                                                          SPGR3180+0309
 1110 FORMAT (//9X,2A10,2A9,A10/)                                           SPGR3190+0310
```

Figure H-2. Listing of ground spur gear computer program (cont'd)

```
1115 FORMAT (///1X,3A10,A2)                                                    $PGR3200=0311
1120 FORMAT (9X,49HVALUES AND DEFINITIONS OF PRIMARY INPUT VARIABLES           $PGR3210=0312
    *,30H (INCH UNITS UNLESS NOTED)     /                                      $PGR3220=0313
    * 2X,16H    (DRIVER)     ,6X,14H    (DRIVEN)                            $PGR3230=0314
    */11H ANP      = ,F10.5,5X,10HANG      = ,F10.5,5X,                       $PGR3240=0315
    *   60H=NUMBER OF TEETH                                                   $PGR3250=0316
    */11H HP       = ,F10.5,5X,10HHG       = ,F10.5,5X,                       $PGR3260=0317
    *   60H=THERMAL CONSTANT (LB,SQRT(SEC,)/IN,DEG, F)                        $PGR3270=0318
    */11H BRKP     = ,F10.5,5X,10HBRKG     = ,F10.5,5X,                       $PGR3280=0319
    *   60H=MAXIMUM TIP BREAK                                                 $PGR3290=0320
    */11H DOPMA    = ,F10.5,5X,10HDOGMA    = ,F10.5,5X,                       $PGR3300=0321
    *   60H=OUTSIDE DIAMETER, MAXIMUM,                                        $PGR3310=0322
    */11H DOPMI    = ,F10.5,5X,10HDOGMI    = ,F10.5,5X,                       $PGR3320=0323
    *   60H=OUTSIDE DIAMETER, MINIMUM                                         $PGR3330=0324
    */11H DRPMA    = ,F10.5,5X,10HDRGMA    = ,F10.5,5X,                       $PGR3340=0325
    *   60H=ROOT DIAMETER, MAXIMUM                                            $PGR3350=0326
    */11H DRPMI    = ,F10.5,5X,10HDRGMI    = ,F10.5,5X,                       $PGR3360=0327
    *   60H=ROOT DIAMETER, MINIMUM                                            $PGR3370=0328
    */11H EP       = ,F10.0,5X,10HEG       = ,E10.0,5X,                       $PGR3380=0329
    *   60H=YOUNG'S MODULUS, PSI,                                             $PGR3390=0330
    *)                                                                        $PGR3400=0331
1125 FORMAT (                                                                 $PGR3410=0332
    * 11H FMINP    = ,F10.5,5X,10HFMING    = ,F10.5,5X,                       $PGR3420=0333
    *   60H=FACE WIDTH, MINIMUM                                               $PGR3430=0334
    */11H PRP      = ,F10.5,5X,10HPRG      = ,F10.5,5X,                       $PGR3440=0335
    *   60H=POISSON'S RATIO                                                   $PGR3450=0336
    */11H RFMIP    = ,F10.5,5X,10HRFMIG    = ,F10.5,5X,                       $PGR3460=0337
    *   60H=ROOT FILLET RADIUS                                                $PGR3470=0338
    */11H TPMAS    = ,F10.5,5X,10HTGMAS    = ,F10.5,5X,                       $PGR3480=0339
    *   60H=ARC OR CHORDAL TOOTH THICKNESS, MAXIMUM,                          $PGR3490=0340
    */11H TPMIS    = ,F10.5,5X,10HTGMIS    = ,F10.5,5X,                       $PGR3500=0341
    *   60H=ARC OR CHORDAL TOOTH THICKNESS, MINIMUM,                          $PGR3510=0342
    */11H BMIN     = ,F10.5,30X, 36H=BACKLASH MINIMUM                         $PGR3520=0343
    */11H BMAX     = ,F10.5,30X, 36H=BACKLASH MAXIMUM                         $PGR3530=0344
    */11H CNSTD    = ,F10.5,30X, 36H=CENTER DISTANCE, STAND, IF ZERO          $PGR3540=0345
    */11H PHIN     = ,F10.5,30X, 36H=PRESSURE ANGLE (DEG,)                    $PGR3550=0346
    */11H PND      = ,F10.5,30X,36H=DIAMETRAL PITCH                           $PGR3560=0347
    *//)                                                                       $PGR3570=0348
1200 FORMAT (//35X,49HVALUES AND DEFINITIONS OF PRELIMINARY CALCULATED        $PGR3580=0349
    *,10HVARIABLES  /                                                         $PGR3590=0350
    * 2X,16H    (DRIVER)     ,6X,14H    (DRIVEN)                            $PGR3600=0351
    */11H ADP      = ,F10.5,5X,10HADG      = ,F10.5,5X,                       $PGR3610=0352
    *   60H=ADDENDUM (IN,)                                                    $PGR3620=0353
    */11H DRP      = ,F10.5,5X,10HDRG      = ,F10.5,5X,                       $PGR3630=0354
    *   60H=BASE CIRCLE DIAMETER                                              $PGR3640=0355
    */11H DODRP    = ,F10.5,5X,10HDODRG    = ,F10.5,5X,                       $PGR3650=0356
    *   60H=OUTSIDE DIAMETER BREAK                                            $PGR3660=0357
    */11H DP       = ,F10.5,5X,10HDG       = ,F10.5,5X,                       $PGR3670=0358
    *   60H=STD, PITCH DIAMETER                                               $PGR3680=0359
    */11H DXP      = ,F10.5,5X,10HDXG      = ,F10.5,5X,                       $PGR3690=0360
    *   60H=NON, STD, PITCH DIAMETER                                          $PGR3700=0361
    */11H WDP      = ,F10.5,5X,10HWDG      = ,F10.5,5X,                       $PGR3710=0362
    *   60H=HEIGHT OR WHOLE DEPTH                                             $PGR3720=0363
    */)                                                                       $PGR3730=0364
1201 FORMAT (11H ANG      = ,F10.5,30X,11H=GEAR RATIO                         $PGR3740=0365
    */11H CNSTD    = ,F10.5,30X, 36H=CALCULATED CENTER                        $PGR3750=0366
    */11H CPN      = ,F10.5,30X, 36H=NORMAL CIRCLE PITCH                      $PGR3760=0367
    */11H PHRA     = ,F10.5,30X, 36H=PRESSURE ANGLE (DEG,)                    $PGR3770=0368
    */11H PXRA     = ,F10.5,30X, 36H=WORKING PRESSURE ANGLE (DEG,)            $PGR3780=0369
    */11H ER       = ,F10.3,30X, 36H=REDUCED MODULUS (PSI,)                   $PGR3790=0370
    */11H PH       = ,F10.5,30X, 36H=BASE PITCH                               $PGR3800=0371
    */11H PDX      = ,F10.5,30X,36H=DIAMETRAL PITCH, WORKING                  $PGR3810=0372
```

Figure H-2. Listing of ground spur gear computer program (cont'd)

```
     */11H RMG      = ,F10.5,30X, 36H=1/GEAR RATIO                                  $PGR3820=0378
     */11H VO       = ,F10.5,30X,                                                   $PGR3830=0379
     =63H=DISTANCE FROM INITIAL INTERFERENCE POINT TO PITCH POINT                   $PGR3840=0375
     */11H WO       = ,F10.5,30X,                                                   $PGR3850=0376
     =63H=DISTANCE FROM SECOND  INTERFERENCE POINT TO PITCH POINT                   $PGR3860=0377
     */11H ZA       = ,F10.5,30X, 36H=PATH OF CONTACT IN APPROACH                   $PGR3870=0378
     */11H ZFN      = ,F10.5,30X, 36H=INVOLUTE PHI FOR STD. CENTERS TO PI          $PGR3880=0379
     = ,20HTCH CIRCLE (RAD.)                                                        $PGR3890=0380
     */11H ZFX      = ,F10.5,30X, 36H=INVOLUTE PHI FOR NON=STD. CENTERS T          $PGR3900=0381
     = ,30HO PITCH CIRCLE (RAD.)                                                    $PGR3910=0382
     */11H ZR       = ,F10.5,30X, 36H=PATH OF CONTACT IN RECESS                    )$PGR3920=0383
1205 FORMAT (/3X,38HARC TOOTH THK, FROM CHORDAL TOOTH THK,/                         $PGR3930=0384
     = 2X,16H    (DRIVER)     ,6X,14H    (DRIVEN)                                  $PGR3940=0385
     */11H TPHIS    = ,F10.5,5X,10HTGMIS    = ,F10.5,5X,                           $PGR3950=0386
     */11H TPHIS    = ,F10.5,5X,10HTGMIS    = ,F10.5/)                             $PGR3960=0387
1206 FORMAT (/3X,42HOPERATING ARC TOOTH THK, AT PITCH DIAMETER/                     $PGR3970=0388
     = 2X,16H    (DRIVER)     ,6X,14H    (DRIVEN)                                  $PGR3980=0389
     */11H TPMAX    = ,F10.5,5X,10HTGMAX    = ,F10.5,5X, 8H=MAXIMUM                $PGR3990=0390
     */11H TPMIN    = ,F10.5,5X,10HTGMIN    = ,F10.5,5X, 8H=MINIMUM                $PGR4000=0391
     */11H PK       = ,F10.5,5X,10HGK       = ,F10.5,5X,                           $PGR4010=0392
     =   60H=ANGLE FROM ORIGIN OF INVOLUTE TO CENTER LINE OF TOOTH (RAD)            $PGR4020=0393
     =  )                                                                           $PGR4030=0394
1127 FORMAT (1H1//35X,48HINPUT VARIABLES FOR SPECIFIED LOOPS AND SECTIO            $PGR4040=0395
     =NS//1X,30HVARIABLES USED IN... RPMP LOOP                                      $PGR4050=0396
     */11H RPMP     = ,F10.2,30X, 36H=RPM DRIVER                                    $PGR4060=0397
     =)                                                                             $PGR4070=0398
1128 FORMAT (                                                                       $PGR4080=0399
     = 11H RINC     = ,F10.2,30X, 36H=RPM DRIVER INCREMENT                          $PGR4090=0400
     */11H RPMX     = ,F10.2,30X, 36H=RPM DRIVER MAXIMUM                            $PGR4100=0401
     =)                                                                             $PGR4110=0402
1140 FORMAT (                                                                       $PGR4120=0403
     */11H HORSES   = ,F10.5,30X, 36H=HORSEPOWER                                    $PGR4130=0404
     =)                                                                             $PGR4140=0405
1141 FORMAT (                                                                       $PGR4150=0406
     = 11H DHP      = ,F10.5,30X, 36H=HORSEPOWER INCREMENT                          $PGR4160=0407
     */11H HPM      = ,F10.5,30X, 36H=MAXIMUM HORSEPOWER                            $PGR4170=0408
     =)                                                                             $PGR4180=0409
1146 FORMAT (/11H P1       = ,F10.5,5X,10HP2       = ,F10.5)                       $PGR4190=0410
1147 FORMAT ( 11H E1       = ,F10.5,5X,10HE2       = ,F10.5)                       $PGR4200=0411
1155 FORMAT (                                                                       $PGR4220=0412
     = 2X,16H    (DRIVER)     ,6X,14H    (DRIVEN)                                  $PGR4230=0413
     */11H AP       = ,F10.5,5X,10HAG       = ,F10.5,5X,                           $PGR4240=0414
     =   60H=THICKNESS OF RIM BELOW ROOT                                            $PGR4250=0415
     */11H PEP      = ,F10.5,5X,10HPEG      = ,F10.5,5X, 13H=PITCH ERROR           $PGR4260=0416
     */11H PMI      = ,F10.5,5X,10HGMI      = ,F10.5,5X,                           $PGR4270=0417
     =   60H=MASS MOMENT OF INERTIA (LB.SEC.SQ.IN.)                                 $PGR4280=0418
     */11H NAT(1)   = ,F10.2,30X, 36H=1ST NATURAL FREQUENCY(RPM)                    $PGR4290=0419
     */11H NAT(2)   = ,F10.2,30X, 36H=2ND NATURAL FREQUENCY(RPM)                    $PGR4300=0420
     */11H NAT(3)   = ,F10.2,30X, 36H=3RD NATURAL FREQUENCY(RPM)                    $PGR4310=0421
     =)                                                                             $PGR4320=0422
1160 FORMAT (                                                                       $PGR4330=0423
     */11H FR1      = ,F9.9,10X, 30H=CONSTANT FRICTION FACTOR                       $PGR4340=0424
     */11H FR2      = ,F9.9,10X, 30H=VARIABLE FRICTION FACTOR                       $PGR4350=0425
     */11H TCON     = ,F9.1,10X, 30H=TEMP DIFFERENCE FACTOR                         $PGR4360=0426
     */11H TEMP     = ,F9.1,10X, 30H=OIL JET TEMPERATURE,F                          $PGR4370=0427
     =)                                                                             $PGR4380=0428
1215 FORMAT (1H1///////7X,2HHP,12X,2HHG,12X,2HTP,12X,2HTG,11X,4HFPCO,              $PGR4390=0429
     =   11X,4HFGCO/)                                                               $PGR4400=0430
1210 FORMAT (1H1///1X,2A7,A10//F11.2,13H = HORSEPOWER/ F11.2,                       $PGR4410=0431
     =         16H = RPM DRIVER   / F11.2,5H = WN)                                 $PGR4420=0432
1211 FORMAT (1H1///1X,2A7,A10//F11.2,13H = HORSEPOWER/F11.2,                        $PGR4430=0433
     =         16H = RPM DRIVER   /F11.2,6H = WN/                                  $PGR4440=0434
```

Figure H-2. Listing of ground spur gear computer program (cont'd)

```
     *        F11.8,7H = TS,F/F11.4,14H = PMEAN,8/SEC)                    SPGR0450
 1230 FORMAT (///3X,2A10,11X,2A10/3X,7A10/)                               SPGR0460
 1220 FORMAT (3X,F8.4,5(6X,F8.4))                                         SPGR0470
 1235 FORMAT (1X,I2,2X,F5.2,3X,F7.1,1X,E10.4,2X,F7.0,5X,F6.2,3X,F6.2,     SPGR0480
     * 3X,E9.3)                                                          SPGR0490
 1250 FORMAT (///9X,A8,3A10/)                                             SPGR0500
C                                                                         SPGR0510
  700 CONTINUE                                                            SPGR0520
      END                                                                 SPGR0530
      SUBROUTINE LDVROL (ROLLRAY,DFBP,DFBG,NXFO,MOD,                      LDVR0000
     *          E1,E2,MARK1,MARK3,EBCP,EECP,KRN,TOFES)                    LDVR0010
      DIMENSION ROLLRAY(KRN,2),TDF(90), DFBP(KRN),DFBG(KRN),PMP(90),      LDVR0020
     *        PMG(90),NX(90),PRMOD(90),NXFO(KRN,2),DFP(90),DFG(90)        LDVR0030
      DATA IM2,IM4,IM5,IM6 /9H = P1    ,9H = P2    ,9H = E1    ,         LDVR0040
     *                      9H = E2    /                                 LDVR0050
      COMMON JA,JB,JC,JD,KAMP,P1,RN,WN,RPMP,LOU,LIN,ANP,ANG,DBP,DBG,      LDVR0060
     *   NODBG,CNSTD,PEP,PEG,ALPHA,OPA,P1,P2,IXT,BET                      LDVR0070
      MARK1=0                                                             LDVR0080
      MARK3=JD+1                                                          LDVR0090
      J=0                                                                 LDVR0100
      XNUM=0.                                                             LDVR0110
C                                                                         LDVR0120
C     CALCULATE DEFLECTIONS,  DFP(I)    /G(I)  AND TOTAL DEFLECTIONS TDF LDVR0130
C                                                                         LDVR0140
      DO 5 I=1,JD                                                         LDVR0150
       DFP(I)=DFBP(I)*WN                                                  LDVR0160
       DFG(I)=DFBG(I)*WN                                                  LDVR0170
       TDF(I)=DFP(I)+DFG(I)                                               LDVR0180
    5 CONTINUE                                                            LDVR0190
C     MODIFICATIONS          (N)=NORMAL CONTACT                           LDVR0200
C     MOD=0          NO MODIFICATION                                      LDVR0210
C     MOD=1          MODIFY GEAR AND PINION TIP                           LDVR0220
C     MOD=2          MODIFY PINION TIP AND ROOT                           LDVR0230
C     MOD=3          MODIFY GEAR TIP AND ROOT                             LDVR0240
C                                                                         LDVR0250
C     PMG(I)         TIP MODIFICATIONS,  A=C (N)                          LDVR0260
C     PMP(I)         ROOT MODIFICATIONS, B=D (N)                          LDVR0270
C                    (PMP(I) IS MOD, FOR ANGLE ONE BASE PITCH AWAY FROM   LDVR0280
C                     ANGLE WHERE PMG(I) IS DETERMINED)                   LDVR0290
C     L2,L1          POINTERS TO ROLLRAY, PIN, ANGLES (COL 1) GEAR (COL 2)LDVR0300
C                                                                         LDVR0310
C     GENERAL EQUATIONS...    PMG(I) = P1*(( EX  -E1)/(EA-E1))            LDVR0320
C                             PMP(I) = P2*(( EY  -E2)/(ED-E2))            LDVR0330
C                    MODIFICATION FACTORS,  P1,P2,E1,E2  ARE GIVEN        LDVR0340
C                    P1 = MODIFICATION AT START OF CONTACT                LDVR0350
C                    E1 = CORRESPONDING ROLL ANGLE                        LDVR0360
C                    P2 = MODIFICATION AT END OF CONTACT                  LDVR0370
C                    E2 = CORRESPONDING ROLL ANGLE                        LDVR0380
C                    EX = ROLL ANGLES  A=C (N)                            LDVR0390
C                    EY = ROLL ANGLES  B=D (N)                            LDVR0400
C                    EA = GEAR OR PINION ANGLES AT POINT =A= ,  EBCP,EECG LDVR0410
C                    ED = GEAR OR PINION ANGLES AT POINT =D= ,  EECP,EECG LDVR0420
C                    J POINTS TO ANGLES ONE BASE PITCH AWAY FROM =I=      LDVR0430
C                                                                         LDVR0440
      I1=1                                                                LDVR0450
      TOFES = TDF(JB)                                                     LDVR0460
      IF (MOD.EQ.0) GO TO 90                                              LDVR0470
      L1=2                                                                LDVR0480
      L2=1                                                                LDVR0490
      IF (MOD.EQ.3) L2=2                                                  LDVR0500
      IF (MOD.EQ.2) L1=1                                                  LDVR0510
      IF (KAMP.EQ.2) GO TO 26                                             LDVR0520
```

Figure H-2. Listing of ground spur gear computer program (cont'd)

```
   20 EA = ROLLRAY(JA,L1)                                                  LDVR0530=0497
      ED = ROLLRAY(JD,L2)                                                  LDVR0540=0498
   25 KAMP=1                                                               LDVR0550=0499
      WRITE  (LOU,900) P1,IM8,P2,IM9,E1,IM5,E2,IM6                         LDVR0560=0500
  900 FORMAT (F11.5,A9,5X,F11.5,A9/F11.5,A9,5X,F11.5,A9)                   LDVR0570=0501
C                                                                          LDVR0580=0502
C     CALCULATE MODIFICATIONS                                              LDVR0590=0503
C                                                                          LDVR0600=0504
   26 J=J8=1                                                               LDVR0610=0505
      DO 30 I=1,JC                                                         LDVR0620=0506
      J=J+1                                                                LDVR0630=0507
      EX=ROLLRAY(I,L1)                                                     LDVR0640=0508
      EY=ROLLRAY(J,L2)                                                     LDVR0650=0509
       PMG(I) = P1 * ((EX-E1)/(EA-E1))                                     LDVR0660=0510
       PMP(I) = P2 * ((EY-E2)/(ED-E2))                                     LDVR0670=0511
      IF(PMG(I).LT.0.0) PMG(I)=0.0                                         LDVR0680=0512
      IF(PMP(I).LT.0.0) PMP(I)=0.0                                         LDVR0690=0513
   30 CONTINUE                                                             LDVR0700=0514
      J=JA=1                                                               LDVR0710=0515
      IF (MOD.EQ.3) GO TO 60                                               LDVR0720=0516
C                                                                          LDVR0730=0517
C     CALCULATE A LOAD VS ROLL ANGLE FOR GEARS WITH TOOTH MODIF.           LDVR0740=0518
C     THAT ARE ONE BASE PITCH APART                                        LDVR0750=0519
C     FOR MOD=1 AND MOD=2                                                  LDVR0760=0520
C                                                                          LDVR0770=0521
   50 DO 55 I=1,JC                                                         LDVR0780=0522
      J=J+1                                                                LDVR0790=0523
      WX(I) = WN*((TDF(J)+PMP(I)-PMG(I))/(TDF(I)+TDF(J)))                  LDVR0800=0524
      WX(J) = WN-WX(I)                                                     LDVR0810=0525
      IF (WX(I).LT.0.) MARK1=I                                             LDVR0820=0526
      IF (WX(J).LT.0.) MARK3=MARK3=1                                       LDVR0830=0527
   55 CONTINUE                                                             LDVR0840=0528
      GO TO 80                                                             LDVR0850=0529
C                                                                          LDVR0860=0530
C     FOR MOD=3                                                            LDVR0870=0531
C                                                                          LDVR0880=0532
   60 DO 65 I=1,JC                                                         LDVR0890=0533
      J=J+1                                                                LDVR0900=0534
      WX(I) = WN*((TDF(J)+PMG(I)-PMP(I))/(TDF(I)+TDF(J)))                  LDVR0910=0535
      WX(J) = WN-WX(I)                                                     LDVR0920=0536
      IF (WX(I).LT.0.) MARK1=I                                             LDVR0930=0537
      IF (WX(J).LT.0.) MARK3=MARK3=1                                       LDVR0940=0538
   65 CONTINUE                                                             LDVR0950=0539
      GO TO 80                                                             LDVR0960=0540
C                                                                          LDVR0970=0541
C     CALCULATE A LOAD VS ROLL ANGLE FOR GEARS WITH NO MODIFICATIONS       LDVR0980=0542
C     THAT ARE ONE BASE PITCH APART                                        LDVR0990=0543
C                                                                          LDVR1000=0544
C                                                                          LDVR1010=0545
   70 J=J8=1                                                               LDVR1020=0546
      DO 75 I=1,JC                                                         LDVR1030=0547
      J=J+1                                                                LDVR1040=0548
      WX(I) = WN*(TDF(J)/(TDF(I)+TDF(J)))                                  LDVR1050=0549
      WX(J) = WN-WX(I)                                                     LDVR1060=0550
      IF (WX(I).LT.0.) MARK1=I                                             LDVR1070=0551
      IF (WX(J).LT.0.) MARK3=MARK3=1                                       LDVR1080=0552
   75 CONTINUE                                                             LDVR1090=0553
C                                                                          LDVR1100=0554
C     CALCULATE LOAD VS ROLL ANGLE FOR ALL ANGLES OF                       LDVR1110=0555
C     SINGLE TOOTH CONTACT                                                 LDVR1120=0556
C                                                                          LDVR1130=0557
   80 K1=JC+1                                                              LDVR1140=0558
```

Figure H-2. Listing of ground spur gear computer program (cont'd)

```
      K2=JB+1                                                                   LDVR1150+0559
      DO 95 I=K1,K2                                                             LDVR1160+0560
      WX(I) = WN                                                                LDVR1170+0561
      PRMOD(I)=0.                                                               LDVR1180+0562
   95 CONTINUE                                                                  LDVR1190+0563
      IF (MOD.EQ.0) GO TO 180                                                   LDVR1200+0564
      J=JA+1                                                                    LDVR1210+0565
      DO 99 I=1,JC                                                              LDVR1220+0566
      J=J+1                                                                     LDVR1230+0567
      PRMOD(I)=PMG(I)                                                           LDVR1240+0568
      PRMOD(J)=PMP(I)                                                           LDVR1250+0569
   99 CONTINUE                                                                  LDVR1260+0570
  127 WRITE (LOU,1002)                                                          LDVR1270+0571
      DO 130 I=1,JD                                                             LDVR1280+0572
      WRITE (LOU,1003) I,(ROLLRAY(I,J),J=1,2), DFP(I), DFG(I),TDF(I),           LDVR1290+0573
     *                  WX(I),PRMOD(I)                                         LDVR1300+0574
  130 CONTINUE                                                                  LDVR1310+0575
      IF (MOD.GT.0) GO TO 205                                                   LDVR1320+0576
  180 WRITE (LOU,1000)                                                          LDVR1330+0577
      DO 100 I=1,JD                                                             LDVR1340+0578
      WRITE (LOU,1001) I,(ROLLRAY(I,J),J=1,2), DFP(I), DFG(I),TDF(I),           LDVR1350+0579
     *                  WX(I)                                                  LDVR1360+0580
  100 CONTINUE                                                                  LDVR1370+0581
 1000 FORMAT (///7X,19HROLL     ANGLES,10X,11HDEFLECTIONS,10X,5HTOTAL,         LDVR1380+0582
     *7X,9HLOAD/6X,6HDRIVER,3X,6HDRIVEN,7X,6HDRIVER,5X,6HDRIVEN,5X,           LDVR1390+0583
     *11HDEFLECTIONS,3X,5HFORCE/)                                            LDVR1400+0584
 1001 FORMAT (1X,I2,  3X,F5.2,9X,F5.2,3(9X,E9.3),3X,F8.1)                       LDVR1410+0585
 1003 FORMAT (1X,I2  ,9X,F5.2,9X,F5.2,3(9X,E9.3),3X,F8.1,2X,E9.3)               LDVR1420+0586
 1002 FORMAT (///7X,19HROLL     ANGLES,10X,11HDEFLECTIONS,10X,5HTOTAL,         LDVR1430+0587
     *7X,9HLOAD/6X,6HDRIVER.3X,6HDRIVEN,7X,6HDRIVER,5X,6HDRIVEN,5X,           LDVR1440+0588
     *11HDEFLECTIONS,3X,5HFORCE,2X,13HMODIFICATIONS/)                        LDVR1450+0589
  205 IF (MARK1.EQ.0.AND.MARK3.GT.JD) GO TO 240                                LDVR1460+0590
  215 IF (MARK1.GT.JA.OR.MARK3.LT.JD) GO TO 230                                LDVR1470+0591
      WXZR=.0002*WN                                                             LDVR1480+0592
      IF (MARK1.EQ.0) GO TO 220                                                 LDVR1490+0593
      IF (ABS(WX(JA)).GT.WXZR) GO TO 230                                        LDVR1500+0594
      IF (MARK3.GT.JD) GO TO 225                                                LDVR1510+0595
  220 IF (ABS(WX(JD)).GT.WXZR) GO TO 230                                        LDVR1520+0596
      WX(JD)=0.                                                                 LDVR1530+0597
      IF (MARK1.EQ.0) GO TO 240                                                 LDVR1540+0598
  225 WX(JA)=0.                                                                 LDVR1550+0599
      GO TO 240                                                                 LDVR1560+0600
  230 KAMP=KAMP+1                                                               LDVR1570+0601
      IF (MARK1.EQ.0) GO TO 235                                                 LDVR1580+0602
      IF (MARK1.GT.IXT/2) GO TO 210                                             LDVR1590+0603
      EP1=ROLLRAY(MARK1,1) * RN                                                 LDVR1600+0604
      EP = ROLLRAY(MARK1+1,1)*RN                                                LDVR1610+0605
      U1 = ABS(WX(MARK1)) * (EP -EP1)/(WX(MARK1+1)+ABS(WX(MARK1)))              LDVR1620+0606
      EBCP=EP1+U1                                                               LDVR1630+0607
      IF (MARK3.GT.JD) GO TO 240                                                LDVR1640+0608
      K=JD-MARK3+1                                                              LDVR1650+0609
      IF (K.GT.IXT/2) GO TO 210                                                 LDVR1660+0610
  235 EP=ROLLRAY(MARK3,1)*RN                                                    LDVR1670+0611
      EP2=ROLLRAY(MARK3-1,1)*RN                                                 LDVR1680+0612
      U2 = WX(MARK3-1) * (EP-EP2)/(WX(MARK3-1)+ABS(WX(MARK3)))                  LDVR1690+0613
      EECP=EP2+U2                                                               LDVR1700+0614
      GO TO 240                                                                 LDVR1710+0615
  210 WRITE (LOU,777)                                                           LDVR1720+0616
  777 FORMAT (/////45H  PROGRAM TERMINATED, NEG. LOADS EXCEED IXT/2)            LDVR1730+0617
      STOP                                                                      LDVR1740+0618
  240 DO 250 I=1,JD                                                             LDVR1750+0619
      WXFO(I,1)=WX(I)                                                           LDVR1760+0620
```

Figure H-2. Listing of ground spur gear computer program (cont'd)

```
  250 CONTINUE                                                          LOVR1770=0621
      RETURN                                                            LOVR1780=0622
      END                                                               LOVR1790=0623
      SUBROUTINE PHI (DEC,F  ,H,T,XDIM,DFS,DX,DB,DR,PGK,AN,RPHI,    EY, PHI 0000=0624
     * PI,RN,JD,FMIN,FCO,KRW)                                          PHI 0010=0625
      DIMENSION DEC(KRW),F(KRW),H(KRW),XDIM(KRW),T(KRW),DFS(KRW),       PHI 0020=0626
     *          DV(90),RV(90),FCO(90),DW(90)                           PHI 0030=0627
      DATA ISEAR /6HSEAR  /                                             PHI 0040=0628
      DO 10 I=1,JD                                                      PHI 0050=0629
      FF    =DR/DEC(I)                                                  PHI 0060=0630
      FRA   =ATAN(SQRT(1.-(FF)**2)/FF)                                  PHI 0070=0631
      FSI   =SIN(FRA)                                                   PHI 0080=0632
      FCO(I)=COS(FRA)                                                   PHI 0090=0633
      FPT   =FSI/FCO(I)                                                 PHI 0100=0634
      F(I) =FPT=PGK                                                     PHI 0110=0635
      DV(I) = DB/COS(F(I))                                              PHI 0120=0636
      RV(I) =DV(I)*.5                                                   PHI 0130=0637
   10 CONTINUE                                                          PHI 0140=0638
C     CALL SUBROUTINES XY AND WEAK WHEN...                              PHI 0150=0639
C                                                                       PHI 0160=0640
   90 CALL XY       (DB,DR,RPHI,PGK,X,Y)                              PHI 0170=0641
      CALL WEAK        (RV,T,H,XDIM,DW,X,Y,RPHI,KRW,JD)                PHI 0180=0642
   50 DO 60 I=1,JD                                                      PHI 0190=0643
      T2=T(I)*2.                                                        PHI 0200=0644
      DFS(I)=(3.0/(EY*FMIN)*((H(I)/T2))      *COS(F(I))                 PHI 0210=0645
   60 CONTINUE                                                          PHI 0220=0646
      RETURN                                                            PHI 0230=0647
      END                                                               PHI 0240=0648
      SUBROUTINE WEAK  (RV,T,H,XDIM,DW,X,Y,RPM,KRW,JD)                  WEAK0000=0649
      DIMENSION T(KRW),H(KRW),RV(KRW),XDIM(KRW),DW(KRW),ALPHA(90)       WEAK0010=0650
C                                                                       WEAK0020=0651
C     SUBROUTINE WEAK CALCS. THE DIA. OF THE WEAKEST SECTION (DW) BY    WEAK0030=0652
C   INSCRIBING THE LARGEST PARABOLA THAT WILL FIT THE GEAR TOOTH SHAPE. WEAK004C=0653
C                                                                       WEAK0050=0654
      DO 80 I=1,JD                                                      WEAK0060=0655
      ALPHA(I)=.1                                                       WEAK0070=0656
      DELTA   =.1                                                       WEAK0080=0657
   10 V = SIN(ALPHA(I))*RPM                                             WEAK0090=0658
      V1 = SQRT((RPM)**2-(V)**2)                                        WEAK0100=0659
C       T =  HALF CHORD AT THE WEAKEST SECTION                          WEAK0110=0660
      T(I)=X-V1                                                         WEAK0120=0661
      YA=T(I)/(SIN(ALPHA(I))/COS(ALPHA(I)))                             WEAK0130=0662
C       H =  TOOTH HEIGHT FROM WEAKEST SECTION TO VERTEX OF PARABOLA    WEAK0140=0663
      H(I)=(RV(I)-Y)+Y                                                  WEAK0150=0664
      YAP=YA*.5                                                         WEAK0160=0665
      IF (YAP-H(I)) 20,90,30                                            WEAK0170=0666
   20 ALPHA(I)=ALPHA(I)-DELTA                                           WEAK0180=0667
      DELTA=.1*DELTA                                                    WEAK0190=0668
      IF (.00000001-DELTA) 10,90,90                                     WEAK0200=0669
   30 ALPHA(I)=ALPHA(I)+DELTA                                           WEAK0210=0670
      GO TO 10                                                          WEAK0220=0671
   90 YB=Y-V                                                            WEAK0230=0672
C       DW  =  WEAKEST SECTION DIAMETER                                 WEAK0240=0673
      DW(I)=SQRT((YB)**2+(T(I))**2)*2.                                  WEAK0250=0674
      Q=ATAN(H(I)/T(I))                                                 WEAK0260=0675
      Q=1.5707963-Q                                                     WEAK0270=0676
C       XDIM=    X DIMENSION                                            WEAK0280=0677
      XDIM(I)=T(I)+(SIN(Q)/COS(Q))                                      WEAK0290=0678
   80 CONTINUE                                                          WEAK0300=0679
      RETURN                                                            WEAK0310=0680
      END                                                               WEAK0320=0681
      SUBROUTINE XY (DB,DR,RPHI,PGK,X,Y)                                XY  0000=0682
```

Figure H-2. Listing of ground spur gear computer program (cont'd)

```
C                                                                       XY  0010+0683
C  SUBROUTINE XY ++CALCULATES COORDINATES TO CENTER OF FILLET RADIUS     XY  0020+0684
C                                                                       XY  0030+0685
      M=(DR/2.)+RPMI                                                    XY  0040+0686
      MM=(DB/2.)+M                                                      XY  0050+0687
      IF (MM)              10,10,12                                     XY  0060+0688
   10 CPR=(DB/B.)/M                                                     XY  0070+0689
      CPRA=ATAN(SQRT(1.-(CPR)**2)/CPR)                                  XY  0080+0690
      OPP=SQRT((M)**2-(DB/2.)**2)                                       XY  0090+0691
      A=OPP-RPMI                                                        XY  0100+0692
      M1=SQRT((A)**2+(DB/2.)**2)                                        XY  0110+0693
      CA=(DB/2.)/M1                                                     XY  0120+0694
      CARA=ATAN(SQRT(1.-(CA)**2)/CA)                                    XY  0130+0695
      ZCA=(SIN(CARA)/COS(CARA))-CARA                                    XY  0140+0696
      B=(CPRA-CARA)-ZCA                                                 XY  0150+0697
      FAPRA=PSK+B                                                       XY  0160+0698
   11 X=SIN(FAPRA)+M                                                    XY  0170+0699
      Y=COS(FAPRA)+M                                                    XY  0180+0700
      RETURN                                                            XY  0190+0701
   12 XX=(DB/2.)+SIN(PSK)                                               XY  0200+0702
      FAPSI=(XX+RPMI)/M                                                 XY  0210+0703
      FAPRA=ATAN(FAPSI/(SQRT(1.-(FAPSI)**2)))                           XY  0220+0704
      GO TO 11                                                          XY  0230+0705
      END                                                               XY  0240+0706
      SUBROUTINE ROLLANG (VO,ZA,ZR,WO,DOPMA,DOGMA,PB,FXTA               ROLL0000+0707
     *                   ,ROLLRAY,RHOP,RHOG,DECP,DECG,VS,VT             ROLL0010+0708
     *                   ,EBCP,EECP,MARK1,MARK2,KRW)                    ROLL0020+0709
      DIMENSION  ROLLRAY(KRW,2),RHOP(KRW),RHOG(KRW),VS(KRW),VT(KRW),    ROLL0030+0710
     *           DECP(KRW),DECG(KRW)                                    ROLL0040+0711
      COMMON JA,JB,JC,JD,KAMP,PI,RN,WN,RPMP,LOU,LIN,ANP,ANG,DBP,DBG,    ROLL0050+0712
     *   DODBG,CNSTD,PEP,PEG,ALPHA,UPA,P1,P2,IXT,BET                    ROLL0060+0713
C     SUBROUTINE ROLLANG                                                ROLL0070+0714
C       CALCULATES..1, EPSILON OD-MAX                                   ROLL0080+0715
C                      2, ROLL ANGLES                                   ROLL0090+0716
C                      3, PROFILE CONTACT RATIOS                        ROLL0100+0717
C                      4, RADIUS OF CURVATURE FOR EACH ROLL ANGLE       ROLL0110+0718
C                      5, SLIDING VELOCITY FOR EACH ROLL ANGLE          ROLL0120+0719
C                      6, SUM VELOCITY FOR EACH ROLL ANGLE              ROLL0130+0720
C                      7, DIAMETER AT ENGAGEMENT CONDITIONS FOR EACH ROLL ROLL0140+0721
C                       ANGLE                                           ROLL0150+0722
C     METHOD OF CALCULATING ROLL ANGLES                                 ROLL0160+0723
C       1, FOR KAMP=1        =CALCULATE PINION ROLL ANGLES AT MAIN POINTSROLL0170+0724
C          FOR KAMP=2        =(ROLL ANGLES ARE TO BE RECALCULATED BECAUSEROLL0180+0725
C                              OF A NEGATIVE LOAD) = CALCULATE MAIN      ROLL0190+0726
C                              POINTS WITH ADJUSTMENTS U1 AND/OR U2      ROLL0200+0727
C       2, USING THESE VALUES CALCULATE ALL PINION AND GEAR ROLL ANGLES ROLL0210+0728
C                                                                       ROLL0220+0729
C     DEFINITIONS OF VARIABLES FOR SUBROUTINE ROLLANG                   ROLL0230+0730
C     KAMP = 1 , ROLL ANGLES CALCULATED WITH NORMAL CONDITIONS          ROLL0240+0731
C          = 2 , ROLL ANGLES RECALCULATED WITH NORMAL CONDITIONS        ROLL0250+0732
C     AMPMA                =PROFILE CONTACT RATIO  (MAXIMUM)            ROLL0260+0733
C     AMPMI                =PROFILE CONTACT RATIO  (MINIMUM)            ROLL0270+0734
C     PINION  GEAR                                                      ROLL0280+0735
C     EOPMA   EOGMI        =EPSILON OD MAX DRIVER                       ROLL0290+0736
C     EOPMI   EOGMA        =EPSILON OD MAX  DRIVEN                      ROLL0300+0737
C     ONEPB   ONEPBG       =ONE BASE PITCH                              ROLL0310+0738
C                                                                       ROLL0320+0739
C     ARRAY DESIGNATION                                                 ROLL0330+0740
C     ROLLRAY         COL.1  =DRIVER ROLL ANGLES                        ROLL0340+0741
C                     COL.2  =DRIVEN GEAR ROLL ANGLES                   ROLL0350+0742
C     VS                     =SLIDING VELOCITIES                        ROLL0360+0743
C     VT                     =SUM VELOCITIES                            ROLL0370+0744
```

Figure H-2. Listing of ground spur gear computer program (cont'd)

```
C     PINION  GEAR                                                          ROLL0380*0795
C     DECP    DECG          *DIAMETERS AT ENGAGEMENT CONDITIONS             ROLL0390*0796
C     RHOP    RHOG          *RADII OF CURVATURE                             ROLL0400*0797
C                                                                           ROLL0410*0798
C                                                                           ROLL0420*0799
C                                                                           ROLL0430*0800
C                                                                           ROLL0440*0801
C                                                                           ROLL0450*0802
C                                                                           ROLL0460*0803
C                                                                           ROLL0470*0804
      EOPMA = SQRT((DOPMA/DBP)**2-1.) /RN                                   ROLL0480*0805
      EOGMA = SQRT((DOGMA/DBG)**2-1.) /RN                                   ROLL0490*0806
      EOPMI=(2.*(VO+HO)-SQRT(DOGMA*DOGMA-(DBG+DBG)))/DBP  /RN               ROLL0500*0807
      FOGMI=(2.*(VO+HO)-SQRT(DOPMA*DOPMA-(DBP+DBP)))/DBG  /RN               ROLL0510*0808
      ONEAP = 2.*(PB/DBP)                                                   ROLL0520*0809
      ONEAPG = 2.*(PB/DBG)                                                  ROLL0530*0810
      GO TO (5,10) KAMP                                                     ROLL0540*0811
C                                                                           ROLL0550*0812
C      MAIN POINTS  (DRIVER ANGLES)                                         ROLL0560*0813
C                 D                                                         ROLL0570*0814
C                 /EECP                                                     ROLL0580*0815
C               B/                A=C, B=D    DOUBLE TOOTH CONTACT        ROLL0590*0816
C               /EESP                                                       ROLL0600*0817
C             C/                        C=B    SINGLE TOOTH CONTACT       ROLL0610*0818
C             /EBSP                                                       ROLL0620*0819
C           A/                                                            ROLL0630*0820
C            EBCP                                                         ROLL0640*0821
C                                                                         ROLL0650*0822
C     PINION  GEAR  NO.   BETWEEN AND INCLUDING POINTS...                 ROLL0660*0823
C      EMP    EMG   IXT   A=C                                             ROLL0670*0824
C      ESTP   ESTG  KXT   C=B                                             ROLL0680*0825
C      ENP    ENG   IXT   B=D  (ONE BASE PITCH FROM POINTS A=C)           ROLL0690*0826
C                                                                         ROLL0700*0827
    5 EBCP = (VO-ZA)     / (DBP/2.)                                       ROLL0710*0828
      EBSP = (VO+ZR-PB) / (DBP/2.)                                       ROLL0720*0829
      EESP = EBCP+ONEBP                                                  ROLL0730*0830
      EECP = EBSP+ONEBP                                                  ROLL0740*0831
      IXT =((1.-(PB/(ZA+ZR)))*20.+.5)/2+2                                ROLL0750*0832
      IF (IXT.LT.2) IXT=3                                                ROLL0760*0833
      KXT=20-2*IXT+1                                                     ROLL0770*0834
      JA=1                                                               ROLL0780*0835
      JC=JA+IXT                                                          ROLL0790*0836
      JB=JA+JC+KXT+1                                                     ROLL0800*0837
      JD=JB+IXT                                                          ROLL0810*0838
      GO TO 20                                                           ROLL0820*0839
   10 IF (MARK1.EQ.0) GO TO 15                                           ROLL0830*0840
      EESP = EBCP+ONEBP                                                  ROLL0840*0841
      IF (MARK3.GT.JD) GO TO 20                                          ROLL0850*0842
   15 EBSP = EECP-ONEBP                                                  ROLL0860*0843
   20 DO 30 I=1,JC                                                       ROLL0870*0844
      J=I-1                                                              ROLL0880*0845
      K=JA+J                                                             ROLL0890*0846
      EMP = EBCP + ((EBSP-EBCP)/IXT)*J                                   ROLL0900*0847
      EMG = (VO+HO)/(DBG/2.) - (EMP*(ANP/ANG))                           ROLL0910*0848
      ENP = EMP + ONEBP                                                  ROLL0920*0849
      ENG = EMG - ONEBPG                                                 ROLL0930*0850
C                                                                        ROLL0940*0851
      ROLLRAY(I,1)=EMP/RN                                                ROLL0950*0852
      ROLLRAY(I,2)=EMG/RN                                                ROLL0960*0853
      ROLLRAY(K,1)=ENP/RN                                                ROLL0970*0854
      ROLLRAY(K,2)=ENG/RN                                                ROLL0980*0855
   30 CONTINUE                                                           ROLL0990*0856
```

Figure H-2. Listing of ground spur gear computer program (cont'd)

```
      K2=KXT+1                                                          ROLL1000*0807
      DO 35 I=1,K2                                                      ROLL1010*0808
      J=I+1                                                             ROLL1020*0809
      K=JC+I                                                            ROLL1030*0810
      FSTP = EBSP + ((EESP-EBSP)/(21+2*IXT))*J                          ROLL1040*0811
      FSTG = (VO+WO)/(DBG/2.) + ESTP*(ANP/ANG)                          ROLL1050*0812
C                                                                       ROLL1060*0813
      ROLLRAY(K,1)=ESTP/RN                                              ROLL1070*0814
      ROLLRAY(K,2)=ESTG/RN                                              ROLL1080*0815
   35 CONTINUE                                                          ROLL1090*0816
      EBCG=ROLLRAY(JA,2) * RN                                           ROLL1100*0817
      AMPMA = ((ANG*(EOPMA*RN-PXTA))+(ANP*(EOPMA*RN+PXTA)))/(2.*PI)     ROLL1110*0818
      AMPMI = ((ANG*(EBCG    -PXTA))+(ANP*(EECP    +PXTA)))/(2.*PI)     ROLL1120*0819
      WRITE  (LOU,1006) (ROLLRAY(JA,I),I=1,2),(ROLLRAY(JC,J),J=1,2),    ROLL1130*0820
     *                  (ROLLRAY(JB,K),K=1,2),(ROLLRAY(JD,L),L=1,2),    ROLL1140*0821
     *                  EOPMA,EOGMI,EOPMI,EOGMA,AMPMA,AMPMI             ROLL1150*0822
C                                                                       ROLL1160*0823
   70 WRITE (LOU,1008)                                                  ROLL1170*0824
      DO 80 I=1,JD                                                      ROLL1180*0825
      EP=ROLLRAY(I,1)*RN                                                ROLL1190*0826
      EG=ROLLRAY(I,2)*RN                                                ROLL1200*0827
      RHOP(I) = EP * (DBP/2.)                                           ROLL1210*0828
      RHOG(I) = (VO+WO) * RHOP(I)                                       ROLL1220*0829
      DECP(I) = SQRT(EP**2+1.) * DBP                                    ROLL1230*0830
      DECG(I) = SQRT(EG**2+1.) * DBG                                    ROLL1240*0831
      VS(I) = (RHOP(I)-(ANP/ANG*RHOG(I)))* ((PI*RPMP)/30.)              ROLL1250*0832
      VT(I) = (RHOP(I)+(ANP/ANG*RHOG(I)))* ((PI*RPMP)/30.)              ROLL1260*0833
      WRITE  (LOU,1009) I,(ROLLRAY(I,J),J=1,2),RHOP(I),RHOG(I),VS(I),   ROLL1270*0834
     *                  VT(I)                                           ROLL1280*0835
   80 CONTINUE                                                          ROLL1290*0836
 1006 FORMAT (/1X,90HROLL ANGLES AT MAIN POINTS,,(IN DEGREES)//         ROLL1300*0837
     *1X,F5.2,9H EBCP,5X,F5.2,9H EBCG,7X,18H= BEGIN CONTACT, A/         ROLL1310*0838
     *1X,F5.2,9H EBSP,5X,F5.2,9H EBSG,7X,28H= BEGIN SINGLE TOOTH CONTACTROLL1320*0839
     *,                                  12H, C  (LPSTC)/              ROLL1330*0840
     *1X,F5.2,9H EESP,5X,F5.2,9H EESG,7X,28H= END SINGLE TOOTH CONTACT, ROLL1340*0841
     *,                                  10HB  (HPSTC)/                ROLL1350*0842
     *1X,F5.2,9H EECP,5X,F5.2,9H EECG,7X,16H= END CONTACT, D/           ROLL1360*0843
     *1X,F5.2,6H EOPMA,4X,F5.2,6H EOGMI,6X,15H= OD MAX DRIVER/          ROLL1370*0844
     *1X,F5.2,6H EOPMI,4X,F5.2,6H EOGMA,6X,15H= OD MAX DRIVEN/          ROLL1380*0845
     *1X,F5.2,6H AMPMA,4X,F5.2,6H AMPMI,6X,23H= PROFILE CONTACT RATIO)  ROLL1390*0846
 1008 FORMAT (/////7X,12HROLL  ANGLES,5X,19HRADIUS OF CURVATURE,10X,    ROLL1400*0847
     *          7HSLIDING,7X,3HSUM/47X,2(6X,8HVELOCITY)/                ROLL1410*0848
     *5X,15HDRIVER    DRIVEN,6X,16HDRIVER    DRIVEN,                   ROLL1420*0849
     *          6X,2(6X,8H(IN/SEC))/)                                   ROLL1430*0850
 1009 FORMAT (1X,I2  ,3X,F5.2,4X,F5.2,5X,F7.4,3X,F7.4,4X,2(7X,F7.2))    ROLL1440*0851
      RETURN                                                            ROLL1450*0852
      END                                                               ROLL1460*0853
      SUBROUTINE FRPHE    (TS,TEMP,WXFO,FRIC,PHE,KRW,JD,L1,VS,FW,ER,    FRPH0000*0854
     *  PHEAV,FR1,FR2,TCON,JB,JC,ROLLRAY,PHET,JA,RPMP,ANP)              FRPH0010*0855
      DIMENSION FRIC(KRW),PHE(KRW),WXFO(KRW,2),VS(KRW),ROLLRAY(KRW,2)  FRPH0020*0856
      DO 90 I=1,JD                                                      FRPH0030*0857
      DFORCE=WXFO(I,L1)                                                 FRPH0040*0858
      IF (DFORCE.NE.0.) GO TO 8                                         FRPH0050*0859
      FRIC(I)=0.                                                        FRPH0060*0860
      GO TO 25                                                          FRPH0070*0861
    8 PVS=DFORCE*((ABS(VS(I)))**(-1./3.))                               FRPH0080*0862
      IF(PVS.LT.200.) GO TO 15                                          FRPH0090*0863
      FRIC(I)=FR1                                                       FRPH0100*0864
      GO TO 25                                                          FRPH0110*0865
   15 FRIC(I)=FR2*(PVS**(-.30))                                         FRPH0120*0866
   25 PHE(I)=FRIC(I)*DFORCE*ABS(VS(I))/9336.                            FRPH0130*0867
   90 CONTINUE                                                          FRPH0140*0868
```

Figure H-2. Listing of ground spur gear computer program (cont'd)

```
      PHE1=0.                                                                  FRPH0150*0869
      J=JC-1                                                                   FRPH0160*0870
      DO 60 I=1,J                                                              FRPH0170*0871
      PHE1=PHE1+(PHE(I)+PHE(I+1))                                              FRPH0180*0872
   60 CONTINUE                                                                 FRPH0190*0873
      PHEAV1=PHE1*(ROLLRAY(JC,1)-ROLLRAY(JA,1))/(8.*J)                         FRPH0200*0874
      PHE2=0.                                                                  FRPH0210*0875
      K1=JC+1                                                                  FRPH0220*0876
      K2=JB-2                                                                  FRPH0230*0877
      KK=K2-K1+1                                                               FRPH0240*0878
      DO 70 I=K1,K2                                                            FRPH0250*0879
      PHE2=PHE2+(PHE(I)+PHE(I+1))                                              FRPH0260*0880
   70 CONTINUE                                                                 FRPH0270*0881
      PHEAV2=PHE2*(ROLLRAY(JB,1)-ROLLRAY(JC,1))/(8.*(KK))                      FRPH0280*0882
      PHE3=0.                                                                  FRPH0290*0883
      J=JD-1                                                                   FRPH0300*0884
      KK=JD-JB                                                                 FRPH0310*0885
      DO 80 I=JB,J                                                             FRPH0320*0886
      PHE3=PHE3+(PHE(I)+PHE(I+1))                                              FRPH0330*0887
   80 CONTINUE                                                                 FRPH0340*0888
      PHEAV3=PHE3*(ROLLRAY(JD,1)-ROLLRAY(JB,1))/((KK)*8.)                      FRPH0345*0889
      PHET=(PHEAV1+PHEAV2+PHEAV3)*ANP/(6.*RPMP)                                FRPH0350*0890
      PHEAV=PHET*RPMP/60.                                                      FRPH0355*0891
      TS=(TCON*((PHEAV)**.80))*TEMP                                            FRPH0360*0892
      RETURN                                                                   FRPH0370*0893
      END                                                                      FRPH0380*0894
      SUBROUTINE FORCE (AP,AG,   CPN,DIP,DIG,EP,EG,FMINP,FMING,FNRA,          FORC0000*0895
     *HORSES,NATPQ,PMI,GMI,PRP,PRG,TPMIS,TGMIS,VA,NDP,NDG,IMT,TDFES)           FORC0010*0896
      COMMON JA,JB,JC,JD,KAMP,PI,RN,NN,RPMP,LOU,LIN,ANP,ANG,DBP,DBG,           FORC0020*0897
     *   NDDBG,CNSTD,PEP,PEG,ALPHA,OPA,P1,P2,IXT,BET                           FORC0030*0898
      PMP=RPMP*(ANP/ANG)                                                       FORC0040*0899
      IF (RPMP.LT.PMPR) PMPR=RPMP                                              FORC0050*0900
      PM = PMI/((DIP/2.)*(DIP/2.))                                             FORC0070*0901
      GM = GMI/((DIG/2.)*(DIG/2.))                                             FORC0080*0902
      EM = (PM*GM)/(PM+GM)                                                     FORC0090*0903
      CB = (1./FMING) * (9.*(NDG/2.)**3/((EG*TGMIS**3))+                       FORC0100*0904
     *     (1./FMINP) * (9.*(NDP/2.)**3/((EP*TPMIS**3)))                      FORC0110*0905
      CN1 = (1./FMING) * ((2.*(1.+PRG)/EG)*((0.1/AG*(CPN*COS(FNRA)))+         FORC0120*0906
     *                          .125))                                         FORC0130*0907
      CN2 = (1./FMINP) * ((2.*(1.+PRP)/EP)*((0.1/AP*(CPN*COS(FNRA)))+         FORC0140*0908
     *                          .125))                                         FORC0150*0909
      CC1=(1./FMING)*(ANG/(6.*(AG/(CPN*COS(FNRA)))**.2)*EG))                   FORC0160*0910
      CC2=(1./FMINP)*(ANP/(6.*(AP/(CPN*COS(FNRA)))**.2)*EP))                   FORC0180*0911
      CC=CC1+CC2                                                               FORC0200*0912
      CR=CB+CN2                                                                FORC0210*0913
      CT=CB+CR+CC                                                              FORC0220*0914
      TS=1./CT                                                                 FORC0230*0915
      TG=1000.*HORSES/PMPR                                                     FORC0240*0916
      V=(PI*DIP/12.)*RPMP                                                      FORC0250*0917
      IF (NATPQ.NE.0.) GO TO 10                                                FORC0260*0918
      T=7.*PI*SQRT(CT*EM)                                                      FORC0270*0919
      NATPQ=60./T                                                              FORC0280*0920
      GO TO 20                                                                 FORC0290*0921
   10 T=60./NATPQ                                                              FORC0300*0922
   20 EE=(PEP*PEG)*TDFES*P1                                                    FORC0310*0923
      PP=(PEP+PEG)*TDFES*(2.*P1)                                               FORC0320*0924
  100 V=(PI*DIP/12.)*RPMP                                                      FORC0340*0925
      BT=PM/12.*(60./V)                                                        FORC0350*0926
      TT = BT/T                                                                FORC0360*0927
      IF (TT-.277) 120,120,110                                                 FORC0365*0928
  110 ET=0.815/SQRT(1.+(6.5*(TT*TT)))                                          FORC0370*0929
      GO TO 130                                                                FORC0380*0930
```

Figure H-2. Listing of ground spur gear computer program (cont'd)

```
      120 FT=1./(1.+(6.+6*(TT*TT)))
      130 DI = EE*FT*TB                                                    FORC0390*0931
          IF (RPMP.GT.PMPR) GO TO 135                                      FORC0400*0932
          DXG = DXP                                                        FORC0410*0933
      135 TI=DI*(DXG/2)                                                    FORC0420*0934
          DF=TG/(TG+TI)                                                    FORC0430*0935
          WRITE (LUU,1001) DI,DF                                           FORC0440*0936
     1001 FORMAT (E11.4,21H =  DYNAMIC INCREMENT/E11.4,18H =  DYNAMIC FACTORFORC0450*0937
         */)                                                               FORC0460*0938
          RETURN                                                           FORC0470*0939
          END                                                              FORC0480*0940
                                                                           FORC0490*0941
                                                                                 *0942
```

Figure H-2. Listing of ground spur gear computer program (cont'd)

VALUES AND DEFINITIONS OF PRIMARY INPUT VARIABLES (INCH UNITS UNLESS NOTED)

(DRIVEN)			(DRIVEN)			
ANP	=	31.00000	ANG	=	75.00000	=NUMBER OF TEETH
AP	=	22.15000	AG	=	22.15000	=THERMAL CONSTANT (LN,SQRT(SEC.)/IN,DEG. F)
BWAP	=	.02129	BWAG	=	.02129	=MAXIMUM TIP BREAK
DOPMA	=	3.00260	DOGMA	=	9.18960	=OUTSIDE DIAMETER, MAXIMUM,
DOPMI	=	3.00000	DOGMI	=	9.18860	=OUTSIDE DIAMETER, MINIMUM
DRPMA	=	3.00000	DRGMA	=	8.82700	=ROOT DIAMETER, MAXIMUM
DRPMI	=	3.00000	DRGMI	=	8.82700	=ROOT DIAMETER, MINIMUM
EP	=	30.+07	EG	=	30.+07	=YOUNG'S MODULUS, PSI,
FWIMP	=	1.87500	FWIMG	=	1.26000	=FACE WIDTH, MINIMUM
PRP	=	.30000	PRG	=	.30000	=POISSON'S RATIO
RFMIP	=	.05500	RFMIG	=	.05000	=ROOT FILLET RADIUS
TPMAS	=	.18530	TGMAS	=	.17730	=ARC OR CHORDAL TOOTH THICKNESS, MAXIMUM,
TPMIS	=	.18430	TGMIS	=	.17630	=ARC OR CHORDAL TOOTH THICKNESS, MINIMUM,
BWIN	=	.00900				=BACKLASH MINIMUM
BWAX	=	.00700				=BACKLASH MAXIMUM
CWSTD	=	0.00000				=CENTER DISTANCE, STAND, IF ZERO
PWIN	=	22.00000				=PRESSURE ANGLE (DEG,)
PWD	=	8.50000				=DIAMETRAL PITCH

VALUES AND DEFINITIONS OF PRELIMINARY CALCULATED VARIABLES

(DRIVEN)			(DRIVEN)			
ADP	=	.10867	ADG	=	.09991	=ADDENDUM (IN,)
DBP	=	3.38199	DBG	=	8.29011	=BASE CIRCLE DIAMETER
DOBMP	=	3.66993	DOBMG	=	9.19020	=OUTSIDE DIAMETER BREAK
DP	=	3.00706	DG	=	8.99118	=STD, PITCH DIAMETER
DIP	=	3.00706	DIG	=	8.99118	=NON, STD, PITCH DIAMETER
HDP	=	.09780	HDG	=	.09660	=HEIGHT OF ANGLE DEPTH
AMG	=	2.95161				=GEAR RATIO
CWSTD	=	5.29912				=CALCULATED CENTER
CPN	=	.36460				=NORMAL CIRCLE PITCH
PWWA	=	22.00000				=PRESSURE ANGLE (DEG,)
PWRA	=	22.00000				=NORMING PRESSURE ANGLE (DEG,)
EN	=	1.29E+07				=REDUCED MODULUS (PSI,)
PB	=	.34264				=BASE PITCH
PDN	=	8.50000				=DIAMETRAL PITCH, NORMING
RMG	=	.33784				=1/GEAR RATIO
VD	=	.08811				=DISTANCE FROM INITIAL INTERFERENCE POINT TO PITCH POINT
WD	=	1.07971				=DISTANCE FROM SECOND INTERFERENCE POINT TO PITCH POINT
ZA	=	.20446				=PATH OF CONTACT IN APPROACH
ZPA	=	.02005				=INVOLUTE PHI FOR STD, CENTERS TO PITCH CIRCLE (RAD,)
ZPR	=	.02005				=INVOLUTE PHI FOR NON-STD, CENTERS TO PITCH CIRCLE (RAD,)
ZR	=	.25219				=PATH OF CONTACT IN RECESS

OPERATING ARC TOOTH THK, AT PITCH DIAMETER

(DRIVEN)			(DRIVEN)			
TPMAX	=	.18530	TGMAX	=	.17730	=MAXIMUM
TPMIN	=	.18430	TGMIN	=	.17630	=MINIMUM
PA	=	.07054	GA	=	.03477	=ANGLE FROM ORIGIN OF INVOLUTE TO CENTER LINE OF TOOTH (RAD)

Figure H-3. Sample ground spur gear computer printout

```
                    INPUT VARIABLES FOR SPECIFIED LOOPS AND SECTIONS

VARIABLES USED IN... RPM LOOP
RPMP    =    8000.00                          =RPM DRIVER

VARIABLES USED IN...HORSEPOWER LOOP

HORSES  =  600.00000                          =HORSEPOWER
DHP     =  100.00000                          =HORSEPOWER INCREMENT
HPM     = 1100.00000                          =MAXIMUM HORSEPOWER

VARIABLES USED IN... MODIF.    LOOP

P1      =     .00095     P2      =     .00035
E1      =   25.00000     E2      =   27.99000

METHOD USED FOR CALCULATING NORMAL FORCE=
1 NORMAL FORCE = STATIC FORCE
2 DYNAMIC FACTOR CALCULATED BY TUPLIN METHOD
     (DRIVER)              (DRIVEN)
AP      =     .79200     AG      =     .31600     =THICKNESS OF RIM BELOW ROOT
PEP     =     .00020     PEG     =     .00020     =PITCH ERROR
PMI     =     .01678     GMI     =     .29669     =MASS MOMENT OF INERTIA (LB,SEC,SQ,IN.)
NAT(1)  =      =0.00                             =1ST NATURAL FREQUENCY(RPM)
NAT(2)  =      =0.00                             =2ND NATURAL FREQUENCY(RPM)
NAT(3)  =      =0.00                             =3RD NATURAL FREQUENCY(RPM)

   VARIABLES USED IN...  FLASH  TEMP   SECTION

FR1     =     .0169          =CONSTANT FRICTION FACTOR
FR2     =     .0802          =VARIABLE FRICTION FACTOR
TCON    =     225.0          =TEMP DIFFERENCE FACTOR
TEMP    =     250.0          =OIL JET TEMPERATURE,F
```

Figure H-3. Sample ground spur gear computer printout (cont'd)

ROLL ANGLE SECTION

ROLL ANGLES AT MAIN POINTS,,(IN DEGREES)

19,68	EBCP	26,60	EBCS	- BEGIN CONTACT, A
28,08	EBBP	29,90	EBBS	- BEGIN SINGLE TOOTH CONTACT, C (LPSTC)
26,29	EEBP	21,87	EEBS	- END SINGLE TOOTH CONTACT, B (HPSTC)
31,78	EECP	19,66	EECS	- END CONTACT, D
33,19	EOPMA	19,85	EOSMI	- OD MAX DRIVER
18,91	EOPMI	27,32	EOSMA	- OD MAX DRIVEN
1,75	AMPMA	1,47	AMPMI	- PROFILE CONTACT RATIO

	ROLL ANGLES		RADIUS OF CURVATURE		SLIDING VELOCITY	SUM VELOCITY
	DRIVER	DRIVEN	DRIVER	DRIVEN	(IN/SEC)	(IN/SEC)
1	19,68	26,60	,9332	1,9297	-294,81	1020,57
2	19,58	26,29	,9597	1,8981	-263,96	1033,75
3	19,48	25,97	,9863	1,8715	-232,12	1046,93
4	17,38	25,60	,8129	1,8999	-200,78	1060,12
5	18,28	25,13	,8395	1,8184	-169,43	1073,30
6	19,18	24,77	,8660	1,7918	-138,09	1086,48
7	20,08	24,40	,8926	1,7652	-106,74	1099,66
8	20,08	24,40	,8926	1,7652	-106,74	1099,66
9	20,77	24,12	,9130	1,7444	-82,73	1109,76
10	21,46	23,84	,9333	1,7245	-58,71	1119,86
11	22,15	23,56	,9537	1,7041	-34,70	1129,96
12	22,84	23,27	,9740	1,6838	-10,69	1140,06
13	23,53	22,99	,9944	1,6634	13,33	1150,16
14	24,22	22,71	,7148	1,6431	37,34	1160,26
15	24,91	22,43	,7351	1,6227	61,35	1170,36
16	25,60	22,15	,7555	1,6023	85,37	1180,46
17	26,29	21,87	,7758	1,5820	109,38	1190,56
18	26,29	21,87	,7758	1,5820	109,38	1190,56
19	27,19	21,50	,8024	1,5554	140,73	1203,74
20	28,09	21,13	,8290	1,5288	172,07	1216,92
21	28,99	20,77	,8556	1,5022	203,41	1230,10
22	29,89	20,40	,8821	1,4757	234,76	1243,29
23	30,79	20,03	,9087	1,4491	266,10	1256,47
24	31,78	19,66	,9353	1,4225	297,45	1269,65

Figure H-3. Sample ground spur gear computer printout (cont'd)

MP	MG	TP	TG	FPCO	FGCO
.0957	.2092	.2856	.2597	.9687	.9870
.0997	.1920	.2815	.2603	.9650	.9842
.0934	.1802	.2779	.2610	.9610	.9119
.0986	.1687	.2734	.2618	.9569	.9136
.0835	.1576	.2695	.2627	.9527	.9158
.0688	.1468	.2658	.2638	.9483	.9179
.0796	.1369	.2623	.2651	.9437	.9200
.0796	.1369	.2623	.2651	.9437	.9200
.0794	.1286	.2598	.2662	.9401	.9217
.0898	.1211	.2579	.2675	.9366	.9233
.0898	.1138	.2552	.2689	.9327	.9249
.0956	.1067	.2537	.2705	.9289	.9265
.1016	.0998	.2519	.2729	.9250	.9281
.1079	.0931	.2497	.2745	.9211	.9296
.1147	.0867	.2482	.2769	.9171	.9312
.1219	.0804	.2468	.2795	.9130	.9327
.1294	.0743	.2456	.2828	.9089	.9343
.1294	.0743	.2455	.2825	.9089	.9343
.1399	.0665	.2441	.2870	.9039	.9363
.1511	.0591	.2428	.2921	.8979	.9382
.1630	.0518	.2418	.2979	.8923	.9402
.1759	.0446	.2409	.3045	.8866	.9421
.1891	.0375	.2401	.3117	.8808	.9440
.2034	.0303	.2394	.3195	.8750	.9459

Figure H-3. Sample ground spur gear computer printout (cont'd)

LOAD FORCE SECTION

600.00 = HORSEPOWER
8000.00 = RPM DRIVER
2795.73 = FN
.08894 = P1 .00035 = P2
25.00000 = E1 27.00000 = E2

	ROLL ANGLES DRIVER	ROLL ANGLES DRIVEN	DEFLECTIONS DRIVER	DEFLECTIONS DRIVEN	TOTAL DEFLECTIONS	LOAD FORCE	MODIFICATIONS
1	19.68	26.60	1.943E-04	7.977E-04	8.970E-04	968.8	9.500E-04
2	15.58	26.29	1.640E-04	7.036E-04	8.676E-04	668.9	3.469E-04
3	16.98	25.87	1.881E-04	6.804E-04	8.685E-04	964.9	2.939E-04
4	17.38	25.50	1.976E-04	6.182E-04	8.158E-04	1313.8	1.908E-04
5	18.28	24.13	2.166E-04	5.770E-04	7.936E-04	1665.7	3.777E-05
6	19.18	24.77	2.372E-04	5.369E-04	7.740E-04	1902.2	0.
7	20.08	24.48	2.595E-04	5.175E-04	7.770E-04	2068.9	0.
8	20.08	24.48	2.595E-04	5.175E-04	7.770E-04	2795.7	0.
9	20.79	24.12	2.777E-04	5.182E-04	7.960E-04	2795.7	0.
10	21.96	23.84	2.970E-04	5.396E-04	7.366E-04	2795.7	0.
11	22.18	23.66	3.174E-04	5.116E-04	7.290E-04	2795.7	0.
12	22.84	23.27	3.388E-04	3.843E-04	7.231E-04	2795.7	0.
13	23.53	22.99	3.619E-04	3.577E-04	7.191E-04	2795.7	0.
14	24.22	22.71	3.858E-04	3.311E-04	7.169E-04	2795.7	0.
15	24.91	22.43	4.099E-04	3.067E-04	7.165E-04	2795.7	0.
16	25.60	22.16	4.358E-04	2.822E-04	7.180E-04	2795.7	0.
17	26.24	21.87	4.629E-04	2.589E-04	7.219E-04	2795.7	0.
18	26.24	21.87	4.629E-04	2.589E-04	7.219E-04	2326.9	0.
19	27.14	21.50	5.000E-04	2.285E-04	7.285E-04	2127.9	0.
20	28.04	21.13	5.391E-04	1.997E-04	7.387E-04	1830.9	5.017E-05
21	28.94	20.77	5.800E-04	1.720E-04	7.520E-04	1482.8	1.251E-04
22	29.84	20.48	6.229E-04	1.453E-04	7.681E-04	1130.1	2.081E-04
23	30.74	20.03	6.676E-04	1.195E-04	7.870E-04	893.6	2.750E-04
24	31.70	19.66	7.191E-04	9.951E-05	8.086E-04	786.0	3.500E-04

Figure H-3. Sample ground spur gear computer printout (cont'd)

FLASH TEMP SECTION

600.00 = HORSEPOWER
8000.00 = RPM DRIVER
2795.73 = PN
399.78 = TS,F
.5763 = PHEAV,B/SEC

NORMAL FORCE = LOAD FORCE

	ROLL ANGLES	LOAD FORCE	FRICTION	HERTZ STRESS	FLASH TEMP F	CTEMP	PHE
1	14.68	468.8	2.2379E-02	74593	18.22	413.00	3.313E-01
2	15.58	668.4	1.9895E-02	87056	18.50	413.29	3.762E-01
3	16.48	964.4	1.7596E-02	102921	18.63	413.41	4.221E-01
4	17.38	1313.0	1.6400E-02	117175	18.59	413.38	4.631E-01
5	18.28	1665.7	1.6400E-02	129622	18.45	413.23	4.959E-01
6	19.18	1902.2	1.6400E-02	136228	16.38	411.18	4.614E-01
7	20.08	2068.4	1.6400E-02	139891	13.27	408.05	3.879E-01
8	20.08	2795.7	1.6400E-02	162619	16.63	411.41	5.292E-01
9	20.77	2795.7	1.6400E-02	160825	12.75	407.53	4.063E-01
10	21.46	2795.7	1.6400E-02	159150	8.96	403.79	2.884E-01
11	22.15	2795.7	1.6400E-02	157585	5.24	400.03	1.704E-01
12	22.84	2795.7	1.6400E-02	156123	1.60	396.38	5.249E-02
13	23.53	2795.7	1.6400E-02	154755	1.98	396.76	6.495E-02
14	24.22	2795.7	1.6400E-02	153477	5.50	400.28	1.834E-01
15	24.91	2795.7	1.6400E-02	152284	8.96	403.79	3.013E-01
16	25.60	2795.7	1.6400E-02	151169	12.37	407.15	4.193E-01
17	26.29	2795.7	1.6400E-02	150129	15.73	410.62	5.372E-01
18	26.29	2326.4	1.6400E-02	136965	13.71	408.44	4.471E-01
19	27.19	2127.4	1.6400E-02	129869	16.34	411.13	5.259E-01
20	28.09	1830.4	1.6400E-02	119558	17.71	412.44	5.534E-01
21	28.99	1482.8	1.6400E-02	106842	17.73	412.51	5.298E-01
22	29.89	1130.1	1.6800E-02	92681	16.47	411.75	4.774E-01
23	30.79	893.6	1.8253E-02	81991	17.40	412.18	4.644E-01
24	31.70	726.8	1.9637E-02	73523	17.81	412.59	4.648E-01

DYNAMIC FACTOR BY TUPLIN METHOD

2.7235E+02 = DYNAMIC INCREMENT
9.0484E-01 = DYNAMIC FACTOR

Figure H-3. Sample ground spur gear computer printout (cont'd)

APPENDIX I
HELICAL GEAR COMPUTER PROGRAM

Program Goal

This program examines parallel-axis helical gears for scoring potential. The analysis follows a pair of teeth from the time that they come into contact until they disengage, examining the conditions in the gear mesh at many intervals (usually 16) during the mesh cycle.

At any interval, the instantaneous line of contact for which the mesh conditions are being examined is divided into several segments. The number of segments may range from two to seven, depending upon the relative length of the instantaneous line of contact. Each segment is then considered, for purposes of analysis, as a narrow spur gear in the normal plane. Loads, velocities, and radii of curvature are found for the center of this narrow spur gear, from which the instantaneous conjunction surface temperature is determined.

Operating parameters are calculated on the basis of static load. These parameters may then be corrected for dynamic loads by applying a dynamic factor, evaluated by a method suggested by Tuplin.[63]

Program Language and Computer Type

The program is written in FORTRAN IV language for a CDC 6000 Series computer, using RUN compiler and SCOPE 3.4 system.

Input Cards

There are nine data cards per set of data. Data sets may be stacked. The program contains a horsepower loop, so the effect on the gears of several equally spaced horsepower levels may be studied.

The program will handle either the pinion or the gear as the driving member. However, the data must be put onto the cards with the driver parameters in the "pinion" categories, regardless of which member is actually the driver.

A description of the cards follows. All units are in inches unless otherwise noted.

Use driver gear parameters for "pinion"

Use driven gear parameters for "gear"

Word	Column	Symbol	Description
Input Card 1	(PRELIMINARY INPUT DATA)		
1	1-10	BDP	Base diameter (pinion)
2	11-20	BDG	Base diameter (gear)
3	21-30	BP	Thermal constant (pinion), lb/°F-in.-$sec^{\frac{1}{2}}$
4	31-40	BG	Thermal constant (gear), lb/°F-in.-$sec^{\frac{1}{2}}$
5	41-50	CTP	Normal circular tooth thickness (pinion)
6	51-60	CTG	Normal circular tooth thickness (gear)
7	61-70	EP	Young's modulus (pinion)
8	71-80	EG	Young's modulus (gear)
Input Card 2			
1	1-10	FWP	Face width (pinion)
2	11-20	FWG	Face width (gear)
3	21-30	ODP	Outside diameter (pinion)
4	31-40	ODG	Outside diameter (gear)
5	41-50	PRP	Poisson's ratio (pinion)
6	51-60	PRG	Poisson's ratio (gear)
7	61-70	RNP	Number of teeth (pinion)
8	71-80	RNG	Number of teeth (gear)

Word	Column	Symbol	Description
Input Card 3			
1	1-10	WDP	Tooth height or whole depth (pinion)
2	11-20	WDG	Tooth height or whole depth (gear)
3	21-30	C	Center distance
4	31-40	CPN	Normal circular pitch
5	41-50	DPN	Normal diametral pitch
6	51-60	HA	Helix angle, deg.
7	61-70	PAN	Normal pressure angle, deg.
Input Card 4	(TEST CONDITIONS)		
1	1-10	RPMP	Rpm of pinion (driver)
2	11-20	TEMP	Oil jet temperature, °F
3	21-25	IT	Number of positions of the line of contact that will be studied, usually 16
Input Card 5	(FRICTION DATA)		
1	1-10	FR1	Friction factor from Eq. (55), (57), (59), or (61)
2	11-20	FR2	Friction factor from Eq. (54), (56), (58), or (60)
3	21-30	TCON	Temperature difference factor from Eq. (69)

Word	Column	Symbol	Description
Input Card 6		(HORSEPOWER LOOP)	
1	1-10	HP	Initial horsepower input
2	11-20	DHP	Horsepower increment. If only one power level is to be used, this must be zero
3	21-30	HPM	Maximum horsepower. If only one power level is to be used, this must be zero
Input Card 7		(METHOD CARD)	
1	1-10	METH	If only static conditions are to be obtained, leave blank; otherwise put a 1 in Col. 10 to calculate a dynamic factor
Input Card 8			If METH is blank, leave this card blank; otherwise:
1	1-10	AP	Thickness of pinion rim below the root. If pinion is solid, this dimension will be the height the pinion extends above the shaft surface.
2	11-20	AG	Thickness of gear rim below the root. If gear is solid, this dimension will be the height the gear extends above the shaft surface.
3	21-30	PEP	Pitch or spacing error (pinion)
4	31-40	PEG	Pitch or spacing error (gear)
5	41-50	PMI	Mass moment of inertia (pinion), $lb\text{-}sec^2\text{-}in.$
6	51-60	PMG	Mass moment of inertia (gear), $lb\text{-}sec^2\text{-}in.$
7	61-70	PMP	Tip profile modification (pinion)
8	71-80	PMG	Tip profile modification (gear)

Word	Column	Symbol	Description
Input Card 9			If METH is blank, leave this card blank. If values are unknown from other sources, leave card blank; otherwise:
1	1-10	RN(1)	Lowest natural frequency of gear system, rpm
2	11-20	RN(2)	Highest natural frequency of gear system, rpm
3	21-30	RN(3)	Natural frequency of teeth acting as a spring, rpm

A sample set of data cards for the helical gear design and operating conditions given in Chapter VIII, Section C, is shown in Figure I-1. The pinion was the driver in this example. The friction factors on Card 5 were determined for plain surfaces, Equations (107) and (108), with a composite surface roughness of 33 μin. AA. Card 6 shows that nine power levels were run, starting at 600 hp, and increasing by 100-hp increments, to a maximum of 1400 hp. Card 7 indicates that a dynamic factor was calculated. As a consequence, Card 8 contains data. No vibration analysis data were available, so Card 9 was left blank.

Computer Program

Figure I-2 shows the listing of the computer program. Control cards are not included.

Sample Printout

Figure I-3 gives the data printout for the input data of Figure I-1. Results are shown for 600 hp only.

The first page of the printout lists the input data for reference purposes. The second page gives some miscellaneous geometry parameters and a listing of the length of the simultaneous lines of contact as the gears pass through mesh; the last column of this list is the sum of all lines of contact at any one position. The next three pages give the details of the behavior in the gear mesh for a single power level. For each value of EFF (designated by f in Fig. 7, Chap. IV), data are displayed for that position of the line of contact. For

example, at EFF(3) = 0.150, the instantaneous line of contact has been divided into 4 segments. At the center of each segment, the roll angle, radii of curvature, sliding and sum velocities, friction, maximum Hertz stress, instantaneous surface temperature rise, instantaneous surface temperature, and instantaneous frictional power loss have been determined. The instantaneous surface temperature, for example, at the center of the first segment is 323.2°F, the maximum for that line of contact. At the bottom of the last page, the natural frequency of the tooth pairs as cantilever beams is given. This value should be well removed from the operating speed for satisfactory dynamic behavior. The dynamic increment and resulting dynamic factor are also given.

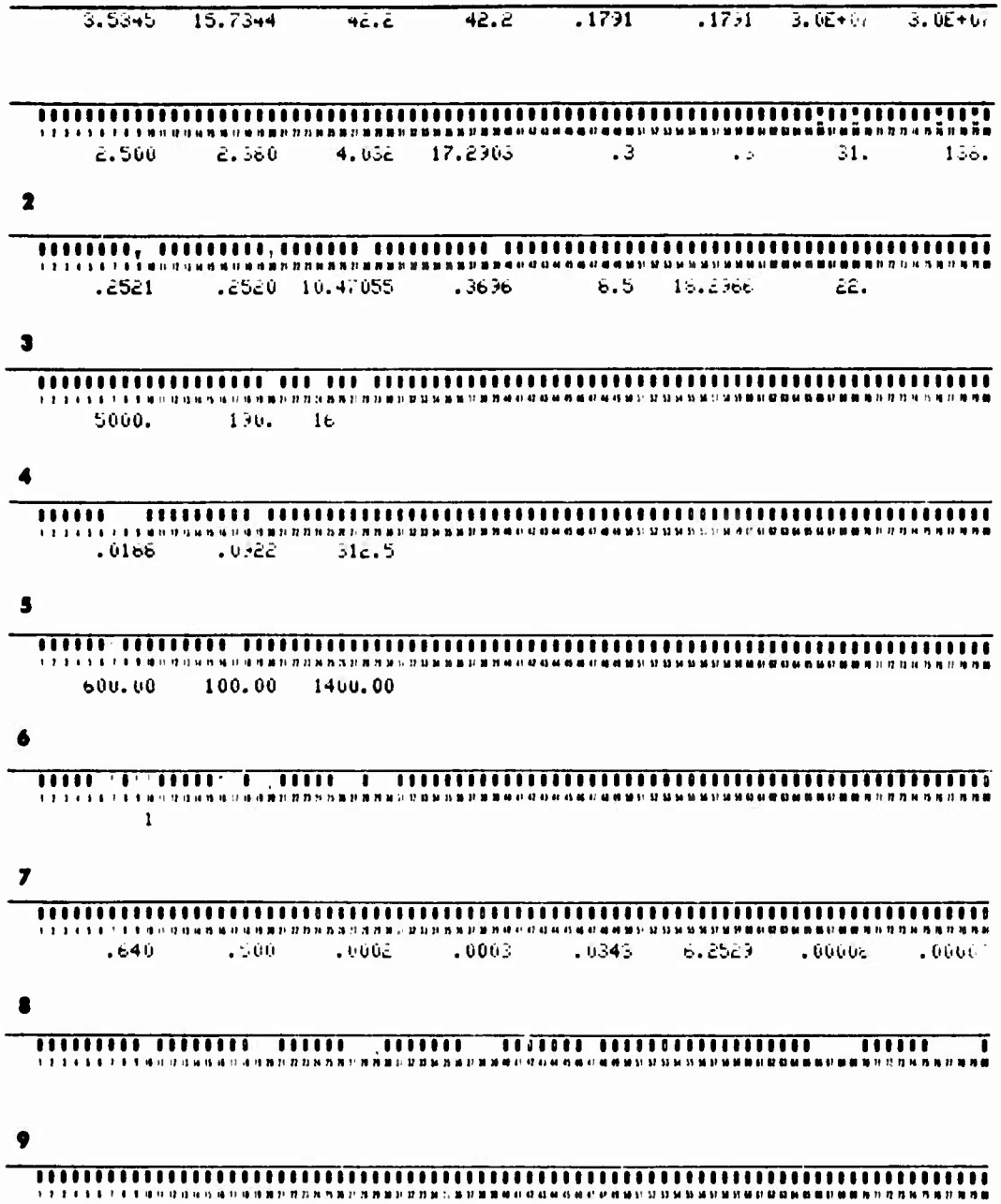

Figure I-1. Sample helical gear computer program data cards

```
      PROGRAM HELICAL (INPUT,OUTPUT,TAPE5=INPUT,TAPE6=OUTPUT)                  HELI0000*0001
      REAL MATFB                                                               HELI0010*0002
      DIMENSION ROLLRAY(11,19,16),XLRY(16),XLFNO(16,6),                        HELI0020*0003
     *          RN(3),METM(1)                                                  HELI0030*0004
      COMMON AG,AP,ADG,ADP,C,   CPN,CTG,CTP,EG,EP,FWB,FWP,GMI,HAR,HP,          HELI0040*0005
     1       IMT,IN,NOUT,ODB,PANR,PDG,PDP,PEG,PEP,PMB,PI,PMI,PMP,RNG,         HELI0050*0006
     2       PMPR,PRB,PRP,RNP,RPMP,VA,WDG,WDP,DFORCE,WN,MATFB                  HELI0060*0007
      DATA IB/4HGEAR/                                                          HELI0070*0008
      IN=5                                                                     HELI0080*0009
      NOUT=6                                                                   HELI0090*0010
      JHN=1                                                                    HELI0100*0011
      JRN=2                                                                    HELI0110*0012
      JRP=3                                                                    HELI0120*0013
      JRG=4                                                                    HELI0130*0014
      JVB=5                                                                    HELI0140*0015
      JVT=6                                                                    HELI0150*0016
      JFR=7                                                                    HELI0160*0017
      JHE=8                                                                    HELI0170*0018
      JDT=9                                                                    HELI0180*0019
      JTC=10                                                                   HELI0190*0020
      JPH=11                                                                   HELI0200*0021
      PI=3.1415926S                                                            HELI0210*0022
      RADIAN=PI/180.                                                           HELI0220*0023
C                                                                              HELI0230*0024
C                                                                              HELI0240*0025
C     DEFINITIONS OF INPUT VARIABLES FOR HELICAL GEAR (INCH UNITS)             HELI0250*0026
C      USE DRIVER VALUES FOR (PINION) ITEMS                                    HELI0260*0027
C      USE DRIVEN VALUES FOR (GEAR) ITEMS                                      HELI0270*0028
C                                                                              HELI0280*0029
C        BDP   =  BASE  DIAMETER (PINION)                                      HELI0290*0030
C        BDG   =  BASE  DIAMETER (GEAR)                                        HELI0300*0031
C        BP    =  THERMAL CONSTANT (PINION),LB,/SQRT(SEC,)IN,DEG,F             HELI0310*0032
C        BG    =  THERMAL CONSTANT (GEAR),LB,/SQRT(SEC,)IN,DEG,F               HELI0320*0033
C        CTP   =  NORMAL CIRCULAR TOOTH THICKNESS (PINION)                     HELI0330*0034
C        CTG   =  NORMAL CIRCULAR TOOTH THICKNESS (GEAR)                       HELI0340*0035
C        EP    =  YOUNGS MODULUS  (PINION)                                     HELI0350*0036
C        EG    =  YOUNGS MODULUS  (GEAR)                                       HELI0360*0037
C        FWP   =  FACE WIDTH (PINION)                                          HELI0370*0038
C        FWG   =  FACE WIDTH (GEAR)                                            HELI0380*0039
C        ODP   =  OUTSIDE DIAMETER (PINION)                                    HELI0390*0040
C        ODG   =  OUTSIDE DIAMETER (GEAR)                                      HELI0400*0041
C        PRP   =  POISSONS RATIO (PINION)                                      HELI0410*0042
C        PRG   =  POISSONS RATIO (GEAR)                                        HELI0420*0043
C        RNP   =  NUMBER OF PINION (DRIVER) TEETH                              HELI0430*0044
C        RNG   =  NUMBER OF GEAR TEETH                                         HELI0440*0045
C        WDP   =  HEIGHT OR WHOLE DEPTH (PINION)                               HELI0450*0046
C        WDG   =  HEIGHT OR WHOLE DEPTH (GEAR)                                 HELI0460*0047
C        C     =  CENTER DISTANCE                                              HELI0470*0048
C        CPN   =  NORMAL CIRCULAR PITCH                                        HELI0480*0049
C        DPN   =  DIAMETRAL PITCH, NORMAL                                      HELI0490*0050
C        HA    =  HELIX ANGLE,DEG,                                             HELI0500*0051
C        PAN   =  PRESSURE ANGLE, NORMAL,DEG,                                  HELI0510*0052
C        RPMP  =  DRIVER RPM                                                   HELI0520*0053
C        TEMP  =  OIL JET TEMPERATURE,DEG,F                                    HELI0530*0054
C        IT    =  INCREMENTS OF EFF (USUALLY 16)                               HELI0540*0055
C        FR1   =  CONSTANT FRICTION FACTOR                                     HELI0550*0056
C        FR2   =  VARIABLE FRICTION FACTOR                                     HELI0560*0057
C        TCON  =  TEMP, DIFFERENCE FACTOR                                      HELI0570*0058
C        HP    =  INITIAL POWER LEVEL, HP                                      HELI0580*0059
C        DHP   =  POWER INCREMENT                                              HELI0590*0060
C        MPH   =  UPPER LIMIT ON HORSEPOWER                                    HELI0600*0061
C        METH  =  USED IF DYNAMIC FACTOR REQ'D,                                HELI0610*0062
```

Figure I-2. Listing of helical gear computer program

```
C        AP    =  THICKNESS OF RIM BELOW ROOT (PINION)                    HELI0620*0063
C        AG    =  THICKNESS OF RIM BELOW ROOT (GEAR)                      HELI0630*0064
C        PEP   =  PITCH ERROR (PINION)                                    HELI0640*0065
C        PEG   =  PITCH ERROR (GEAR)                                      HELI0650*0066
C        PMI   =  MASS MOMENT OF INERTIA OF PINION,LB,SEC,SQ,-IN.         HELI0660*0067
C        GMI   =  MASS MOMENT OF INERTIA OF GEAR,LB,SEC,SQ,-IN.           HELI0670*0068
C        PMP   =  PROFILE MODIFICATION (PINION)                           HELI0680*0069
C        PMG   =  PROFILE MODIFICATION (GEAR)                             HELI0690*0070
C        RN(1) =  LOWEST SHAFT NAT. FREQ.,RPM                             HELI0700*0071
C        RN(2) =  HIGHEST SHAFT NAT. FREQ.,RPM                            HELI0710*0072
C        RN(3) =  TOOTH SPRING NAT. FREQ.,RPM                             HELI0720*0073
C                                                                         HELI0730*0074
C     DEFINITIONS OF PRELIMINARY CALCULATED VARIABLES FOR HELICAL GEAR    HELI0740*0075
C                                                                         HELI0750*0076
C        ADP   =  ADDENDUM (PINION)                                       HELI0760*0077
C        ADG   =  ADDENDUM (GEAR)                                         HELI0770*0078
C        PDP   =  PITCH DIAMETER (PINION)                                 HELI0780*0079
C        PDG   =  PITCH DIAMETER (GEAR)                                   HELI0790*0080
C        ZA    =  PATH OF CONTACT IN APPROACH                             HELI0800*0081
C        VO    =  DISTANCE FROM FIRST INTERFERENCE POINT TO PITCH POINT   HELI0810*0082
C        VA    =  DISTANCE FROM FIRST INTERFERENCE TO START OF CONTACT    HELI0820*0083
C        WA    =  DISTANCE FROM SECOND INTERFERENCE TO START OF CONTACT   HELI0830*0084
C        PHA   =  BASE HELIX ANGLE                                        HELI0840*0085
C        ZR    =  PATH OF CONTACT IN RECESS                               HELI0850*0086
C        Z     =  PATH OF CONTACT                                         HELI0860*0087
C        BPN   =  NORMAL BASE PITCH                                       HELI0870*0088
C        BPT   =  TRANSVERSE BASE PITCH                                   HELI0880*0089
C        ZD    =  DISTANCE FROM PITCH POINT TO LPSTC                      HELI0890*0090
C        ZC    =  DISTANCE FROM PITCH POINT TO HPSTC                      HELI0900*0091
C        ER    =  REDUCED MODULUS                                         HELI0910*0092
C        FMP   =  FACE CONTACT RATIO                                      HELI0920*0093
C        TMP   =  TRANSVERSE CONTACT RATIO                                HELI0930*0094
C        RHOP  =  RADIUS  OF CURVATURE AT CONTACT (PINION)                HELI0940*0095
C        RHOG  =  RADIUS  OF CURVATURE AT CONTACT (GEAR)                  HELI0950*0096
C        RHOE  =  EFFECTIVE RADIUS  OF CURVATURE                          HELI0960*0097
C        RANGLP=  PINION ROLL ANGLE                                       HELI0970*0098
C        RANGPL=  PINION ROLL ANGLE TO LPSTC                              HELI0980*0099
C        RANGPH=  PINION ROLL ANGLE TO HPSTC                              HELI0990*0100
C        W(N)  =  INCREMENT OF DISPLACEMENT ALONG Z                       HELI1000*0101
C                                                                         HELI1010*0102
C     READ INPUT VARIABLES FOR HELICAL GEAR                               HELI1020*0103
C                                                                         HELI1030*0104
    1 READ (IN,1001) BDP,BDG,BP,BG,CTP,CTG,EP,EG,                        HELI1040*0105
     *                FWP,FWG,ODP,ODG,PRP,PRG,RNP,RNG,                   HELI1050*0106
     *                WDP,WDG,C,CPN,DPN,HA,PAN,                          HELI1060*0107
     *                RPMP,TEMP,IT,                                      HELI1070*0108
     *                FR1,FR2,TCON                                       HELI1080*0109
 1001 FORMAT (6F10.5,2E10.1/8F10.5/7F10.5/2F10.2,I5/8F10.4,F10.1)        HELI1090*0110
      IF (EOF,IN) 220,2                                                  HELI1100*0111
    2 READ (IN,1002) NP,DNP,NPM                                          HELI1110*0112
 1002 FORMAT (3F10.2)                                                    HELI1120*0113
      READ (IN,1003) METH                                                HELI1130*0114
 1003 FORMAT (I10)                                                       HELI1140*0115
      IF (METH.NE.1) GO TO 3                                             HELI1150*0116
      READ (IN,1004) AP,AG,PEP,PEG,PMI,GMI,PMP,PMG,RN(1),RN(2),RN(3)     HELI1160*0117
 1004 FORMAT (8F10.5/3F10.2)                                             HELI1170*0118
    3 WRITE (NOUT,1000)                                                  HELI1180*0119
      WRITE (NOUT,1005) BDP,BDG,BP,BG,CTP,CTG,EP,EG,                     HELI1190*0120
     *                FWP,FWG,ODP,ODG,PRP,PRG,RNP,RNG                    HELI1200*0121
 1005 FORMAT (35X,29HVALUES AND DEFINITIONS OF PRIMARY INPUT VARIABLES/  HELI1210*0122
     *,26H (INCH UNITS UNLESS NOTED)/                                    HELI1220*0123
     * 2X,16H   (DRIVER)      ,6X,19H      (DRIVEN)                     HELI1230*0124
```

Figure I-2. Listing of helical gear computer program (cont'd)

```
     */11H BDP      = ,F10.5,5X,10HBDG      = ,F10.6,5X,                    HELI1240-0125
     *    60H=BASE CIRCLE DIAMETER                                          HELI1250-0126
     */11H BP       = ,F10.5,5X,10HBG       = ,F10.5,5X,                    HELI1260-0127
     *    60H=THERMAL CONSTANT (LB./SQRT(SEC.))IN.DEG.F)                    HELI1270-0128
     */11H CTP      = ,F10.5,5X,10HCTG      = ,F10.5,5X,                    HELI1280-0129
     *    60H=NORMAL CIRCLE TOOTH THICKNESS                                 HELI1290-0130
     */11H EP       = ,E10.0,5X,10HEG       = ,E10.0,5X,                    HELI1300-0131
     *    60H=YOUNG'S MODULUS, PSI.                                         HELI1310-0132
     */11H FWP      = ,F10.5,5X,10HFWG      = ,F10.5,5X,                    HELI1320-0133
     *    60H=FACE WIDTH                                                    HELI1330-0134
     */11H ODP      = ,F10.5,5X,10HODG      = ,F10.5,5X,                    HELI1340-0135
     *    60H=OUTSIDE DIAMETER                                              HELI1350-0136
     */11H PRP      = ,F10.5,5X,10HPRG      = ,F10.5,5X,                    HELI1360-0137
     *    60H=POISSON'S RATIO                                               HELI1370-0138
     */11H RNP      = ,F10.5,5X,10HRNG      = ,F10.6,5X,                    HELI1380-0139
     *    60H=NUMBER OF TEETH                                               HELI1390-0140
     *)                                                                     HELI1400-0141
      WRITE (NOUT,1006) WDP,WDG,C,CPN,DPN,HA,PAN,RPMP,TEMP,IT,              HELI1410-0142
     *                  FR1,FR2,TCON                                        HELI1420-0143
1006 FORMAT (                                                               HELI1430-0144
     * 11H WDP      = ,F10.5,5X,10HWDG      = ,F10.5,5X,                    HELI1440-0145
     *    60H=HEIGHT OR WHOLE DEPTH                                         HELI1450-0146
     */11H C        = ,F10.6,30X, 36H=CENTER DISTANCE                      HELI1460-0147
     */11H CPN      = ,F10.5,30X, 36H=NORMAL CIRCLE PITCH                  HELI1470-0148
     */11H DPN      = ,F10.6,30X, 36H=DIAMTERAL PITCH                      HELI1480-0149
     */11H HA       = ,F10.5,30X, 36H=HELIX ANGLE (DEG.)                   HELI1490-0150
     */11H PAN      = ,F10.5,30X, 36H=PRESSURE ANGLE (DEG.)                HELI1500-0151
     */11H RPMP     = ,F10.2,30X, 36H=RPM DRIVER                           HELI1510-0152
     */11H TEMP     = ,F10.2,30X, 36H=OIL JET TEMPERATURE (DEG.F)          HELI1520-0153
     */11H IT       = ,I10,  30X,36H=INCREMENTS OF EFF                     HELI1530-0154
     */11H FR1      = ,F10.4,30X,36H=CONSTANT FRICTION FACTOR              HELI1540-0155
     */11H FR2      = ,F10.4,30X,36H=VARIABLE FRICTION FACTOR              HELI1550-0156
     */11H TCON     = ,F10.1,30X,36H=TEMP DIFFERENCE FACTOR                HELI1560-0157
     *)                                                                     HELI1570-0158
      WRITE (NOUT,1007) HP,DHP,HPM                                          HELI1580-0159
1007 FORMAT (//36H INPUT VARIABLES FOR HORSEPOWER LOOP/                     HELI1590-0160
     * 11H HP       = ,F10.3,30X, 36H=INITIAL HORSEPOWER                   HELI1600-0161
     */11H DHP      = ,F10.3,30X, 36H=HORSEPOWER INCREMENT                 HELI1610-0162
     */11H HPM      = ,F10.3,30X, 36H=MAXIMUM HORSEPOWER                   HELI1620-0163
     *)                                                                     HELI1630-0164
      WRITE (NOUT,1008)                                                     HELI1640-0165
1008 FORMAT (//42H METHOD USED FOR CALCULATING NORMAL FORCE=)               HELI1650-0166
      I=1                                                                   HELI1660-0167
      WRITE (NOUT,1009) I                                                   HELI1670-0168
1009 FORMAT (1X,I2,26H NORMAL FORCE=STATIC FORCE)                           HELI1680-0169
      I=2                                                                   HELI1690-0170
    6 IF (METH.NE.1) GO TO 20                                               HELI1700-0171
      WRITE (NOUT,1010) I                                                   HELI1710-0172
1010 FORMAT (1X,I2,43H DYNAMIC FACTOR CALCULATED BY TUPLIN METHOD)          HELI1720-0173
      WRITE (NOUT,1012) AP,AG,PEP,PEG,PMI,GMI,PMP,PMG,RN(1),RN(2),RN(3)     HELI1730-0174
1012 FORMAT (//47H INPUT VARIABLES FOR DYNAMIC FORCE CALCULATIONS/          HELI1740-0175
     * 2X,16H    (DRIVER)     ,6X,14H      (DRIVEN)                       HELI1750-0176
     */11H AP       = ,F10.5,5X,10HAG       = ,F10.5,5X,                    HELI1760-0177
     *    60H=THICKNESS OF RIM BELOW ROOT                                   HELI1770-0178
     */11H PEP      = ,F10.5,5X,10HPEG      = ,F10.6,5X, 13H=PITCH ERROR    HELI1780-0179
     */11H PMI      = ,F10.5,5X,10HGMI      = ,F10.5,5X,                    HELI1790-0180
     *    60H=MASS MOMENT OF INERTIA (LB.SEC.SQ.IN.)                        HELI1800-0181
     */11H PMP      = ,F10.5,5X,10HPMG      = ,F10.5,5X,                    HELI1810-0182
     *    60H=PROFILE MODIFICATION                                          HELI1820-0183
     */11H RN(1)    = ,F10.2,30X, 36H=1ST NATURAL FREQUENCY (RPM)          HELI1830-0184
     */11H RN(2)    = ,F10.2,30X, 36H=2ND NATURAL FREQUENCY (RPM)          HELI1840-0185
     */11H RN(3)    = ,F10.2,30X, 36H=3RD NATURAL FREQUENCY (RPM)          HELI1850-0186
```

Figure I-2. Listing of helical gear computer program (cont'd)

```
     *)                                                                 HELI1860*0187
C                                                                       HELI1870*0188
C        PRELIMINARY CALCULATIONS FOR HELICAL GEAR TEST.                HELI1880*0189
C                                                                       HELI1890*0190
   20 FW=AMIN1(FNP,FNG)                                                 HELI1900*0191
      PANR=PAN*RADIAN                                                   HELI1910*0192
      HAR=HA*RADIAN                                                     HELI1920*0193
      PDP=2.*(C/(1.+RNG/RNP))                                           HELI1930*0194
      PDG=2.*C-PDP                                                      HELI1940*0195
      ADP=(ODP-PDP)/2.                                                  HELI1950*0196
      ADG=(ODG-PDG)/2.                                                  HELI1960*0197
      ZA = (SQRT((ODG*ODG)-(BDG*BDG))-SQRT((PDG*PDG)-(BDG*BDG))) / 2.   HELI1970*0198
      VO = SQRT((PDP*PDP)-(BDP*BDP)) / 2.                               HELI1980*0199
      VA = VO-ZA                                                        HELI1990*0200
      HA = (SQRT(ODG*ODG-(BDG*BDG)))/2.                                 HELI2000*0201
      BHAR= ASIN(SIN(HAR)*COS(PANR))                                    HELI2010*0202
      ZR = (SQRT((ODP*ODP)-(BDP*BDP))-SQRT((PDP*PDP)-(BDP*BDP))) / 2.   HELI2020*0203
      Z  = ZA+ZR                                                        HELI2030*0204
      BPN = CPN * COS(PANR)                                             HELI2040*0205
      BPT = PI*BDP/RNP                                                  HELI2050*0206
      ZD = BPT-ZR                                                       HELI2060*0207
      ZC = BPT-ZA                                                       HELI2070*0208
      ER = 1. / (((1.-(PRP*PRP))/EP+((1.-(PRG*PRG))/EG))*2.)           HELI2080*0209
      WRITE (NOUT,1000)                                                 HELI2090*0210
      WRITE (NOUT,1013) ADP,ADG,PDP,PDG,BHAR,BPN,BPT,ER                 HELI2100*0211
 1013 FORMAT (//35X,*9HVALUES AND DEFINITIONS OF PRELIMINARY CALCULATED HELI2110*0212
     *,10HVARIABLES  /                                                  HELI2120*0213
     * 1X,26H(INCH UNITS UNLESS NOTED) /                                HELI2130*0214
     * 2X,16H   (DRIVER)      ,6X,14H      (DRIVEN)                    HELI2140*0215
     */11H ADP      = ,F10.5,5X,10HADG      = ,F10.5,5X,                HELI2150*0216
     *   60H=ADDENDUM (IN.)                                             HELI2160*0217
     */11H PDP      = ,F10.5,5X,10HPDG      = ,F10.5,5X,                HELI2170*0218
     *   60H=PITCH DIAMETER                                             HELI2180*0219
     */11H BHAR     = ,F10.6,30X, 36H=BASE HELIX ANGLE (RADIANS)       HELI2190*0220
     */11H BPN      = ,F10.6,30X, 36H=NORMAL BASE PITCH                HELI2200*0221
     */11H BPT      = ,F10.6,30X, 36H=TRANSVERSE BASE PITCH            HELI2210*0222
     */11H ER       = ,F10.3,30X, 35H=REDUCED MODULUS (PSI)           )HELI2220*0223
      WRITE (NOUT,1014) VA,HA,Z,ZA,ZC,ZD,ZR                             HELI2230*0224
 1014 FORMAT (                                                          HELI2240*0225
     * 11H VA       = ,F10.6,30X, 59H=DISTANCE FROM FIRST INTERFERENCE POHELI2250*0226
     *INT TO START OF CONTACT                                          HELI2260*0227
     */11H HA       = ,F10.6,30X, 60H=DISTANCE FROM SECOND INTERFERENCE PHELI2270*0228
     *OINT TO START OF CONTACT                                         HELI2280*0229
     */11H Z        = ,F10.5,30X, 36H=PATH OF CONTACT                  HELI2290*0230
     */11H ZA       = ,F10.5,30X, 36H=PATH OF CONTACT IN APPROACH      HELI2300*0231
     */11H ZC       = ,F10.5,30X, 36H=DISTANCE FROM PITCH POINT TO HPSTC HELI2310*0232
     */11H ZD       = ,F10.5,30X, 36H=DISTANCE FROM PITCH POINT TO LPSTC HELI2320*0233
     */11H ZR       = ,F10.5,30X, 30H=PATH OF CONTACT IN RECESS       )HELI2330*0234
      WRITE (NOUT,9090)                                                 HELI2340*0235
 9090 FORMAT (///////1X,*9HCALCULATIONS OF XL FOR EACH VALUE OF EFF//)  HELI2350*0236
      ICASE=1                                                           HELI2360*0237
      RANGPL = (VO-ZD)/(BDP/2.)/RADIAN                                  HELI2370*0238
      RANGPH = (VO+ZC)/(BDP/2.)/RADIAN                                  HELI2380*0239
      FMP = FW * TAN(HAR)/(CPN/COS(HAR))                                HELI2390*0240
      TMP = Z/(BPN/COS(HAR))                                            HELI2400*0241
      FSIN = FW*SIN(BHAR)                                               HELI2410*0242
      FCOS = FW * COS(BHAR)                                             HELI2420*0243
      ZCOS = Z *COS(BHAR)                                               HELI2430*0244
      IF (Z.LT.FSIN) ICASE=ICASE+1                                      HELI2440*0245
C                                                                       HELI2450*0246
C        DEFINITIONS FOR T LOOP VARIABLES                               HELI2460*0247
C        EFF    =  INDEPENDENT VARIABLE                                 HELI2470*0248
```

Figure I-2. Listing of helical gear computer program (cont'd)

```
C                (EFF WILL BE INCREMENTED BY DEF AND T   IT    TIMES    HELI2480*0249
C                 WHERE T=0...(IT-1))                                    HELI2490*0250
C       XLRY  =  ARRAY THAT STORES VALUES OF XL                          HELI2500*0251
C       BETA  =  INCREMENT OF BPN                                        HELI2510*0252
C       BINC  =  POSITIVE AND NEGATIVE INCREMENT OF BETA                 HELI2520*0253
C       XBETA =  UPPER AND LOWER LIMITS OF BETA                          HELI2530*0254
C                                                                        HELI2540*0255
C       TEST FOR THE NO. OF INCREMENTS OF BPN                            HELI2550*0256
C                                                                        HELI2560*0257
      BETA=0.                                                            HELI2570*0258
      TEST=0.                                                            HELI2580*0259
   30 BETA=BETA+1.                                                       HELI2590*0260
      TEST=0.+BETA*BPN                                                   HELI2600*0261
      IF (TEST.GT.(ZCOS+FSIN)) GO TO 35                                  HELI2610*0262
      GO TO 30                                                           HELI2620*0263
   35 XBETA=BETA-1.                                                      HELI2630*0264
      DEF = (ZCOS+FSIN)/(IT-1)                                           HELI2640*0265
C                                                                        HELI2650*0266
C     START T LOOP                                                       HELI2660*0267
      DO 130 L=1,IT                                                      HELI2670*0268
      LXL=0                                                              HELI2680*0269
      BETA=0.                                                            HELI2690*0270
      BINC=1.                                                            HELI2700*0271
C                                                                        HELI2710*0272
C     A, CHOOSE F                                                        HELI2720*0273
C                                                                        HELI2730*0274
      TL=L                                                               HELI2740*0275
      T=TL-1.                                                            HELI2750*0276
      EFF=DEF*T                                                          HELI2760*0277
   45 GO TO (50,55) ICASE                                                HELI2770*0278
C                                                                        HELI2780*0279
C     B, (CASE I)                                                        HELI2790*0280
C                                                                        HELI2800*0281
   50 A0=0.                                                              HELI2810*0282
      A1=FSIN                                                            HELI2820*0283
      A2=ZCOS                                                            HELI2830*0284
      A1A2=A1+A2                                                         HELI2840*0285
      GO TO 60                                                           HELI2850*0286
C                                                                        HELI2860*0287
C     B, (CASE II)                                                       HELI2870*0288
C                                                                        HELI2880*0289
   55 A0=0.                                                              HELI2890*0290
      A1=ZCOS                                                            HELI2900*0291
      A2=FSIN                                                            HELI2910*0292
      A1A2=A1+A2                                                         HELI2920*0293
   60 IF (EFF.GT.A0.AND.EFF.LT.A1A2) GO TO 62                            HELI2930*0294
      XL=0.                                                              HELI2940*0295
      GO TO 70                                                           HELI2950*0296
   62 IF (EFF.GT.A1) GO TO 64                                            HELI2960*0297
      XL = EFF*((1./TAN(BHAR))+TAN(BHAR))                                HELI2970*0298
      GO TO 70                                                           HELI2980*0299
   64 IF (EFF.GT.A2.OR.EFF.EQ.A2) GO TO 66                               HELI2990*0300
      IF (ICASE.EQ.2) GO TO 65                                           HELI3000*0301
      XL = FW * (COS(BHAR)+(SIN(BHAR)*TAN(BHAR)))                        HELI3010*0302
      GO TO 70                                                           HELI3020*0303
   65 XL = Z*(SIN(BHAR)+(COS(BHAR)*(1./TAN(BHAR))))                      HELI3030*0304
      GO TO 70                                                           HELI3040*0305
   66 XL = FW * (COS(BHAR)+SIN(BHAR)*TAN(BHAR))+(Z*(SIN(BHAR)+COS(BHAR)) HELI3050*0306
     1        *(1./TAN(BHAR))))-(EFF*(TAN(BHAR)+(1./TAN(BHAR))))        HELI3060*0307
C                                                                        HELI3070*0308
C     C, STORE VALUE OF XL                                               HELI3080*0309
C                                                                        HELI3090*0310
```

Figure I-2. Listing of helical gear computer program (cont'd)

```
   70 LXL=LXL+1                                                          HELI3100+0311
      XLRY(LXL) =XL                                                      HELI3110+0312
      IF (BETA.NE.0.) GO TO 105                                          HELI3120+0313
C                                                                        HELI3130+0314
C     D. EVALUATE XL AGAINST...          AND CHOOSE APPROPRIATE K        HELI3140+0315
C                                        K MUST BE AN EVEN NO.           HELI3150+0316
C                                                                        HELI3160+0317
      KKK=2                                                              HELI3170+0318
      K=8                                                                HELI3180+0319
      KK=12                                                              HELI3190+0320
      IF (XL.LT.(FW/5.)) K=KKK                                           HELI3200+0321
      IF (XL.GT.(FW/2.)) K=KK                                            HELI3210+0322
C                                                                        HELI3220+0323
C     E. CALCULATE HO,H,H(N)                                             HELI3230+0324
C                                                                        HELI3240+0325
   80 HO = (EFF-FW*SIN(BHAR))/COS(BHAR)                                  HELI3250+0326
      IF (HO.LT.0.) HO=0.                                                HELI3260+0327
      H =EFF/COS(BHAR)                                                   HELI3270+0328
      IF (H.GT.Z) H=Z                                                    HELI3280+0329
      K2=K/2                                                             HELI3290+0330
      DO 90 N=1,K2                                                       HELI3300+0331
      NN=N-1                                                             HELI3310+0332
      HN = HO+((H-HO)/K)*(2*NN+1)                                        HELI3320+0333
C                                                                        HELI3330+0334
C     F. CALCULATE FOR EACH VALUE OF H(N)....                            HELI3340+0335
C                                                                        HELI3350+0336
      RANGLP = (VA+HN)/(BDP/2.)                                          HELI3360+0337
      RHOP = (1./COS(BHAR))*(VA+HN)                                      HELI3370+0338
      RHOG = (1./COS(BHAR))*(RA-HN)                                      HELI3380+0339
      VP = RHOP*RPMP*(PI/30.)                                            HELI3390+0340
      VG = RHOG*RPMP*(RNP/RNG)*(PI/30.)                                  HELI3400+0341
      VS=ABS(VP-VG)                                                      HELI3410+0342
      VT=VP+VG                                                           HELI3420+0343
C                                                                        HELI3430+0344
C     G. STORE                                                           HELI3440+0345
C                                                                        HELI3450+0346
      ROLLRAY(N,JHN,L) = HN                                              HELI3460+0347
      ROLLRAY(N,JRN,L) = RANGLP/RADIAN                                   HELI3470+0348
      ROLLRAY(N,JRP,L) = RHOP                                            HELI3480+0349
      ROLLRAY(N,JRG,L) = RHOG                                            HELI3490+0350
      ROLLRAY(N,JVS,L) = VS                                              HELI3500+0351
      ROLLRAY(N,JVT,L) = VT                                              HELI3510+0352
   90 CONTINUE                                                           HELI3520+0353
      XLFNO(L,1)=K2                                                      HELI3530+0354
      XLFNO(L,2)=EFF                                                     HELI3540+0355
      XLFNO(L,3)=XL                                                      HELI3550+0356
C                                                                        HELI3560+0357
C     H. CALCULATE A NEW EFF                                             HELI3570+0358
C                                                                        HELI3580+0359
  105 IF (XBETA.EQ.BETA) GO TO 107                                       HELI3590+0360
  106 BETA=BETA+BINC                                                     HELI3600+0361
      EFF = XLFNO(L,2)+BETA*BPN                                          HELI3610+0362
      GO TO 60                                                           HELI3620+0363
  107 IF (XBETA.LT.0.) GO TO 110                                         HELI3630+0364
      BINC=-BINC                                                         HELI3640+0365
      BETA=0.                                                            HELI3650+0366
      XBETA=-XBETA                                                       HELI3660+0367
      GO TO 106                                                          HELI3670+0368
C                                                                        HELI3680+0369
C     I. TOTAL ALL XLS                                                   HELI3690+0370
C                                                                        HELI3700+0371
  110 XBETA=ABS(XBETA)                                                   HELI3710+0372
```

Figure I-2. Listing of helical gear computer program (cont'd)

```
      XLT=0.                                                            HELI3720.0373
      IF (LXL.NE.1) GO TO 111                                           HELI3730.0374
      XLT=XLRAY(LXL)                                                    HELI3740.0375
      GO TO 118                                                         HELI3750.0376
  111 DO 115 I=1,LXL                                                    HELI3760.0377
      XLT=XLT+XLRAY(I)                                                  HELI3770.0378
  115 CONTINUE                                                          HELI3780.0379
      WRITE (NOUT,9091) (XLRAY(I),I=1,LXL),XLT                          HELI3790.0380
 9091 FORMAT (16(2X,F6.3))                                              HELI3800.0381
C                                                                       HELI3810.0382
C     J. STORE XLTOT                                                    HELI3820.0383
C                                                                       HELI3830.0384
  118 XLFNO(L,3)=XLT                                                    HELI3840.0385
  130 CONTINUE                                                          HELI3850.0386
C                                                                       HELI3860.0387
C     START HP LOOP                                                     HELI3870.0388
C                                                                       HELI3880.0389
  135 HT = 126000.*HP/(RPMP*PDP)                                        HELI3890.0390
      WN = HT/(COS(HAR)*COS(PANR))                                      HELI3900.0391
      IHT=1                                                             HELI3910.0392
      DFORCE=WN                                                         HELI3920.0393
      GO TO 145                                                         HELI3930.0394
  138 I...METH.NE.1) GO TO 200                                          HELI3940.0395
      I...=2                                                            HELI3950.0396
      NATFO=RN(3)                                                       HELI3960.0397
      CALL FORCE                                                        HELI3970.0398
      GO TO 200                                                         HELI3980.0399
  145 CALL SHFR (JRP,JRG,JVS,JFR,JPH,XLFNO,ROLLRAY,ER,IT,DFORCE,        HELI3990.0400
     *      RNP,Z,BDP,PI, FR1,FR2,YCON,TEMP,TS,PHEAV,FRIC)             HELI4000.0401
      DO 160 L=1,IT                                                     HELI4010.0402
      XL=XLFNO(L,4)                                                     HELI4020.0403
      K2=XLFNO(L,1)                                                     HELI4030.0404
      K=2*K2                                                            HELI4040.0405
      XLTOT=XLFNO(L,3)                                                  HELI4050.0406
  166 DO 150 N=1,K2                                                     HELI4060.0407
      RHOP=ROLLRAY(N,JRP,L)                                             HELI4070.0408
      RHOG=ROLLRAY(N,JRG,L)                                             HELI4080.0409
      RHOE = 488(RHOP*RHOG/(RHOP+RHOG))                                 HELI4090.0410
      VS=ROLLRAY(N,JVS,L)                                               HELI4100.0411
      VT=ROLLRAY(N,JVT,L)                                               HELI4110.0412
      FRIC  = ROLLRAY(N,JFR,L)                                          HELI4120.0413
      IF (XLTOT.GT.0.) GO TO 167                                        HELI4130.0414
      WRITE (NOUT,9999) XLTOT                                           HELI4140.0415
 9999 FORMAT (9H XLTOT = ,E13.4)                                        HELI4150.0416
      ROLLRAY(N,JDT,L) = 9.                                             HELI4160.0417
      GO TO 150                                                         HELI4170.0418
  167 IF(DFORCE.GT.0.) GO TO 168                                        HELI4180.0419
      WRITE (NOUT,8888) DFORCE                                          HELI4190.0420
 8888 FORMAT (9H DFORCE = ,E13.4)                                       HELI4200.0421
      ROLLRAY(N,JDT,L) = 8.                                             HELI4210.0422
      GO TO 150                                                         HELI4220.0423
  168 CONTINUE                                                          HELI4230.0424
      IF(L.EQ.1.OR.L.EQ.IT) GO TO 165                                   HELI4240.0425
      DT = .201 * (FRIC*((DFORCE/XLTOT)**(3./4.))*(ER**(1./4.))/        HELI4250.0426
     1       (RHOE**(1./4.)) ) *(ABS(RHOP -(RNP/RNG*RHOG))*SQRT(RPMP)/  HELI4260.0427
     2       (RP*SQRT(RHOP)+(RG*SQRT(RNP/RNG*RHOG))))*(COS(PHAR)/       HELI4270.0428
     3       SQRT(COS(HAR)))                                            HELI4280.0429
      GO TO 169                                                         HELI4290.0430
  165 DT=0.                                                             HELI4300.0431
  169 CTEMP=TS+DT                                                       HELI4310.0432
      HERTZ = .3989*SQRT((DFORCE*XL)/(K/2*XLTOT)*(ER/RHOE))             HELI4320.0433
      ROLLRAY(N,JDT,L) = DT                                             HELI4330.0434
```

Figure I-2. Listing of helical gear computer program (cont'd)

```
      ROLLRAY(N,JTC,L)=CTEMP                                                    HELI0340
      ROLLRAY(N,JHE,L)=HERTZ                                                    HELI0350
  150 CONTINUE                                                                  HELI0360
  160 CONTINUE                                                                  HELI0370
C                                                                               HELI0380
C     START PRINTING LOOP                                                       HELI0390
C                                                                               HELI0400
      K2T=63                                                                    HELI0410
  170 DO 190 L=1,IT                                                             HELI0420
      K2=XLFNO(L,1)                                                             HELI0430
      K2T=K2T+K2+5                                                              HELI0440
      IF (K2T.LT.58) GO TO 179                                                  HELI0450
      WRITE (NOUT,1021) HP,FMP,RANGPL,TB,RPMP,TMP,RANGPM,PHEAV,WN               HELI0460
      K2T=K2+5                                                                  HELI0470
  179 WRITE (NOUT,1015)  L,(XLFNO(L,J),J=2,3),XLFNO(L,5)                        HELI0480
      DO 180 N=1,K2                                                             HELI0490
      WRITE (NOUT,1017) N,(ROLLRAY(N,J,L),J=1,11)                               HELI0500
  180 CONTINUE                                                                  HELI0510
  190 CONTINUE                                                                  HELI0520
  199 GO TO (138,200) IMT                                                       HELI0530
  200 HP=HP+DHP                                                                 HELI0540
      IF (HP.LE.HPM) GO TO 135                                                  HELI0550
      GO TO 1                                                                   HELI0560
 1000 FORMAT (1H1)                                                              HELI0570
 1015 FORMAT (///5X,9HEFF(,I2,9H) = ,F6.3,7X,7HLTOT = ,F8.4,5X,                 HELI0580
     1   20HNORMAL TOOTH LOAD = ,F12.2/7X,9HM(N),3X,6HRANGLP,3X,9HRMOP,         HELI0590
     2   9X,9HRMOG,3X,7HVB(IPB),2X,7HVT(IPB),3X,9HFRIC,9X,9HMERTZ(MX),          HELI0600
     3   9X,5HOT(F),2X,5HCTEMP,2X,10HPHE(B/SEC))                                HELI0610
 1017 FORMAT (2X,I2,2X,F5.3,3(3X,F5.2),2X,F7.2,2X,F8.2,1X,F6.4,3X,F8.1,         HELI0620
     12(3X,F5.1),3X,F6.4,4X,F6.2)                                               HELI0630
 1021 FORMAT (1H1,13HMORSEPOWER = ,F8.2,5X,6HFMP = ,F8.3,5X,                    HELI0640
     * 9HRANGPL = ,F5.2,8X,11HTB,DEG F = ,F5.1/14H RPM DRIVER = ,F8.2,         HELI0650
     * 5X,6HTMP = ,F8.3,5X,9HRANGPM = ,F5.2,5X,14HPHEAV,B/SEC = ,F7.4/         HELI0660
     * 14H WN,LB.     = ,F8.2)                                                 HELI0670
  220 CONTINUE                                                                  HELI0680
      END                                                                       HELI0690
      SUBROUTINE SBFR (JRP,JRG,JVB,JFR,JPM,XLFNO,ROLLRAY,ER,IT,DFORCE,          SBFR0000
     *      RMP,Z,BDP,PI, FR1,FR2,TCON,TEMP,TB,PHEAV,FRIC)                      SBFR0010
      DIMENSION ROLLRAY(11,14,16),XLFNO(16,5)                                   SBFR0020
      DO 20 L=1,IT                                                              SBFR0030
      K2=XLFNO(L,1)                                                             SBFR0040
      K2=K2                                                                     SBFR0050
      XLTOT=XLFNO(L,3)                                                          SBFR0060
      XL=XLFNO(L,4)                                                             SBFR0070
      PHET=0.                                                                   SBFR0080
      DO 10 N=1,K2                                                              SBFR0090
      RMOP = ROLLRAY(N,JRP,L)                                                   SBFR0100
      RMOG = ROLLRAY(N,JRG,L)                                                   SBFR0110
      RMOE = ABS((RMOP*RMOG)/(RMOP+RMOG))                                       SBFR0120
      VB=ROLLRAY(N,JVB,L)                                                       SBFR0130
      IF (L.EQ.1.OR.L.EQ.IT) GO TO 11                                           SBFR0140
    8 PVB=(DFORCE*XL)/(    XLTOT)*((ABS(VB))**(-1./3.))                         SBFR0145
      IF(PVB.LT.200.) GO TO 15                                                  SBFR0150
      FRIC=FR1                                                                  SBFR0160
      GO TO 25                                                                  SBFR0170
   15 FRIC=FR2*(PVB**(-.30))                                                    SBFR0180
      GO TO 25                                                                  SBFR0190
   11 FRIC=0.                                                                   SBFR0197
   25 IF (L.EQ.1.OR.L.EQ.IT) GO TO 17                                           SBFR0200
      PHE=FRIC*(DFORCE*XL)/(K/2*XLTOT)*VB*(1./9336.)                            SBFR0210
      GO TO 27                                                                  SBFR0220
   17 PHE=0.                                                                    SBFR0230
```

Figure I-2. Listing of helical gear computer program (cont'd)

```
   87 ROLLRAY(N,JFR,L)=FRIC                                                  SBFR0250=0497
      ROLLRAY(N,JPN,L) = PHE                                                SBFR0260=0498
      PHET=PHET+PHE                                                         SBFR0265=0499
   10 CONTINUE                                                              SBFR0270=0500
      XLFNO(L,5)=PHET                                                       SBFR0280=0501
   20 CONTINUE                                                              SBFR0290=0502
      PHEAV=0.                                                              SBFR0310=0503
      KX=IT-1                                                               SBFR0320=0504
      DO 30 L=1,KX                                                          SBFR0330=0505
      PHEAV=PHEAV+XLFNO(L,5)+XLFNO(L+1,5)                                   SBFR0340=0506
   30 CONTINUE                                                              SBFR0350=0507
      PHEAV=(PHEAV+RNP*2)/(KX*2.*BDP*PI)                                    SBFR0360=0508
   40 TS=(TCON*((PHEAV)**.80))*TEMP                                         SBFR0370=0509
      DO 50 L=1,IT                                                          SBFR0372=0510
      XL=XLFNO(L,4)                                                         SBFR0373=0511
      XLTOT=XLFNO(L,3)                                                      SBFR0374=0512
      XLD=DFORCE*XL/XLTOT                                                   SBFR0376=0513
      XLFNO(L,5)=XLD                                                        SBFR0377=0514
   50 CONTINUE                                                              SBFR0378=0515
      RETURN                                                                SBFR0380=0516
      END                                                                   SBFR0390=0517
      SUBROUTINE FORCE                                                      FORC0000=0518
      REAL NATFQ                                                            FORC0010=0519
      COMMON AG,AP,BDG,BDP,C,   CPN,CTG,CTP,EG,EP,FNG,FNP,GMI,HAR,HP,       FORC0020=0520
     1       IMT,IN,NOUT,DDG,PANR,PDG,PDP,PEG,PEP,PMG,PI,PMI,PMP,RNG,       FORC0030=0521
     2       PMPR,PRG,PRP,RNP,RPMP,VA,WDG,WDP,DFORCE,WN,NATFQ                FORC0040=0522
C                                                                            FORC0050=0523
C     DEFINITION OF CALCULATED VARIABLES FOR HELICAL GEAR DYNAMIC FACTOR     FORC0060=0524
C                                                                            FORC0070=0525
C        PM    =  MASS OF PINION AT PITCH LINE,LB,SEC,SQ,/IN,                FORC0080=0526
C        GM    =  MASS OF GEAR AT PITCH LINE,LB,SEC,SQ,/IN,                  FORC0090=0527
C        EM    =  EQUIVALENT MASS,LB,SEC,SQ,/IN,                             FORC0100=0528
C        CB    =  COMPLIANCE OF TOOTH IN BENDING,IN,                         FORC0110=0529
C        CR    =  COMPLIANCE OF TOOTH RIM FLEXURE,IN,                        FORC0120=0530
C        CC    =  COMPLIANCE OF RIM IN CIRCUMF, DIRECTION,IN,                FORC0130=0531
C        CT    =  TOTAL COMPLIANCE INCHES/LB, PER IN, WIDTH                  FORC0140=0532
C        TS    =  TOOTH STIFFNESS, LB/IN, PER IN, WIDTH                      FORC0150=0533
C        TG    =  LOW SPEED SHAFT TORQUE,IN,-LB,                             FORC0160=0534
C        V     =  PITCH LINE VELOCITY,FPM                                     RC0170=0535
C        EE    =  EFFECTIVE ERROR                                            ORC0180=0536
C        ST    =  TIME FOR 1 TOOTH PULSE,SEC,                                ORC0190=0537
C        TT    =  RATIO OF TIME OF INTRODUCTION OF                           FORC0200=0538
C                 ERROR TO NATURAL PERIOD                                    FORC0210=0539
C        DF    =  DYNAMIC FACTOR                                             FORC0220=0540
C        NATFQ =  TOOTH SPRING FREQ,,RPM                                     FORC0230=0541
C                                                                            FORC0240=0542
C     PRELIMINARY CALCULATIONS                                               FORC0250=0543
C                                                                            FORC0260=0544
      PMPR=RPMP*(RNP/RNG)                                                    FORC0270=0545
      IF(RPMP.LT.PMPR) PMPR=RPMP                                             FORC0280=0546
  300 PM = PMI /((PDP/2.)*(PDP/2.))                                          FORC0290=0547
      GM = GMI /((PDG/2.)*(PDG/2.))                                          FORC0300=0548
      EM = (PM*GM)/(PM+GM)                                                   FORC0310=0549
      CB=(12/PI)*((WDG/2)**2)/(EG*(CTG)**3)+                                 FORC0320=0550
     1   (12/PI)*((WDP/2)**2)/(EP*(CTP)**3)                                  FORC0330=0551
      CR1= (1./FNG) * ((2.*(1.+PRG)/EG)*((0.1/AG*(CPN*COS(PANR)))+.125)*FORC0340=0552
     1                    (1./COS(HAR)))                                    FORC0350=0553
      CR2= (1./FNP) * ((2.*(1.+PRP)/EP)*((0.1/AP*(CPN*COS(PANR)))+.125)*FORC0360=0554
     1                    (1./COS(HAR)))                                    FORC0370=0555
      CR = CR1+CR2                                                           FORC0380=0556
      CC1 = (1./FNG)*(RNG*(1./COS(HAR))/(6.*(AG/(CTG*COS(PANR))+.2)*EG))FORC0390=0557
      CC2 = (1./FNP)*(RNP*(1./COS(HAR))/(6.*(AP/(CTP*COS(PANR))+.2)*EP))FORC0400=0558
```

Figure I-2. Listing of helical gear computer program (cont'd)

```
      CC = CC1+CC2                                                      FORC0910
      CT = CB+CA+CC                                                     FORC0920
      TS = 1./CT                                                        FORC0930
      TG = 63000.*HP / RMPR                                             FORC0940
      V  = (PI*PDP/12.) * RPMP                                          FORC0950
      EE = PEP + PEG + PMG                                              FORC0960
      PP = (PEP+PEG)*(2.*PMG)                                           FORC0970
      IF (NATFQ.NE.0.) GO TO 10                                         FORC0980
      T3=2.*PI*SQRT(CT*EM)                                              FORC0990
      NATFQ=60./T3                                                      FORC0500
      WRITE (NOUT,1023) NATFQ                                           FORC0510
 1023 FORMAT (///1X,19HTOOTH NAT. FREQ. = ,F10.1,9H RPM)                FORC0520
      GO TO 350                                                         FORC0530
   10 T3=60./NATFQ                                                      FORC0540
C                                                                       FORC0550
C     CALCULATION OF DYNAMIC FACTOR BY TUPLIN METHOD                    FORC0560
C                                                                       FORC0570
  350 RT = CPN *(1./COS(HAR))/12. * (60./V)                             FORC0580
      TT = RT/T3                                                        FORC0590
      IF (TT-.277) 370,370,360                                          FORC0600
  360 ET = 0.815 / SQRT(1.+(6.6*(TT*TT)))                               FORC0610
      GO TO 380                                                         FORC0620
  370 ET = 1./(1.+(6.6*(TT*TT)))                                        FORC0630
  380 DI = EE*ET*TS                                                     FORC0640
      IF (RPMP.GT.RMPR) GO TO 381                                       FORC0650
      PDG=PDP                                                           FORC0660
  381 TI=DI*(PDG/2.)                                                    FORC0670
      DF=TG/(IG*TI)                                                     FORC0680
      WRITE (NOUT,1022) DI,DF                                           FORC0690
 1022 FORMAT (/E11.4,29H = DYNAMIC INCREMENT,LB./E11.4,                 FORC0700
     *  19H = DYNAMIC FACTOR)                                          FORC0710
      RETURN                                                            FORC0720
      END                                                               FORC0730
                                                                        *0592
```

Figure I-2. Listing of helical gear computer program (cont'd)

```
                    VALUES AND DEFINITIONS OF PRIMARY INPUT VARIABLES
(INCH UNITS UNLESS NOTED)
   (DRIVER)                    (DRIVEN)
BDP     =    3,53950    BDG     =   15,73990    =BASE CIRCLE DIAMETER
BP      =   92,20000    BG      =   92,20000    =THERMAL CONSTANT (LB,/SQRT(SEC,)IN,DEG,F)
CTP     =     ,17910    CTG     =     ,17910    =NORMAL CIRCLE TOOTH THICKNESS
EP      =      3E+07    EG      =      3E+07    =YOUNG'S MODULUS, PSI,
FWP     =    2,50000    FWG     =    2,38000    =FACE WIDTH
ODP     =    4,03200    ODG     =   17,29030    =OUTSIDE DIAMETER
PRP     =     ,30000    PRG     =     ,30000    =POISSON'S RATIO
RNP     =   31,00000    RNG     =  138,00000    =NUMBER OF TEETH
WDP     =     ,25210    WDG     =     ,25200    =WEIGHT OR WHOLE DEPTH
C       =  10,970550                            =CENTER DISTANCE
CPN     =     ,36960                            =NORMAL CIRCLE PITCH
DPN     =    8,500000                           =DIAMTERAL PITCH
HA      =   18,2°,60                            =HELIX ANGLE (DEG,)
PAN     =   22,30000                            =PRESSURE ANGLE (DEG,)
RPMP    =    6000,00                            =RPM DRIVER
TEMP    =     190,00                            =OIL JET TEMPERATURE (DEG,F)
IT      =         16                            =INCREMENTS OF EFF
FR1     =      ,0188                            =CONSTANT FRICTION FACTOR
FR2     =      ,0922                            =VARIABLE FRICTION FACTOR
TCON    =      312,5                            =TEMP DIFFERENCE FACTOR

INPUT VARIABLES FOR HORSEPOWER LOOP
HP      =    600,000                            =INITIAL HORSEPOWER
DHP     =    100,000                            =HORSEPOWER INCREMENT
HPM     =   1400,000                            =MAXIMUM HORSEPOWER

METHOD USED FOR CALCULATING NORMAL FORCE=
 1 NORMAL FORCE=STATIC FORCE
 2 DYNAMIC FACTOR CALCULATED BY TUPLIN METHOD

INPUT VARIABLES FOR DYNAMIC FORCE CALCULATIONS
   (DRIVER)                    (DRIVEN)
AP      =     ,66000    AG      =     ,50000    =THICKNESS OF RIM BELOW ROOT
PEP     =     ,00020    PEG     =     ,00030    =PITCH ERROR
PMI     =     ,03430    GMI     =    6,25240    =MASS MOMENT OF INERTIA (LB,SEC,SQ,IN,)
PMP     =     ,00000    PMG     =     ,00000    =PROFILE MODIFICATION
RN(1)   =      =0,00                            =1ST NATURAL FREQUENCY (RPM)
RN(2)   =      =0,00                            =2ND NATURAL FREQUENCY (RPM)
RN(3)   =      =0,00                            =3RD NATURAL FREQUENCY (RPM)
```

Figure I-3. Sample helical gear computer printout

VALUES AND DEFINITIONS OF PRELIMINARY CALCULATED VARIABLES

(INCH UNITS UNLESS NOTED)

(DRIVER)			(DRIVEN)			
ADP	=	,09537	ADG	=	,09523	=ADDENDUM (IN.)
PDP	=	3,84127	PDG	=	17,09983	=PITCH DIAMETER
BHAR	=	,295352				=BASE HELIX ANGLE (RADIANS)
BPN	=	,342687				=NORMAL BASE PITCH
BPT	=	,358192				=TRANSVERSE BASE PITCH
ER	=	3,297E+07				=REDUCED MODULUS (PSI)
VA	=	,515873				=DISTANCE FROM FIRST INTERFERENCE POINT TO START OF CONTACT
WA	=	3,584101				=DISTANCE FROM SECOND INTERFERENCE POINT TO START OF CONTACT
Z	=	,45922				=PATH OF CONTACT
ZA	=	,23623				=PATH OF CONTACT IN APPROACH
ZC	=	,12196				=DISTANCE FROM PITCH POINT TO HPSTC
ZD	=	,14020				=DISTANCE FROM PITCH POINT TO LPSTC
ZR	=	,21799				=PATH OF CONTACT IN RECESS

CALCULATIONS OF XL FOR EACH VALUE OF EFF

0,000	1,231	1,560	,356	0,000	0,000	0,000	3,198
,270	1,500	1,317	,087	0,000	0,000	0,000	3,174
,540	1,560	1,047	0,000	0,000	0,000	0,000	3,198
,810	1,560	,777	0,000	0,000	0,000	0,000	3,198
1,080	1,560	,507	0,000	0,000	0,000	0,000	3,198
1,349	1,468	,238	0,000	,119	0,000	0,000	3,174
1,560	1,198	0,000	0,000	,389	0,000	0,000	3,198
1,560	,928	0,000	0,000	,659	0,000	0,000	3,198
1,560	,659	0,000	0,000	,928	0,000	0,000	3,198
1,560	,389	0,000	0,000	1,198	0,000	0,000	3,198
1,349	,119	0,000	0,000	1,468	,238	0,000	3,174
1,080	0,000	0,000	0,000	1,560	,507	0,000	3,198
,810	0,000	0,000	0,000	1,560	,777	0,000	3,198
,540	0,000	0,000	0,000	1,560	1,047	0,000	3,198
,270	0,000	0,000	0,000	1,500	1,317	,087	3,174
0,000	0,000	0,000	0,000	1,231	1,560	,356	3,198

Figure I-3. Sample helical gear computer printout (cont'd)

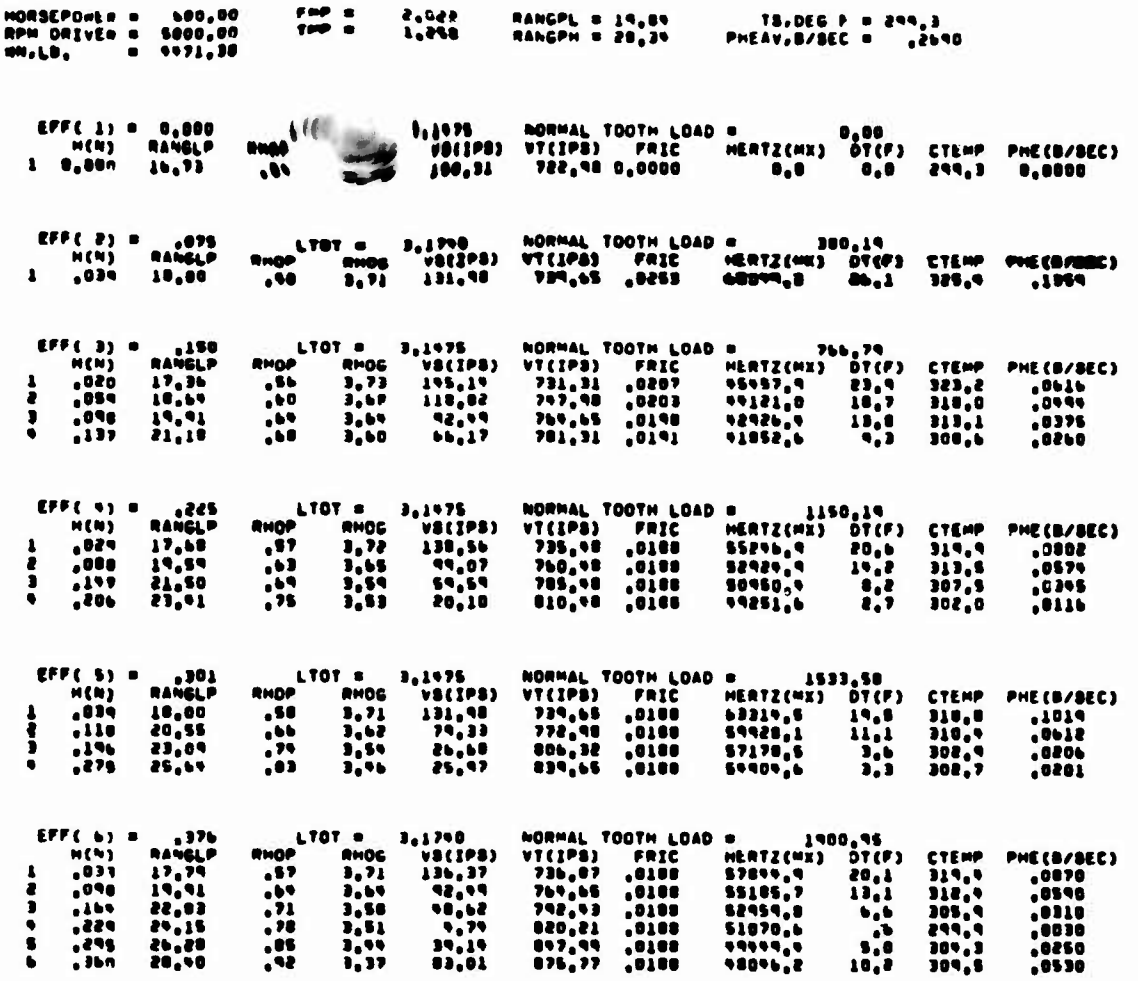

HORSEPOWER = 600.00 FMP = 2.022 RANGPL = 14.89 TB,DEG F = 299.3
RPM DRIVER = 5000.00 TMP = 1.998 RANGPN = 28.34 PHEAV,B/SEC = .2640
HP,LB, = 9971.38

EFF(1) = 0.000 NORMAL TOOTH LOAD = 0.00

	M(N)	RANGLP	RMOP	RMOG	VS(IPS)	VT(IPS)	FRIC	HERTZ(MX)	DT(F)	CTEMP	PHE(B/SEC)
1	0.000	16.93	.00		100.31	722.98	0.0000	0.0	0.0	299.3	0.0000

EFF(2) = .075 LTOT = 3.1998 NORMAL TOOTH LOAD = 380.14

	M(N)	RANGLP	RMOP	RMOG	VS(IPS)	VT(IPS)	FRIC	HERTZ(MX)	DT(F)	CTEMP	PHE(B/SEC)
1	.039	18.88	.48	3.71	131.98	954.65	.0253	[illegible]	26.1	325.4	.1964

EFF(3) = .150 LTOT = 3.1975 NORMAL TOOTH LOAD = 766.79

	M(N)	RANGLP	RMOP	RMOG	VS(IPS)	VT(IPS)	FRIC	HERTZ(MX)	DT(F)	CTEMP	PHE(B/SEC)
1	.020	17.36	.56	3.73	195.19	731.31	.0207	95497.9	23.9	323.2	.0616
2	.059	18.69	.60	3.69	118.82	747.98	.0203	99121.0	18.7	318.0	.0999
3	.098	19.91	.64	3.64	92.99	764.65	.0198	92926.9	13.8	313.1	.0375
4	.137	21.18	.68	3.60	66.17	781.31	.0191	91852.6	9.3	308.6	.0260

EFF(4) = .245 LTOT = 3.1975 NORMAL TOOTH LOAD = 1150.19

	M(N)	RANGLP	RMOP	RMOG	VS(IPS)	VT(IPS)	FRIC	HERTZ(MX)	DT(F)	CTEMP	PHE(B/SEC)
1	.029	17.68	.57	3.72	138.56	735.98	.0188	55296.9	20.6	319.9	.0802
2	.088	19.59	.63	3.65	99.07	760.98	.0188	52929.9	14.2	313.5	.0574
3	.147	21.50	.69	3.59	59.59	785.98	.0188	50950.9	8.2	307.5	.0345
4	.206	23.41	.75	3.53	20.10	810.98	.0188	49251.6	2.7	302.0	.0116

EFF(5) = .301 LTOT = 3.1975 NORMAL TOOTH LOAD = 1533.58

	M(N)	RANGLP	RMOP	RMOG	VS(IPS)	VT(IPS)	FRIC	HERTZ(MX)	DT(F)	CTEMP	PHE(B/SEC)
1	.039	18.00	.58	3.71	131.98	739.65	.0188	63219.5	14.8	318.8	.1019
2	.118	20.55	.66	3.62	79.33	772.98	.0188	59928.1	11.1	310.9	.0612
3	.196	23.09	.74	3.54	26.68	806.32	.0188	57178.5	3.6	302.9	.0206
4	.275	25.64	.83	3.46	25.97	839.65	.0188	54909.6	3.3	302.7	.0201

EFF(6) = .376 LTOT = 3.1998 NORMAL TOOTH LOAD = 1900.95

	M(N)	RANGLP	RMOP	RMOG	VS(IPS)	VT(IPS)	FRIC	HERTZ(MX)	DT(F)	CTEMP	PHE(B/SEC)
1	.031	17.79	.57	3.71	136.37	736.87	.0188	57899.9	20.1	319.9	.0870
2	.098	19.91	.64	3.64	92.99	764.65	.0188	55185.7	13.1	312.9	.0548
3	.166	22.03	.71	3.58	48.62	792.43	.0188	52954.8	6.6	305.9	.0310
4	.229	24.15	.78	3.51	4.24	820.21	.0188	51070.6	.6	299.9	.0038
5	.295	26.28	.85	3.44	39.10	847.99	.0188	49444.9	5.8	304.3	.0250
6	.364	28.40	.92	3.37	83.01	875.77	.0188	48046.2	10.2	309.5	.0530

Figure I-3. Sample helical gear computer printout (cont'd)

HORSEPOWER = 600.00 FMP = 2.022 RANGPL = 19.89 TS,DEG F = 299.3
RPM DRIVER = 5000.00 TMP = 1.268 RANGPM = 28.34 PMEAV,B/SEC = .2690
WN,LB. = 9971.38

EFF(7) = .951 LTOT = 3.1975 NORMAL TOOTH LOAD = 2216.85

	M(N)	RANGLP	RMOP	RMOG	VS(IPS)	VT(IPS)	FRIC	HERTZ(MX)	DT(F)	CTEMP	PME(B/SEC)
1	.038	17.95	.58	3.71	132.99	739.09	.0188	62221.9	19.7	319.0	.0489
2	.114	20.91	.66	3.63	82.20	771.17	.0188	58993.3	11.6	310.9	.0612
3	.189	22.86	.74	3.55	31.46	803.24	.0188	56359.6	9.2	303.6	.0234
4	.265	25.32	.82	3.47	19.28	835.32	.0188	54160.9	2.5	301.8	.0193
5	.341	27.77	.90	3.39	70.02	867.39	.0188	52311.7	8.7	308.1	.0521
6	.416	30.22	.97	3.31	120.76	899.47	.0188	50738.3	14.6	313.9	.0898

EFF(8) = .926 LTOT = 3.1975 NORMAL TOOTH LOAD = 2216.85

	M(N)	RANGLP	RMOP	RMOG	VS(IPS)	VT(IPS)	FRIC	HERTZ(MX)	DT(F)	CTEMP	PME(B/SEC)
1	.038	17.95	.58	3.71	132.99	739.09	.0188	62221.9	19.7	319.0	.0489
2	.114	20.91	.66	3.63	82.20	771.17	.0188	58993.3	11.6	310.9	.0612
3	.189	22.86	.74	3.55	31.46	803.24	.0188	56359.6	9.2	303.6	.0234
4	.265	25.32	.82	3.47	19.28	835.32	.0188	54160.9	2.5	301.8	.0193
5	.341	27.77	.90	3.39	70.02	867.39	.0188	52311.7	8.7	308.1	.0521
6	.416	30.22	.97	3.31	120.76	899.47	.0188	50738.3	14.6	313.9	.0898

EFF(9) = .901 LTOT = 3.1975 NORMAL TOOTH LOAD = 2216.85

	M(N)	RANGLP	RMOP	RMOG	VS(IPS)	VT(IPS)	FRIC	HERTZ(MX)	DT(F)	CTEMP	PME(B/SEC)
1	.038	17.95	.58	3.71	132.99	739.09	.0188	62221.9	19.7	319.0	.0489
2	.114	20.91	.66	3.63	82.20	771.17	.0188	58993.3	11.6	310.9	.0612
3	.189	22.86	.74	3.55	31.46	803.24	.0188	56359.6	9.2	303.6	.0234
4	.265	25.32	.82	3.47	19.28	835.32	.0188	54160.9	2.5	301.8	.0193
5	.341	27.77	.90	3.39	70.02	867.39	.0188	52311.7	8.7	308.1	.0521
6	.416	30.22	.97	3.31	120.76	899.47	.0188	50738.3	14.6	313.9	.0898

EFF(10) = .876 LTOT = 3.1975 NORMAL TOOTH LOAD = 2216.85

	M(N)	RANGLP	RMOP	RMOG	VS(IPS)	VT(IPS)	FRIC	HERTZ(MX)	DT(F)	CTEMP	PME(B/SEC)
1	.038	17.95	.58	3.71	132.99	739.09	.0188	62221.9	19.7	319.0	.0489
2	.114	20.91	.66	3.63	82.20	771.17	.0188	58993.3	11.6	310.9	.0612
3	.189	22.86	.74	3.55	31.46	803.24	.0188	56359.6	9.2	303.6	.0234
4	.265	25.32	.82	3.47	19.28	835.32	.0188	54160.9	2.5	301.8	.0193
5	.341	27.77	.90	3.39	70.02	867.39	.0188	52311.7	8.7	308.1	.0521
6	.416	30.22	.97	3.31	120.76	899.47	.0188	50738.3	14.6	313.9	.0898

EFF(11) = .752 LTOT = 3.1740 NORMAL TOOTH LOAD = 1900.95

	M(N)	RANGLP	RMOP	RMOG	VS(IPS)	VT(IPS)	FRIC	HERTZ(MX)	DT(F)	CTEMP	PME(B/SEC)
1	.094	19.78	.69	3.65	95.19	762.99	.0188	55335.9	13.5	312.8	.0607
2	.160	21.90	.71	3.58	51.31	790.72	.0188	53046.0	7.0	306.3	.0327
3	.226	24.02	.77	3.51	7.43	818.50	.0188	51178.3	1.0	300.3	.0047
4	.291	26.15	.84	3.44	36.44	846.28	.0188	49592.3	4.6	303.4	.0232
5	.356	28.27	.91	3.37	80.32	874.06	.0188	48126.9	9.4	309.2	.0512
6	.421	30.39	.98	3.31	124.19	901.84	.0188	46893.8	14.9	314.2	.0792

Figure I-3. Sample helical gear computer printout (cont'd)

```
HORSEPOWER =   600.00      FMP =    2.022      RANGPL = 19.89       TB,DEG F = 299.3
RPM DRIVE  =  5000.00      TMP =    1.258      RANGPH = 28.39     PHEAV,B/SEC =   .2690
WN,LB.     =  9971.38

  EFF(12) =    .827        LTOT =   3.1975     NORMAL TOOTH LOAD =      1533.58
     M(N)    RANGLP   RHOP    RHOG     VB(IPS)  VT(IPS)    FRIC     HERTZ(MX)   DT(F)   CTEMP   PHE(B/SEC)
1    .174    22.59    .73     3.56     38.15   799.05    .0188     57732.4      8.2     304.5     .0295
2    .256    25.08    .81     3.98     49.58   832.39    .0188     55365.5      1.9     301.2     .0112
3    .336    27.63    .89     3.39     67.16   868.72    .0188     53386.9      8.9     307.7     .0518
4    .419    30.18    .97     3.31    119.81   899.06    .0188     51713.3     19.5     313.8     .0925

  EFF(13) =    .902        LTOT =   3.1975     NORMAL TOOTH LOAD =      1150.19
     M(N)    RANGLP   RHOP    RHOG     VB(IPS)  VT(IPS)    FRIC     HERTZ(MX)   DT(F)   CTEMP   PHE(B/SEC)
1    .298    24.77    .80     3.99      7.92   828.22    .0188     58189.1      1.8     300.4     .0096
2    .307    26.68    .86     3.93     47.91   853.72    .0188     56892.9      6.8     306.3     .0275
3    .366    28.59    .92     3.36     86.90   879.23    .0188     55662.6     18.7     310.8     .0503
4    .428    30.50    .98     3.30    126.39   903.23    .0188     54619.8     15.2     319.5     .0732

  EFF(14) =    .977        LTOT =   3.1975     NORMAL TOOTH LOAD =       766.79
     M(N)    RANGLP   RHOP    RHOG     VB(IPS)  VT(IPS)    FRIC     HERTZ(MX)   DT(F)   CTEMP   PHE(B/SEC)
1    .319    26.99    .87     3.92     53.99   857.39    .0188     38077.5      6.8     306.1     .0208
2    .356    28.27    .91     3.37     80.32   874.86    .0196     37935.7     18.3     309.6     .0321
3    .398    29.59    .95     3.33    106.69   890.73    .0201     36899.8     13.9     313.8     .0439
4    .439    30.81    .99     3.29    132.97   907.39    .0205     36299.7     17.9     316.7     .0560

  EFF(15) =   1.052        LTOT =   3.1980     NORMAL TOOTH LOAD =       380.19
     M(N)    RANGLP   RHOP    RHOG     VB(IPS)  VT(IPS)    FRIC     HERTZ(MX)   DT(F)   CTEMP   PHE(B/SEC)
1    .419    30.18    .97     3.31    119.81   899.06    .0250     51496.7     19.2     310.5     .1222

  EFF(16) =   1.127        LTOT =   3.1975     NORMAL TOOTH LOAD =         0.00
     M(N)    RANGLP   RHOP    RHOG     VB(IPS)  VT(IPS)    FRIC     HERTZ(MX)   DT(F)   CTEMP   PHE(B/SEC)
1    .499    31.95    1.01    3.27    196.13   915.73 0.0000          0.0       0.0     299.3     0.0000

TOOTH NAT. FREQ. =   113671.5 RPM

1.9871E+02 = DYNAMIC INCREMENT,LB.
9.5379E-01 = DYNAMIC FACTOR
```

Figure I-3. Sample helical gear computer printout (cont'd)

APPENDIX J
SPIRAL BEVEL GEAR COMPUTER PROGRAM

Program Goal

This program examines spiral bevel gears for scoring potential. The analysis follows a pair of teeth from the time they engage until they separate, examining the conditions in the gear mesh at a number of intervals (usually 20) during the mesh cycle. The area of contact is assumed to be elliptical. Geometric parameters, velocities, loads, and temperatures are evaluated at the center of the contact ellipse. The method of analysis generally follows that of Coleman.[66]

Operating parameters are calculated on the basis of static load. These parameters may be corrected by applying a dynamic factor.

Program Language and Computer Type

The program is written in FORTRAN IV language for a CDC 6000 Series computer, using RUN compiler and SCOPE 3.4 system.

Input Cards

There are six data cards per set of data. Data sets may be stacked. The program contains both rpm and a horsepower loop, so the effect of changes in these operating variables on gear behavior may be studied.

Either the gear or the pinion may be the driver. However, data must be entered as applicable to the pinion or the gear, regardless of which drives. The program will evaluate conditions for either left- or right-hand rotation of the driver or, in the case of a reversing gear drive, both directions.

A description of the cards follows. All units are in inches unless otherwise noted.

Word	Column	Symbol	Description
Input Card 1	(PRELIMINARY INPUT DATA)		
1	1-10	RNP	Number of pinion teeth
2	11-20	RNG	Number of gear teeth

Word	Column	Symbol	Description
Input Card 1 (Cont'd)			
3	21-30	AP	Pinion addendum
4	31-40	AG	Gear addendum
5	41-50	BP	Pinion thermal constant, $lb/°F\text{-}in.sec^{\frac{1}{2}}$
6	51-60	BG	Gear thermal constant, $lb/°F\text{-}in.\text{-}sec^{\frac{1}{2}}$
7	61-70	DEDP	Pinion dedendum angle, deg
8	71-80	DEDG	Gear dedendum angle, deg
Input Card 2			
1	1-10	EP	Young's modulus, pinion
2	11-20	EG	Young's modulus, gear
3	21-30	PRP	Poisson's ratio, pinion
4	31-40	PRG	Poisson's ratio, gear
5	41-50	PA	Pressure angle, deg
6	51-60	SA	Spiral angle, deg
7	61-70	SIGMA	Shaft angle, deg
8	71-80	FW	Face width
Input Card 3			
1	1-10	PD	Diametral pitch
2	11-20	DRIVE	Driving gear; use: PIN = pinion GEAR = gear

Word	Column	Symbol	Description
Input Card 3 (Cont'd)			
3	21-30	ROT	Rotation of driver as seen looking toward apex; use: CW = clockwise CCW = counterclockwise REV = reverse
4	31-40	HAND	Hand of driver spiral; use: RH = right-hand LH = left-hand
5	41-50	M	Number of divisions of the line of contact that will be studied, usually 20
Input Card 4 (FRICTION AND TEMPERATURE)			
1	1-10	TEMP	Oil jet temperature, °F
2	11-20	FR1	Friction factor from Eq. (55), (57), (59), or (61)
3	21-30	FR2	Friction factor from Eq. (54), (56), (58), or (60)
4	31-40	TCON	Temperature difference factor from Eq. (69)
Input Card 5 (RPM LOOP)			
1	1-10	RPMP	Pinion rpm
2	11-20	RINC	Rpm pinion increment. Blank or zero if only one rpm
3	21-30	RPMX	Maximum pinion rpm. Blank or zero if only one rpm
Input Card 6 (HORSEPOWER LOOP)			
1	1-10	HPO	Initial horsepower

Word	Column	Symbol	Description
Input Card 6 (Cont'd)			
2	11-20	HINC	Horsepower increment. Blank or zero if only one horsepower
3	21-30	HPMX	Maximum horsepower. Blank or zero if only one horsepower

A sample set of data cards for the spiral bevel gear design and operating conditions given in Chapter VIII, Section D, is shown in Figure J-1. The pinion is the driver, turns CW, and has a left-hand spiral, as shown on Card 3. Card 4 contains friction factors calculated for plain surfaces with a composite surface roughness of 33 μin. AA, using Equations (111) and (112). Only one rpm was required as shown by Card 5, and Card 6 shows that 10 hp levels were run, starting at 300 hp to a maximum of 1200 hp.

Computer Program

Figure J-2 shows a listing of the computer program. Control cards are not included.

Sample Printout

Figure J-3 gives the data printout for the data input of Figure J-1. Results are shown for 600 hp only.

The first page lists the input data for reference purposes. The second page gives the results of the preliminary calculations. The third page lists, for M + 1 positions across the plane of action, those variables that are independent of the power level. These are velocities and some geometric parameters. The next page gives, again for M + 1 positions across the plane of action, those parameters such as load, instantaneous surface temperature, and instantaneous frictional power loss that are power-dependent.

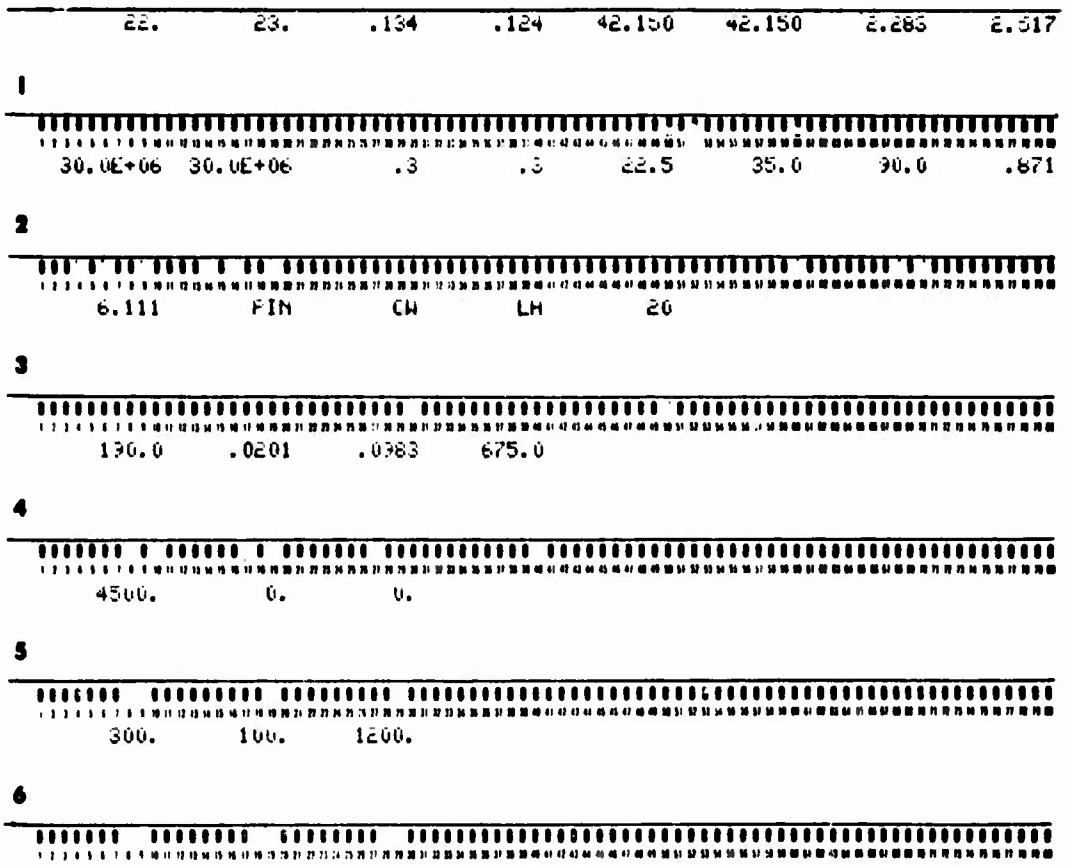

Figure J-1. Sample spiral bevel gear computer program data cards

```
      PROGRAM SCIFF (INPUT,OUTPUT,TAPE5=INPUT,TAPE6=OUTPUT)                  SBEV0000.0001
      DIMENSION EFFRY(30,10)                                                 SBEV0010.0002
      DATA IGEAR/3HGEAR/,IPIN/3HPIN /,IREV/3HREV/,ICW/3HCW /,                SBEV0020.0003
     1     ICCW/3HCCW/,ILH/2HLH/,IRH/2HRH/                                   SBEV0030.0004
      JEF=1                                                                  SBEV0040.0005
      JVS=2                                                                  SBEV0050.0006
      JVT=3                                                                  SBEV0060.0007
      JPH=4                                                                  SBEV0070.0008
      JHD=5                                                                  SBEV0080.0009
      JFR=6                                                                  SBEV0090.0010
      JSP=7                                                                  SBEV0100.0011
      JHOT=8                                                                 SBEV0110.0012
      JOH=9                                                                  SBEV0120.0013
      JRH=10                                                                 SBEV0130.0014
      IN=5                                                                   SBEV0140.0015
      NOUT=6                                                                 SBEV0150.0016
      PI=3.14159265                                                          SBEV0160.0017
      RADIAN=PI/180.                                                         SBEV0170.0018
C                                                                            SBEV0180.0019
C     DEFINITIONS OF INPUT VARIABLES FOR SPIRAL BEVEL GEARS (INCH UNITS)     SBEV0190.0020
C                                                                            SBEV0200.0021
C        ANP   = NUMBER OF PINION TEETH                                      SBEV0210.0022
C        ANG   = NUMBER OF GEAR TEETH                                        SBEV0220.0023
C        AP    = ADDENDUM (PINION)                                           SBEV0230.0024
C        AG    = ADDENDUM (GEAR)                                             SBEV0240.0025
C        HP    = THERMAL CONSTANT (PINION),LB./SQRT(SEC.)IN.DEG.F            SBEV0250.0026
C        HG    = THERMAL CONSTANT (GEAR),LB./SQRT(SEC.)IN.DEG.F              SBEV0260.0027
C        DEDP  = DEDENDUM ANGLE (PINION),DEG.                                SBEV0270.0028
C        DEDG  = DEDENDUM ANGLE (GEAR),DEG.                                  SBEV0280.0029
C        EP    = YOUNG'S MODULUS (PINION),PSI                                SBEV0290.0030
C        EG    = YOUNG'S MODULUS (GEAR),PSI                                  SBEV0300.0031
C        PRP   = POISSON'S RATIO (PINION)                                    SBEV0310.0032
C        PRG   = POISSON'S RATIO (GEAR)                                      SBEV0320.0033
C        PA    = NORMAL PRESSURE ANGLE, DEG.                                 SBEV0330.0034
C        QA    = SPIRAL ANGLE,DEG.                                           SBEV0340.0035
C        SIGMA = SHAFT ANGLE,DEG.                                            SBEV0350.0036
C        FW    = FACE WIDTH                                                  SBEV0360.0037
C        PD    = DIAMETRAL PITCH                                             SBEV0370.0038
C        DRIVE = DRIVING GEAR                                                SBEV0380.0039
C        ROT   = ROTATION OF DRIVER (LOOKING TOWARD APEX)                    SBEV0390.0040
C        HAND  = HAND OF DRIVER SPIRAL                                       SBEV0400.0041
C        L     = NUMBER OF INCREMENTS OF EFF (USUALLY 20)                    SBEV0410.0042
C        TEMP  = OIL JET TEMPERATURE,DEG.F                                   SBEV0420.0043
C        FR1   = CONSTANT FRICTION FACTOR                                    SBEV0430.0044
C        FR2   = VARIABLE FRICTION FACTOR                                    SBEV0440.0045
C        TCON  = TEMP. DIFFERENCE FACTOR                                     SBEV0450.0046
C        RPMP  = PINION RPM                                                  SBEV0460.0047
C        RINC  = RPM PINION INCREMENT                                        SBEV0470.0048
C        RPMX  = RPM PINION MAXIMUM                                          SBEV0480.0049
C        HPO   = INITIAL HORSEPOWER                                          SBEV0490.0050
C        HINC  = HORSEPOWER INCREMENT                                        SBEV0500.0051
C        HPMX  = MAXIMUM HORSEPOWER                                          SBEV0510.0052
C                                                                            SBEV0520.0053
C     DEFINITIONS OF PRELIMINARY CALCULATED VARIABLES (INCH UNITS)           SBEV0530.0054
C                                                                            SBEV0540.0055
C        A     = MEAN CONE DISTANCE                                          SBEV0550.0056
C        ALFP  = ADDENDUM ANGLE (PINION),DEG.                                SBEV0560.0057
C        ALFG  = ADDENDUM ANGLE (GEAR),DEG.                                  SBEV0570.0058
C        AMP   = MEAN ADDENDUM (PINION)                                      SBEV0580.0059
C        AMG   = MEAN ADDENDUM (GEAR)                                        SBEV0590.0060
C        AO    = CONE DISTANCE                                               SBEV0600.0061
C        ABA   = MEAN BASE SPIRAL ANGLE,RADIANS                              SBEV0610.0062
```

Figure J-2. Listing of spiral bevel gear computer program

```
C        CP     = MATERIAL LOAD FACTOR                                          SBEV0620
C        CR     = MODIFIED CONTACT RATIO                                        SBEV0630
C        DP     = PITCH DIAMETER (PINION)                                       SBEV0640
C        DG     = PITCH DIAMETER (GEAR)                                         SBEV0650
C        DRHODP = MEAN RADIUS OF CURVATURE (PINION)                             SBEV0660
C        DRHODG = MEAN RADIUS OF CURVATURE (GEAR)                               SBEV0670
C        ETASQ  = A PARAMETER                                                   SBEV0680
C        FAC    = A FACTOR                                                      SBEV0690
C        FI     = INERTIA FACTOR                                                SBEV0700
C        FMP    = FACE CONTACT RATIO                                            SBEV0710
C        GAMP   = PITCH ANGLE (PINION),RADIANS                                  SBEV0720
C        GAMG   = PITCH ANGLE (GEAR),RADIANS                                    SBEV0730
C        OMEGP  = PINION SPEED,RAD/SEC                                          SBEV0740
C        PN     = MEAN NORMAL BASE PITCH                                        SBEV0750
C        PRNP   = PITCH RADIUS IN MEAN NORMAL SECTION (PINION)                  SBEV0760
C        PRNG   = PITCH RADIUS IN MEAN NORMAL SECTION (GEAR)                    SBEV0770
C        PZ     = A PARAMETER                                                   SBEV0780
C        RBNP   = BASE RADIUS IN MEAN NORMAL SECTION (PINION)                   SBEV0790
C        RBNG   = BASE RADIUS IN MEAN NORMAL SECTION (GEAR)                     SBEV0800
C        RP     = PITCH RADIUS IN MEAN TRANSVERSE SECTION (PINION)              SBEV0810
C        RG     = PITCH RADIUS IN MEAN TRANSVERSE SECTION (GEAR)                SBEV0820
C        RONP   = OUTSIDE RADIUS IN MEAN NORMAL SECTION (PINION)                SBEV0830
C        RONG   = OUTSIDE RADIUS IN MEAN NORMAL SECTION (GEAR)                  SBEV0840
C        TMP    = TRANSVERSE CONTACT RATIO                                      SBEV0850
C        ZN     = LENGTH OF ACTION IN NORMAL PLANE                              SBEV0860
C                                                                               SBEV0870
C                                                                               SBEV0880
C     READ INPUT VARIABLES FOR SPIRAL BEVEL GEARS                               SBEV0890
C                                                                               SBEV0900
  100 READ (IN,9004) RNP,RNG,AP,AG,BP,BG,DEDP,DEDG,                            SBEV0910
     2               EP,EG,PRP,PRG,PA,SA,SIGMA,FW,                             SBEV0920
     3               PD,DRIVE,ROT,HAND,M,                                      SBEV0930
     4               TEMP,FR1,FR2,TCON                                         SBEV0940
 9004 FORMAT (2F10.0,6F10.3/2E10.2,5F10.2,F10.3/F10.3,3,3A10,I10/              SBEV0950
     1   1F10.1,3F10.4)                                                        SBEV0960
      IF (EOF,IN) 600,150                                                      SBEV0970
  150 READ (IN,9005) RPMP,RINC,RPMX                                            SBEV0980
      READ (IN,9005) HPO,HINC,HPMX                                             SBEV0990
 9005 FORMAT (3F10.2)                                                          SBEV1000
      WRITE (NOUT,9010) RNP,RNG,AP,AG,BP,BG,DEDP,DEDG,EP,EG,PRP,PRG           SBEV1010
      WRITE (NOUT,9011) PA,SA,SIGMA,FW,PD,DRIVE,ROT,HAND,M,                   SBEV1020
     *       TEMP,FR1,FR2,TCON                                                 SBEV1030
 9010 FORMAT (1H1,////30X,41HVALUES AND DEFINITIONS OF INPUT VARIABLES,//      SBEV1040
     * 26H (INCH UNITS UNLESS NOTED)/                                          SBEV1050
     * 2X,16H     (PINION)     ,6X,16H          (GEAR),                       SBEV1060
     */11H RNP      = ,F10.4,5X,10H RNG     = ,F10.4,5X,                     SBEV1070
     *   40H=NUMBER OF TEETH                                                   SBEV1080
     */11H AP       = ,F10.4,5X,10H AG      = ,F10.4,5X,                     SBEV1090
     *   40H=ADDENDUM                                                          SBEV1100
     */11H BP       = ,F10.4,5X,10H BG      = ,F10.4,5X,                     SBEV1110
     *   40H=THERMAL CONSTANT,LB./SQRT(SEC.)IN.DEG.F                           SBEV1120
     */11H DEDP     = ,F10.4,5X,10H DEDG    = ,F10.4,5X,                     SBEV1130
     *   40H=DEDENDUM ANGLE,DEG.                                               SBEV1140
     */11H EP       = ,E10.2,5X,10H EG      = ,E10.2,5X,                     SBEV1150
     *   40H=YOUNG'S MODULUS,PSI                                               SBEV1160
     */11H PRP      = ,F10.4,5X,10H PRG     = ,F10.4,5X,                     SBEV1170
     *   40H=POISSON'S RATIO                                                   SBEV1180
     *)                                                                        SBEV1190
 9011 FORMAT (                                                                 SBEV1200
     * 11H PA       = ,F10.2,30X,36H=NORMAL PRESSURE ANGLE,DEG.              SBEV1210
     */11H SA       = ,F10.2,30X,36H=SPIRAL ANGLE,DEG.                       SBEV1220
     */11H SIGMA    = ,F10.2,30X,36H=SHAFT ANGLE,DEG.                        SBEV1230
```

Figure J-2. Listing of spiral bevel gear computer program (cont'd)

```
     */11H FW       = ,F10.4,30X,36H=FACE WIDTH                                  SBEV1240-0125
     */11H PD       = ,F10.2,30X,36H=DIAMETRAL PITCH                             SBEV1250-0126
     */11H DRIVE    = ,A10  ,30X,36H=DRIVING GEAR                                SBEV1260-0127
     */11H ROT      = ,A10  ,30X,36H=ROTATION OF DRIVER                          SBEV1270-0128
     */11H HAND     = ,A10  ,30X,36H=HAND OF DRIVER SPIRAL                       SBEV1280-0129
     */11H N        = ,I10  ,30X,36H=NUMBER OF INCREMENTS OF EFF                 SBEV1290-0130
     */11H TEMP     = ,F10.2,30X,36H=OIL JET TEMPERATURE,DEG,F                   SBEV1300-0131
     */11H FR1      = ,F10.4,30X,36H=CONSTANT FRICTION FACTOR                    SBEV1310-0132
     */11H FR2      = ,F10.4,30X,36H=VARIABLE FRICTION FACTOR                    SBEV1320-0133
     */11H TCON     = ,F10.2,30X,36H=TEMP.DIFFERENCE FACTOR                      SBEV1330-0134
     *)                                                                          SBEV1340-0135
      WRITE (NOUT,9006) RPMP                                                     SBEV1350-0136
      IF (RINC.EQ.0.) GO TO 252                                                  SBEV1360-0137
      WRITE (NOUT,9007) RINC,RPMX                                                SBEV1370-0138
  252 WRITE (NOUT,9008) HPO                                                      SBEV1380-0139
      IF (HINC.EQ.0.) GO TO 253                                                  SBEV1390-0140
      WRITE (NOUT,9009) HINC,HPMX                                                SBEV1400-0141
 9006 FORMAT (   //35X,48HINPUT VARIABLES FOR SPECIFIED LOOPS AND SECTIOSBEV1410-0142
     *NS//1X,30HVARIABLES USED IN,,, RPMP LOOP                                   SBEV1420-0143
     */11H RPMP     = ,F10.2,30X, 36H=RPM PINION                                 SBEV1430-0144
     *)                                                                          SBEV1440-0145
 9007 FORMAT (                                                                   SBEV1450-0146
     * 11H RINC     = ,F10.2,30X, 36H=RPM PINION INCREMENT                       SBEV1460-0147
     */11H RPMX     = ,F10.2,30X, 36H=RPM PINION MAXIMUM                         SBEV1470-0148
     *)                                                                          SBEV1480-0149
 9008 FORMAT (                                                                   SBEV1490-0150
     * //1X,35HVARIABLES USED IN,,,HORSEPOWER LOOP                              SBEV1500-0151
     */11H HPO      = ,F10.2,30X, 36H=HORSEPOWER                                 SBEV1510-0152
     *)                                                                          SBEV1520-0153
 9009 FORMAT (                                                                   SBEV1530-0154
     * 11H HINC     = ,F10.2,30X, 36H=HORSEPOWER INCREMENT                       SBEV1540-0155
     */11H HPMX     = ,F10.2,30X, 36H=MAXIMUM HORSEPOWER                         SBEV1550-0156
     *//)                                                                        SBEV1560-0157
C                                                                               SBEV1570-0158
C                                                                               SBEV1580-0159
C    DEFINITIONS OF CALCULATED LOOP VARIABLES FOR SPIRAL BEVEL GEAR -           SBEV1590-0160
C       ALF1  = ANGLE THE PINION VELOCITY MAKES WITH PITCH LINE IN              SBEV1600-0161
C               RADIANS,                                                        SBEV1610-0162
C       ALF2  = ANGLE THE GEAR VELOCITY MAKES WITH PITCH LINE IN                SBEV1620-0163
C               RADIANS,                                                        SBEV1630-0164
C       AB    = SEMI-AXIS OF CONTACT ELLIPSE, IN,                               SBEV1640-0165
C       BB    = SEMI-AXIS OF CONTACT ELLIPSE, IN,                               SBEV1650-0166
C       DELT  = CONJUNCTION TEMPERATURE RISE, DEG, F                            SBEV1660-0167
C       D1    = DISTANCE THE CONTACT AREA MOVES OVER A POINT ON                 SBEV1670-0168
C               SURFACE OF PINION, IN,                                          SBEV1680-0169
C       D2    = DISTANCE THE CONTACT AREA MOVES OVER A POINT ON                 SBEV1690-0170
C               SURFACE OF GEAR, IN,                                            SBEV1700-0171
C       EFF   = THE INDEPENDENT VARIABLE, DISTANCE FROM CENTER OF               SBEV1710-0172
C               SURFACE OF ACTION TO LINE OF CONTACT MEASURED                   SBEV1720-0173
C               IN THE NORMAL DIRECTION, IN,                                    SBEV1730-0174
C       ETA1  = FACTOR IN LOAD SHARING RATIO                                    SBEV1740-0175
C       FRIC  = FRICTION COEFFICIENT,                                           SBEV1750-0176
C       HP    = HORSEPOWER,                                                     SBEV1760-0177
C       OMEG  = INCLINATION ANGLE BETWEEN LINE OF CONTACT AND THE               SBEV1770-0178
C               PITCH LINE IN THE TANGENT PLANE IN RADIANS,                     SBEV1780-0179
C       Q     = CONTACT STRESS, PSI,                                            SBEV1790-0180
C       RHO   = RELATIVE RADIUS OF CURVATURE, IN,                               SBEV1800-0181
C       RHOG  = RADIUS OF PROFILE CURVATURE AT PITCH POINT ON GEAR              SBEV1810-0182
C               IN THE MEAN NORMAL SECTION, IN,                                 SBEV1820-0183
C       RHOP  = RADIUS OF PROFILE CURVATURE AT PITCH POINT ON PINION            SBEV1830-0184
C               IN THE MEAN NORMAL SECTION, IN,                                 SBEV1840-0185
C       RHO1  = RADIUS OF PROFILE CURVATURE ON PINION, IN,                      SBEV1850-0186
```

Figure J-2. Listing of spiral bevel gear computer program (cont'd)

```
C        RHO2   = RADIUS OF PROFILE CURVATURE ON GEAR, IN,                    SBEV1860*0187
C        SG     = LENGTH OF LINE OF CONTACT THRU CRITICAL POINT, IN,         SBEV1870*0188
C        SR     = LOAD SHARING RATIO                                         SBEV1880*0189
C        VF     = LENGTHWISE SLIDING VELOCITY, IN/SEC,                       SBEV1890*0190
C        VFG    = LENGTHWISE SLIDING VELOCITY OF GEAR, IN/SEC,               SBEV1900*0191
C        VFP    = LENGTHWISE SLIDING VELOCITY OF PINION, IN/SEC,             SBEV1910*0192
C        VFT    = LENGTHWISE SUM VELOCITY, IN/SEC,                           SBEV1920*0193
C        VPT    = PROFILE SUM VELOCITY, IN/SEC,                              SBEV1930*0194
C        VT     = RESULTANT SUM VELOCITY , IN/SEC,                           SBEV1940*0195
C        VN     = TANGENTIAL VELOCITY VECTOR, IN/SEC,                        SBEV1950*0196
C        VP     = PROFILE SLIDING VELOCITY, IN/SEC,                          SBEV1960*0197
C        VPG    = PROFILE SLIDING VELOCITY OF GEAR, IN/SEC,                  SBEV1970*0198
C        VPP    = PROFILE SLIDING VELOCITY OF PINION, IN/SEC,                SBEV1980*0199
C        VS     = RESULTANT SLIDING VELOCITY, IN/SEC,                        SBEV1990*0200
C        V1     = RESULTANT ABSOLUTE VELOCITY OF PINION, IN/SEC,             SBEV2000*0201
C        V2     = RESULTANT ABSOLUTE VELOCITY OF GEAR, IN/SEC,               SBEV2010*0202
C        WD     = DYNAMIC LOAD, LB,                                          SBEV2020*0203
C        WT     = MAXIMUM TANGENTIAL LOAD AT HEEL PITCH POINT, LB,           SBEV2030*0204
C        Z0     = DISTANCE FROM PITCH LINE TO CRITICAL POINT IN THE MEAN     SBEV2040*0205
C                 NORMAL SECTION,IN,                                         SBEV2050*0206
C                                                                            SBEV2060*0207
C                                                                            SBEV2070*0208
C                                                                            SBEV2080*0209
C     PERFORM PRELIMINARY CALCULATIONS                                       SBEV2090*0210
C                                                                            SBEV2100*0211
  253 SIGMAR=SIGMA*RADIAN                                                    SBEV2110*0212
      PAR=PA*RADIAN                                                          SBEV2120*0213
      SAR=SA*RADIAN                                                          SBEV2130*0214
      ALFP = DFDG                                                            SBEV2140*0215
      ALFG = DFDP                                                            SBEV2150*0216
      ALFPR=ALFP*RADIAN                                                      SBEV2160*0217
      ALFGR=ALFG*RADIAN                                                      SBEV2170*0218
      DP = RNP/PD                                                            SBEV2180*0219
      DG = RNG/PD                                                            SBEV2190*0220
      ANGLE = (180.-SIGMA)*RADIAN                                            SBEV2200*0221
      GAMP=ATAN(SIN(SIGMAR)/((RNG/RNP) +COS(SIGMAR)))                        SBEV2210*0222
  270 GAMG = SIGMAR-GAMP                                                     SBEV2220*0223
      IF (ABS(GAMG-PI/2.).GT..0015) GO TO 274                                SBEV2230*0224
  272 GAMGT=1000.                                                            SBEV2240*0225
      GAMGC=.0001                                                            SBEV2250*0226
      GO TO 278                                                              SBEV2260*0227
  274 GAMGT=TAN(GAMG)                                                        SBEV2270*0228
      GAMGC=COS(GAMG)                                                        SBEV2280*0229
  278 AO = DG/(2.*SIN(GAMG))                                                 SBEV2290*0230
      A = AO-FW/2.                                                           SBEV2300*0231
      RP = (A/AO)*(DP/(2.*COS(GAMP)))                                        SBEV2310*0232
      RG = (A/AO)*(DG/(2.*GAMGC))                                            SBEV2320*0233
      AMP = AP-(FW/2.)*TAN(ALFPR)                                            SBEV2330*0234
      AMG = AG-(FW/2.)*TAN(ALFGR)                                            SBEV2340*0235
      RNP = RP*((1./COS(SAR))*(1./COS(SAR)))                                 SBEV2350*0236
      RNG = RG*((1./COS(SAR))*(1./COS(SAR)))                                 SBEV2360*0237
      RAP= RNP*COS(PAR)                                                      SBEV2370*0238
      RAG =RNG*COS(PAR)                                                      SBEV2380*0239
      RONP =RNP*AMP                                                          SBEV2390*0240
      RONG =RNG*AMG                                                          SBEV2400*0241
      DRHOP = SQRT((RONP*RONP)-(RAP*RAP))-RNP*SIN(PAR)                       SBEV2410*0242
      DRHOG = SQRT((RONG*RONG)-(RAG*RAG))-RNG*SIN(PAR)                       SBEV2420*0243
      ZN = DRHOP+DRHOG                                                       SBEV2430*0244
      YK2=FW/AO*((2.-FW/AO)/(2.*(1.-FW/AO)))                                 SBEV2440*0245
      FWP=AO*PD/PI*(YK2*TAN(SAR   )-(1./3.*((YK2*TAN(SAR   ))**3)))          SBEV2450*0246
      P2 = (A/AO)*((PI*COS(SAR))/(COS(PAR)*((COS(SAP)*COS(SAR))              SBEV2460*0247
     1             +(TAN(PAR)*TAN(PAR)))))                                   SBEV2470*0248
```

Figure J-2. Listing of spiral bevel gear computer program (cont'd)

```
      TMP = (ZN*PD)/P2                                                          SBEV2480*0248
      CR = SQRT(TMP*TMP+FMP*FMP)                                                SBEV2490*0250
      BSA=ACOS((COS(PAR)*SQRT(COS(BAR)*COS(BAR)+TAN(PAR)*TAN(PAR)))             SBEV2500*0251
      BSA=BSA/RADIAN                                                            SBEV2510*0252
      PN = (A/AO)*(PI/PD)*COS(BAR)*COS(PAR)                                     SBEV2520*0253
      IF (FAC.NE.0.) GO TO 285                                                  SBEV2530*0254
      FAC = (RNG-RNP)/(3.2*RNG*9.8*RNP)                                         SBEV2540*0255
  285 ETASQ = (ZN*ZN*COS(BSA)**2)*(FW*PW)*(SIN(BSA)*SIN(BSA))                   SBEV2550*0256
      CP = SQRT(1.5/(PI*(((1.-PRP*PRP)/EP)+((1.-PRG*PRG)/EG))))                 SBEV2560*0257
   40 FI=1.0                                                                    SBEV2570*0258
   50 G1=GAMP/RADIAN                                                            SBEV2580*0259
      G2=GAMG/RADIAN                                                            SBEV2590*0260
      BS=BSA/RADIAN                                                             SBEV2600*0261
      WRITE  (NOUT,9002) ALFP,ALFG,AMP,AMG,DP,DG,DRHOP,DRHOG,G1,G2,            SBEV2610*0262
     *                   PRNP,PRNG,RBNP,RBNG,RONP,RONG                        SBEV2620*0263
      WRITE (NOUT,9003) RP,RG,A,AO,BSA,CP,ETASQ,FAC,FI,P2,PN,ZN,               SBEV2630*0264
     *                  TMP,FMP,CR                                            SBEV2640*0265
 9002 FORMAT (1H1,/////9X,35HO U T P U T  D A T A  S E C T I O N////           SBEV2650*0266
     *2X,8H(PINION),16X,6H(GEAR)                                              SBEV2660*0267
     */11H ALFP     = ,F10.5,5X,10HALFG     = ,F10.5,5X,                      SBEV2670*0268
     *63H=ADDENDUM ANGLE (DEG.)                                               SBEV2680*0269
     */11H AMP      = ,F10.5,5X,10HAMG      = ,F10.5,5X,                      SBEV2690*0270
     *63H=MEAN ADDENDUM (IN.)                                                 SBEV2700*0271
     */11H DP       = ,F10.5,5X,10HDG       = ,F10.5,5X,                      SBEV2710*0272
     *63H=PITCH DIAMETER (IN.)                                                SBEV2720*0273
     */11H DRHOP    = ,F10.5,5X,10HDRHOG    = ,F10.5,5X,                      SBEV2730*0274
     *63H=MEAN RADIUS OF CURVATURE (IN.)                                      SBEV2740*0275
     */11H GAMP     = ,F10.5,5X,10HGAMG     = ,F10.5,5X,                      SBEV2750*0276
     *63H=PITCH ANGLE (DEG.)                                                  SBEV2760*0277
     */11H PRNP     = ,F10.5,5X,10HPRNG     = ,F10.5,5X,                      SBEV2770*0278
     *63H=PITCH RADIUS IN MEAN NORMAL SECTION (IN.)                           SBEV2780*0279
     */11H RBNP     = ,F10.5,5X,10HRBNG     = ,F10.5,5X,                      SBEV2790*0280
     *63H=BASE RADIUS IN MEAN NORMAL SECTION (IN.)                            SBEV2800*0281
     */11H RONP     = ,F10.5,5X,10HRONG     = ,F10.5,5X,                      SBEV2810*0282
     *63H=OUTSIDE RADIUS IN MEAN NORMAL SECTION (IN.)                         SBEV2820*0283
     *)                                                                       SBEV2830*0284
 9003 FORMAT (                                                                SBEV2840*0285
     * 11H RP       = ,F10.5,5X,10HRG       = ,F10.5,5X,                      SBEV2850*0286
     *63H=PITCH RADIUS IN MEAN TRANSVERSE SECTION (IN.)                       SBEV2860*0287
     */11H A        = ,F10.5,30X,37H=MEAN CONE DISTANCE (IN.)                 SBEV2870*0288
     */11H AO       = ,F10.5,30X,37H=CONE DISTANCE (IN.)                      SBEV2880*0289
     */11H BSA      = ,F10.5,30X,37H=MEAN BASE SPIRAL ANGLE (DEG.)            SBEV2890*0290
     */11H CP       = ,F10.3,30X,37H=MATERIAL LOAD FACTOR (SQRT(LB./IN.))     SBEV2900*0291
     */11H ETASQ    = ,F10.5,30X,37H=SQUARE OF TOTAL LENGTH OF ACTION IN      SBEV2910*0292
     *                        15HNORMAL SECTION /                             SBEV2920*0293
     *                   52X,37HWITHIN CONTACT ELLIPSE, (SQUARE IN.)          SBEV2930*0294
     */11H FAC      = ,F10.5,30X,37H=A FACTOR                                 SBEV2940*0295
     */11H FI       = ,F10.5,30X,37H=INERTIA FACTOR                           SBEV2950*0296
     */11H P2       = ,F10.5,30X,37H=FACTOR IN TRANSVERSE CONTACT RATIO       SBEV2960*0297
     */11H PN       = ,F10.5,30X,37H=MEAN NORMAL BASE PITCH (IN.)             SBEV2970*0298
     */11H ZN       = ,F10.5,30X,37H=LENGTH OF ACTION IN NORMAL PLANE         SBEV2980*0299
     */11H TMP      = ,F10.5,30X,37H=TRANSVERSE CONTACT RATIO                 SBEV2990*0300
     */11H FMP      = ,F10.5,30X,37H=FACE CONTACT RATIO                       SBEV3000*0301
     */11H CR       = ,F10.2,30X,37H=MODIFIED CONTACT RATIO                   SBEV3010*0302
     *)                                                                       SBEV3020*0303
C                                                                             SBEV3030*0304
C     BEGIN HORSEPOWER LOOP FOR SPIRAL BEVEL GEAR.                            SBEV3040*0305
C                                                                             SBEV3050*0306
      RPLOOP=RPMP                                                             SBEV3060*0307
  290 RPM=RPLOOP                                                              SBEV3070*0308
  295 HP=HPO                                                                  SBEV3080*0309
      WRITE (NOUT,9013)                                                       SBEV3090*0310
```

Figure J-2. Listing of spiral bevel gear computer program (cont'd)

```
  297 NUM=0                                                              SBEV3100.0311
      VT = (HP*6300.)/(RPMP*(DP/2.))                                     SBEV3110.0312
C                                                                        SBEV3120.0313
C     BEGIN LOOP FOR THE INDEPENDENT VARIABLE EFF.                       SBEV3130.0314
C                                                                        SBEV3140.0315
      IXREV=2                                                            SBEV3150.0316
      XXM=1.                                                             SBEV3160.0317
      IF (IROT.EQ.IREV)  GO TO 280                                       SBEV3170.0318
      IXREV=1                                                            SBEV3180.0319
      IF (IDRIVE.EQ.IGEAR) XXM=-XXM                                      SBEV3190.0320
      IF (IHAND.EQ.IRH) XXM=-XXM                                         SBEV3200.0321
      IF (IROT.EQ.ICCW) XXM=-XXM                                         SBEV3210.0322
  280 MM=1                                                               SBEV3220.0323
      DO 381 I=1,MM                                                      SBEV3230.0324
      J=I-1                                                              SBEV3240.0325
      EFF = .5*(SQRT(ETASQ)/2.)+(SQRT(ETASQ)/2.**2.-J/MM)                SBEV3250.0326
      EFFAV(I,JEF)=EFF                                                   SBEV3260.0327
      RAD = ETASQ-4.*(EFF*EFF)                                           SBEV3270.0328
      IF (RAD) 381,300,300                                               SBEV3280.0329
  300 ETA1 = SQRT(RAD)                                                   SBEV3290.0330
      FIRST =((ZN+ZN*EFF+(COS(BSA)*COS(FBA)))/ETASQ)*ZN/2.               SBEV3300.0331
      SECOND = ((PN*ZN*ETA1*SIN(BSA))/ETASQ )                            SBEV3310.0332
  310 ZO = FIRST+(XXM*FAC*SECOND)*ORMOG                                  SBEV3320.0333
  320 VN=PI*RPMP/30.*A*SIN(GAMP)*COS(BAR)                                SBEV3330.0334
      VFP = VN*(TAN(BAR)+ABS(ZO)*SIN(PAR)*(TAN(BAR)/(A*TAN(GAMP)))*      SBEV3340.0335
     1          ABS(ZO)*COS(PAR)*(1./(A*COS(BAR))))                      SBEV3350.0336
      VFG = VN*(TAN(BAR)-ABS(ZO)*SIN(PAR)*(TAN(BAR)/(A*GAMGT))*          SBEV3360.0337
     1          ABS(ZO)*COS(PAR)*(1./(A*COS(BAR))))                      SBEV3370.0338
      VF  = VFP+VFG                                                      SBEV3380.0339
      VPP = VN*(SIN(PAR)+ABS(ZO)*(1./(A*TAN(GAMP))))                     SBEV3390.0340
      VPG = VN*(SIN(PAR)-ABS(ZO)*(1./(A*GAMGT)))                         SBEV3400.0341
      VP  = VPP+VPG                                                      SBEV3410.0342
      VFT = VFP+VFG                                                      SBEV3420.0343
      VPT = VPP+VPG                                                      SBEV3430.0344
      VT  = SQRT(VFT*VFT+VPT*VPT)                                        SBEV3440.0345
      VS  = SQRT(VF*VF+VP*VP)                                            SBEV3450.0346
      EFFAV(I,JVS)=VS                                                    SBEV3460.0347
      EFFAV(I,JVT)=VT                                                    SBEV3470.0348
      V1  = SQRT(VFP*VFP+VPP*VPP)                                        SBEV3480.0349
      V2  = SQRT(VFG*VFG+VPG*VPG)                                        SBEV3490.0350
      SUM = 0.0                                                          SBEV3500.0351
      DO 340 KN=1,100                                                    SBEV3510.0352
      RAD = (ETA1*ETA1-4.*KN*PN*(KN*PN-2.*EFF))**2                       SBEV3520.0353
      IF (RAD) 350,330,330                                               SBEV3530.0354
  330 SUM = SUM+SQRT(RAD)                                                SBEV3540.0355
  340 CONTINUE                                                           SBEV3550.0356
      WRITE (NOUT,9015) SUM                                              SBEV3560.0357
      STOP                                                               SBEV3570.0358
  350 SUM1 = 0.                                                          SBEV3580.0359
      DO 370 KN=1,100                                                    SBEV3590.0360
      RAD = (ETA1*ETA1-4.*KN*PN*(KN*PN-2.*EFF))**2                       SBEV3600.0361
      IF (RAD) 380,360,360                                               SBEV3610.0362
  360 SUM1 = SUM1+SQRT(RAD)                                              SBEV3620.0363
  370 CONTINUE                                                           SBEV3630.0364
      WRITE (NOUT,9016) SUM1                                             SBEV3640.0365
      STOP                                                               SBEV3650.0366
  380 IF (ETA1.NE.0.) GO TO 381                                          SBEV3660.0367
      ETA1=.00001                                                        SBEV3670.0368
  381 ET1CUB=ETA1**3                                                     SBEV3680.0369
      ET2CUB = ET1CUB+SUM+SUM1                                           SBEV3690.0370
      SR = ET1CUB/ET2CUB                                                 SBEV3700.0371
      WNB=T*ABS(A/AO)*3R*PI/(COS(PAR)*COS(BAR))                          SBEV3710.0372
```

Figure J-2. Listing of spiral bevel gear computer program (cont'd)

```
      SG = FW*ZW*COS(BBA)*(ETA1/ETABB)                                  BBEV3720*0373
382   EFFRY(I,JWD)=WN                                                   BBEV3730*0374
      RHOP = (RP*SIN(PAR))/(COS(BBA)*COS(BBA))                          BBEV3740*0375
      RHOG = (RG*SIN(PAR))/(COS(BBA)*COS(BBA))                          BBEV3750*0376
      RHO1 = RHOP*ZO                                                    BBEV3760*0377
      RHO2 = RHOG*ZO                                                    BBEV3770*0378
      RHOE = ABS((RHO1*RHO2)/(RHO1+RHO2))                               BBEV3780*0379
384   Q = CP*SQRT((WN)/(RHOE*SG))                                       BBEV3790*0380
      OMEG = ATAN(SIN(PAR)*TAN(BAR))                                    BBEV3800*0381
      ALF1 = ATAN(VPP/VRP)                                              BBEV3810*0382
      ALF2 = ATAN(VPG/VFG)                                              BBEV3820*0383
      AS = SG/2.                                                        BBEV3830*0384
      BS = (1./(PI*CP*CP))*Q*RHOE                                       BBEV3840*0385
      D1 = 2.*SQRT((AS*AS*BS*BS)/(AS*AS*(SIN(ALF1+OMEG))**2+BS*BS       BBEV3850*0386
     1             *(COS(ALF1+OMEG))**2))                               BBEV3860*0387
      D2 = 2.*SQRT((AS*AS*BS*BS)/(AS*AS*(SIN(ALF2+OMEG))**2+BS*BS       BBEV3870*0388
     1             *(COS(ALF2+OMEG))**2))                               BBEV3880*0389
      BOT=RP*SQRT(V1/D1)+BG*SQRT(V2/D2)                                 BBEV3890*0390
385   EFFRY(I,JBOT)=BOT                                                 BBEV3900*0391
      EFFRY(I,JRH)=RHOE                                                 BBEV3910*0392
      EFFRY(I,JQ)=Q                                                     BBEV3920*0393
      EFFRY(I,JBR)=BR                                                   BBEV3930*0394
      IF (MPO.NE.MP) GO TO 383                                          BBEV3940*0395
      NUM=NUM+1                                                         BBEV3950*0396
      WRITE (NOUT,9015) NUM,EFF,VS,VT,V1,V2,ZO,BR,RHOE                  BBEV3960*0397
383 CONTINUE                                                            BBEV3970*0398
      NUM=0                                                             BBEV3980*0399
      CALL FRCTN (EFFRY,MM,JVS,JFR,JPM,JWD,TS,PHEAV,TEMP,FR1,FR2,TCON,  BBEV3990*0400
     1            ZW,RP,RBA,M,RMP,RADIAN,GAMP)                          BBEV4000*0401
      WRITE (NOUT,9017) MP,MT,PHEAV,TS,RPMP                             BBEV4010*0402
      WRITE (NOUT,9018)                                                 BBEV4020*0403
      DO 430 I=1,MM                                                     BBEV4030*0404
      EFF=EFFRY(I,JEF)                                                  BBEV4040*0405
      VS=EFFRY(I,JVS)                                                   BBEV4050*0406
      VT=EFFRY(I,JVT)                                                   BBEV4060*0407
      FRTC=EFFRY(I,JFR)                                                 BBEV4070*0408
      PHE=EFFRY(I,JPM)                                                  BBEV4080*0409
      WN=EFFRY(I,JWD)                                                   BBEV4090*0410
      BR=EFFRY(I,JBR)                                                   BBEV4100*0411
      BOT=EFFRY(I,JBOT)                                                 BBEV4110*0412
      Q=EFFRY(I,JQ)                                                     BBEV4120*0413
      RHOE=EFFRY(I,JRH)                                                 BBEV4130*0414
      IF (Q.GT.10..OR.Q.EQ.10.) GO TO 389                               BBEV4140*0415
      FRIC=0.                                                           BBEV4150*0416
      PHE=0.                                                            BBEV4160*0417
      Q=0.                                                              BBEV4170*0418
389   DELT = (.89*Q*FRIC*VS)/BOT                                        BBEV4180*0419
392   CTEMP=TS+DELT                                                     BBEV4190*0420
420   NUM=NUM+1                                                         BBEV4200*0421
      WRITE (NOUT,9019) NUM,EFF,DELT,CTEMP,WN,Q,FRIC,PHE                BBEV4210*0422
430   CONTINUE                                                          BBEV4220*0423
440   CONTINUE                                                          BBEV4230*0424
      IF (ITYPEV.EQ.1) GO TO 500                                        BBEV4240*0425
      IXREV=1                                                           BBEV4250*0426
      XXMS=XXM                                                          BBEV4260*0427
      GO TO 200                                                         BBEV4270*0428
500   MP=MP+MINC                                                        BBEV4280*0429
      IF (MP.LE.MPMX) GO TO 297                                         BBEV4290*0430
      RPMP=RPMP+RINC                                                    BBEV4300*0431
      IF (RPMP.LE.RPMX) GO TO 295                                       BBEV4310*0432
      GO TO 100                                                         BBEV4320*0433
600   WRITE (NOUT,9022)                                                 BBEV4330*0434
```

Figure J-2. Listing of spiral bevel gear computer program (cont'd)

```
      STOP                                                                  SBEV0340*0035
9013 FORMAT (1H1/////8X,68H VARIABLES CALCULATED INDEPENDENT OF HORSEPO SBEV0350*0036
     *WER (INCHES AND IN./SEC)///9X,3HEFF,11X,2HVS,11X,2HVT,11X,2HV1,   SBEV0360*0037
     *11X,2HV2,11X,2HZO,11X,2HSR,10X,4HRMOE/)                           SBEV0370*0038
9014 FORMAT (1X,I2,1H.,2X,9(E10.3,3X))                                   SBEV0380*0039
9015 FORMAT (54H VALUE OF INDEX KN IN CALCULATION OF ETA2 HAS EXCEEDED, SBEV0390*0040
     1       48H ALPHA LIMIT OF 100 = SERIES SUM OF 100 TERMS = ,       SBEV0400*0041
     2       E9.4)                                                      SBEV0410*0042
9016 FORMAT (54H VALUE OF INDEX KN IN CALCULATION OF ETA2 HAS EXCEEDED, SBEV0420*0043
     1       48H BETA  LIMIT OF 100 = SERIES SUM OF 100 TERMS = ,       SBEV0430*0044
     2       E9.4)                                                      SBEV0440*0045
9017 FORMAT (1H1/////3X,F8.1,19H  = HORSEPOWER/                          SBEV0450*0046
     *                  1X,F10.1,11H  = WT, LB,/                        SBEV0460*0047
     *                  1X,E10.3,19H  = PMEAV, BTU/SEC,/                SBEV0470*0048
     *                  1X,F10.2,19H  = TS, DEG, F/                     SBEV0480*0049
     *                  1X,F10.1,19H  = PINION RPM/)                    SBEV0490*0050
9018 FORMAT (5X,6HMAX,6HERTZ,6X,3HPHE/9X,3HEFF,9X,4HDT,F,5X,            SBEV0500*0051
     *       3HCTEMP,F,9X,5HAN,LB,8X,10HSTRESS,PSI,8X,4HFRIC,           SBEV0510*0052
     *       5X,7HBTU/SEC/)                                             SBEV0520*0053
9022 FORMAT (22H1END OF INPUT PROBLEMS)                                  SBEV0530*0054
9019 FORMAT (1X,I2,1H.,2X,E10.3,9X,F5.1,6X,F5.1,6X,F8.1,3X,E9.3,9X,     SBEV0540*0055
     *       F5.4,8X,E9.3)                                              SBEV0550*0056
      END                                                               SBEV0560*0057
      SUBROUTINE FRCTN (EFFRY,MM,JVS,JFR,JPH,JHD,TS,PHEAV,TEMP,         FRCTN000*0058
     1                  FR1,FR2,TCON,ZN,RP,BSA,M,RNP,RADIAN,GAMP)       FRCTN010*0059
      DIMENSION EFFRY(30,10)                                            FRCTN020*0060
      DO 30 I=1,MM                                                      FRCTN030*0061
      WN=EFFRY(I,JHD)                                                   FRCTN050*0062
      IF (WN.NE.0.) GO TO 5                                             FRCTN060*0063
      FRIC=0.                                                           FRCTN070*0064
      GO TO 27                                                          FRCTN080*0065
    5 VS=(EFFRY(I,JVS))                                                 FRCTN090*0066
      WVS=WN*(VS**(-1./3.))                                             FRCTN100*0067
      IF (WVS.LT.200.) GO TO 15                                         FRCTN110*0068
      FRIC=FR1                                                          FRCTN120*0069
      GO TO 27                                                          FRCTN130*0070
   15 FRIC=FR2*(WVS**(-.30))                                            FRCTN140*0071
   27 PHE = FRIC*WN*VS/9338.                                            FRCTN150*0072
      EFFRY(I,JPH)=PHE                                                  FRCTN160*0073
      EFFRY(I,JFR)=FRIC                                                 FRCTN170*0074
   30 CONTINUE                                                          FRCTN180*0075
      PHET = 0.                                                         FRCTN190*0076
      DO 45 I=1,M                                                       FRCTN200*0077
      PHET=PHET+(EFFRY(I,JPH)+EFFRY(I+1,JPH))                           FRCTN210*0078
   45 CONTINUE                                                          FRCTN220*0079
      PHEAV = (PHET/(2.*M))*RNP*ZN*COS(BSA)/(RP*RADIAN*360.*COS(GAMP))  FRCTN230*0080
      TS=(TCON*((PHEAV)**.80))+TEMP                                     FRCTN240*0081
      RETURN                                                            FRCTN250*0082
      END                                                               FRCTN260*0083
                                                                        *0084
```

Figure J-2. Listing of spiral bevel gear computer program (cont'd)

VALUES AND DEFINITIONS OF INPUT VARIABLES

(INCH UNITS UNLESS NOTED)

(PINION)			(GEAR)			
[illegible]	=	22.0000	[illegible]	=	23.0000	=NUMBER OF TEETH
[illegible]	=	.1250	[illegible]	=	.1250	=ADDENDUM
[illegible]	=	92.1500	[illegible]	=	92.1500	=THERMAL CONSTANT,LB./SQRT(SEC.)IN.DEG.F
[illegible]	=	2.2830	[illegible]	=	2.5170	=DEDENDUM ANGLE,DEG.
[illegible]	=	3.00E+07	[illegible]	=	3.00E+07	=YOUNG'S MODULUS,PSI
[illegible]	=	.3000	[illegible]	=	.3000	=POISSON'S RATIO
[illegible]	=	20.00				=NORMAL PRESSURE ANGLE,DEG.
[illegible]	=	35.00				=SPIRAL ANGLE,DEG.
SIGMA	=	90.00				=SHAFT ANGLE,DEG.
[illegible]	=	.0710				=FACE WIDTH
[illegible]	=	6.11				=DIAMETRAL PITCH
[illegible]	=	PIN				=DRIVING GEAR
[illegible]	=	CW				=ROTATION OF DRIVER
[illegible]	=	LH				=HAND OF DRIVER SPIRAL
N	=	20				=NUMBER OF INCREMENTS OF EFF
[illegible]	=	190.00				=OIL JET TEMPERATURE,DEG.F
[illegible]	=	.0091				=CONSTANT FRICTION FACTOR
[illegible]	=	.0003				=VARIABLE FRICTION FACTOR
TCON	=	675.00				=TEMP.DIFFERENCE FACTOR

INPUT VARIABLES FOR SPECIFIED LOOPS AND SECTIONS

VARIABLES USED IN... RPMP LOOP

[illegible]	=	9500.00	=RPM PINION

VARIABLES USED IN...HORSEPOWER LOOP

HPO	=	300.00	=HORSEPOWER
HINC	=	100.00	=HORSEPOWER INCREMENT
[illegible]	=	1200.00	=MAXIMUM HORSEPOWER

Figure J-3. Sample spiral bevel gear computer printout

OUTPUT DATA SECTION

	(PINION)		(GEAR)		
ALFP	= 2.51700	ALFG	= 2.28300	=ADDENDUM ANGLE (DEG.)
AMP	= .11986	AMG	= .10669	=MEAN ADDENDUM (IN.)
DP	= 3.60007	DG	= 3.76370	=PITCH DIAMETER (IN.)
DRMOP	= .27398	DRMOG	= .25793	=MEAN RADIUS OF CURVATURE (IN.)
GAMP	= 43.72697	GAMG	= 46.27303	=PITCH ANGLE (DEG.)
PRNP	= 3.04137	PRNG	= 3.37879	=PITCH RADIUS IN MEAN NORMAL SECTION (IN.)
RBNP	= 2.85605	RBNG	= 3.12160	=BASE RADIUS IN MEAN NORMAL SECTION (IN.)
RONP	= 3.20623	RONG	= 3.48593	=OUTSIDE RADIUS IN MEAN NORMAL SECTION (IN.)
RP	= 2.07984	RG	= 2.26720	=PITCH RADIUS IN MEAN TRANSVERSE SECTION (IN.)
A	= 2.16863			=MEAN CONE DISTANCE (IN.)
AO	= 2.60913			=CONE DISTANCE (IN.)
BBA	= 31.99975			=MEAN BASE SPIRAL ANGLE (DEG.)
CP	= 2805.405			=MATERIAL LOAD FACTOR (SQRT(LB.)/IN.)
ETAS	= .35910			=SQUARE OF TOTAL LENGTH OF ACTION IN NORMAL SECTION WITHIN CONTACT ELLIPSE, (SQUARE IN.)
FAC	= .00619			=A FACTOR
FI	= 1.00000			=INERTIA FACTOR
F2	= 2.75202			=FACTOR IN TRANSVERSE CONTACT RATIO
PN	= .32400			=MEAN NORMAL BASE PITCH (IN.)
ZN	= .53191			=LENGTH OF ACTION IN NORMAL PLANE
TMP	= 1.17960			=TRANSVERSE CONTACT RATIO
FMP	= 1.99199			=FACE CONTACT RATIO
MR	= 1.96			=MODIFIED CONTACT RATIO

Figure J-3. Sample spiral bevel gear computer printout (cont'd)

VARIABLES CALCULATED INDEPENDENT OF HORSEPOWER (INCHES AND IN./SEC)

	EFF	VB	VT	V1	V2	ZO	BR	RHOE
1.	-2.996E-01	8.919E+01	8.925E+02	9.699E+02	3.898E+02	-1.618E-01	9.099E-15	5.580E-01
2.	-2.647E-01	7.916E+01	8.519E+02	9.553E+02	3.979E+02	-1.931E-01	8.010E-02	5.612E-01
3.	-2.397E-01	6.955E+01	8.600E+02	9.558E+02	9.054E+02	-1.858E-01	1.699E-01	5.690E-01
4.	-2.097E-01	6.008E+01	8.606E+02	9.563E+02	9.133E+02	-1.085E-01	3.155E-01	5.665E-01
5.	-1.798E-01	5.053E+01	8.772E+02	9.570E+02	9.210E+02	-9.139E-02	9.319E-01	5.687E-01
6.	-1.498E-01	9.107E+01	8.858E+02	9.577E+02	9.288E+02	-7.926E-02	5.966E-01	5.707E-01
7.	-1.198E-01	3.163E+01	8.999E+02	9.585E+02	9.362E+02	-6.719E-02	6.628E-01	5.729E-01
8.	-8.989E-02	2.220E+01	9.030E+02	9.594E+02	9.438E+02	-9.015E-02	7.812E-01	5.739E-01
9.	-5.992E-02	1.279E+01	9.117E+02	9.603E+02	9.519E+02	-2.313E-02	8.992E-01	5.751E-01
10.	-2.996E-02	3.901E+00	9.209E+02	9.613E+02	9.598E+02	-6.199E-03	9.428E-01	5.761E-01
11.	0.	9.978E+00	9.179E+02	9.610E+02	9.569E+02	1.001E-02	1.000E+00	5.760E-01
12.	2.996E-02	1.539E+01	9.093E+02	9.600E+02	9.993E+02	2.779E-02	9.928E-01	5.773E-01
13.	5.992E-02	2.969E+01	9.007E+02	9.591E+02	9.918E+02	9.955E-02	8.992E-01	5.778E-01
14.	8.989E-02	3.903E+01	8.922E+02	9.583E+02	9.843E+02	6.163E-02	7.812E-01	5.775E-01
15.	1.198E-01	9.838E+01	8.837E+02	9.575E+02	9.768E+02	7.838E-02	6.628E-01	5.772E-01
16.	1.498E-01	5.265E+01	8.753E+02	9.568E+02	9.692E+02	9.520E-02	5.966E-01	5.767E-01
17.	1.798E-01	6.193E+01	8.669E+02	9.562E+02	9.618E+02	1.180E-01	9.319E-01	5.759E-01
18.	2.097E-01	7.118E+01	8.584E+02	9.557E+02	9.543E+02	1.287E-01	3.155E-01	5.744E-01
19.	2.397E-01	8.039E+01	8.503E+02	9.552E+02	9.469E+02	1.494E-01	1.969E-01	5.737E-01
20.	2.697E-01	8.953E+01	8.422E+02	9.549E+02	9.395E+02	1.619E-01	8.010E-02	5.722E-01
21.	2.996E-01	9.829E+01	8.344E+02	9.546E+02	9.322E+02	1.777E-01	9.939E-22	5.706E-01

Figure J-3. Sample spiral bevel gear computer printout (cont'd)

```
     600.0  = HORSEPOWER
    9666.6  = HT, LB.
1.975E-01   = PHEAV, BTU/SEC.
     375.0  = TB, DEG. F
    9600.0  = PINION RPM
```

	EPI	DT,F	CTEMP,F	WN,LB	MAX.HERTZ STRESS,PSI	FRIC	PHI BTU/SEC
1.	-2.996E-01	0.0	375.0	.0	0.	.0000	0.
2.	-2.647E-01	23.5	397.9	911.3	1.921E+05	.0250	8.723E-02
3.	-2.347E-01	25.5	399.9	1808.6	1.892E+05	.0201	1.510E-01
4.	-2.097E-01	27.5	401.9	1620.9	2.199E+05	.0201	2.099E-01
5.	-1.797E-01	26.0	401.2	2217.0	2.920E+05	.0201	2.913E-01
6.	-1.548E-01	24.9	398.9	2007.0	2.612E+05	.0201	2.482E-01
7.	-1.148E-01	28.0	395.2	3402.0	2.791E+05	.0201	2.316E-01
8.	-8.484E-02	16.0	390.9	4011.6	2.467E+05	.0201	1.917E-01
9.	-5.992E-02	10.0	389.9	4617.2	2.138E+05	.0201	1.278E-01
10.	-2.996E-02	2.0	377.2	5090.2	1.864E+05	.0201	3.733E-02
11.	0.	5.0	379.9	5135.0	1.870E+05	.0201	6.609E-02
12.	2.996E-02	18.0	387.2	5090.2	2.266E+05	.0201	1.699E-01
13.	5.992E-02	19.3	393.7	4617.2	2.191E+05	.0201	2.456E-01
14.	8.484E-02	24.5	398.9	4011.6	2.958E+05	.0201	2.939E-01
15.	1.148E-01	28.5	402.9	3402.0	2.780E+05	.0201	3.175E-01
16.	1.548E-01	31.3	405.7	2807.0	2.599E+05	.0201	3.182E-01
17.	1.798E-01	32.0	407.3	2217.0	2.985E+05	.0201	2.957E-01
18.	2.047E-01	32.6	407.8	1620.9	2.178E+05	.0201	2.483E-01
19.	2.347E-01	29.5	403.9	1808.6	1.876E+05	.0201	1.746E-01
20.	2.647E-01	26.9	401.3	911.3	1.908E+05	.0253	9.988E-02
21.	2.996E-01	0.0	375.9	.0	0.	.0000	0.

Figure J-3. Sample spiral bevel gear computer printout (cont'd)

APPENDIX K
CALCULATION OF AVERAGE FRICTIONAL POWER LOSS

As explained in Chapter VII, Section B, the average frictional power loss, ϕ_{av}, for a gear set is derived basically from Equation (72). However, due to the way the analyses were made (Chap. VII, Sect. D, E, and F), the detailed computing procedures differed for the three different gear types. These computations will now be illustrated by reference to the three specific gear types examined in Chapter VIII, the computer printouts for which at 600 hp were presented in Appendixes H, I, and J.

Spur Gears

For the ground spur gear set operating at 600 hp under the conditions stated in Chapter VIII, Section B, the instantaneous f, W, V_s, and ϕ' values vs. the pinion roll angle, ϵ, as given in Figure H-3, are summarized in Table K-1. Contact line positions 1 through 7 represent a double tooth contact region with $\Delta\epsilon_1 = 20.08 - 14.68 = 5.40°$, divided into 6 equal intervals. Contact line positions 8 through 17 represent a single tooth contact region with $\Delta\epsilon_2 = 26.29 - 20.08 = 6.21°$, divided into 9 equal intervals. Contact line positions 18 through 24 represent a double tooth contact region with $\Delta\epsilon_3 = 31.70 - 26.29 = 5.41°$, divided into 6 equal intervals. Note that at any contact line position, $\phi' = f W V_s/9336$ as tabulated.

Because the roll angle intervals into which $\Delta\epsilon_1$, $\Delta\epsilon_2$, and $\Delta\epsilon_3$ are divided are not of equal magnitude, the integration of the ϕ' vs. ϵ curve is made separately for each region and summed as implied in Equation (72), so

$$\sum \int \phi'(\epsilon)\, d\epsilon = \text{Area}_1 + \text{Area}_2 + \text{Area}_3$$

$$= \bar{h}_1 \Delta\epsilon_1 + \bar{h}_2 \Delta\epsilon_2 + \bar{h}_3 \Delta\epsilon_3 \qquad \text{(K-1)}$$

where $\bar{h}_1$, $\bar{h}_2$, and $\bar{h}_3$ are the average heights of the ϕ' vs. ϵ curves in regions 1, 2, and 3. Using the trapezoidal rule for integration in the computer program, one may write

TABLE K-1. INSTANTANEOUS ϕ' VALUES
(GROUND SPUR GEARS, 600 hp)

Contact line position	ϵ, deg.	f	W, lb	V_s, ips	ϕ', Btu/sec
1	14.68	0.022379	468.8	294.81	0.3313
2	15.58	0.019895	668.4	263.46	0.3752
3	16.48	0.017596	964.9	232.12	0.4221
4	17.38	0.016400	1313.0	200.78	0.4631
5	18.28	0.016400	1665.7	169.43	0.4957
6	19.18	0.016400	1902.2	138.09	0.4614
7	20.08	0.016400	2068.9	106.74	0.3879
8	20.08	0.016400	2795.7	106.74	0.5242
9	20.77	0.016400	2795.7	82.73	0.4063
10	21.46	0.016400	2795.7	58.71	0.2884
11	22.15	0.016400	2795.7	34.70	0.1704
12	22.84	0.016400	2795.7	10.69	0.0 '5
13	23.53	0.016400	2795.7	13.33	0.0655
14	24.22	0.016400	2795.7	37.34	0.1834
15	24.91	0.016400	2795.7	61.35	0.3013
16	25.60	0.016400	2795.7	85.37	0.4193
17	26.29	0.016400	2795.7	109.38	0.5372
18	26.29	0.016400	2326.9	109.38	0.4471
19	27.19	0.016400	2127.4	140.73	0.5259
20	28.09	0.016400	1830.9	172.07	0.5534
21	28.99	0.016400	1482.8	203.41	0.5298
22	29.89	0.016800	1130.1	234.76	0.4774
23	30.79	0.018253	893.6	266.10	0.4649
24	31.70	0.019637	726.8	297.45	0.4548

$$\bar{h} = \frac{1}{2n}\left[\sum_{i=1}^{n}(\phi_i' + \phi_{i+1}')\right] \qquad \text{(K-2)}$$

where n = number of elemental intervals

ϕ_i' = ϕ' value at the beginning of interval i

ϕ_{i+1}' = ϕ' value at the end of interval i

Applying Equation (K-2) to the ϕ' values in Table K-1, one obtains

$$\bar{h}_1 = \frac{1}{2 \times 6}(\phi_1' + 2\phi_2' + \ldots\ldots + 2\phi_6' + \phi_7') = 0.42952$$

$$\bar{h}_2 = \frac{1}{2 \times 9}(\phi_8' + 2\phi_9' + \ldots\ldots + 2\phi_{16}' + \phi_{17}') = 0.26864$$

$$\bar{h}_3 = \frac{1}{2 \times 6}(\phi_{18}' + 2\phi_{19}' + \ldots\ldots + 2\phi_{23}' + \phi_{24}') = 0.50039$$

and $A_1 = \bar{h}_1 \Delta\epsilon_1 = 0.42952 \times 5.40 = 2.31941$

$A_2 = \bar{h}_2 \Delta\epsilon_2 = 0.26864 \times 6.21 = 1.66825$

$A_3 = \bar{h}_3 \Delta\epsilon_3 = 0.50039 \times 5.41 = 2.70711$

Thus, by Equation (K-1),

$$\sum\int \phi'(\epsilon)\, d\epsilon = A_1 + A_2 + A_3 = 6.69477$$

and by Equation (72) and noting that $N_p = 31$,

$$\phi_{av} = \left[\sum\int \phi'(\epsilon)\, d\epsilon\right]\frac{N_p}{360}$$

$$= 6.69477 \times 31/360$$

$$= 0.5765 \text{ Btu/sec}$$

which compares with $\phi_{av} = 0.5763$ Btu/sec given in the computer printout (Fig. H-3) and tabulated in Table 8 (Chap. VIII); the slight numerical difference is due to the rounding off of significant places in the calculation given herein.

Helical Gears

For the helical gear set operating at 600 hp under the conditions stated in Chapter VIII, Section C, the instantaneous f, W, V_s, and ϕ'' values vs. the contact line position, taken from or calculated from data given in Figure I-3, are summarized in Table K-2. Note from Chapter VII, Section E, that in order to obtain the value of ϕ'' at any contact line position, the contributions of the several "elemental spur gears" on this contact line should be summed up. For example, referring to contact line position 3 in Figure I-3, this contact line is divided into four elemental spur gears at a total normal load of 766.79 lb, or at a normal load of 766.79/4 = 191.7 lb for each elemental spur gear. Therefore, the elemental contribution to ϕ'' at this contact line is, from data given in Figure I-3,

$$\phi''_3 = (0.0207 \times 191.70 \times 145.14)/9336$$

$$+ (0.0203 \times 191.70 \times 118.82)/9336$$

$$+ (0.0198 \times 191.70 \times 92.49)/9336$$

$$+ (0.0191 \times 191.70 \times 66.17)/9336$$

$$= 0.0616 + 0.0494 + 0.0375 + 0.0260$$

$$= 0.1745 \text{ Btu/sec}$$

where the quantities 0.0616, 0.0494, 0.0375, and 0.0260 are given in the computer printout; but their sum, $\phi''_3 = 0.1745$ Btu/sec, is stored in the computer program. If this process is repeated for all contact line positions, the appropriate values of ϕ'' will be as in Table K-2.

To calculate ϕ_{av}, it is convenient to transform Equation (85) to the form

TABLE K-2. INSTANTANEOUS ϕ'' VALUES
(HELICAL GEARS, 600 hp)

Contact line position	f	W, lb	V_s, ips	ϕ'', Btu/sec
1	0	0	158.31	0
2	0.0253	380.19	131.98	0.1359
3	-	766.79	-	0.1745
4	-	1150.19	-	0.1837
5	-	1533.59	-	0.2038
6	-	1900.95	-	0.2580
7	-	2216.85	-	0.3397
8	-	2216.85	-	0.3397
9	-	2216.85	-	0.3397
10	-	2216.85	-	0.3397
11	-	1900.95	-	0.2517
12	-	1533.58	-	0.1850
13	-	1150.19	-	0.1556
14	-	766.79	-	0.1528
15	0.0250	380.19	119.81	0.1222
16	0	0	146.13	0

$$\phi_{av} = (\bar{h}\,\Delta\epsilon)\,\frac{N_p}{360} \qquad \text{(K-3)}$$

where $\bar{h}$, the average contribution for a pair of teeth as contact moves across the plane of action, is, by applying Equation (K-2),

$$\bar{h} = \frac{1}{2n}\left[\sum_{i=1}^{n}(\phi_i'' + \phi_{i+1}'')\right]$$

$$= \frac{1}{2 \times 15}(\phi_1' + 2\phi_2'' + \ldots\ldots + 2\phi_{15}'' + \phi_{16}'')$$

$$= 0.2121 \text{ Btu/sec}$$

Now, the angle through which the pinion turns as contact moves across the plane of action is, from Equation (86),

$$\Delta\epsilon = \frac{2Z}{d_b} \cdot \frac{180}{\pi}$$

$$= \frac{2 \times 0.45422}{3.53450} \cdot \frac{180}{\pi} = 14.7262°$$

Substituting the calculated $\bar{h}$ and $\Delta\epsilon$ into Equation (K-3), and noting that $N_p = 31$,

$$\phi_{av} = 0.2121 \times 14.7262 \times 31/360$$

$$= 0.2690 \text{ Btu/sec}$$

which is the value given in the computer printout (Fig. I-3) and tabulated in Table 10 (Chap. VIII).

Spiral Bevel Gears

For the spiral bevel gear set operating at 600 hp under the conditions stated in Chapter VIII, Section D, the instantaneous f, W, V_s, and ϕ'' values vs. the contact line position, as taken from Figure J-3, are summarized in Table K-3.

To calculate ϕ_{av}, it is convenient to transform Equation (88)

TABLE K-3. INSTANTANEOUS ϕ'' VALUES
(SPIRAL BEVEL GEARS, 600 hp)

Contact line position	f	W, lb	V_s, ips	ϕ'', Btu/sec
1	0	0	89.14	0
2	0.0250	411.3	79.16	0.0872
3	0.0201	1008.6	69.55	0.1510
4	0.0201	1620.4	60.02	0.2094
5	0.0201	2217.8	50.53	0.2413
6	0.0201	2807.0	41.07	0.2482
7	0.0201	3402.0	31.63	0.2316
8	0.0201	4011.6	22.20	0.1917
9	0.0201	4617.2	12.79	0.1272
10	0.0201	5098.2	3.40	0.0373
11	0.0201	5135.0	5.98	0.0661
12	0.0201	5098.2	15.34	0.1684
13	0.0201	4617.2	24.69	0.2455
14	0.0201	4011.6	34.03	0.2939
15	0.0201	3402.0	43.35	0.3175
16	0.0201	2807.0	52.65	0.3182
17	0.0201	2217.8	61.93	0.2957
18	0.0201	1620.4	71.18	0.2483
19	0.0201	1008.6	80.39	0.1746
20	0.0253	411.3	89.53	0.0999
21	0	0	98.29	0

again to the form of Equation (K-3) given previously for helical gears. Thus

$$\bar{h} = \frac{1}{2n}\left[\sum_{i=1}^{n} (\phi_i'' + \phi_{i+1}'')\right]$$

$$= \frac{1}{2 \times 20} (\phi_1'' + 2\phi_2'' + \ldots\ldots + 2\phi_{20}'' + \phi_{21}'')$$

$$= 0.1877 \text{ Btu/sec}$$

Now, the angle through which the pinion turns as contact moves across the plane of action is, from Equation (89),

$$\Delta\epsilon = \frac{Z}{A \sin \gamma} \cdot \frac{180}{\pi}$$

$$= \frac{Z_N \cos \psi_b}{A \sin \gamma} \cdot \frac{180}{\pi}$$

$$= \frac{0.53141 \cos (31.99975°)}{2.16863 \sin (43.72697°)} \cdot \frac{180}{\pi} = 17.2255°$$

Substituting the calculated $\bar{h}$ and $\Delta\epsilon$ into Equation (K-3), and noting that $N_p = 22$,

$$\phi_{av} = 0.1877 \times 17.2255 \times 22/360$$

$$= 0.1975 \text{ Btu/sec}$$

which is the value given in the computer printout (Fig. J-3) and tabulated in Table 12 (Chap. VIII).

LIST OF SYMBOLS

a	addendum, in.
a	major semiwidth of Hertzian ellipse, in.
B	minor width of Hertzian rectangle, in.
b	dedendum, in.
b	minor semiwidth of Hertzian ellipse, in.
C	center distance, in.
C	fitting constant in $(T_s - T_j)$ vs. ϕ equation for disks
C'	fitting constant in $(T_s - T_j)$ vs. ϕ_{av} equation for gears
C_o	fitting constant in $(T_o - T_j)$ vs. ϕ equation for disks
C'_o	fitting constant in $(T_o - T_j)$ vs. ϕ_{av} equation for gears
c	specific heat of gear material, in./°F
c	specific heat of oil, Btu/lb-°F
D	pitch diameter of gear, in.
d	pitch diameter of pinion, in.
D_b	base diameter of gear, in.
d_b	base diameter of pinion, in.
D_o	outside diameter of gear, in.
d_o	outside diameter of pinion, in.
E	Young's modulus, psi
E^*	Equivalent Young's modulus, psi
e	angular misalignment, deg

LIST OF SYMBOLS (Cont'd)

e	pitch error, in.
e_a	apparent tooth error, in.
e_e	effective tooth error, in.
e_f	effective pitch error, in.
F	face width, in.
F_i	dynamic normal tooth load increment, lb
f	coefficient of friction
G	gear ratio
h_m	minimum EHD film thickness without side flow and inlet-shear thermal corrections, μin.
h'_m	minimum EHD film thickness with side flow and inlet-shear thermal corrections, μin.
K_i	inertia factor (AGMA)
K_v	dynamic factor (AGMA)
k	thermal conductivity of gear material, lb/°F-sec
k	thermal conductivity of oil, Btu/ft-°F-sec
L	total length of lines of contact for all tooth pairs simultaneously in contact, in.
ℓ	elemental segment on a line of contact, in.
M	sliding-to-sum velocity ratio
m_c	transverse contact ratio
m_f	face contact ratio

LIST OF SYMBOLS (Cont'd)

m_N	load sharing ratio
m_o	modified contact ratio
m_t	total contact ratio
N_g	number of teeth in gear
N_p	number of teeth in pinion
n_g	rotative speed of gear, rpm
n_p	rotative speed of pinion, rpm
P	diametral pitch, $in.^{-1}$
P	power transmitted, hp
P_A	actual scoring-limited power-transmitting capacity, hp
P_I	ideal scoring-limited power-transmitting capacity, hp
p	pressure, psi
p	transverse circular pitch, in.
p_b	transverse base pitch, in.
p_N	normal base pitch, in.
R	equivalent radius of curvature, in.
S	surface roughness, μin. rms (AGMA)
S_d	dynamic factor
S_m	misalignment factor
T	temperature, °F
T	torque, in.-lb

LIST OF SYMBOLS (Cont'd)

T_c	maximum instantaneous conjunction surface temperature, °F
T_{cr}	critical temperature, °F
T_j	oil jet temperature, °F
T_o	conjunction-inlet oil temperature, °F
T_s	quasi-steady surface temperature, °F
ΔT	maximum instantaneous conjunction surface temperature rise, °F
V_1	surface velocity of body 1, ips
V_2	surface velocity of body 2, ips
V_g	surface velocity of gear, ips
V_p	surface velocity of pinion, ips
V_s	sliding velocity, ips
V_t	sum velocity, ips
V_t	pitchline velocity, fpm
W	normal tooth load, lb
w	unit normal tooth load, ppi
W_d	dynamic normal tooth load, lb
W_t	tangential tooth load, lb
w_t	unit tangential tooth load, lb
Z	length of path of contact in transverse plane, in.

LIST OF SYMBOLS (Cont'd)

α	pressure-viscosity coefficient of oil, psi^{-1}
β	Blok's thermal coefficient of gear material, $lb/°F\text{-}in.\text{-}sec^{\frac{1}{2}}$
Γ	pitch angle of gear, deg
γ	pitch angle of pinion, deg
Δ	profile modification, in.
δ	composite surface roughness of one surface, μin. AA
δ_c	composite surface roughness of mating surfaces, μin. AA
δ_i	initial composite surface roughness of mating surfaces, μin. AA
δ_m	normal tooth deflection, in.
ϵ	roll angle, deg
θ	load angle, deg
Λ	EHD film thickness ratio
μ	absolute viscosity of oil, cp
ν	kinematic viscosity of oil, cs
ν	Poisson's ratio of gear material
ρ	density of gear material, $lb/in.^3$
ρ	density of oil, g/ml
ρ_g	radius of curvature of gear tooth, in.
ρ_p	radius of curvature of pinion tooth, in.
ϕ	pressure angle, deg

LIST OF SYMBOLS (Cont'd)

ϕ	frictional power loss, Btu/sec
ϕ_{av}	average frictional power loss, Btu/sec
ϕ_n	pressure angle in normal plane, deg
ψ	helix angle, deg
ψ	spiral angle, deg
ψ_b	base helix angle, deg
ψ_b	base spiral angle, deg
ω_g	angular velocity of gear, rad/sec
ω_p	angular velocity of pinion, rad/sec